
Theses and Dissertations

Spring 2014

Potential opioid receptor modulators derived from novel stilbenes

Alyssa Michelle Hartung
University of Iowa

Copyright 2014 Alyssa Michelle Hartung

This dissertation is available at Iowa Research Online: <http://ir.uiowa.edu/etd/3093>

Recommended Citation

Hartung, Alyssa Michelle. "Potential opioid receptor modulators derived from novel stilbenes." PhD (Doctor of Philosophy) thesis, University of Iowa, 2014.
<http://ir.uiowa.edu/etd/3093>.

Follow this and additional works at: <http://ir.uiowa.edu/etd>

 Part of the [Chemistry Commons](#)

POTENTIAL OPIOID RECEPTOR MODULATORS DERIVED FROM NOVEL
STILBENES

by
Alyssa Michelle Hartung

A thesis submitted in partial fulfillment
of the requirements for the Doctor of
Philosophy degree in Chemistry
in the Graduate College of
The University of Iowa

May 2014

Thesis Supervisor: Professor David F. Wiemer

Graduate College
The University of Iowa
Iowa City, Iowa

CERTIFICATE OF APPROVAL

PH.D. THESIS

This is to certify that the Ph.D. thesis of

Alyssa Michelle Hartung

has been approved by the Examining Committee
for the thesis requirement for the Doctor of Philosophy
degree in Chemistry at the May 2014 graduation.

Thesis Committee: _____
David F. Wiemer, Thesis Supervisor

James B. Gloer

F. Christopher Pigge

Alexei V. Tivanski

Robert J. Kerns

The more you learn, the more you realize how little you know.

Socrates

ACKNOWLEDGMENTS

The amount of patience and encouragement provided by my advisor has not gone unnoticed. Dr. Wiemer is an immensely kind person and a true leader. I feel fortunate to have worked with him. I'm so grateful for my labmates and their friendship, common love for coffee, and helpful chemistry discussions. I am especially thankful for the instruction provided by Dr. John Kodet in my first year, and for his patience in answering my questions. I would also like to thank Kevyn Gardner, John Stanley, Dr. Rocky Barney, and Dr. Jeffrey Neighbors for the roles they played in supporting this project. The efforts of Dr. Hernán Navarro (RTI International) in providing bioassay data are greatly appreciated, as well as the contributions by Dr. Liu-Chen (Temple University) and Dr. Larry Toll (SRI International) in providing cell lines for the assays. I'd like to thank the faculty and staff of the Chemistry Department, all of whom are extremely gracious and capable. Thanks to all of our funding sources including the National Institutes of Health, National Cancer Institute, Center for Research, and the Roy J. Carver Charitable Trust. Thank you so very much to Mom, Dad, and Steven. Your guidance and unending encouragement means the world to me. Last but not least, I have profound gratitude for my husband, Kevin. Your daily support is a constant reminder to celebrate (even the small) accomplishments and enjoy the present.

ABSTRACT

The stilbene structure is part of many biologically active natural products, and these compounds can be attractive targets for chemical synthesis. A convergent synthetic design can be utilized in order to install the central olefinic moiety by way of organophosphorus compounds. This design has been employed to prepare a number of natural products, including the potent anti-cancer compounds known as the schweinfurthins and many analogues thereof. Not only do all these structures consist of a stilbenoid scaffold, but all are partially terpenoid in nature as well. Striking similarities to the schweinfurthins would become apparent following the isolation of a new group of compounds, which would later become known as the pawhuskins.

In 2004, Belofsky and co-workers reported a small set of prenylated stilbenes that they named pawhuskins. Pawhuskins A–C were isolated from the common North American purple prairie clover (*Dalea purpurea*) collected near Pawhuska, Oklahoma. Belofsky's findings support an ethnomedical use, because the pawhuskins were shown to modulate opioid receptors through displacement of a nonselective radioactive antagonist ($^3\text{[H]}$ -naloxone) striatal tissue taken from rat brain. Pawhuskin A was the most potent member of the family, making it one of a small group of compounds that does not contain a basic nitrogen atom but that still exhibits effects on the opiate receptor system. This activity is surprising given the absence of the traditional pharmacophore, a 6-membered piperidine ring containing a basic nitrogen. In these studies, we will report the opioid receptor binding affinity and selectivity of pawhuskin A using a functional assay based on [^{35}S]GTP- γ -S binding.

Because of our well-established history of synthesizing prenylated stilbenes, and the unique biological activity of the pawhuskins, we embarked on a synthetic effort targeted at pawhuskin analogues. The preparation of sixteen analogues will be presented. The structure-activity relationship studies of twenty compounds correlated to illuminate

more information on the novel pawhuskin pharmacophore will also be reported. Efforts toward preparation of more water-soluble structures similar to the pawhuskins will also be described. The interrelated studies involving pawhuskin analogue synthesis and elucidation of the novel pharmacophore, as well as interesting chemical findings, will be discussed in detail.

TABLE OF CONTENTS

LIST OF TABLES	vii
LIST OF FIGURES	viii
LIST OF ABBREVIATIONS.....	xv
CHAPTER	
1. BRIEF HISTORY OF STILBENOID SYNTHESIS IN THE WIEMER GROUP; THE PAWHUSKINS AND ASSOCIATED BIOLOGICAL ACTIVITY	1
2. STRUCTURAL ANALOGUES OF PAWHUSKIN A: PROBING THE IMPORTANCE OF A-RING SUBSTITUENTS.....	15
3. STRUCTURAL ANALOGUES OF PAWHUSKIN A: PROBING THE IMPORTANCE OF B-RING SUBSTITUENTS	28
4. STRUCTURAL ANALOGUES OF PAWHUSKIN C: ASSESSING THE SIGNIFICANCE OF VARYING THE ISOPRENOID CHAIN	49
5. DISCOVERY OF A NEW REGIOISOMER IN A DIRECTED <i>ORTHO</i> METALLATION REACTION	59
6. SYNTHESIS OF A NEW CORE LINKAGE: AN EXTENSION OF PROMISING ANALOGUES	74
7. SUMMARY AND FUTURE DIRECTIONS.....	91
8. EXPERIMENTAL PROCEDURES.....	94
APPENDIX: SELECTED NMR SPECTRA.....	132
REFERENCES	242

LIST OF TABLES

Table

1.	Pawhuskins A and C opioid receptor affinity and selectivity.....	13
2.	The opioid receptor affinity of analogue 46	21
3.	The opioid receptor affinity of analogues 54, 56, and 58	24
4.	The opioid receptor affinity of analogue 64	26
5.	The opioid receptor affinity and selectivity of analogues 64, 79, and 77	35
6.	The opioid receptor affinity of analogues 81, 83, and 85	37
7.	The opioid receptor affinity of analogues 86, 88, and 90	40
8.	The opioid receptor affinity of analogue 91	41
9.	The opioid receptor affinity of analogues 110 and 113 and Schweinfurthin J (100).....	54
10.	The opioid receptor affinity of the natural products Schweinfurthin C (3), Mappain (8), and Schweinfurthin I (101)	56
11.	The opioid receptor selectivity of Schweinfurthin J (100)	57
12.	The effect of temperature on product ratio in directed <i>ortho</i> metallation	69
13.	Calculated partition coefficients	76

LIST OF FIGURES

Figure

1.	Schweinfurthins, Vedelianin, and Mappain.....	2
2.	<i>D. purpurea</i> isolates: Pawhuskins A–C and Petalostemumol	4
3.	Traditional opioid receptor modulators with a common <i>N</i> -methyl-piperidine core.....	5
4.	Structures of non-nitrogenous opioid receptor modulators.....	7
5.	Retrosynthesis of Pawhuskin C showing common phosphonate synthon 23	9
6.	Initial preparation of phosphonate 23	10
7.	Efficient preparation of phosphonate 23	11
8.	Convergent retrosynthetic analysis of Pawhuskin A	12
9.	Representative graph of the antagonist activity of pawhuskin A in the KOP receptor affinity assay. Each data point represents the mean and SEM of duplicate samples.....	16
10.	Retrosynthesis of analogues 46 , 54 , 56 , 58 , and 64	17
11.	Synthesis of aldehyde 34	18
12.	Preparation of phosphonate 44	19
13.	Condensation and hydrolysis to provide compound 46	20
14.	Preparation of phosphonates 48 , 50 , and 52	22
15.	Condensations and hydrolyses to provide analogues 54 , 56 , and 58	23
16.	Formation of phosphonate 62	25
17.	Condensation and hydrolysis to provide compound 64	26
18.	Retrosynthesis of analogues 79 , 81 , 83 , 85 , 86 , 88 , 90 , and 91	29
19.	Synthesis of aldehyde 66	30
20.	Preparation of phosphonate 73	31
21.	Formation of phosphonate 75	32
22.	Pawhuskin analogues 64 and 77	33
23.	Condensation and hydrolysis to provide analogue 79	34

24.	Condensations and hydrolyses to provide analogues 81 , 83 , and 85	36
25.	Condensations and hydrolyses to afford analogues 86 and 88	38
26.	Condensation and hydrolysis to provide analogue 90	39
27.	Divergence of compound 81 to provide analogue 91	41
28.	Pawhuskin A and the opioid receptors in brief.....	43
29.	Representative graph of the antagonist activity of compound 79 in the KOP receptor affinity assay. Each data point represents the mean and SEM of duplicate samples.....	44
30.	Representative graph of the antagonist activity of compound 90 in the DOP receptor affinity assay. Each data point represents the mean and SEM of duplicate samples.....	46
31.	Preparation of mono methylated B–ring isomers	47
32.	Pawhuskin C and structurally similar compounds.....	50
33.	Retrosynthesis of analogues 110 and 113	51
34.	Formation of phosphonate 104	52
35.	Condensations and hydrolyses to provide analogues 110 and 113	53
36.	Linear strategy toward Schweinfurthin C.....	60
37.	Revised retrosynthesis of Schweinfurthin C from Vanillin.....	61
38.	Synthesis of alkylated arene 127 toward Schweinfurthins F and G	62
39.	Synthesis of aldehyde 30 toward Pawhuskin A.....	64
40.	A new regioisomeric product 61 of a published DOM procedure.....	65
41.	Structures of Pawhuskin A analogues 79 and 90	66
42.	The effect of a bulky protecting group in product distribution.....	71
43.	Unsuccessful halogen–metal exchange toward compound 130	72
44.	Active stilbenes 79 and 90 and respective target amides.....	75
45.	Retrosynthesis of analogues 131 and 132	77
46.	Synthesis of amines 139 and 140	78
47.	Synthesis of acetanilide 142	79
48.	Amide model reactions	80

49.	Preparation of carboxylic acids 149 and 152	82
50.	Attempted carbodiimide coupling reactions	84
51.	Attempted recycling of compound 154	85
52.	Synthesis of amide 155	86
53.	Retrosynthesis of analogues 131 and 132 via imine.....	87
54.	Synthesis of imine 159	88
55.	Potential applications of the amide core linkage	90
56.	Selective KOP receptor antagonist JD <i>Tic</i> (161).....	93
A-1.	¹ H NMR spectrum of compound 37	133
A-2.	¹³ C NMR spectrum of compound 37	134
A-3.	¹ H NMR spectrum of compound 38	135
A-4.	¹³ C NMR spectrum of compound 38	136
A-5.	¹ H NMR spectrum of compound 34	137
A-6.	¹³ C NMR spectrum of compound 34	138
A-7.	¹ H NMR spectrum of compound 45	139
A-8.	¹³ C NMR spectrum of compound 45	140
A-9.	¹ H NMR spectrum of compound 46	141
A-10.	¹³ C NMR spectrum of compound 46	142
A-11.	¹ H NMR spectrum of compound 53	143
A-12.	¹³ C NMR spectrum of compound 53	144
A-13.	¹ H NMR spectrum of compound 54	145
A-14.	¹³ C NMR spectrum of compound 54	146
A-15.	¹ H NMR spectrum of compound 55	147
A-16.	¹³ C NMR spectrum of compound 55	148
A-17.	¹ H NMR spectrum of compound 56	149
A-18.	¹³ C NMR spectrum of compound 56	150
A-19.	¹ H NMR spectrum of compound 57	151

A-20.	¹³ C NMR spectrum of compound 57	152
A-21.	¹ H NMR spectrum of compound 58	153
A-22.	¹³ C NMR spectrum of compound 58	154
A-23.	¹ H NMR spectrum of compound 61	155
A-24.	¹³ C NMR spectrum of compound 61	156
A-25.	¹ H NMR spectrum of compound 62	157
A-26.	¹³ C NMR spectrum of compound 62	158
A-27.	¹ H NMR spectrum of compound 63	159
A-28.	¹³ C NMR spectrum of compound 63	160
A-29.	¹ H NMR spectrum of compound 64	161
A-30.	¹³ C NMR spectrum of compound 64	162
A-31.	¹ H NMR spectrum of compound 70	163
A-32.	¹³ C NMR spectrum of compound 70	164
A-33.	¹ H NMR spectrum of compound 71	165
A-34.	¹³ C NMR spectrum of compound 71	166
A-35.	¹ H NMR spectrum of compound 66	167
A-36.	¹³ C NMR spectrum of compound 66	168
A-37.	¹ H NMR spectrum of compound 72	169
A-38.	¹ H NMR spectrum of compound 73	170
A-39.	¹ H NMR spectrum of compound 75	171
A-40.	¹³ C NMR spectrum of compound 75	172
A-41.	¹ H NMR spectrum of compound 78	173
A-42.	¹³ C NMR spectrum of compound 78	174
A-43.	¹ H NMR spectrum of compound 79	175
A-44.	¹³ C NMR spectrum of compound 79	176
A-45.	¹ H NMR spectrum of compound 80	177
A-46.	¹³ C NMR spectrum of compound 80	178

A-47. ^1H NMR spectrum of compound 81	179
A-48. ^{13}C NMR spectrum of compound 81	180
A-49. ^1H NMR spectrum of compound 82	181
A-50. ^{13}C NMR spectrum of compound 82	182
A-51. ^1H NMR spectrum of compound 83	183
A-52. ^{13}C NMR spectrum of compound 83	184
A-53. ^1H NMR spectrum of compound 84	185
A-54. ^{13}C NMR spectrum of compound 84	186
A-55. ^1H NMR spectrum of compound 85	187
A-56. ^{13}C NMR spectrum of compound 85	188
A-57. ^1H NMR spectrum of compound 86	189
A-58. ^{13}C NMR spectrum of compound 86	190
A-59. ^1H NMR spectrum of compound 87	191
A-60. ^{13}C NMR spectrum of compound 87	192
A-61. ^1H NMR spectrum of compound 88	193
A-62. ^{13}C NMR spectrum of compound 88	194
A-63. ^1H NMR spectrum of compound 89	195
A-64. ^{13}C NMR spectrum of compound 89	196
A-65. ^1H NMR spectrum of compound 90	197
A-66. ^{13}C NMR spectrum of compound 90	198
A-67. ^1H NMR spectrum of compound 91	199
A-68. ^{13}C NMR spectrum of compound 91	200
A-69. ^1H NMR spectrum of compound 94	201
A-70. ^{13}C NMR spectrum of compound 94	202
A-71. HSQC spectrum of compound 94	203
A-72. HMBC spectrum of compound 94	204
A-73. ^1H NMR spectrum of compound 95	205

A-74. ¹³ C NMR spectrum of compound 95	206
A-75. HSQC spectrum of compound 95	207
A-76. HMBC spectrum of compound 95	208
A-77. ¹ H NMR spectrum of compound 93	209
A-78. ¹³ C NMR spectrum of compound 93	210
A-79. ¹ H NMR spectrum of compound 109	211
A-80. ¹³ C NMR spectrum of compound 109	212
A-81. ¹ H NMR spectrum of compound 112	213
A-82. ¹³ C NMR spectrum of compound 112	214
A-83. ¹ H NMR spectrum of compound 128	215
A-84. ¹³ C NMR spectrum of compound 128	216
A-85. ¹ H NMR spectrum of compound 129	217
A-86. ¹³ C NMR spectrum of compound 129	218
A-87. ¹ H NMR spectrum of compound 130	219
A-88. ¹³ C NMR spectrum of compound 130	220
A-89. ¹ H NMR spectrum of compound 138	221
A-90. ¹³ C NMR spectrum of compound 138	222
A-91. ¹ H NMR spectrum of compound 139	223
A-92. ¹³ C NMR spectrum of compound 139	224
A-93. ¹ H NMR spectrum of compound 140	225
A-94. ¹³ C NMR spectrum of compound 140	226
A-95. ¹ H NMR spectrum of compound 142	227
A-96. ¹³ C NMR spectrum of compound 142	228
A-97. ¹ H NMR spectrum of compound 145	229
A-98. ¹³ C NMR spectrum of compound 145	230
A-99. ¹ H NMR spectrum of compound 150	231
A-100. ¹³ C NMR spectrum of compound 150	232

A-101.	^1H NMR spectrum of compound 151	233
A-102.	^{13}C NMR spectrum of compound 151	234
A-103.	^1H NMR spectrum of compound 149	235
A-104.	^{13}C NMR spectrum of compound 149	236
A-105.	^1H NMR spectrum of compound 152	237
A-106.	^{13}C NMR spectrum of compound 152	238
A-107.	^1H NMR spectrum of compound 154	239
A-108.	^1H NMR spectrum of compound 155	240
A-109.	^{13}C NMR spectrum of compound 155	241

LIST OF ABBREVIATIONS

Å	Angstrom
Ac	Acetate
Anal.	Analysis
Aq.	Aqueous
br	Broad
Bu	Butyl
C	Celsius
calcd	Calculated
<i>cLogP</i>	Calculated octanol–water partition coefficient
CAN	Ceric ammonium nitrate
d	Doublet
DBU	1,8-Diazabicyclo[5.4.0]undec-7-ene
DCM	Dichloromethane
DCC	N,N'-dicyclohexylcarbodiimide
dd	Doublet of doublets
DEPT	Distortionless enhancement by polarization transfer (NMR)
DHP	Dihydropyran
DIPEA	Diisopropylethylamine
DMF	Dimethylformamide
DMS	Dimethyl sulfide
DOP	Delta (δ) opioid (receptor)
dt	Doublet of triplets
EDC	N-(3-Dimethylaminopropyl)-N'-ethylcarbodiimide hydrochloride
EI	Electron Impact

ESI	Electrospray ionization
Et	Ethyl
g	Gram
h	Hour
HOBt	1-Hydroxybenzotriazole hydrate
HPLC	High performance liquid chromatography
HRMS	High resolution mass spectroscopy
HWE	Horner–Wadsworth–Emmons
Hz	Hertz
Imid.	Imidazole
iPr	Isopropyl
<i>J</i>	Coupling constant
KHMDS	Potassium hexamethyl disilazane
KOP	Kappa (κ) opioid (receptor)
LDA	Lithium diisopropylamide
<i>LogP</i>	Octanol–water partition coefficient
m	Multiplet
M	Molar
Me	Methyl
MeCN	Acetonitrile
mg	Milligram
mL	Milliliter
mmol	Millimole
MOM	Methoxymethyl
Ms	Methanesulfonyl
MOP	Mu (μ) opioid (receptor)
<i>m/z</i>	Mass/charge

<i>n</i> -BuLi	<i>n</i> -Butyllithium
NP	Natural product
NBS	N-bromosuccinimide
NCI	National Cancer Institute
NMR	Nuclear magnetic resonance
Pyr.	pyridine
PDC	Pyridinium dichromate
PPTS	Pyridinium <i>p</i> -toluenesulfonate
q	Quartet
rt	Room temperature
s	Singlet
sat.	Saturated
t	Triplet
TBAF	Tetrabutylammonium fluoride
TBAI	Tetrabutylammonium iodide
THP	Tetrahydropyran
TBS	<i>tert</i> -Butyldimethylsilyl
TEA	Triethylamine
TFAA	Trifluoroacetic anhydride
THF	Tetrahydrofuran
TLC	Thin layer chromatography
TMEDA	Tetramethylethylenediamine
TMS	Trimethylsilyl
Ts	<i>p</i> -Toluene sulfonyl
TsOH	<i>p</i> -Toluene sulfonic acid

CHAPTER 1
BRIEF HISTORY OF STILBENOID SYNTHESIS IN THE WIEMER
GROUP; THE PAWHUSKINS AND ASSOCIATED BIOLOGICAL
ACTIVITY

Stilbenoid synthesis has been a focus of our research group for many years.¹ A convergent synthetic design can be utilized in order to install the central olefinic moiety by way of organophosphorus compounds. This design has been employed to prepare a number of natural products, including the potent anti-cancer compounds known as the schweinfurthins and many analogues thereof. Some of these targeted natural products are shown in Figure 1, and include schweinfurthins A (**1**),² B (**2**),³⁻⁷ C (**3**),¹ E (**4**),⁴ F (**5**),^{3,8,9} and G (**6**),⁸ as well as the structurally related vedelianin (**7**)¹⁰ and mappain (**8**).¹¹ Not only do all of these structures consist of a stilbenoid scaffold, but all are partially of a terpenoid nature. The expertise developed while carrying out the synthesis of these compounds would become of great value following the isolation of a new class of natural products, which would become known as the pawhuskin family.¹²

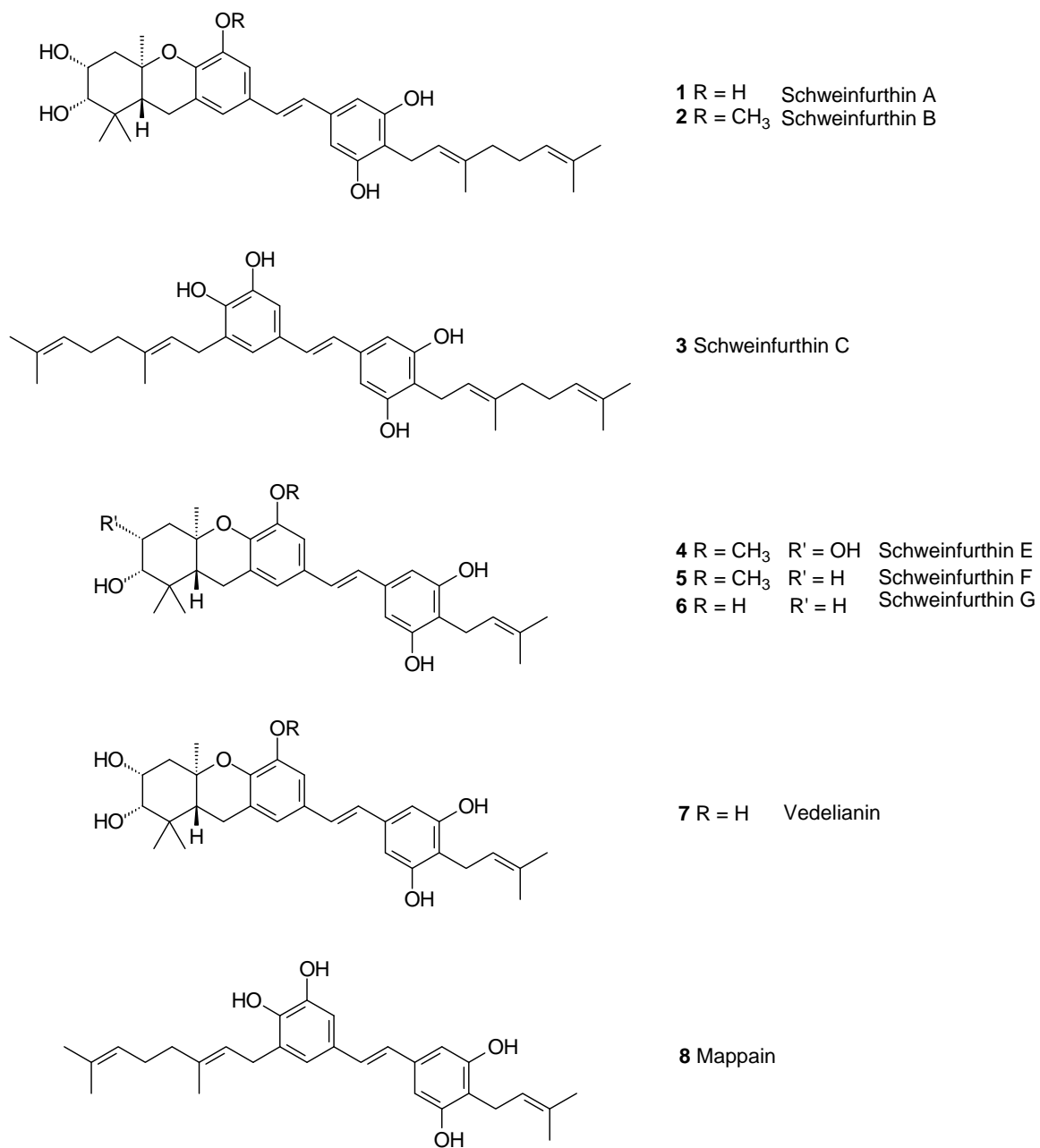


Figure 1. Schweinfurthins, Vedelianin, and Mappain

In 2004, Belofsky and co-workers reported a small set of prenylated stilbenes that they named the pawhuskins.¹² This family of compounds was isolated from the common North American purple prairie clover (*Dalea purpurea*) collected near Pawhuska, Oklahoma. The isolates included three new prenylated stilbenes, pawhuskins A–C (**9–11**, Figure 2), as well as the known petalostemumol (**12**).^{12–14} Extracts of this plant reportedly have been made into teas and used by Native American peoples as a prophylactic and for treatment of various ailments.^{15,16} Belofsky's findings support this ethnomedical use, because the pawhuskins were shown to modulate opioid receptors by displacement of a nonselective radioactive antagonist (³[H]–naloxone) in rat brain striatal tissue.^{12,16} The naloxone ligand was chosen in part because it has similar affinities for the three major types of opioid receptors, which include the G-protein-coupled kappa (κ), delta (δ), and mu (μ) receptors.^{12,17} The total displacement of naloxone was characterized by functional inhibition constants (K_i). The reported K_i of pawhuskins A, B, and C, and petalostemumol were $0.29 \pm 0.11 \mu\text{M}$, $11.4 \pm 7.9 \mu\text{M}$, $4.2 \pm 3.6 \mu\text{M}$, and $>100 \mu\text{M}$, respectively.¹² Pawhuskin A was the most potent member of the family. Thus, it is among a small group of compounds not containing a basic nitrogen atom that has exhibited effects on the opiate receptor system.¹⁶ This activity is surprising given the absence of the traditional opioid pharmacophore, which encompasses a 6-membered piperidine ring containing a basic nitrogen.¹²

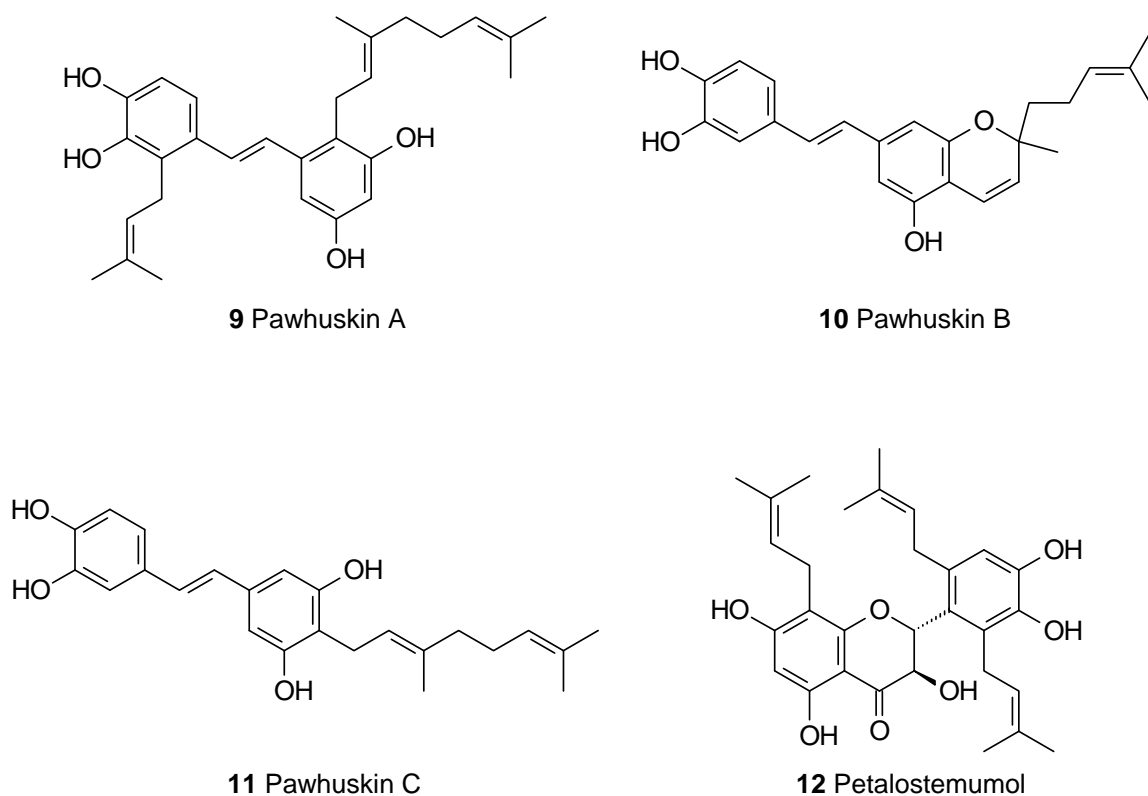


Figure 2. *D. purpurea* isolates: Pawhuskins A–C and Petalostemumol

Traditional opioid receptor modulators have been isolated from the opium poppy plant (*Papaver somniferum*) and all contain the piperidine pharmacophore. These extensively studied analgesics include morphine (**13**), codeine (**14**), and thebaine (**15**, Figure 3).¹⁷ These opium constituents can be used to manage pain by way of opioid receptor activation. Morphine is commonly referred to as the gold standard among analgesics,^{17,18} and is fairly selective ($\delta/\mu = 50$, $\kappa/\mu = 176$) for the μ -receptor ($K_i = 1.8$ nM).¹⁹ Unfortunately, many adverse side-effects, including tolerance, constipation, respiratory depression, nausea, and dependence^{17,20,21} are correlated with analgesics

which include this common piperidine core. As a result, the need for improved and atypical opioid receptor modulators is of great concern in the scientific community. As summarized by T. E. Prisinzano,¹⁷ a medicinal chemist who has studied non-nitrogenous opioid receptor ligands extensively, “identifying new opioid receptor probes (might have) the greatest potential for activity with reduced side-effects.”

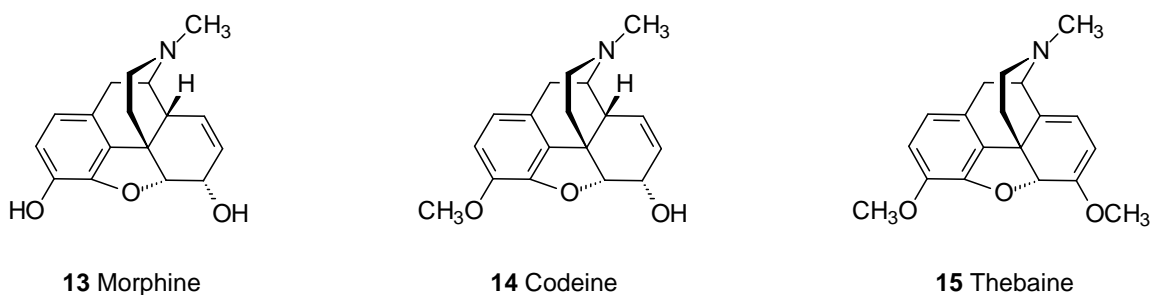


Figure 3. Traditional opioid receptor modulators with a common *N*-methyl-piperidine core

Several opioid receptor modulators not containing a basic nitrogen atom have been isolated from natural sources. The most studied compound is salvinorin A (**16**, Figure 4), a potent hallucinogen isolated from the Mexican sage, *Salvia divinorum*.²² Salvinorin A has been shown to be a κ -opioid (KOP) receptor agonist, and KOP receptor ligands have become of interest with respect to studies of addiction and other disorders.²³ Two total syntheses of salvinorin A have been reported,^{24,25} but modifications of the isolated natural product have driven more extensive structure-activity studies.²⁶⁻³² The non-nitrogenous compound dioflorin (**17**), a prenylated flavonoid, was isolated from the Brazilian vine *Dioclea grandiflora* through activity-guided fractionation³³⁻³⁵ and also was shown to have analgesic activity.³⁶ While more extensive efforts to categorize the

opioid receptor binding of dioflorin have not yet been reported, bioassays with a series of other natural flavonoids including catechin (**18**) and hesperetin (**19**) have been conducted and demonstrate that this scaffold may have considerable potential for development of opioid receptor ligands.³⁷ Other structural subtypes with opioid-binding activity are becoming more common,³⁸⁻⁴⁰ including stilbenoids more reminiscent of the pawhuskins such as resveratrol (**20**)^{41,42} and, more recently, chlorophorin (**21**).⁴³

In terms of its opioid activity, salvinorin A (**16**) has been shown to be a functional agonist.^{17,44} Dioflorin (**17**) and other isolates of *Dioclea* display morphine-like analgesia that is inhibited by naloxone, a nonspecific opioid receptor antagonist, so they are presumably agonists as well.³⁵ While the flavan-3-ol catechin (**18**) had good activity as an antagonist at the KOP receptor ($K_e = 320$ nM), the closely related flavanone hesperetin (**19**) had no activity at the μ , δ , or κ receptors.³⁷ The work of Sobolev and co-workers on peanut phytoalexins such as stilbene **21** determined the selectivity of these compounds against each opioid receptor, but these compounds have not yet been fully characterized using functional assays.^{16,43}

In these studies, we will report the opioid receptor binding affinity and selectivity of pawhuskin A using a functional assay based on [³⁵S]GTP- γ -S binding.¹⁶ We will also report results of structure-activity relationship studies of the new pawhuskin-related analogues constructed in order to elucidate the novel pawhuskin pharmacophore. Both analogue syntheses and interesting chemical findings will be explained in detail. To fully appreciate the significance of these results as they guide further compound design, first it is important to understand more of the biochemical pathways associated with the opioid receptors.

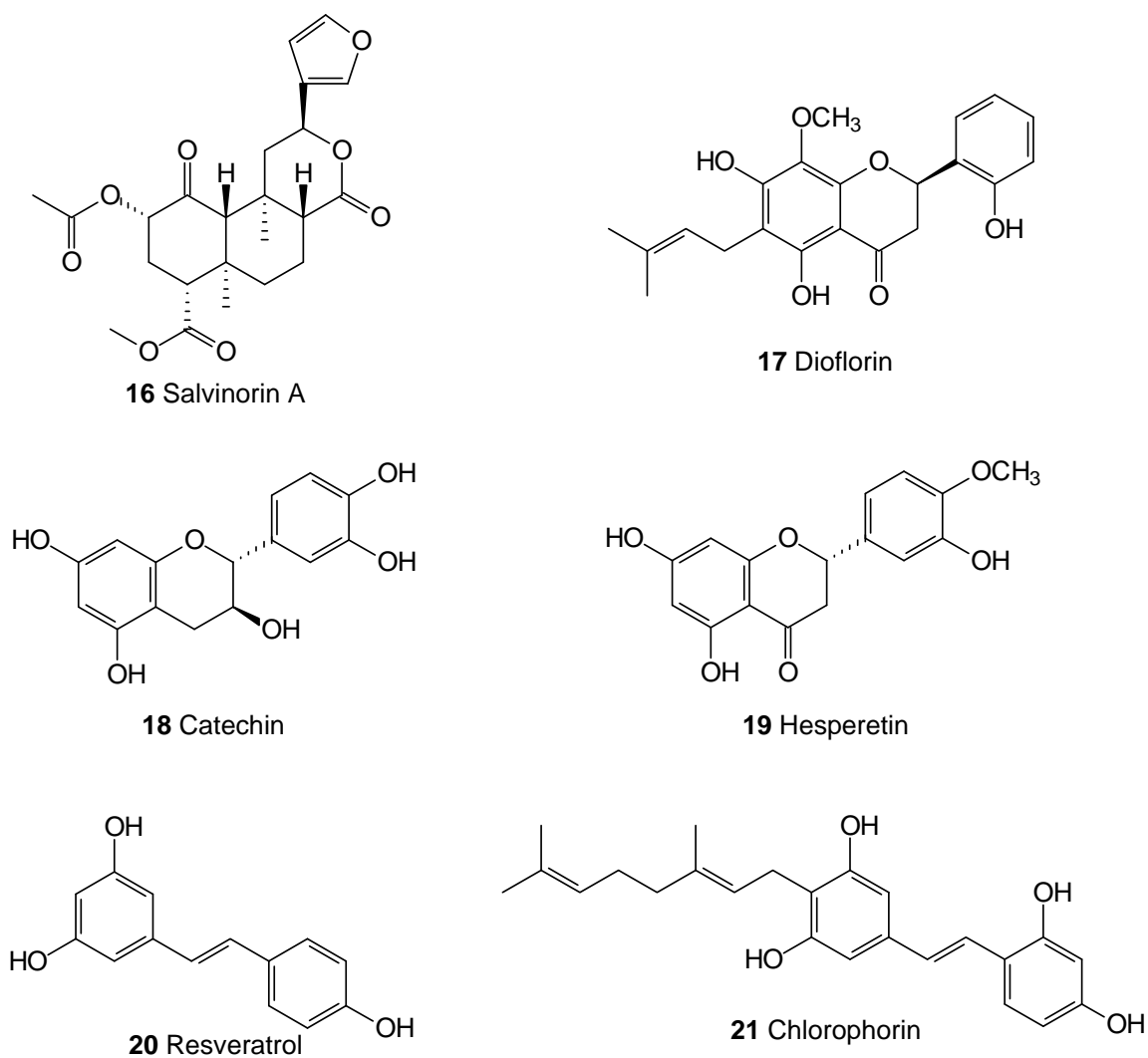


Figure 4. Structures of non-nitrogenous opioid receptor modulators

As previously mentioned, the opioid receptors are members of the G-protein-coupled (GPCRs) class of receptors, and three major subtypes have been characterized including κ , δ , and μ .^{17,21,45} The opioid receptors occur in multiple locations throughout the human body, including the central and peripheral nervous systems, and heart, lungs, and liver, as well as the gastrointestinal tract.⁴⁶ The κ receptors are activated by

endogenous peptides known as dynorphins,⁴⁵ while the μ -opioid (MOP) and δ -opioid (DOP) receptors are activated by endogenous peptides known as endorphins and enkephalins, respectively.^{45,46} Once a ligand activates the GPCRs, there is a conformational change within the receptor.⁴⁷ GTP is then exchanged for GDP on the α subunit of the G protein. This allows dissociation of the $G\alpha$ unit from the $\beta\gamma$ heterodimer. This will lead to extracellular responses, e.g., reduction in the sensation of pain, through inhibition of adenylyl cyclase, K^+ channel activation, and Ca^+ channel inhibition.^{47,48}

The opioid receptors also indirectly regulate the release of the neurotransmitter dopamine. MOP receptor agonists increase the release of dopamine,⁴⁵ this supports early studies showing that μ activation elevates mood.⁴⁹ As mentioned above, there are a number of adverse side-effects associated with μ agonists including tolerance, dependence, and respiratory depression. The MOP antagonists naloxone and naltrexone are used to treat the unwanted side-effects of analgesics.⁵⁰ Dopamine levels also are increased upon DOP activation, and recent studies have shown that δ stimulation may lead to neuroprotection making for a suitable treatment of Parkinson's disease and a potential stroke preventative.⁴⁶ DOP receptor antagonists are useful in many therapeutic settings, including treatment of neurological conditions, drug/alcohol abuse, and gastritis, in addition to cardiovascular and respiratory disorders.⁵¹ KOP receptors agonists decrease the release of dopamine,⁴⁵ confirming that κ activation can result in dysphoria and hallucinogen activity.⁴⁹ Up-regulation of the endogenous κ ligand dynorphin is a natural response to stress, leading to decreased dopamine levels.²⁰ This has led to the investigation of κ antagonism as a mode of treating mood disorders such as anxiety and depression,^{21,52} as well as stress-induced craving of stimulant drugs of abuse.^{21,53}

Because of our well-established history of synthesizing prenylated stilbenes, and the unique biological activity of the pawhuskins, we embarked on a synthetic effort targeted at these compounds. Our efforts to characterize the pawhuskin-opioid receptor

activity began with the synthesis of the schweinfurthin–reminiscent pawhuskin C (**11**). That work, reported in 2005,⁵⁴ employed a convergent, late–stage Horner–Wadsworth–Emmons (HWE) condensation to install the central *trans*–stilbene olefin (Figure 5). The known phosphonate reagent **23** has been utilized in the syntheses of schweinfurthins A–C (**1–3**),^{1,2,7} as well as the synthetic analogue 3–deoxyschweinfurthin B (**22**).⁵⁵

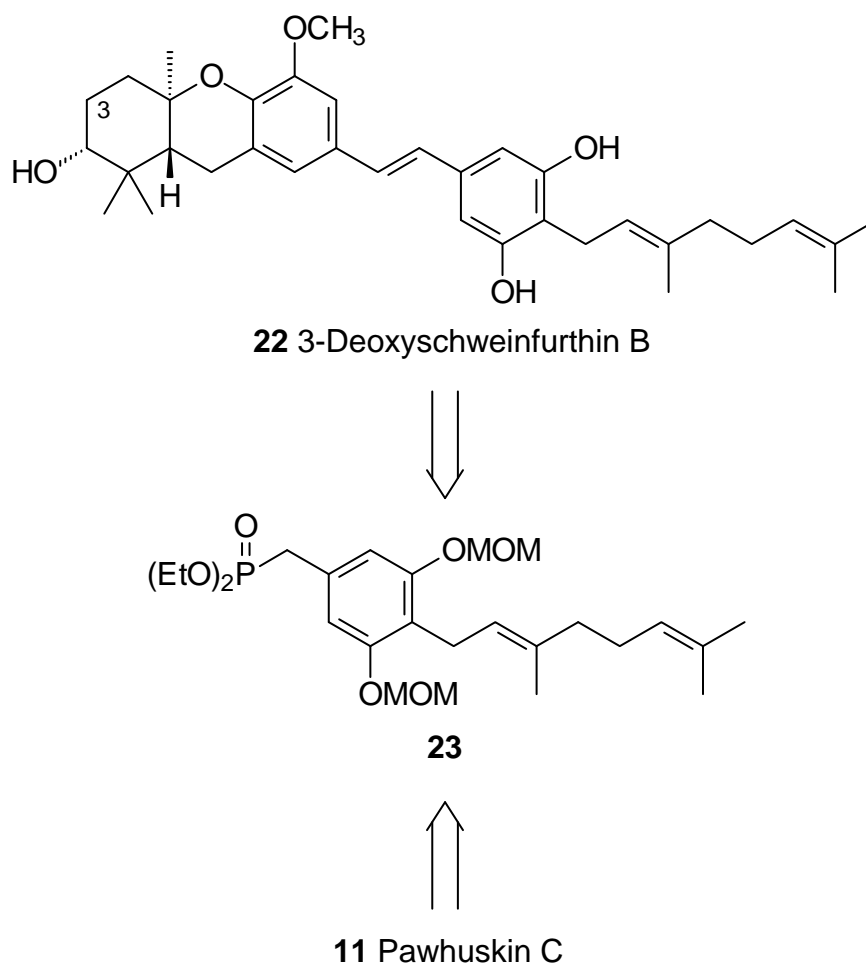


Figure 5. Retrosynthesis of Pawhuskin C showing common phosphonate synthon **23**

The preparation of phosphonate **23** was first reported in 1999.¹ For that synthesis, the commercial ester **24** (Figure 6) was treated with MOMCl in the presence of NaH, and subsequent reduction provided benzyl alcohol **25**. The alcohol was protected by reaction with TBSCl prior to the directed *ortho* metallation, in which the lithium reagent was alkylated with geranyl bromide. The geranylated arene **27** underwent silyl removal with TBAF to afford alcohol **28** (in 5 steps from compound **24**). Reaction of alcohol **28** with methanesulfonyl chloride provided the intermediate mesylate, and then treatment with NaI gave iodide **29**. Phosphonylation through reaction with P(OEt)₃ provided the corresponding phosphonate **23** in quantitative yield. Horner–Wadsworth–Emmons olefination with with respective aldehydes followed by MOM hydrolysis provided targets **1–3**, and **22**.^{1,2,7,55}

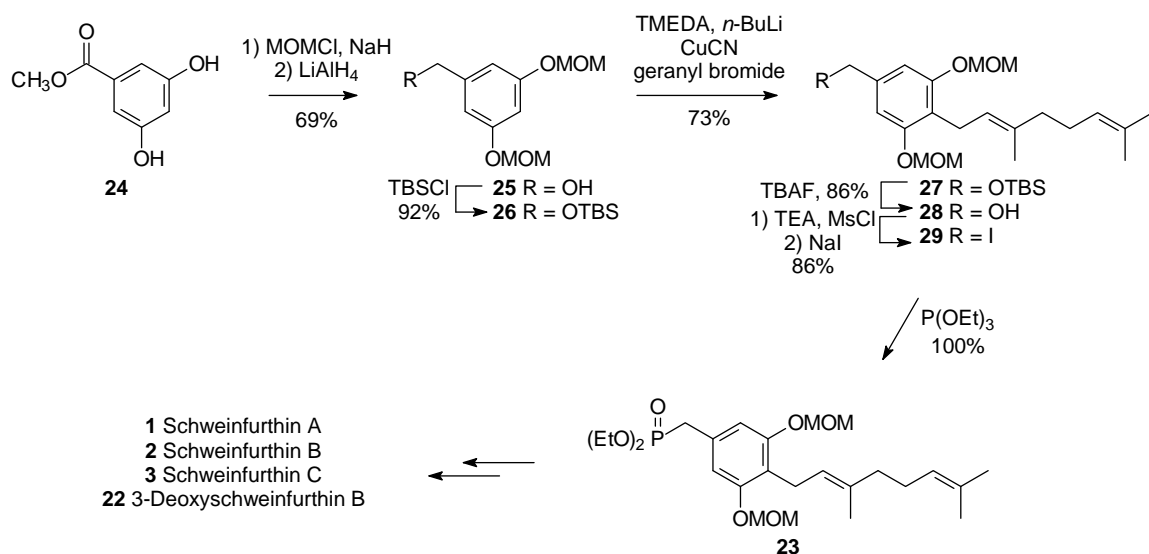


Figure 6. Initial preparation of phosphonate **23**

The synthesis of pawhuskin C would include a more efficient preparation of phosphonate **23** than previously reported during work on the schweinfurthins. The

installation of a protecting group on alcohol **25** prior to the directed *ortho* metallation was abrogated. Alcohol **25** (Figure 7) underwent directed *ortho* metallation upon treatment with excess base, forming the dianion intermediate followed by alkylation to directly provide alcohol **28** in 3 steps from compound **24**. Compound **28** then was advanced to afford the phosphonate **23** as previously described. This variation thereby reduced the overall number of steps in the preparation of phosphonate **23** by two, including the installation and removal of the protecting group.

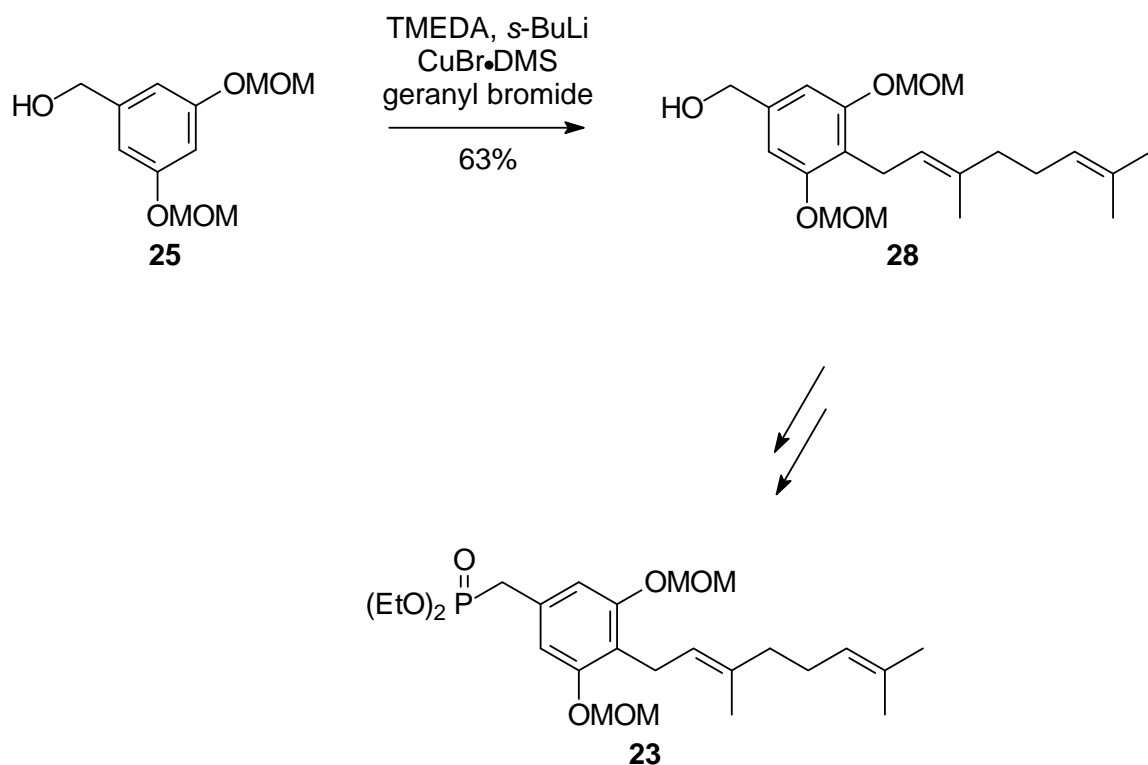


Figure 7. Efficient preparation of phosphonate **23**

The reported synthesis of pawhuskin A (**9**) followed soon after.⁵⁶ This prenylated stilbene was different from the schweinfurthins in the sense that the position of the prenyl and geranyl units would require new routes to the coupling partners. A late-stage HWE condensation of aldehyde **30** (Figure 8) and phosphonate **31** would install the central *trans*-stilbene moiety. This work, reported in 2008,⁵⁶ paved the way for many analogues to come. Synthesis of the natural bioactive pawhuskins provided benchmarks for our study of structure–activity relationships.

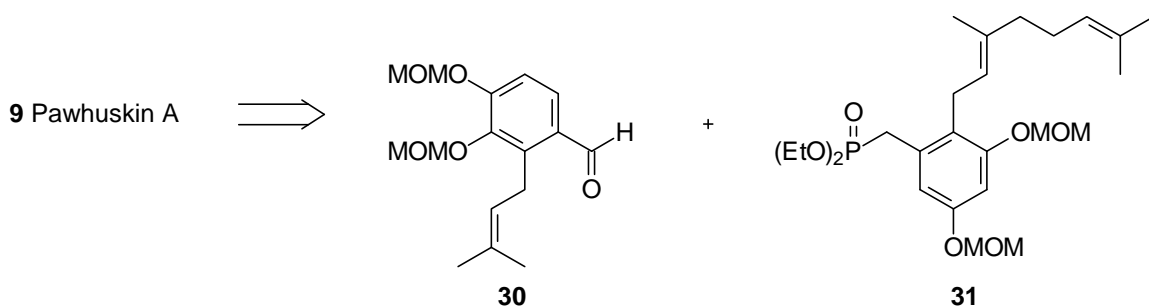


Figure 8. Convergent retrosynthetic analysis of Pawhuskin A

The screening process used by our collaborator Dr. Hernán Navarro, RTI International, is similar to that used by the group that published the isolation and nonselective opioid receptor activity of the pawhuskins.¹² In our study, synthetic pawhuskins A and C were pre-screened for intrinsic and antagonistic activity at a concentration of 10 μ M in the [³⁵S]GTP- γ -S binding assay at the human κ , μ , and δ opioid receptors overexpressed in Chinese hamster ovary cells. Compounds identified as antagonists were characterized for functional antagonism (K_e) and selectivity by measuring the ability of the test compounds to inhibit stimulated [³⁵S]GTP- γ -S binding produced by one of three selective agonists DAMGO (μ), DPDPE (δ), or U69,593 (κ).

Agonist concentration–response curves were determined in the presence or absence of a single concentration of test compound.¹⁶

More recent efforts have focused on the exploration of opioid activity in this family by determination of the selectivity of pawhuskins A and C for human κ (KOP), μ (MOP), and δ (DOP) receptors. Even at 10 μM concentrations, pawhuskin A and pawhuskin C were found to have no intrinsic agonist activity at any of these receptors in the [³⁵S]GTP- γ -S binding assay. However, further testing showed antagonist activity at all three of the opioid receptor subtypes. Pawhuskin A (**9**, Table 1) is modestly selective for the κ receptor, with a K_e of 203 nM ($\delta/\kappa = 14.5$, $\mu/\kappa = 2.9$). Pawhuskin C (**11**) also displayed some antagonist activity at the KOP receptor ($K_e = 25 \mu\text{M}$), but was much less potent and selective ($\delta/\kappa = 1.6$, $\mu/\kappa = 1.4$) than compound **9**.¹⁶ The data from assays of pawhuskin A will be discussed in further detail in Chapter 2.

Compound	apparent affinity of competitive antagonists (K_e) in μM			Selectivity	
	KOP	DOP	MOP	δ/κ	μ/κ
Pawhuskin A	0.2	2.9	0.57	14.5	2.9
Pawhuskin C	25	41	35	1.6	1.4

Table 1. Pawhuskins A and C opioid receptor affinity and selectivity¹⁶

While the natural product salvinorin A (**16**) and many of its analogues are KOP receptor **agonists**, there are only limited examples of non–nitrogenous KOP receptor **antagonists** including some flavanoids.³⁷ Pawhuskin A rivals the potency of the flavonoids, although catechin (**18**) displayed higher selectivity versus the other opioid

receptors ($\mu/\kappa > 31$). However improved KOP receptor selectivity might be uncovered by a synthetic exploration based upon the pawhuskin's stilbene scaffold. Synthetic efforts along these lines are encouraged by the recent interest in KOP receptor antagonists as potential treatments for stimulant abuse. Such agents might be of particular value as potential preventatives for relapse. While there has been some interest in using KOP agonists for treatment of substance abuse, compounds such as salvinorin A have been accompanied by serious side-effects including potent hallucinogen activity.

There is a significant relationship between relapse to stimulant abuse and stress.⁵⁷ Indeed encounters with stressors, and even images that induce stress, have been shown to induce craving in stimulant abusers.^{58,59} The potent KOP receptor antagonist JD1c⁶⁰ has been shown to block stress induced cocaine seeking behavior and also has demonstrated antidepressant-like activity.⁶¹ This result was confirmed and expanded to show that pretreatment with the κ -opioid antagonist arodyn prevented stress-related induction of cocaine-conditioned place preference in rats,⁶² which further heightens interest in κ -selective antagonists such as pawhuskin A.

In conclusion, the pawhuskin scaffold resembles that of the anti-cancer schweinfurthins. The opioid receptor activity of the pawhuskins is surprising given the absence of a piperidine core. Studies to elucidate more detail on the novel pawhuskin pharmacophore began with the synthesis of pawhuskins A and C. In the next several chapters, the synthesis of sixteen pawhuskin analogues will be described. Unique synthetic findings will be explained in detail. In total, twenty compounds will be assayed for pawhuskin-like activity at the opioid receptors in the same manner as described above. This will allow several conclusions to be drawn, including at least some of the necessary feature(s) for pawhuskin-opioid receptor activity and how the affinity and selectivity for certain receptors has been increased. In addition, approaches toward replacement of the central *trans*-stilbene olefin with a new core linkage that may be more biologically attractive will be described.

CHAPTER 2
STRUCTURAL ANALOGUES OF PAWHUSKIN A: PROBING THE
IMPORTANCE OF A-RING SUBSTITUENTS

As part of an ongoing interest in natural prenylated stilbenes with biological activity,^{2,10} we have undertaken studies to elucidate the character and receptor subtype selectivity of opioid modulation by pawhuskins. As previously described, this effort already has led to the synthesis of both pawhuskins A (**9**)⁵⁶ and C (**11**).⁵⁴ Pawhuskin A demonstrated antagonist activity at the κ , δ , and μ receptors, with $K_e = 0.20, 2.9,$ and $0.57 \mu\text{M}$, respectively, and thus some κ -selectivity ($\delta/\kappa = 14.5, \mu/\kappa = 2.9$).¹⁶ Assays with κ -selective agonist, U69,593, are displayed in Figure 9 in which log concentration of agonist was plotted against the percent basal binding. The addition of various concentrations of pawhuskin A caused a rightward shift in the agonist concentration response curve, and its antagonism was surmountable, suggesting a competitive mode of antagonism.^{16,63} The agonist alone displayed an EC_{50} of 192 nM. In the presence of pawhuskin A (1 μM concentration), the EC_{50} was increased to 1140 nM.

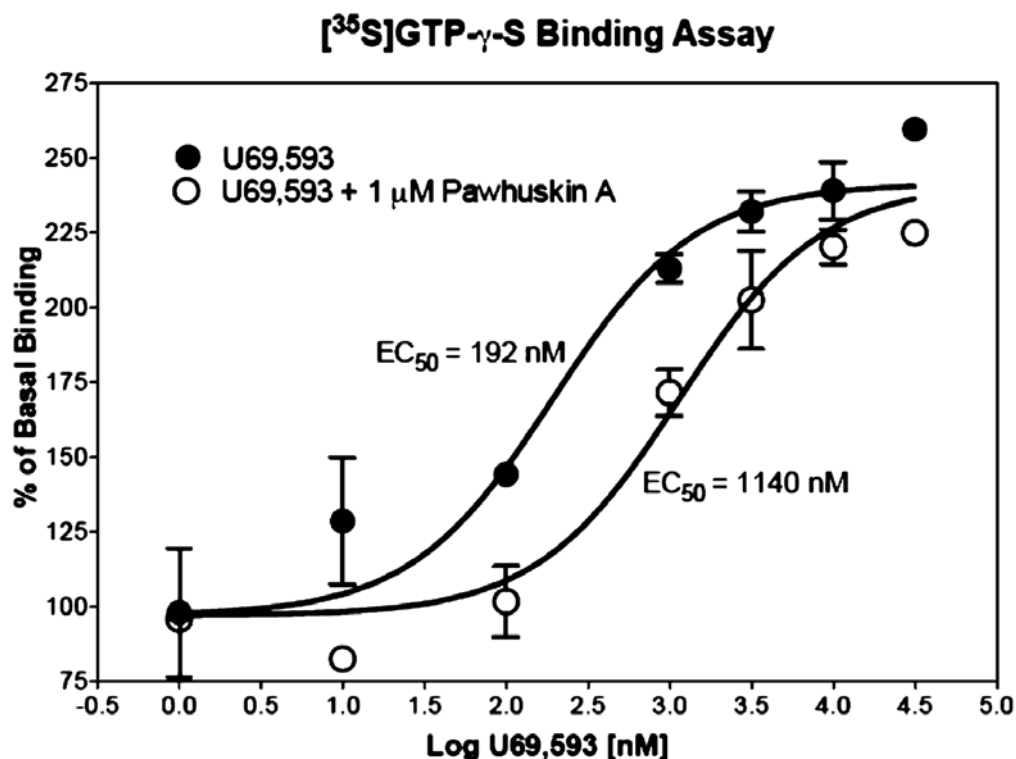


Figure 9. Representative graph of the antagonist activity of pawhuskin A in the KOP receptor affinity assay. Each data point represents the mean and SEM of duplicate samples.¹⁶

Our approach to exploration of the structure–activity relationships of pawhuskin A analogues took advantage of a core strategy that we have used in the synthesis of other natural stilbenes (Figure 10).^{5,6,64} A disconnection of the central olefinic moiety (**32**) through a Horner–Wadsworth–Emmons (HWE) transform allows choice of phosphonate coupling partners such as **33** and aldehydes such as **34**, although the reversed pairing also is viable.^{8,65} This permits maximum convergence and also provides for divergence through condensations of one aldehyde with several phosphonates or one phosphonate with several aldehydes.⁶⁶ To begin exploration of the pharmacophore of pawhuskin A, as

well as essential binding motifs for κ -selective antagonist activity, we undertook syntheses aimed at preparation of a small set of analogues through this strategy.

Phenolic H-bonding is important to the KOP receptor selectivity of the antagonist JD_Tic and other members of the phenylpiperidine class of opioid receptor modulators.⁶⁷ Furthermore, as in past studies of salvinorin A (**16**),¹⁷ the absence of a readily ionizable group that would form salt bridges with an opioid receptor suggested that attention should be directed at the H-bonding groups of pawhuskin A. Thus, we chose to prepare a number of methylated analogues to assess the importance of H-bond donation from the various hydroxy groups without a significant change in electron donation.¹⁶ In addition, the effect on opioid receptor activity of the presence and position of the C-5 prenyl group within the A-ring now was of interest.

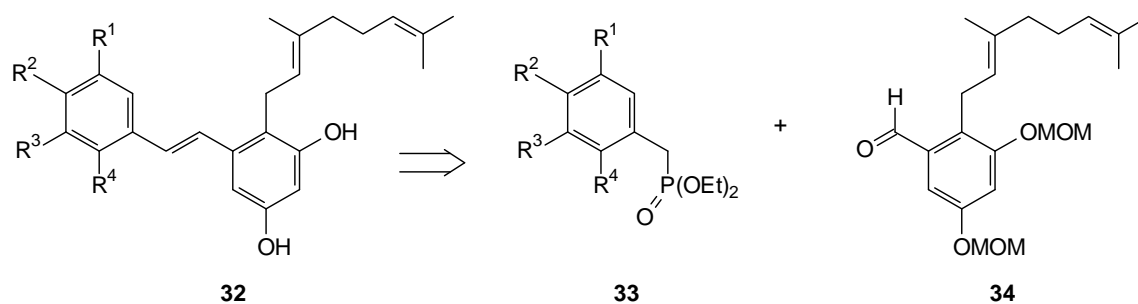


Figure 10. Retrosynthesis of analogues **46**, **54**, **56**, **58**, and **64**

Synthesis of the first B-ring aldehyde **34** (Figure 11) began with commercial methyl 3,5-dihydroxybenzoate (**35**). Conversion of ester **35** to the known compound 3,5-bis(methoxymethoxy)benzyl alcohol (**36**)⁵⁴ was done by a two-step process including MOM protection and reduction.⁵⁶ Treatment of alcohol **36** with NBS allowed formation of the intermediate aryl bromide, and in the presence of DHP and PPTS, the

acetal **37** was formed in quantitative yield. The lithiated arene was formed by reaction with *n*-BuLi, and subsequent treatment with geranyl bromide resulted in formation of compound **38**. The THP acetal was selectively hydrolyzed without substantial loss of the MOM groups by treatment with TsOH in methanol to afford the benzylic alcohol **39**. Oxidation to the corresponding aldehyde **34** then was achieved by treatment of the benzylic alcohol **39** with MnO₂.¹⁶

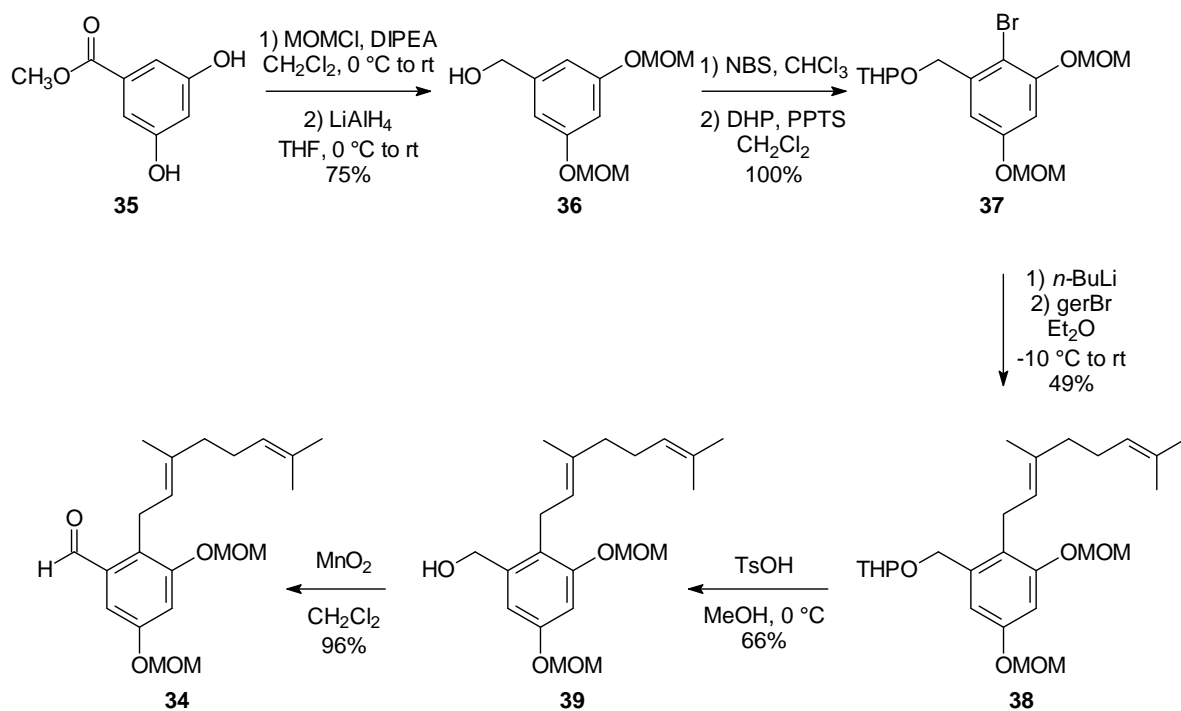


Figure 11. Synthesis of aldehyde **34**

The complementary phosphonate reagent **44** (Figure 12) was assembled in order to evaluate the significance of H-bond donation from the *meta* position within the A-ring of pawhuskin A. Commercial isovanillin (**40**) was allowed to react with 2-methyl-3-

butyn-2-ol to afford the ether **41** in moderate yield. Partial reduction of the acetylene was achieved in the presence of H₂ and Lindlar's catalyst. Subsequent exposure of the allyl ether to reflux in toluene allowed a [3,3]-sigmatropic rearrangement to provide the corresponding prenylated arene **42**. MOM protection gave the known intermediate aldehyde,⁶⁸ and NaBH₄ reduction of the carbonyl group in methanol gave benzyl alcohol **43** in high yield.¹⁶ Treatment of this alcohol with methansulfonyl chloride and then LiBr made available the intermediate bromide. Standard work-up followed by treatment with P(OEt)₃ at 90 °C provided the desired phosphonate **44**.¹⁶

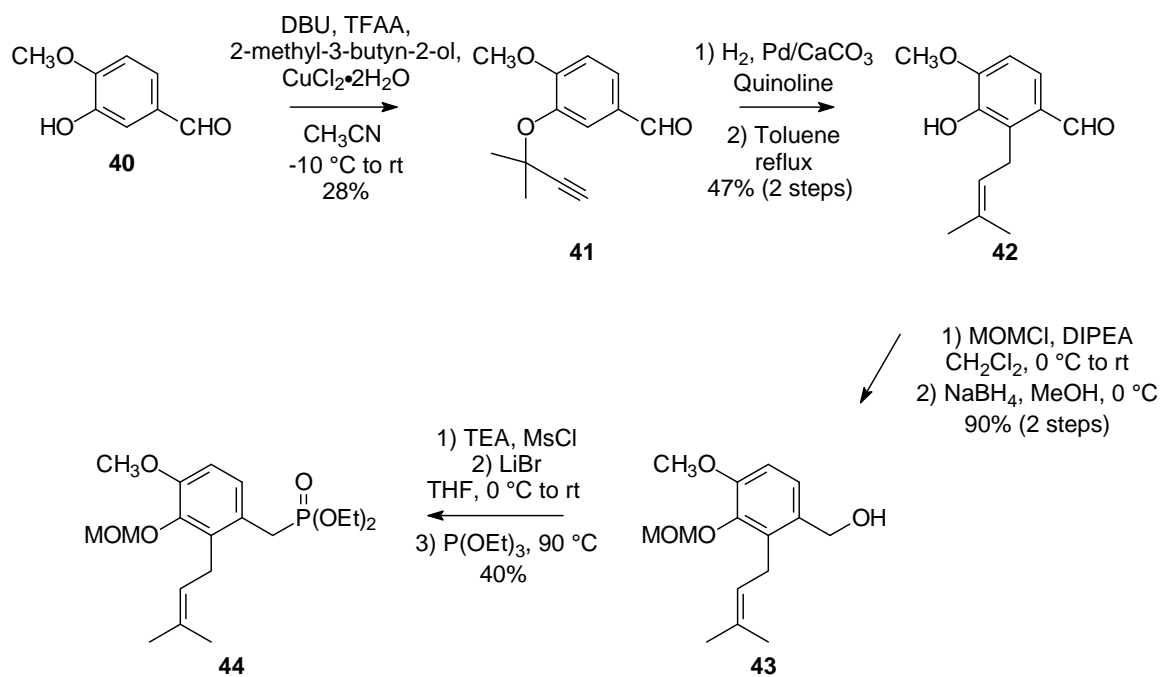


Figure 12. Preparation of phosphonate **44**

Next, an analogue interrogating the importance of the A-ring *para* H-bond donation site was assembled. Compound **45**, the immediate precursor to target **46**

(Figure 13), was formed from a Horner–Wadsworth–Emmons condensation of phosphonate **44** with aldehyde **34** in the presence of KHMDS. Hydrolysis of the MOM protecting groups was carried out under acidic conditions to make available stilbene **46**,¹⁶ an analogue of pawhuskin A featuring a specifically blocked H–bond donation site at the *para* position of the A–ring.

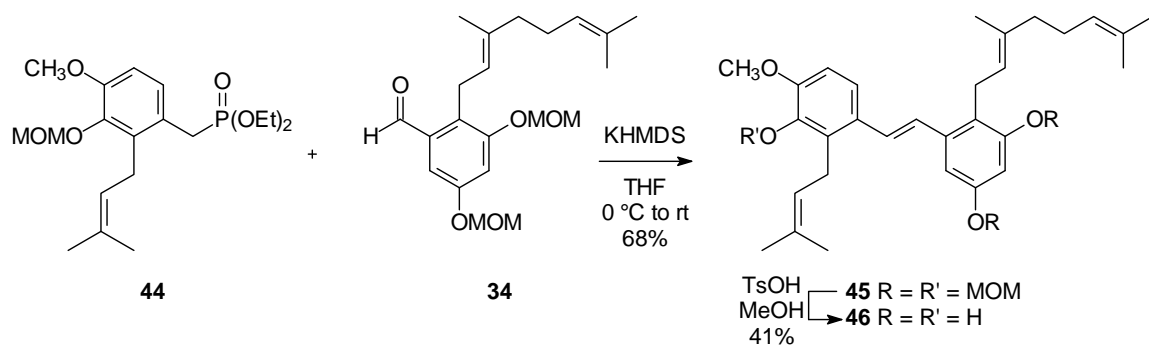


Figure 13. Condensation and hydrolysis to provide compound **46**

A small set of analogues containing the natural B–ring of pawhuskin A was the initial goal. In order to test whether the analogues displayed pawhuskin A–like activity, once the compounds were in hand they were initially screened for intrinsic and antagonistic activity at 10 μM in the [³⁵S]GTP– γ -S binding assay in Chinese hamster ovary cells. The ability of the test compounds to inhibit binding between the opioid receptor and the selective antagonist was measured and characterized by functional antagonism (K_e). Agonist concentration–response curves were determined in the presence or absence of the test compounds.¹⁶

The removal of the *para* H–bond donation site from pawhuskin A, as shown in compound **46**, completely eliminated the competitive antagonism at the KOP, DOP, and MOP receptors (Table 2) up to the highest concentration tested. In fact, weak negative allosteric modulation at the KOP and MOP receptors was observed with this analogue. Therefore, this particular H–bond donation site appears to be critical for affinity with the opioid receptors.

Compound	apparent affinity of competitive antagonists (K_e) in μM			IC_{50} of negative allosteric modulators in μM	
	KOP	DOP	MOP	KOP	MOP
Pawhuskin A	0.2	2.9	0.57	NA	NA
46	>10	>10	>10	0.46	>10

Table 2. The opioid receptor affinity of analogue **46**

The implication of removing the A–ring prenyl group from pawhuskin A was assessed through the preparation of simplified phosphonate **48**. Through parallel reactions, the HWE reagents **50** and **52** also were made. Preparation of these fairly simple phosphonates (Figure 14) began with the known 3,4–bis(methoxymethoxy)benzyl alcohol (**47**),⁵⁶ 4–(methoxymethoxy)benzyl alcohol (**49**),⁶⁹ and 3–(methoxymethoxy)benzyl alcohol (**51**).⁷⁰ In each case, the alcohol was treated with methanesulfonyl chloride to give an intermediate mesylate. Treatment of each mesylate with LiBr afforded the corresponding bromide, and standard Arbuzov reactions with triethyl phosphite provided the three benzyl phosphonates **48**,⁷¹ **50**, and **52**. The latter

was completed in significantly higher yield than the others, perhaps because it was done at a time when there was more extensive experience with this particular reaction.

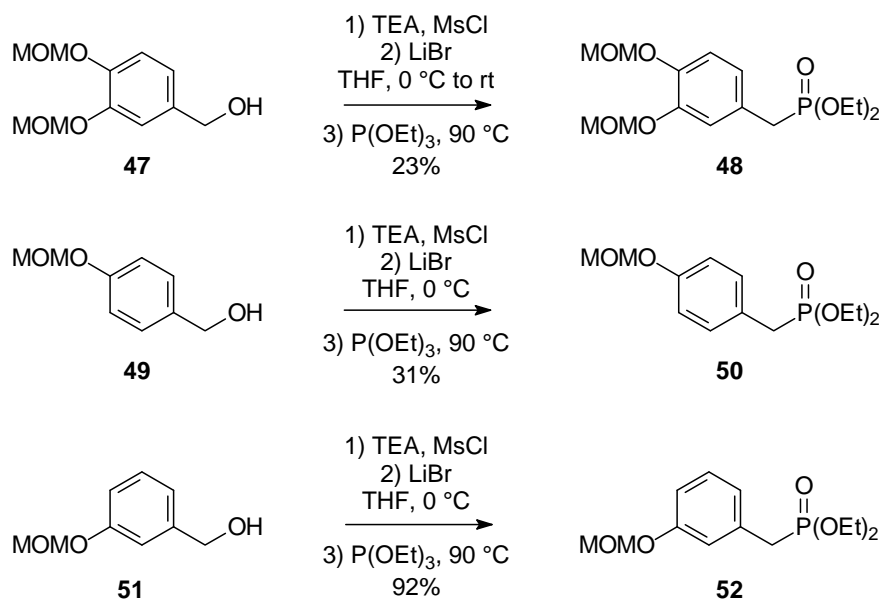


Figure 14. Preparation of phosphonates **48**, **50**, and **52**

The significance of the steric presence of the C-5 prenyl group within the A-ring was examined through preparation of analogues **54**,¹⁶ **56**, and **58**. This set of stilbenes was constructed by separate condensations of aldehyde **34** with phosphonates **48**, **50**, and **52** (Figure 15), which generally proceeded in attractive yields. Subsequent hydrolysis of the protecting groups in the resulting stilbenes allowed formation of analogues **54**, **56**, and **58**. This set of compounds features formal removal of the A-ring prenyl group, as well as complete deletion of a *meta* or *para* H-bond donation and accepting site.

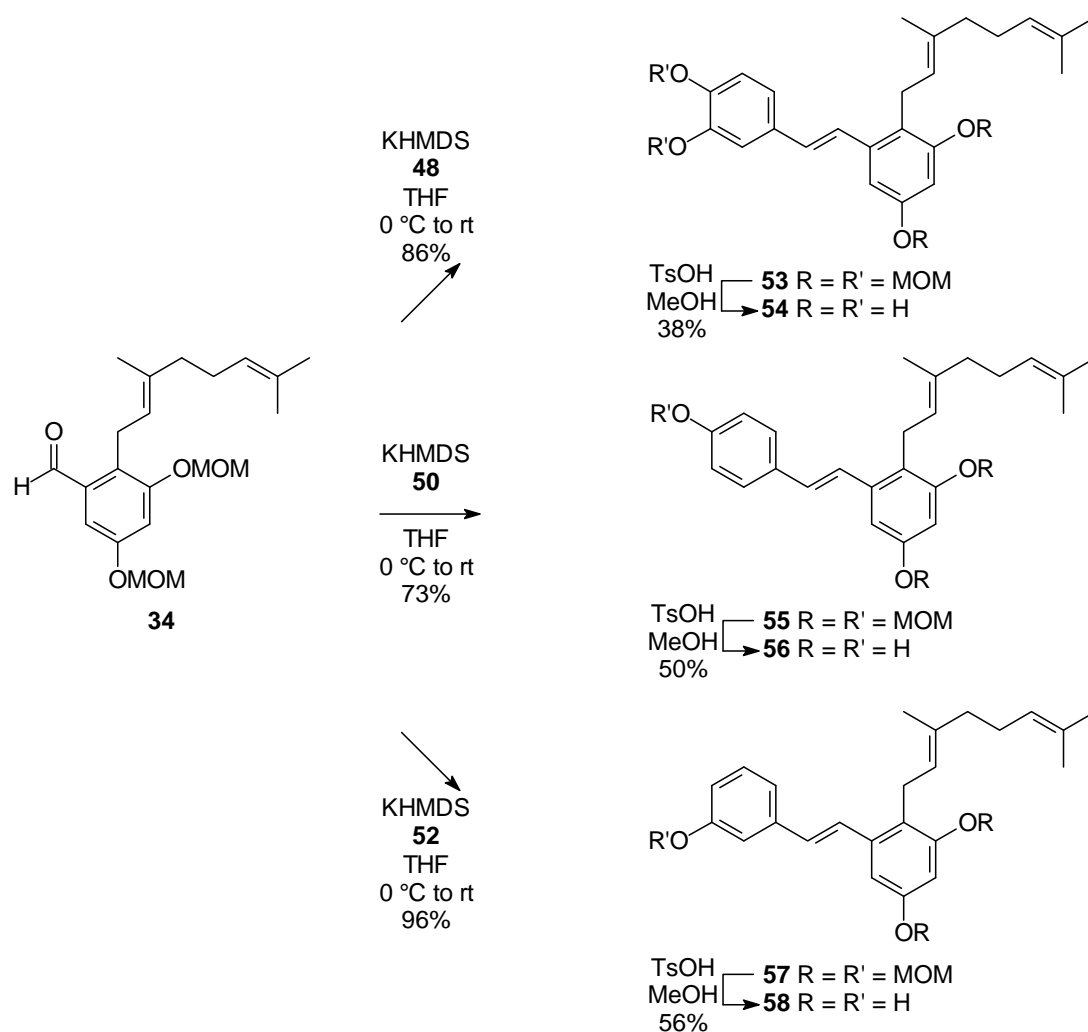


Figure 15. Condensations and hydrolyses to provide analogues **54**, **56**, and **58**

The apparent affinity of analogues **54**,¹⁶ **56**, and **58** is displayed in Table 3. Removal of the A-ring prenyl group diminished competitive antagonism at the opioid receptors, regardless of the presence of the *para* and/or *meta* H-bond donation and/or

accepting site(s). From this study, it is now clear that the presence of this C–5 alkyl group is important to analogue–receptor binding.

Compound	apparent affinity of competitive antagonists (K_e) in μM			IC_{50} of negative allosteric modulators in μM	
	KOP	DOP	MOP	KOP	MOP
Pawhuskin A	0.2	2.9	0.57	NA	NA
54	>10	>10	>10	>10	>10
56	>3	>10	>3	NA	NA
58	>10	>10	>10	>10	>10

Table 3. The opioid receptor affinity of analogues **54**,¹⁶ **56**, and **58**

The consequence of relocating the prenyl group within the A–ring was assessed through the preparation of the more functionalized phosphonate **62** (Figure 16). This reagent was prepared from the known alcohol 3,4–bis(methoxymethoxy)benzyl alcohol **47**, which in turn is available in just two steps from commercial 3,4–dihydroxybenzaldehyde (**59**).⁵⁶ The prenylated arene **61** was delivered upon use of a directed *ortho* metallation/transmetallation/alkylation protocol.⁵⁶ The regiochemistry was established by ¹H NMR: the doublets within the aromatic region had a coupling constant (J) of approximately 2 Hz indicating *meta*–coupled aromatic hydrogens.

The alcohol **61** was subsequently treated with methanesulfonyl chloride, then LiBr to provide the intermediate mesylate and bromide, respectively. Finally, treatment with triethylphosphite at an elevated temperature resulted in formation of benzyl phosphonate **62**.¹⁶

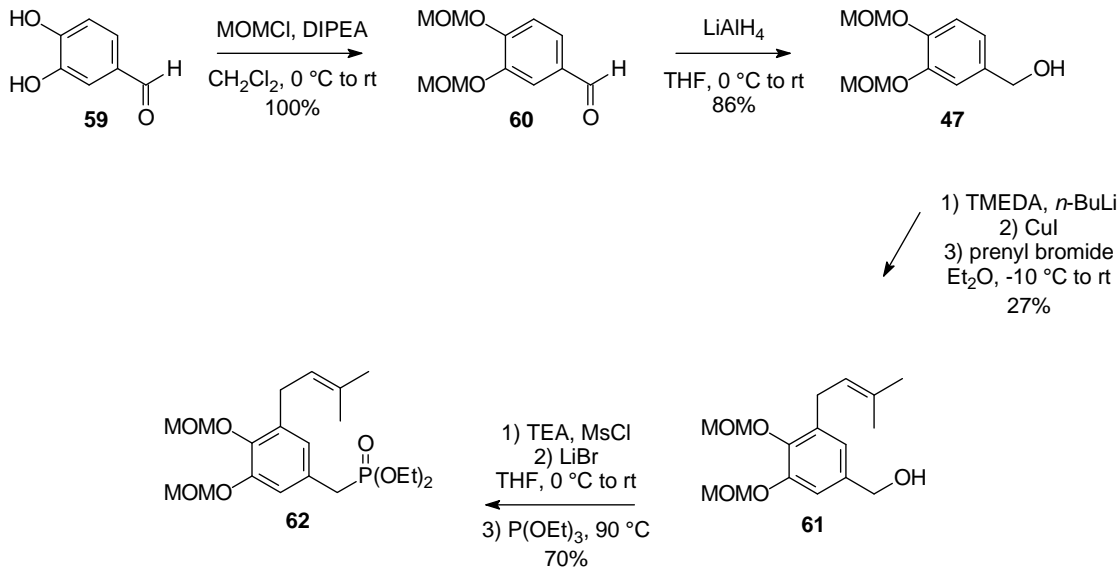


Figure 16. Formation of phosphonate **62**

Not only the presence, but also the position of the C-5 prenyl substituent within the A-ring was analyzed. Analogue **64** (Figure 17) features a *meta* A-ring alkyl group (relative to the central stilbene) which is isomeric in comparison to pawhuskin A which bears an *ortho* prenyl group. To access this analogue, an HWE condensation of phosphonate **62** with aldehyde **34** in the presence of KHMDS was conducted, and the reaction resulted in formation of stilbene **63**. Acid hydrolysis of the MOM protecting groups provided the A-ring analogue **64**, which is regioisomeric to pawhuskin A.

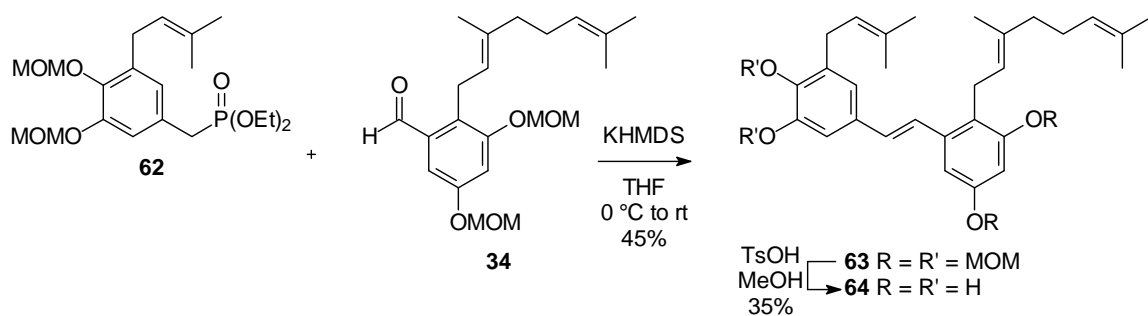


Figure 17. Condensation and hydrolysis to provide compound **64**

Competitive antagonism at the opioid receptors diminished in the reorganized prenyl analogue **64** (Table 4), even though the B–ring substructure of pawhuskin A is completely intact. However, it is important to note that compound **64** displayed 35%, 54%, and 16% agonist activity at 10 μM at the KOP, DOP, MOP receptors, respectively, compared to control E_{max} . These data will be revisited in Chapter 3, as a comparison standard for analogues made up of this A–ring, but with variations within the B–ring of the natural product pawhuskin A. The position of the A–ring C–5 substituent group will prove to be a significant factor in receptor selectivity.

Compound	apparent affinity of competitive antagonists (K_e) in μM			IC_{50} of negative allosteric modulators in μM	
	KOP	DOP	MOP	KOP	MOP
Pawhuskin A	0.2	2.9	0.57	NA	NA
64	>10	>10	>10	NA	NA

Table 4. The opioid receptor affinity of analogue **64**

In conclusion, a number of structural analogues of pawhuskin A featuring only A-ring variations were prepared. The methyl ether **46** tested the importance of the hydroxyl group *para* to the stilbene linkage and its relationship to pawhuskin-receptor affinity. Compounds **54**, **56**, and **58** confirmed the importance of the presence of the C-5 substituent group. At this point, the significance of the position of the prenyl functionality was not yet completely clear. This concept, and test compound **64**, will be revisited in Chapter 3, along with the preparation and opioid receptor analysis of several new compounds with further variations on the pawhuskin scaffold.

CHAPTER 3

STRUCTURAL ANALOGUES OF PAWHUSKIN A: PROBING THE IMPORTANCE OF B-RING SUBSTITUENTS

As described in the previous chapters, a small set of pawhuskin A analogues has been prepared to assess the importance of A-ring H-bond donation to receptor binding. Bioassays on these compounds demonstrated that the hydroxyl group *para* to the stilbene linkage was critical for ligand-receptor binding because mono methylation of this hydroxyl group diminished competitive antagonism at all of the opioid receptors. In addition, it was found that the A-ring prenyl group was an important factor for binding. Analogues featuring a left-half lacking the prenyl group or the *para* H-bond donation site displayed weak affinity for all opioid receptor subtypes. This chapter will detail analogues with A-ring features parallel to those discussed in Chapter 2, but with variations in the B-ring which would entail blocked sites of H-bond donation. Such compounds would be based upon the representative stilbene **65** which could be seen arising from phosphonate **33** and aldehyde **66** through a Horner-Wadsworth-Emmons condensation reaction as shown in Figure 18. We prepared a number of analogues to assess the significance of the H-bond donation/accepting sites and steric properties within the B-ring. As a result of this study, a crucial finding emerged regarding the significance of the position of the prenyl group within the pawhuskin A-ring and implications on opioid receptor selectivity.

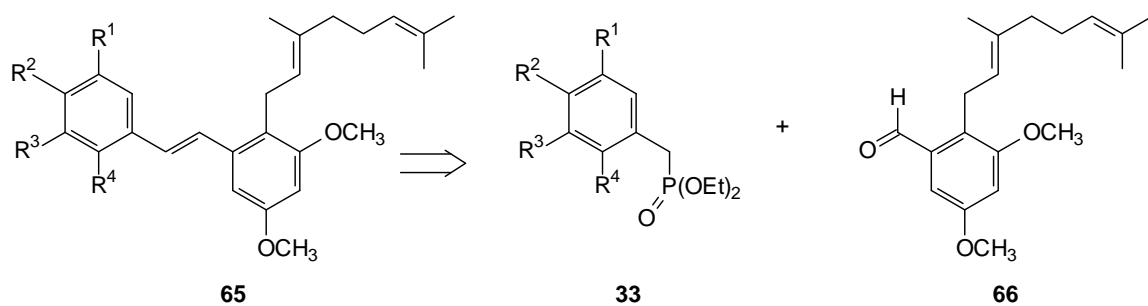


Figure 18. Retrosynthesis of analogues **79**, **81**, **83**, **85**, **86**, **88**, **90**, and **91**

Synthesis of the aldehyde **66** (Figure 19) began with commercial methyl 3,5-dihydroxybenzoate **35**. Compound **35** was methylated and then reduced to afford alcohol **67**. Conversion of this benzyl alcohol to the known aryl bromide **68** was achieved in high yield upon treatment with NBS.⁷² Protection of the alcohol as the THP acetal and a metallation/transmetallation/alkylation sequence provided geranylated arene **70** in modest yield.^{16,73} Hydrolysis of the THP acetal under acidic conditions allowed formation of benzyl alcohol **71**, and subsequent oxidation provided the corresponding aldehyde coupling partner (**66**).¹⁶ Preparation of this aldehyde required a sequence of 5 steps from commercial starting material **67**, but proceeded in 11% overall yield.

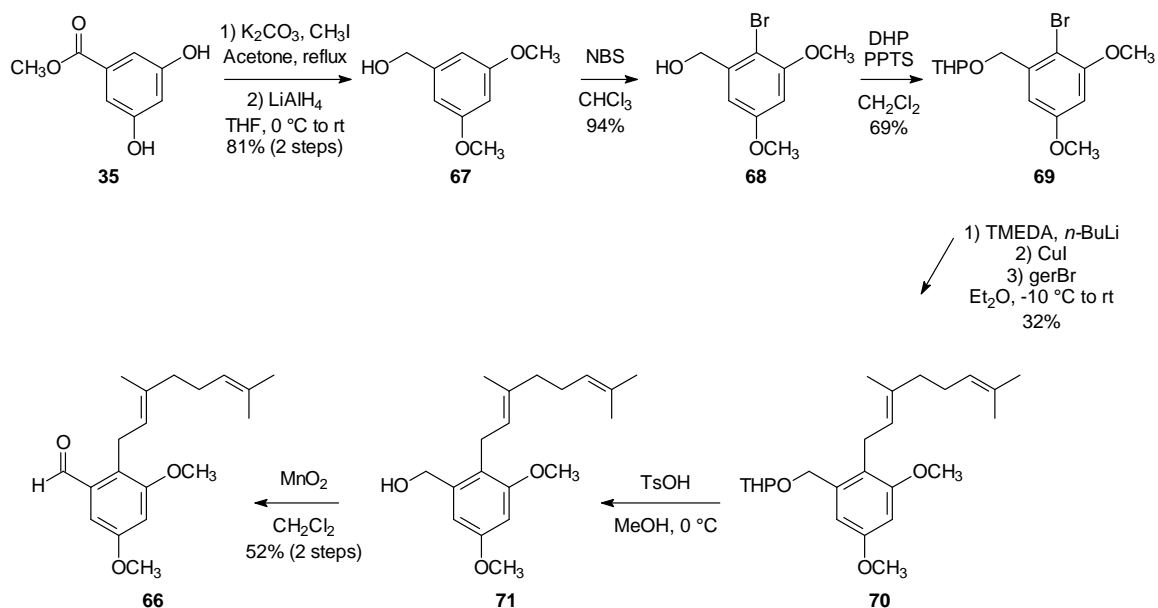


Figure 19. Synthesis of aldehyde **66**

To prepare the complementary phosphonate **73** (Figure 20) a two-step sequence from the known phosphonate **44** was required.¹⁶ The synthesis of compound **44** was discussed in Chapter 2. To begin the preparation of compound **73**, hydrolysis of the MOM protecting group in **44** gave phenol **72**. Standard reaction with iodomethane and base afforded the dimethylated phosphonate **73**.¹⁶

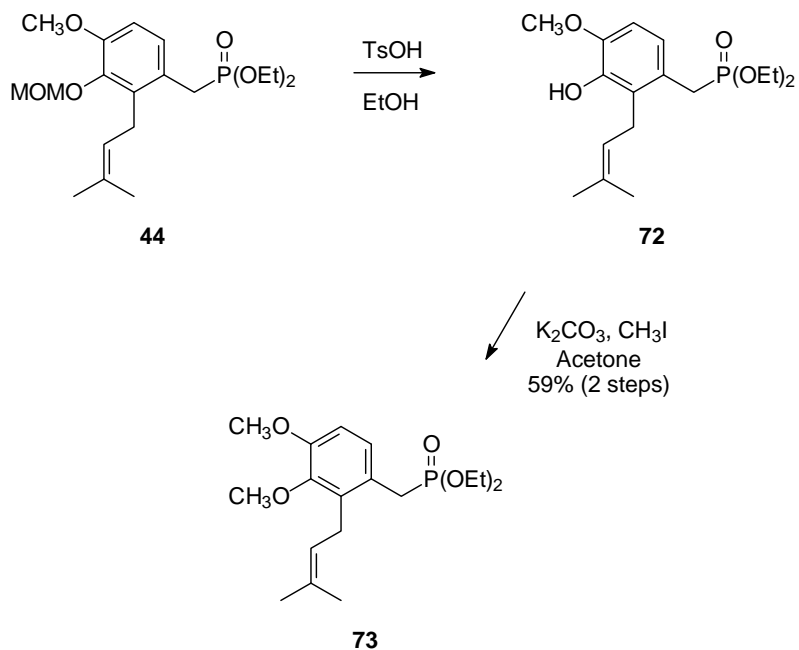


Figure 20. Preparation of phosphonate **73**

Preparation of the pawhuskin A left-half phosphonate **75** began with commercial 3,4-dihydroxybenzaldehyde (**59**, Figure 21). The known alcohol **47**⁷⁴ was readily formed via MOM protection of aldehyde **59** followed by reduction. As previously published, the prenylated arene **74** was made available by directed *ortho* metallation;⁵⁶ this particular reaction will be discussed in more detail in Chapter 5. Conversion of alcohol **74** to the phosphonate **75** was accomplished through the intermediate mesylate and bromide.

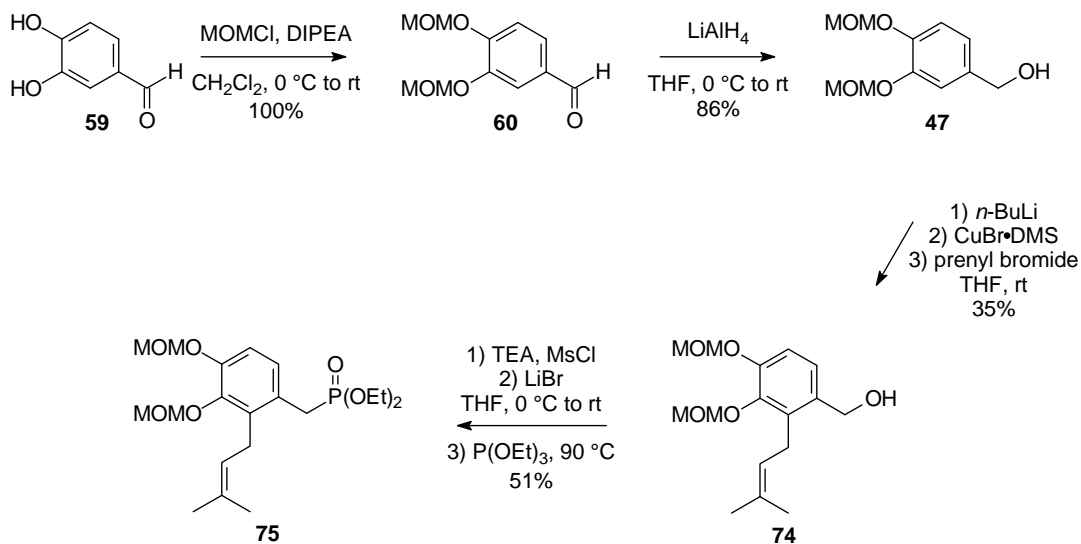


Figure 21. Formation of phosphonate **75**

Preparation of stilbene **64** from phosphonate **62** and aldehyde **34** was discussed in Chapter 2 (Figure 22). This compound features a relocated prenyl group within the A-ring. Likewise, Kevyn D. Gardner has prepared the related compound **77** from phosphonate **62** through an HWE condensation with the aldehyde she prepared, compound **76**. Compound **77** highlights the same relocated prenyl group, in addition to blocked H-bond donation within the B-ring, and a tolyl group as a prenyl group mimic. The tolyl group is shorter than the natural C-10 length, but has more π character. These compounds and their respective opioid receptor data will be revisited with analysis later in this chapter.

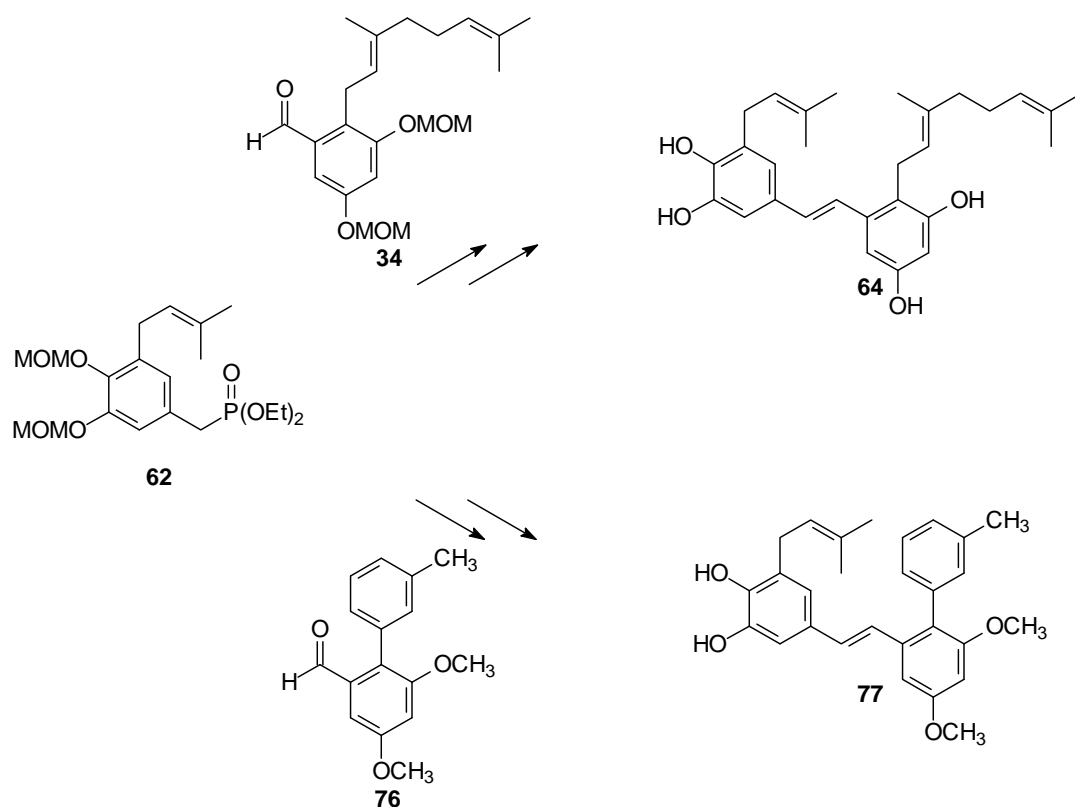


Figure 22. Pawhuskin analogues **64** and **77**

A small set of analogues derived from the aldehyde **66** was assembled, highlighting blocked B-ring H-bond donation sites. First, a compound featuring the 3,4,5-substitution pattern within the A-ring was targeted. In the presence of KHMDS, condensation of phosphonate **62** with aldehyde **66** resulted in formation of stilbene **78** (Figure 23). Both MOM protecting groups were then hydrolyzed under standard acidic conditions to provide the desired analogue **79**.¹⁶

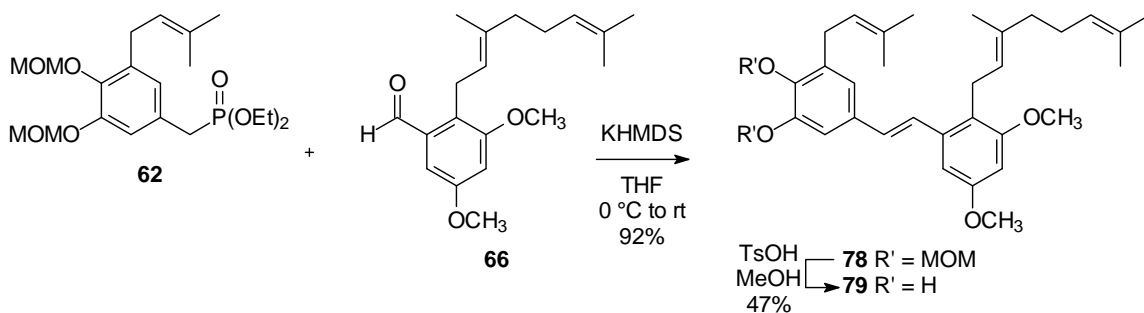


Figure 23. Condensation and hydrolysis to provide analogue **79**

Test compound **64** highlighted a 3,4,5-substituted A-ring, and assays revealed that affinity for all of the opioid receptors was lost (Table 5). Transposition of the A-ring prenyl group in the presence of blocked B-ring H-bond donation sites, as shown in compound **79** (Table 5), shows that these changes reestablished affinity for the KOP receptor ($K_e = 150$ nM). Affinity for the κ receptor increased by a factor >67 , in comparison to compound **64**, with no detectable gain in affinity for the δ or μ receptors. In fact, analogue **79** showed better binding affinity to the κ receptor than pawhuskin A itself, and also demonstrated dramatically improved selectivity (δ/κ at least 4-fold larger and μ/κ at least 20-fold larger for compound **79** than for pawhuskin A). Indeed we could not find antagonist activity at the μ or δ receptors for compound **79** up to the highest concentrations typically tested (10 μ M). This compound demonstrates that methylation of the malonate-derived hydroxyl groups on the pawhuskin A scaffold does not abrogate the KOP receptor antagonist activity on this stilbene structure.¹⁶ With respect to compound **79**, replacement of the geranyl substituent in the B-ring with an aryl group as shown in target compound **77**, completely sacrifices activity at the opioid receptors. Based on these data, the nature of the B-ring substituent appears to be an important factor in opioid receptor binding.

Compound	apparent affinity of competitive antagonists (K_e) in μM			Selectivity	
	KOP	DOP	MOP	δ/κ	μ/κ
Pawhuskin A	0.2	2.9	0.57	14.5	2.9
64	>10	>10	>10	-	-
79	0.15	>10	>10	>67	>67
77	>10	>10	>10	-	-

Table 5. The opioid receptor affinity and selectivity of analogues **64**, **79**,¹⁶ and **77**

In order to test the hypothesis that the alkyl substituent in the A-ring is integral for opioid receptor affinity, aldehyde **66** was condensed with the simplified phosphonates **48**, **50**, and **52** in the presence of base (Figure 24). In earlier HWE condensations, such as the reaction between compounds **66** and **48** to form stilbene **80**, the base NaH was used as a dispersion in mineral oil. Due to the inherent hydrophobic character of this family of compounds, this formulation made it more difficult to isolate the stilbene product from unwanted mineral oil and at times there were significant impurities in the ¹H NMR spectrum of the stilbene products. This separation was problematic even when the mixture of base and mineral oil was washed repeatedly with hexanes prior to the reaction. The alternate base KHMDS was selected shortly after preparation of the initial targets and used as a commercial solution in THF or toluene. With this base, the HWE condensations of aldehyde **66** and phosphonates **50** and **52** proceeded smoothly, and provided stilbenes **82** and **84** in satisfactory yield. Following acidic hydrolysis of the MOM protecting groups, the desired target compounds **81**,¹⁶ **83**, and **85** were obtained,

and all three compounds were screened for opioid receptor activity. Unfortunately, compound **83** was obtained in lower yield than compounds **81** and **85**, but given its limited bioactivity (*vide infra*), efforts to improve this sequence were not pursued.

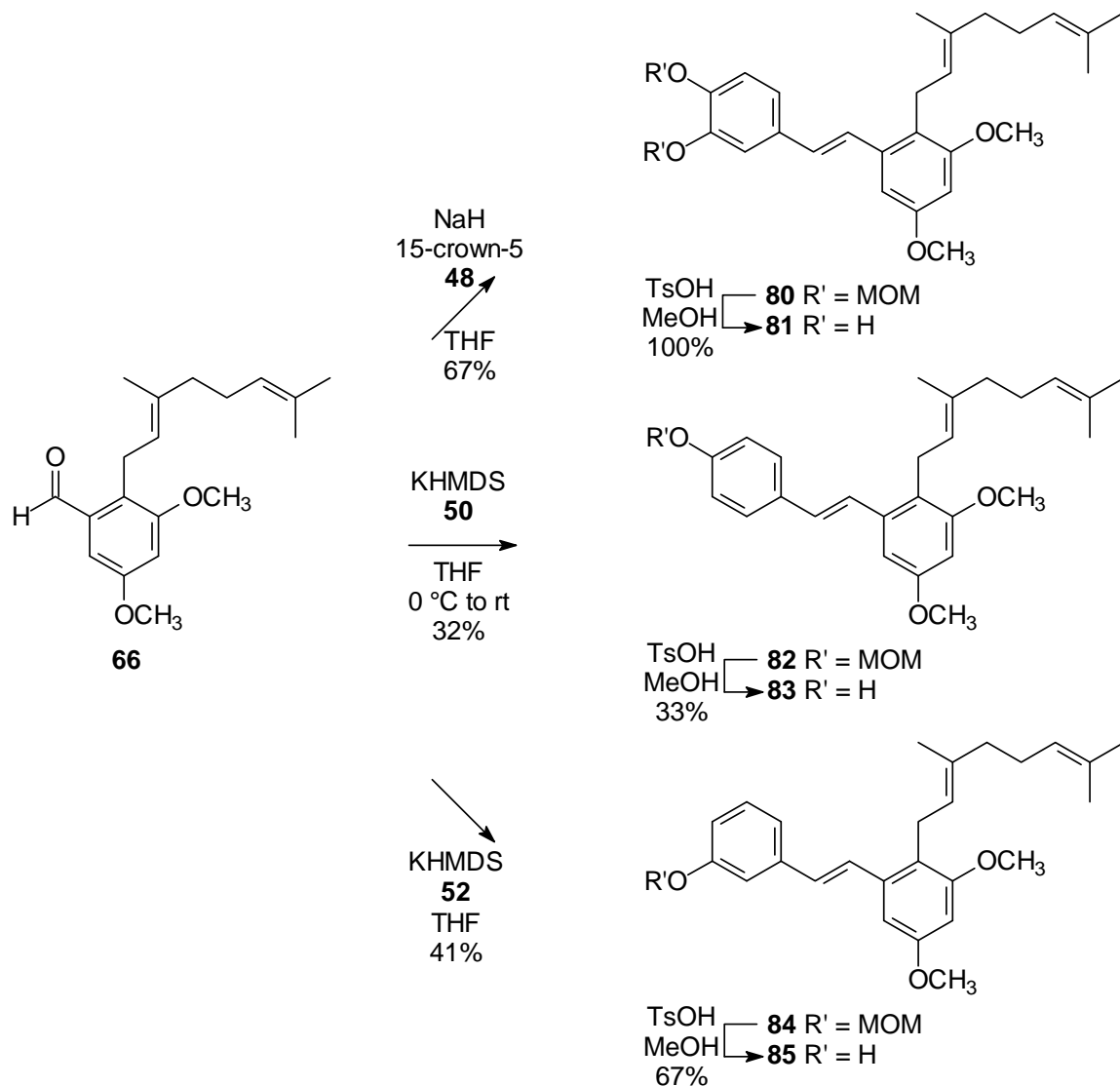


Figure 24. Condensations and hydrolyses to provide analogues **81**,¹⁶ **83**, and **85**

As expected based upon the results reported in Chapter 2 for targets **54**, **56**, and **58**, the apparent affinity for the opioid receptors was lost in compounds featuring

complete removal of the alkyl substituent in the A–ring, regardless of B–ring hydrogen bond contacts (Table 6). Analogues **81** and **85** displayed little to no competitive antagonism. Compound **83** demonstrated weak affinity for a negative allosteric site.

Compound	apparent affinity of competitive antagonists (K_e) in μM			IC_{50} of negative allosteric modulators in μM	
	KOP	DOP	MOP	KOP	MOP
Pawhuskin A	0.2	2.9	0.57	-	-
81	>10	>10	>10	-	-
83	-	-	-	3.26	0.56
85	>3	>10	>3	-	-

Table 6. The opioid receptor affinity of analogues **81**,¹⁶ **83**, and **85**

Coupling of aldehyde **66** and phosphonate **73** via HWE condensation afforded the fully methylated pawhuskin A analogue **86** (Figure 25).¹⁶ This analogue would mimic the steric footprint of pawhuskin A, and clarify the importance of the H–bond donors in both rings. Condensation of aldehyde **66** and phosphonate **44** followed by hydrolysis of the MOM group upon treatment with TsOH in methanol provided analogue **88**.¹⁶ Exposing the A–ring *meta* hydroxyl contact alone would not be expected to reestablish affinity for the opioid receptors based on the findings with compound **46**. Compound **86** also was prepared from stilbene **88** upon treatment with NaH and iodomethane in good yield.¹⁶ It was expected that the yield to prepare compound **86** might be higher over the 3 steps from phosphonate **44** to phosphonate **73** (previously described in Figure 20), and finally olefination with aldehyde **66**, because the convergence is done later in the

sequence. However, both routes to the tetramethyl compound **86** were accomplished in 18% yield over 3 steps.

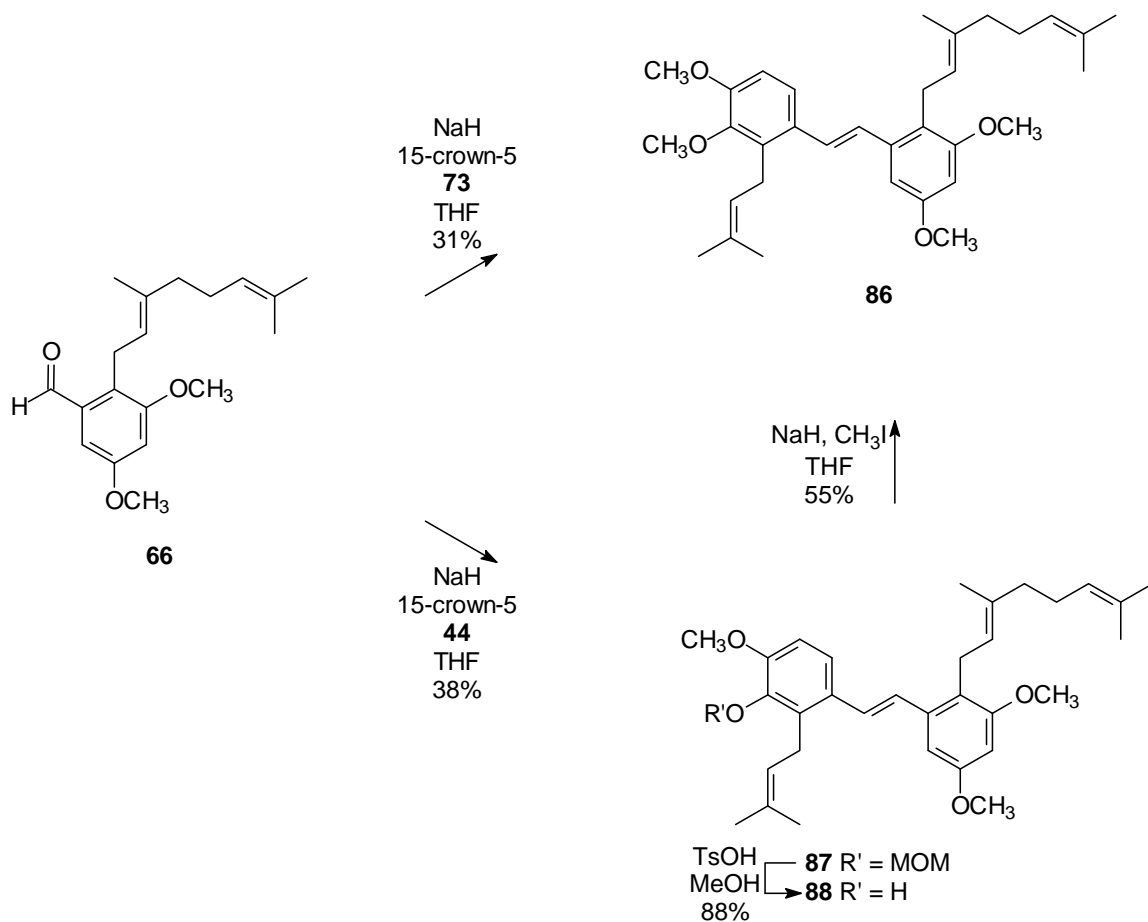


Figure 25. Condensations and hydrolyses to afford analogues **86** and **88**

With analogues **86** and **88** in hand, it was possible to probe the impact of elimination of the *para* H-bond contact in addition to the *meta* contact. This was an interesting target, because of the already established importance of the A-ring *para* hydroxyl functional group and the exciting activity of compound **79**. Bioassays with analogue **90** (Figure 26) would allow comparison of the relative activity of the two alkyl regioisomers. Therefore coupling of phosphonate **75** with aldehyde **66** was conducted to obtain the stilbene **89**. Following MOM deprotection of the MOM acetal **89**, compound **90** was available for those comparisons.

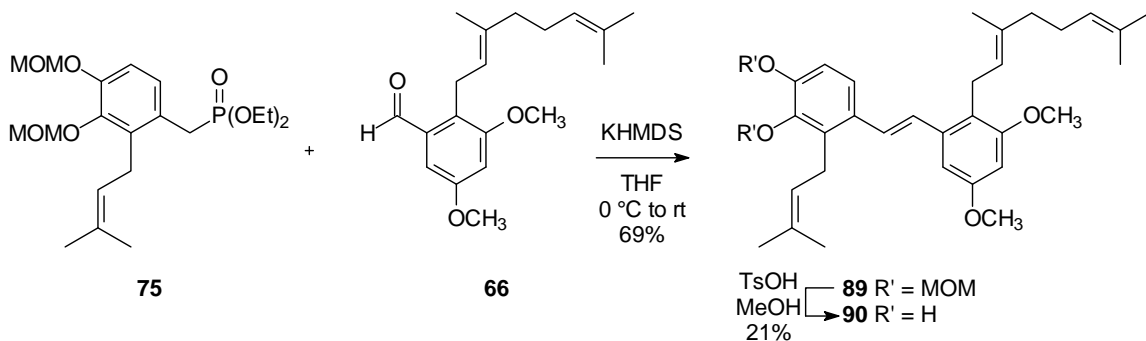


Figure 26. Condensation and hydrolysis to provide analogue **90**

Bioassays on the new stilbenes prepared above allowed a host of comparisons. Full methylation of pawhuskin A, as shown in target compound **86** (Table 7) completely destroyed affinity for the KOP, DOP, and MOP receptors. Exposure of the A-ring *meta* H-bond donation contact (**88**) did not restore affinity for these receptors, and confirms the importance of hydrogen bonding to these receptors. However, exposing the *para* H-bond contact in addition to the *meta* contact, as shown in compound **90** greatly increased affinity for the δ receptor ($K_e = 25$ nM) and not the κ receptor. This is a remarkable finding given the affinity of stilbene **79** for the κ receptor. This indicates that the position

of the C-5 prenyl group upon the A-ring is integral to receptor selectivity. Analogue **90** is approximately 400 times more selective for the δ receptor than the κ receptor. In addition, the previous finding that removal of H-bond donation within the B-ring does not abrogate KOP receptor antagonist activity is also true for this interaction with the DOP receptor.

Compound	apparent affinity of competitive antagonists (K_e) in μM			Selectivity	
	KOP	DOP	MOP	δ/κ	μ/κ
Pawhuskin A	0.2	2.9	0.57	14.5	2.9
86	>10	>10	>10	-	-
88	>10	>10	>10	-	-
90	>10	0.025	ND	<0.0025	ND

Table 7. The opioid receptor affinity of analogues **86**,¹⁶ **88**,¹⁶ and **90**

Because the fully methylated variation on pawhuskin A (stilbene **86**) was inactive, removal of the analogues' A-ring prenyl group would not be expected to reestablish opioid receptor affinity. It was discovered previously that removal of this carbon chain functionality in addition to methylation of the *para* hydroxyl group was not favorable. Bioassays with target compound **91** (Figure 27) might serve to reinforce both of these points. The earlier preparation of compound **81** allowed formation of permethylated analogue **91** upon treatment with weak base (K_2CO_3) and iodomethane.¹⁶

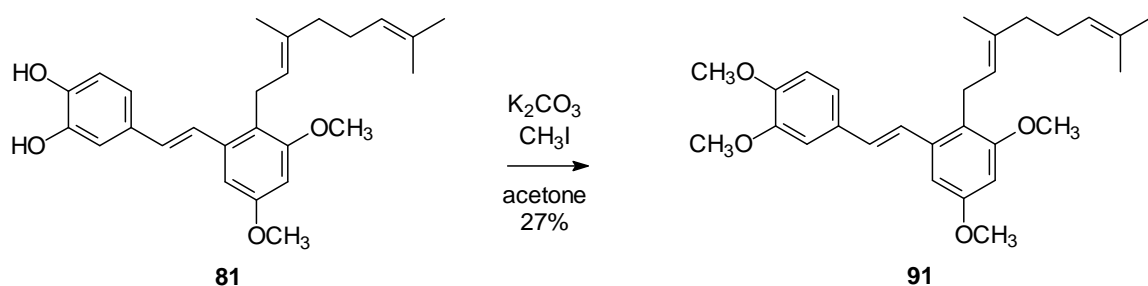


Figure 27. Divergence of compound **81** to provide analogue **91**

As mentioned above, the full methylation of pawhuskin A shown in structure **86** diminished antagonist activity at all three opioid receptor subtypes. Formal removal of the A-ring prenyl group as shown in compound **81** also weakened receptor affinity. As expected based on our evolving understanding of the pharmacophore, compound **91** (Table 8) was inactive. This finding once again confirms that the *para* H-bond donation site and the prenyl group in the A-ring are significant factors in pawhuskin binding to the opioid receptors.

Compound	apparent affinity of competitive antagonists (K_e) in μM			IC ₅₀ of negative allosteric modulators in μM	
	KOP	DOP	MOP	KOP	MOP
Pawhuskin A	0.2	2.9	0.57	-	-
91	>10	>10	>10	-	-

Table 8. The opioid receptor affinity of analogue **91**¹⁶

In summary, several analogues where H-bond donation within the B-ring was eliminated by methylation have been made. Compounds **79** and **90** helped to demonstrate that methylation of the malonate derived-hydroxyl groups does not abrogate affinity for the opioid receptors. Compound **77**, the variation of stilbene **79** with an aryl substituent on the B-ring, helped to demonstrate that the geranyl length chain is desirable for KOP receptor antagonist activity. Compounds **81**, **83**, **85**, and **91** were simplified by formal removal of the A-ring prenyl group and tested. Based on the assay of these four compounds and the conclusions discussed in Chapter 2 from the data of analogues **54**, **56**, and **58**, the prenyl functionality is key in binding to the receptors. Methylation of the *para* position in the A-ring destroyed opioid receptor affinity; this was observed in Chapter 2, and confirmed in Chapter 3 through synthesis and bioassays of compounds **86**, **88**, and **91**.

The findings of Chapter 2 and Chapter 3 are summarized in Figure 28. In pawhuskin A, the presence of the *para* H-bond is a key to opioid receptor binding. The presence and position of the A-ring prenyl group is significant to activity, but the position of this alkyl group determines the selectivity whether it be κ or δ . The removal of the B-ring hydrogen bond donors by methylation does not abrogate binding to the opioid receptors. The length of the alkyl substituent in the B-ring is seemingly important in opioid receptor binding, as demonstrated through studies where this was replaced with a *m*-tolyl group.

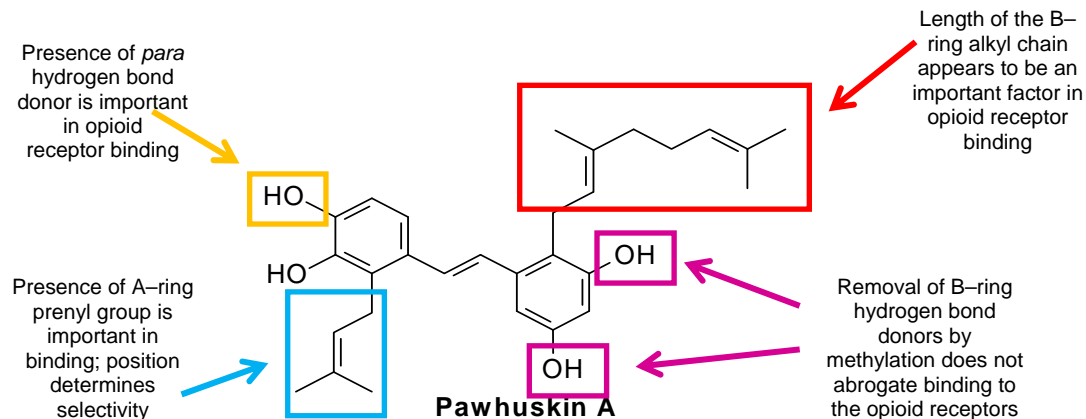


Figure 28. Pawhuskin A and the opioid receptors in brief

The studies presented to this point describe a total of fourteen pawhuskin A analogues that have been prepared. Once aldehydes **34** and **66** were in hand, a number of stilbene variations could be prepared and tested for opioid receptor activity. The most noteworthy compounds are **79** and **90**. The isomeric pawhuskin A analogue **79** (Figure 29) exhibited greater affinity and selectivity for the KOP receptor than pawhuskin A itself, indicating that this shikimate-derived ring is a key for κ -opioid receptor binding.¹⁶ The displacement of the known κ agonist, U69,593, from the KOP receptor by compound **79** is shown below. The percent basal binding increases as the concentration of the agonist increases. The curve for the agonist alone is depicted, as well as the agonist in the presence of the ligand **79**. The rightward shift of the curve is an indication of a competitive mode of antagonism. The EC_{50} of the agonist alone is 184 nM. In the presence of compound **79**, the EC_{50} of the agonist is 4250 nM or ~20-fold greater. Compound **79** shows significantly greater selectivity for the KOP than PF-04455242, which was advanced to Phase 1 clinical trials for alcohol dependency, albeit with significantly lower potency (~150 nM vs 3 nM).^{16,20,45} While the study of KOP agonists

for treatment of pain and addiction has been moving forward, their potential may be limited by side effects such as hallucinations and dysphoria. This makes the discovery of additional classes of opioid receptor antagonists appealing. Therefore, this stilbene scaffold may present new opportunities for the discovery of compounds with utility in the treatment of addiction and depression.¹⁶

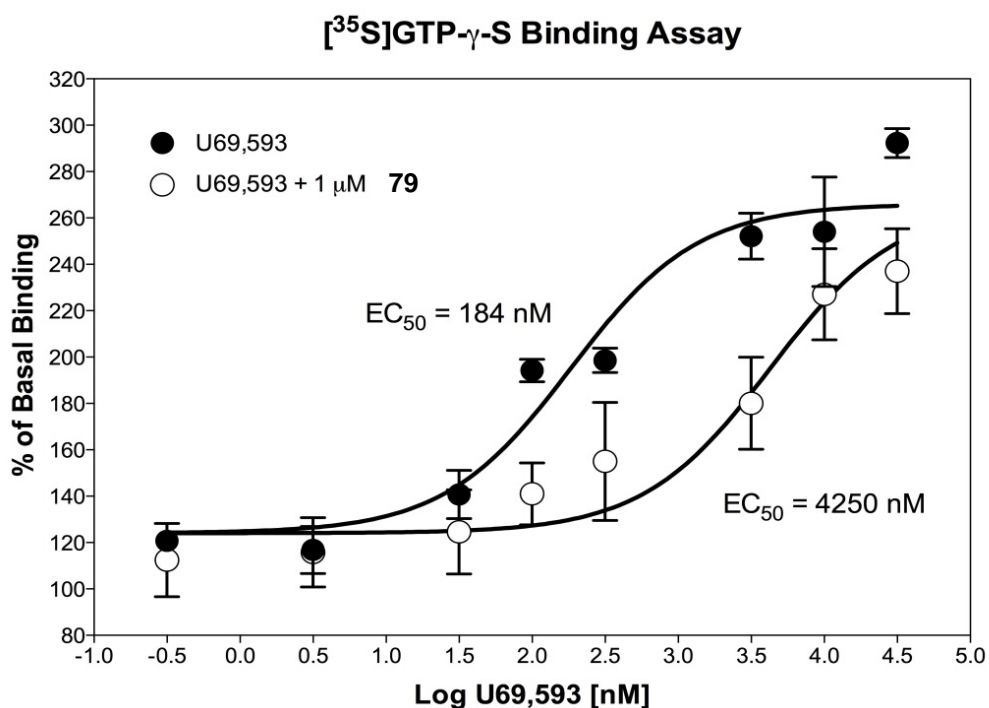


Figure 29. Representative graph of the antagonist activity of compound **79** in the KOP receptor affinity assay. Each data point represents the mean and SEM of duplicate samples.

Analogue **90** (Figure 30) exhibited substantial affinity and selectivity for the DOP receptor, indicating again that the shikimate-derived ring is a key for opioid receptor selectivity. The displacement of the known δ agonist, DPDPE, from the DOP receptor is

shown below. With increasing concentration of agonist, the percent basal binding increased. Again the curve for the known agonist bound to the receptors is shown, in addition to the curve for the bound agonist in the presence of test compound **90**. The curves suggest a competitive mode of antagonism, similar to that of pawhuskin A. The EC_{50} of the agonist alone is 13.2 nM, and in the presence of compound **90**, the EC_{50} of the agonist is increased to 6600 nM or approximately 500-fold greater. Analogues **79** and **90** exhibited greater affinity for the opioid receptors than pawhuskin A, albeit stilbene **90** is selective for the δ receptor. The only distinction between these compounds is the position of the prenyl substituent. As discussed in Chapter 1, DOP receptor antagonists, such as compound **90**, are potential therapies for drug and alcohol abuse as well as neurological conditions, and other disorders.⁵¹

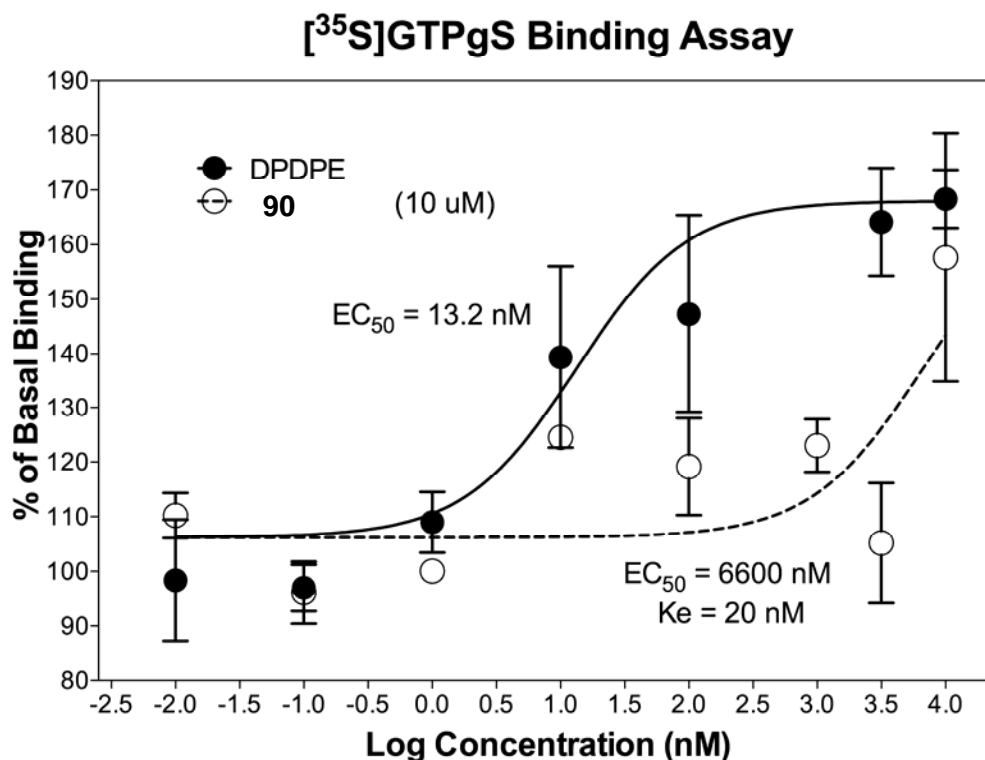


Figure 30. Representative graph of the antagonist activity of compound **90** in the DOP receptor affinity assay. Each data point represents the mean and SEM of duplicate samples.

In the future, the preparation of the mono methyl B–ring aldehydes **96** and **97** (Figure 31) should be revisited. Aldehydes **96** and **97** are accessible from commercial methyl 3,5–dihydroxybenzoate **35**. Upon treatment of ester **35** with $\text{BF}_3 \cdot \text{OEt}_2$ and geraniol, electrophilic aromatic substitution provided compound **92**. Methylated products **93–95** were formed in the presence of potassium carbonate and iodomethane. The mono methylated compounds **94** and **95** were identified by HMBC experiments. A few simple conversions of esters **94** and **95** would provide aldehydes **96** and **97**, respectively. HWE

olefination reactions of these aldehydes with phosphonate **75**, followed by MOM deprotection would afford analogues **98** and **99**. Bioassay of these targets might tell which one (or both) H-bond contact(s) within the B-ring is (are) essential for pawhuskin A binding.

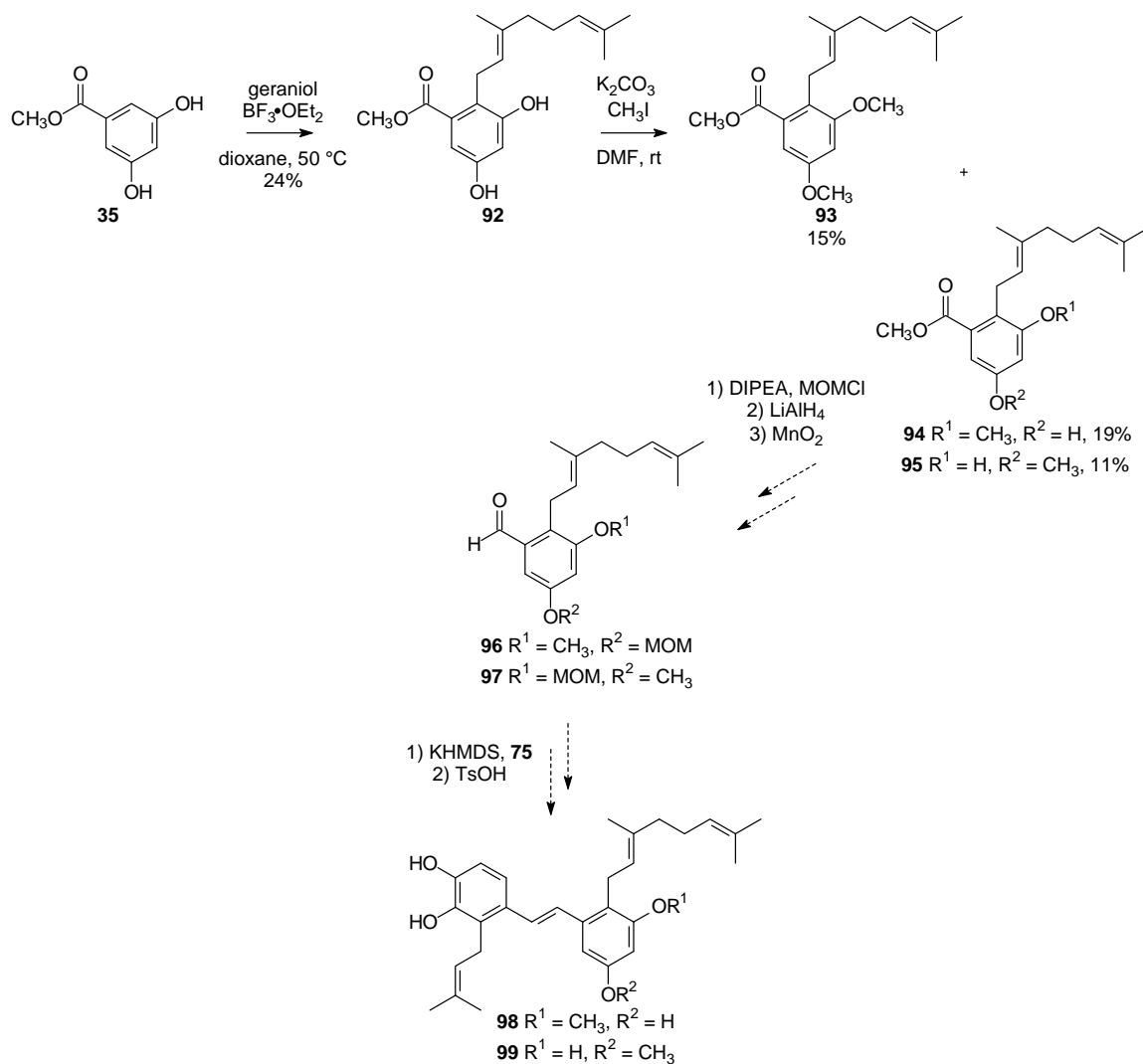


Figure 31. Preparation of mono methylated B-ring isomers

The studies encompass variations as simple as selective methylation of hydroxyl groups in order to assess the significance of H-bond donation to the receptor site without a significant change in electron donation. A more challenging evaluation required the assessment of steric effects by variation of the length and position of the isoprenoid chains. These initial findings should allow further compound design and certainly guide the preparation of pawhuskin A-like analogues with more drug-like characteristics. Similarly, a small set of easily accessible pawhuskin C analogues has been constructed and the same method was utilized in order to test the compounds' affinity for the opioid receptors. These studies will be presented in the following chapter.

CHAPTER 4
STRUCTURAL ANALOGUES OF PAWHUSKIN C: ASSESSING THE
SIGNIFICANCE OF VARYING THE ISOPRENOID CHAIN

Pawhuskin A was found to be the most active member of the *D. purpurea* isolates by Belofsky and coworkers.¹² The reported affinity (K_i) was $0.29 \pm 0.11 \mu\text{M}$ in their opioid receptor assay, in which the nonselective antagonist $^3\text{[H]}$ -naloxone was displaced from striatal rat tissue. The second most active isolate was pawhuskin C (**11**), with a $K_i = 4.2 \pm 3.6 \mu\text{M}$. Because a number of pawhuskin C-like synthons were easily accessible through our previous studies of the pawhuskins and the anti-cancer schweinfurthins,^{54,55,64,75} a small number of test compounds of this chemotype was prepared. The results of this study would illuminate the importance of the hydrophobic substituent on the B-ring. This set includes the natural products schweinfurthin J (**100**, Figure 32) and schweinfurthin I (**101**), which were isolated from the African plant *M. schweinfurthii* and provided to us by colleagues at the National Cancer Institute-Frederick.^{76,77} The bioassay data also will encompass schweinfurthin C (**3**)¹ and mappain (**8**),¹¹ which were prepared by the Wiemer group as reported elsewhere.

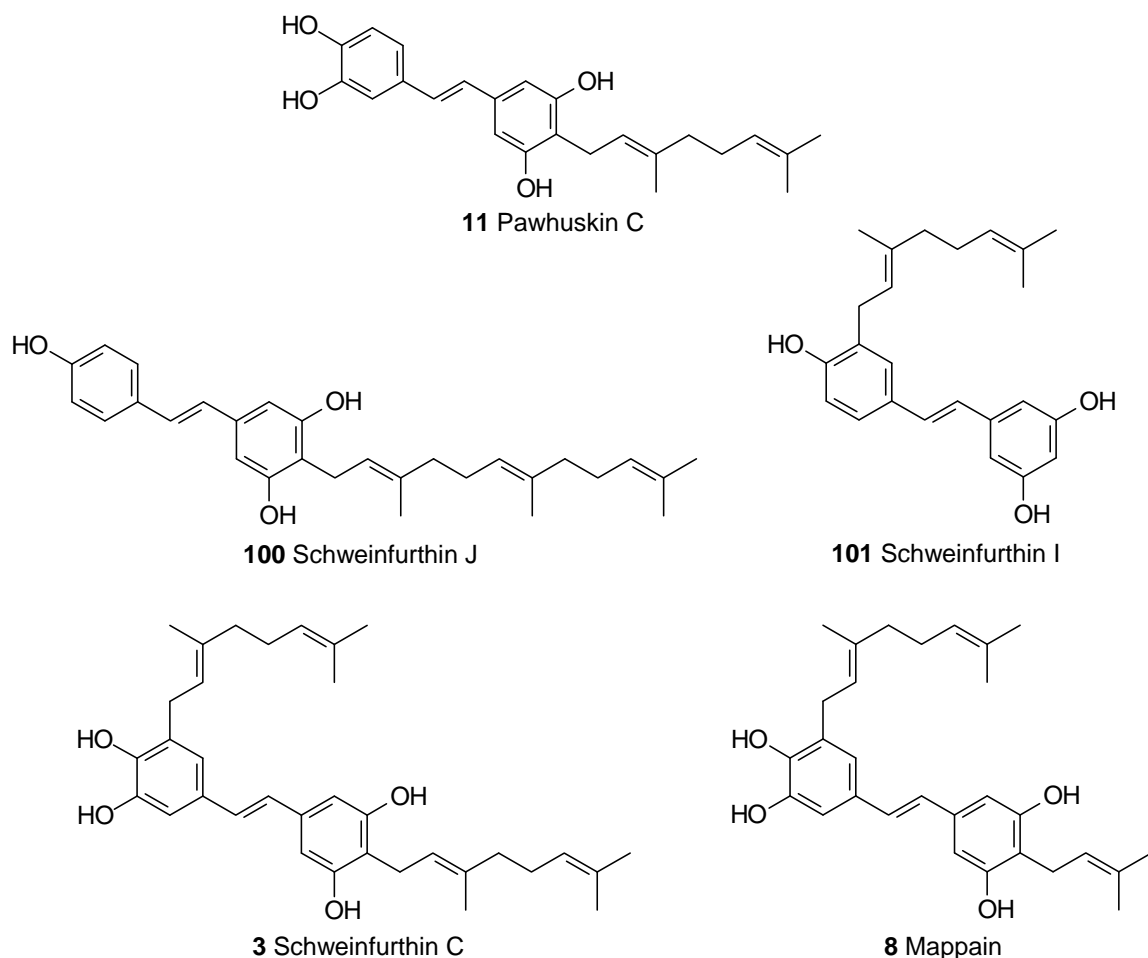


Figure 32. Pawhuskin C and structurally similar compounds

As described above, a disconnection of the central olefinic moiety by Horner–Wadsworth–Emmons condensation involving reversed pairing is viable.^{8,65} Stilbenes prepared in Chapters 2 and 3 were retrosynthetically described from a left half phosphonate and a right half aldehyde. Because the left half phosphonate was known⁸ and available for this study, the synthesis in this chapter would entail a condensation of a left half aldehyde **103** and the right half phosphonate **104** in order to provide the representative stilbene **102** (Figure 33).

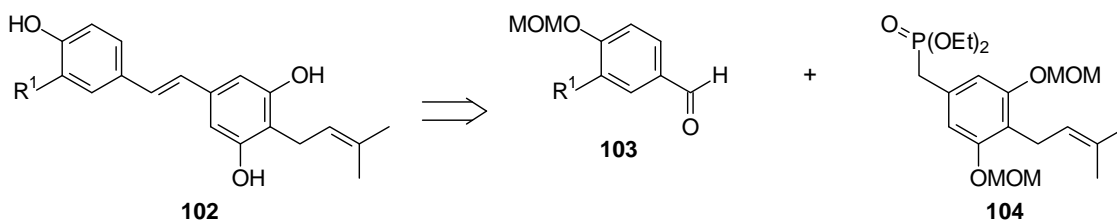
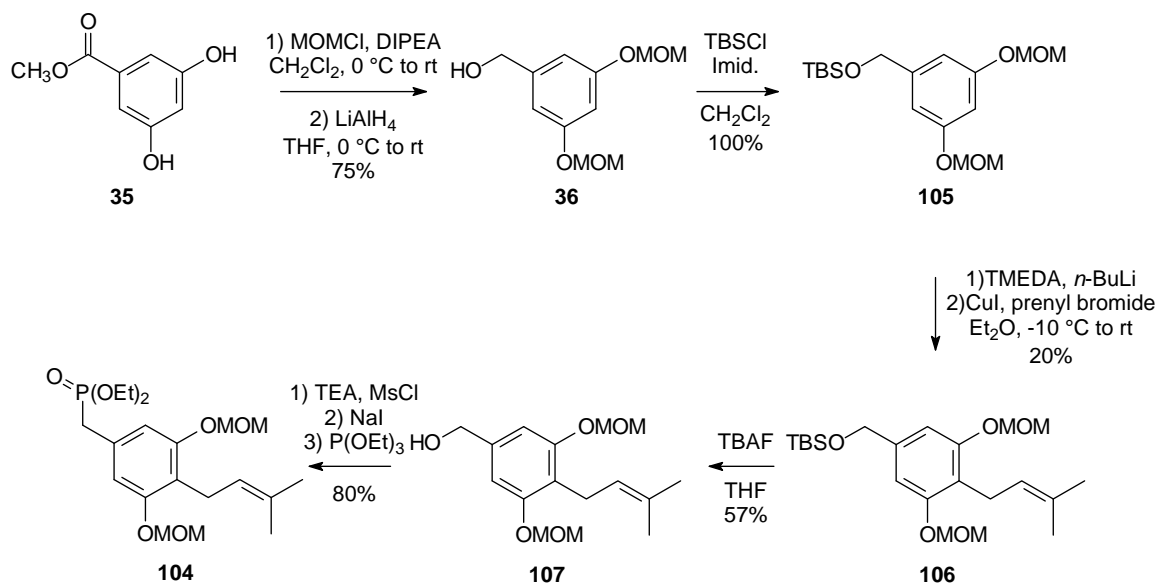


Figure 33. Retrosynthesis of analogues **110** and **113**

Synthesis of the required phosphonate **104** (Figure 34) began with commercial methyl 3,5-dihydroxybenzoate (**35**). Compound **35** underwent MOM protection and reduction smoothly to provide the known 3,5-bis(methoxymethoxy)benzyl alcohol **36**.⁵⁴ Treatment of compound **36** with TBSCl in the presence of imidazole allowed formation of the silyl ether **105**.⁵⁴ Directed *ortho* metallation of the silyl ether **105**⁵⁴ allowed formation of the known prenylated arene **106**.⁶⁶ Removal of the silyl protecting group in the presence of TBAF,⁵⁴ followed by standard Arbuzov conditions^{9,54} through the intermediate mesylate and bromide, allowed formation of the known phosphonate **104**.^{8,9} Analogues of this type would allow us to evaluate the significance of the 10-carbon chain of the natural product.

Figure 34. Formation of phosphonate **104**

A small set of analogues based upon the HWE reagent **104** was desired in order to determine the significance of the isoprenoid functional group on the pawhuskin C scaffold. Phosphonate **104**^{8,9} (Figure 35) was used to access the prenylated pawhuskin C analogue **110**^{78,79} and the natural product *trans*-arachidin-2 (**113**).^{78,79} Condensation of phosphonate **104** with the known aldehyde **108**⁵⁴ gave the protected stilbene **109**. Hydrolysis of the four MOM acetals of compound **109** gave stilbene **110**. The closely related compound **112** was formed through an HWE condensation of phosphonate **104** with the known aldehyde **111**⁸⁰ in the presence of KHMDS. The use of the MOM protecting group for all the hydroxyl groups of compound **112** allowed deprotection to stilbene **113** in a single step, which is more efficient than the previous synthesis.⁸¹ While the potential H-bond contacts of stilbene **110** remained consistent with those of

pawhuskin C, the natural product **113** featured a deleted H-bond donation/accepting site at the *meta* position of the A-ring.

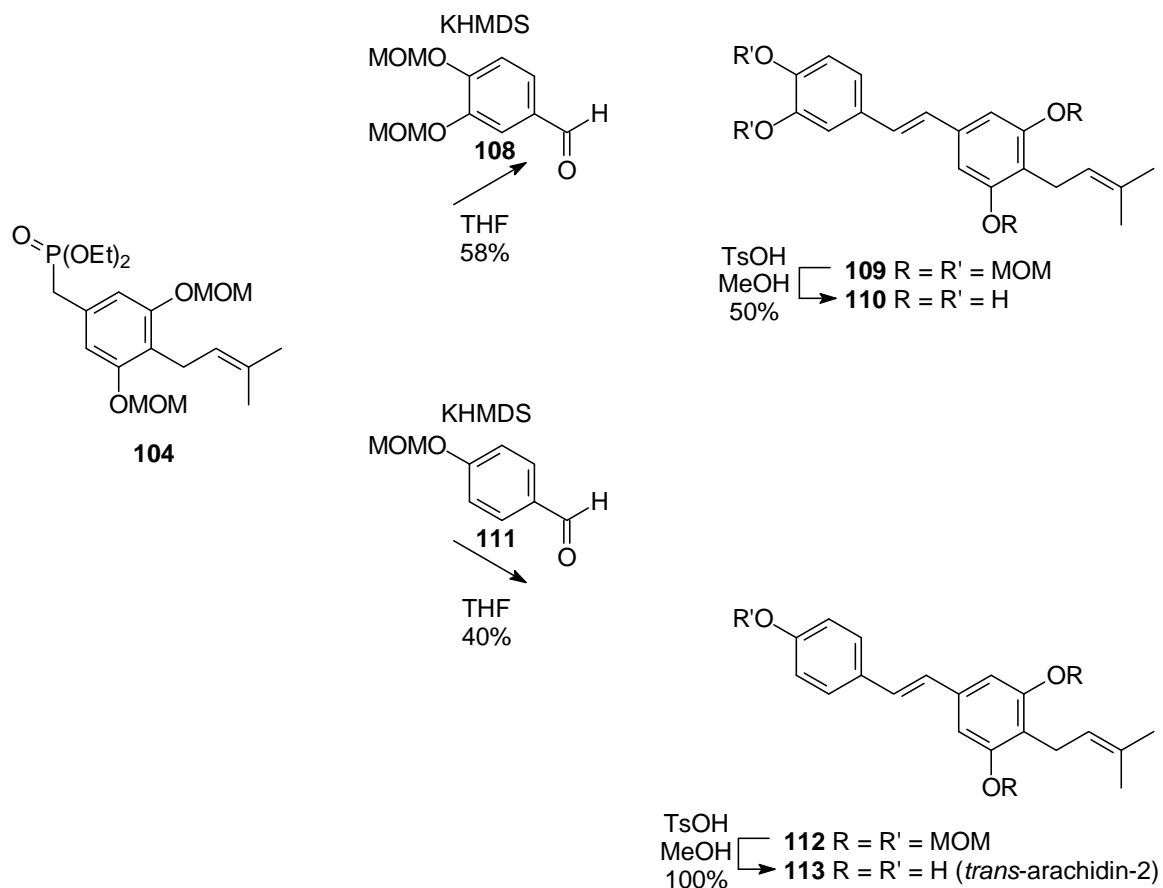


Figure 35. Condensations and hydrolyses to provide analogues **110** and **113**

Similar to the work described in Chapters 2 and 3, the compounds initially were screened for intrinsic and antagonistic activity at 10 μ M in the G-protein coupled receptor assay. The ability to displace the agonists from the opioid receptors was measured and characterized by K_e .¹⁶

Test compound **110** (Table 9) highlighted a shortened prenyl-length chain, as compared to pawhuskin C which bears a geranyl-length chain. From our assays with this compound it is clear that the apparent affinity for all of the opioid receptors was minimal. Further simplification, entailing removal of the *meta* H-bond donation and accepting site, as shown in compound **113**, completely diminished competitive antagonism and only an extremely weak affinity for a negative allosteric site was observed. However, in schweinfurthin J (**100**), the case where the alkyl chain is lengthened to C-15 while the *meta* phenolic hydroxyl group is still absent vis-à-vis pawhuskin C, displacement of the opioid receptor agonists increases, especially at the MOP receptor ($K_e = 3 \mu\text{M}$). This data indicates the alkyl chain length is an important factor in opioid receptor activity. Similar findings were observed in Chapter 3, albeit the pawhuskin A analogues feature an *ortho* substituted prenyl group rather than the *para* substitution pattern that is shown here.

Compound	apparent affinity of competitive antagonists (K_e) in μM			IC ₅₀ of negative allosteric modulators in μM	
	KOP	DOP	MOP	KOP	MOP
Pawhuskin C	25	41	35	-	-
110	>10	>10	>10	-	-
113	-	-	-	>10	>10
100	9	6	3	-	-

Table 9. The opioid receptor affinity¹⁶ of analogues **110** and **113** and Schweinfurthin J (**100**)

A small set of other natural products also was tested for opioid receptor activity. Schweinfurthin C (**3**, Table 10) is structurally very similar to pawhuskin C; it can be

viewed as an analogue with an added steric factor in the geranyl-length chain within the A-ring. Though affinity for the κ receptor was lost with schweinfurthin C, the affinity for the δ and μ receptors increased from $K_e = 41 \mu\text{M}$ and $35 \mu\text{M}$ in pawhuskin C, to $K_e = 13 \mu\text{M}$ and $14 \mu\text{M}$ respectively in compound **3**. The natural product mappain (**8**) is comparable to schweinfurthin C (**3**) in structure, and similar to prepared analogues **110** and **113** in that it contains a shortened alkyl chain in the B-ring. With this compound the affinity for the KOP receptor was regained, and the K_e at the MOP receptor decreased to $29 \mu\text{M}$. Schweinfurthin I (**101**) entails complete removal of the B-ring alkyl group, as well as a deleted phenolic hydroxyl group at the *meta* position within the A-ring. With these changes, the activity at the μ receptor was completely lost. It is apparent that the steric and hydrophobic character of the geranyl chain of pawhuskin C is important for its MOP receptor affinity. Shortening the isoprenoid chain diminishes affinity, and as shown before lengthening the chain to a farnesyl-length increases affinity for the μ receptor. However, although the C-15 isoprenoid increases affinity for the MOP receptor, the calculated functional antagonism is still weak ($K_e = 3 \mu\text{M}$).

Compound	apparent affinity of competitive antagonists (K_{ρ}) in μM			IC ₅₀ of negative allosteric modulators in μM	
	KOP	DOP	MOP	KOP	MOP
Pawhuskin C	25	41	35	-	-
3	>100	13	14	-	-
8	11	10	29	-	-
101	13	11	>100	-	-

Table 10. The opioid receptor affinity of the natural products Schweinfurthin C (**3**), Mappain (**8**), and Schweinfurthin I (**101**)

In summary, analogues featuring variations in isoprenoid chain length were prepared or secured from colleagues, tested in functional assays, and the assay results were analyzed. Analogues **110**, **113**, and schweinfurthin J (**100**) revealed the significance of the hydrophobic geranyl functionality in pawhuskin C. Shortening this group to a prenyl length is unfavorable for opioid receptor affinity, whereas lengthening it to a farnesyl (C-15) length is favorable for both activity and μ receptor selectivity. Schweinfurthin J (**100**, Table 11) is 2 times more selective for the μ receptor than δ , and 3 times more selective for the μ receptor than that of κ . Shortening the geranyl chain in schweinfurthin C (**3**) to a prenyl chain as shown in mappain (**8**), decreased affinity for the MOP receptor. Similarly, complete removal of the isoprenoid group from the B-ring completely eliminated activity at the μ receptor.

Compound	apparent affinity of competitive antagonists (K_e) in μM			Selectivity	
	KOP	DOP	MOP	δ/κ	μ/κ
Pawhuskin C	25	41	35	1.6	1.4
100	9	6	3	0.67	0.33

Table 11. The opioid receptor selectivity of Schweinfurthin J (**100**)¹⁶

Of the pawhuskin C analogues, schweinfurthin J (**100**) was the only compound to demonstrate appreciable activity in these G–protein coupled receptor binding assays. Schweinfurthin J, with a weak K_e of 3 μM for the MOP receptor and limited selectivity ($\delta/\kappa = 0.67$, $\mu/\kappa = 0.33$), is the only stilbene we have studied that shows selectivity for the μ –opioid receptor. Interestingly, schweinfurthin J is also closely related to chlorophorin, which was shown by Sobolev and co–workers to lower agonist binding to the κ and δ receptors to an equal extent but to have no substantial effect on the binding of agonists to the μ –opioid receptor.^{16,43} It would be interesting to target new analogues of pawhuskin C with yet an even more hydrophobic character, e.g. the geranylgeranyl (C–20) or geranylfarnesyl (C–25) analogues. This may allow for increased affinity for the μ –receptor, and eventually the limit to which the receptor will tolerate the increased steric bulk would be established.

The G–protein coupled receptor assay used for screening the synthetic pawhuskin A and pawhuskin C analogues appears to be an efficient method for identifying potency and selectivity at the opioid receptors. Screening such compounds with minor structural differences from the parent compounds might reduce the impact of variables such as the

analogues' water solubility or metabolic stability. Ultimately, the more active compounds should be tested in much more complex animal assays.

CHAPTER 5
DISCOVERY OF A NEW REGIOISOMER IN A DIRECTED *ORTHO*
METALLATION REACTION

The utility of directed *ortho* metallation (DOM) was explored in the preparation of schweinfurthin C (**3**, Figure 36). The work reported in 1999 described an attempt at linear construction toward the doubly geranylated stilbene scaffold utilizing a late-stage DOM reaction.¹ Horner–Wadsworth–Emmons coupling of aldehyde **114** and phosphonate **115** in the presence of NaH gave *E*-stilbene **116**. Removal of the *t*-butyldimethylsilyl group was achieved upon treatment with TBAF in good yield. Reaction of phenol **117** with sodium metal and geranyl bromide provided the *C*-alkylated product **118** in 14% yield, and the *O*-alkylated product **119** in 6% yield. Unfortunately, virtually no starting material was recovered from this reaction, which meant that recycling of compound **117** was not an option. Because only traces of the desired *C*-alkylated product **118** were obtained, attempts toward schweinfurthin C (**3**) via use of a late-stage DOM reaction to alkylate the A-ring were abandoned.

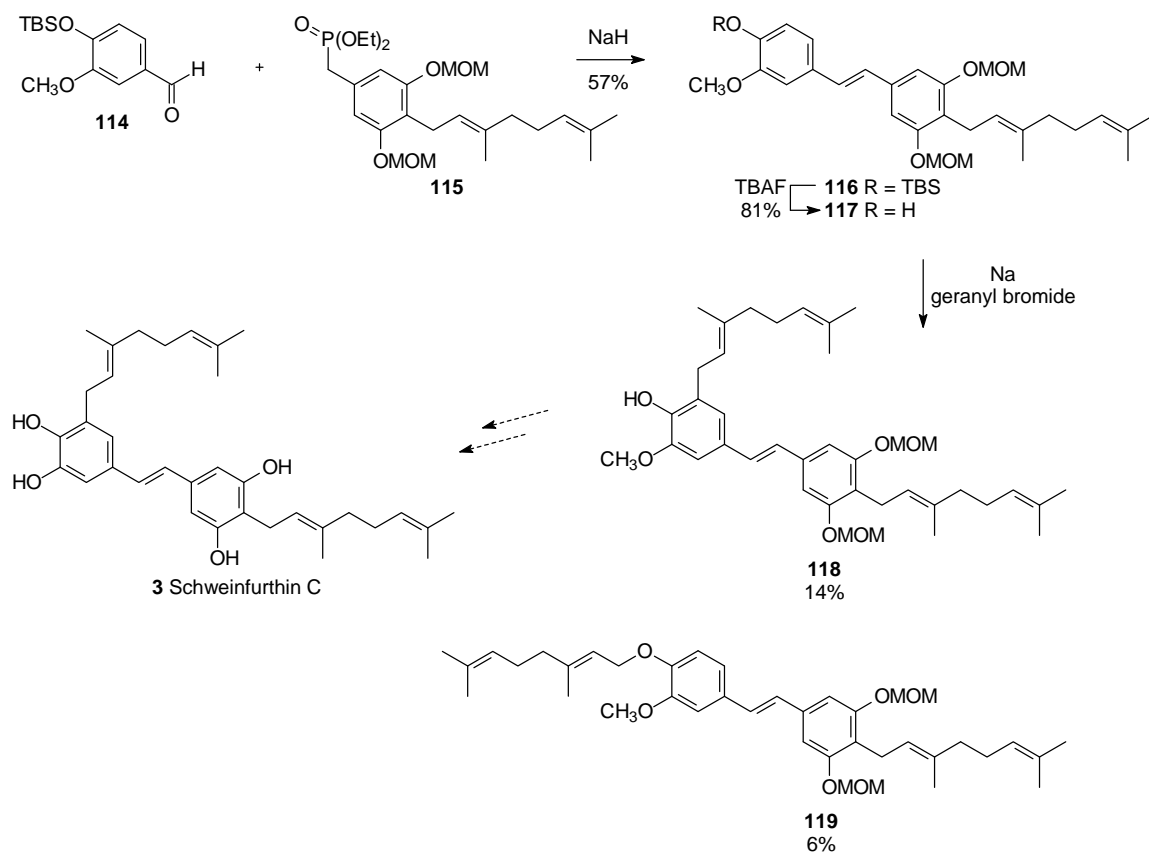


Figure 36. Linear strategy toward Schweinfurthin C¹

An alternate preparation of schweinfurthin C (**3**) involved a late-stage convergent sequence through aldehyde **120** (Figure 37), which would be derived from commercial vanillin (**121**).¹ This approach proved to be viable and thus was employed in the total syntheses of virtually all of the schweinfurthins^{3,4,6-9,75} as well as vedelianin (**7**)¹⁰ and mappain (**8**).¹¹ Syntheses of all of these natural products were published in the years following the first synthesis of schweinfurthin C.¹

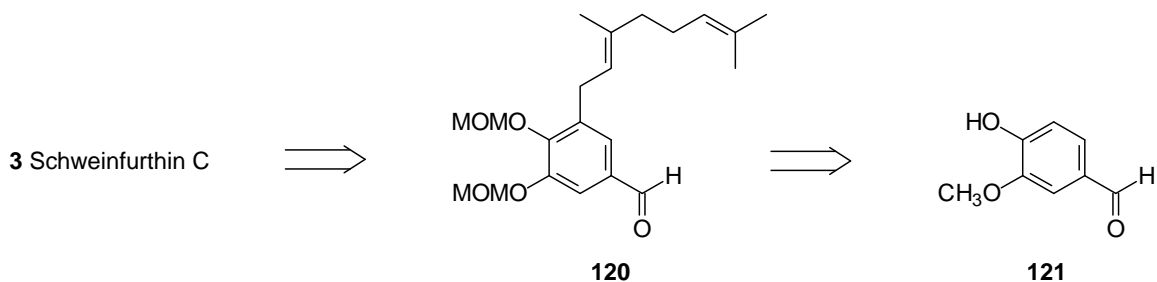


Figure 37. Revised retrosynthesis of Schweinfurthin C from Vanillin

The more structurally complex schweinfurthins, such as schweinfurthins F (**5**) and G (**6**), were assembled in a parallel manner to the preparation of schweinfurthin C (**3**). As reported in this 2008 publication, the geranylated arene **127** (Figure 38) was derived from bromovanillin (**122**) in 5 steps and 61% yield,⁸ or 6 steps and ~60% yield from the commercial starting material vanillin (**121**). Demethylation of bromovanillin (**122**) made available aldehyde **123**. MOM protection of the hydroxyl group followed by NaBH₄ reduction of the aldehyde provided benzyl alcohol **125**. The alcohol was protected in the presence of TBSCl and imidazole to obtain the silyl ether **126**. Finally, halogen–metal exchange effectively delivered the C–alkylated product **127** upon treatment with *n*-BuLi and geranyl bromide. Further modifications of this general approach would eventually make available schweinfurthins F (**5**) and G (**6**).⁸ It should be noted that these substitution patterns (i.e. *meta*-coupled aromatic hydrogens) consistently are observed as characteristic doublets with a coupling constant $J = \sim 2$ Hz in the ¹H NMR spectra (e.g. compounds **122–127**).⁸

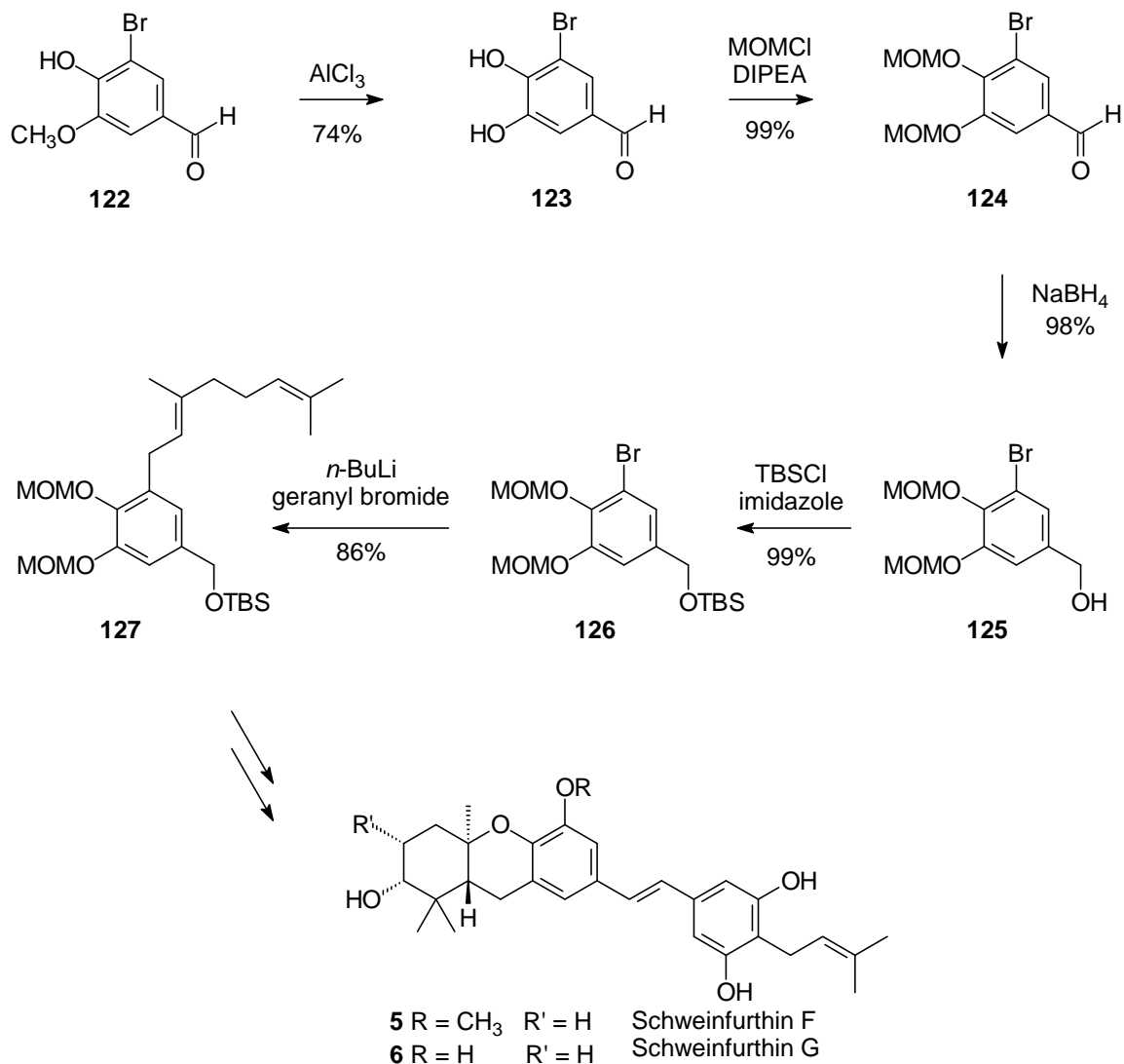


Figure 38. Synthesis of alkyated arene **127** toward Schweinfurthins F and G⁸

A new regioisomer of this alkyated arene would be prepared efficiently in the convergent sequence toward pawhuskin A (**9**) by way of a DOM strategy.⁵⁶ As shown in Figure 39, MOM protection of 3,4-dihydroxybenzaldehyde (**59**) followed by reduction with LiAlH₄ would provide the alcohol and DOM precursor **47**. Dianion formation in the

presence of *n*-BuLi, subsequent cuprate formation, and eventual alkylation with prenyl bromide made available the prenylated arene **74**. Confirmation of the regiochemistry was accomplished upon inspection of ¹H NMR spectrum. As expected for *ortho*-coupled aromatic hydrogens, the coupling observed in the aromatic hydrogens was $J = \sim 8$ Hz. This intermediate would be oxidized upon treatment with MnO₂ to provide the aldehyde **30** for HWE condensation. This work, published in 2008,⁵⁶ would serve as a starting point for synthesis of pawhuskin A analogues.

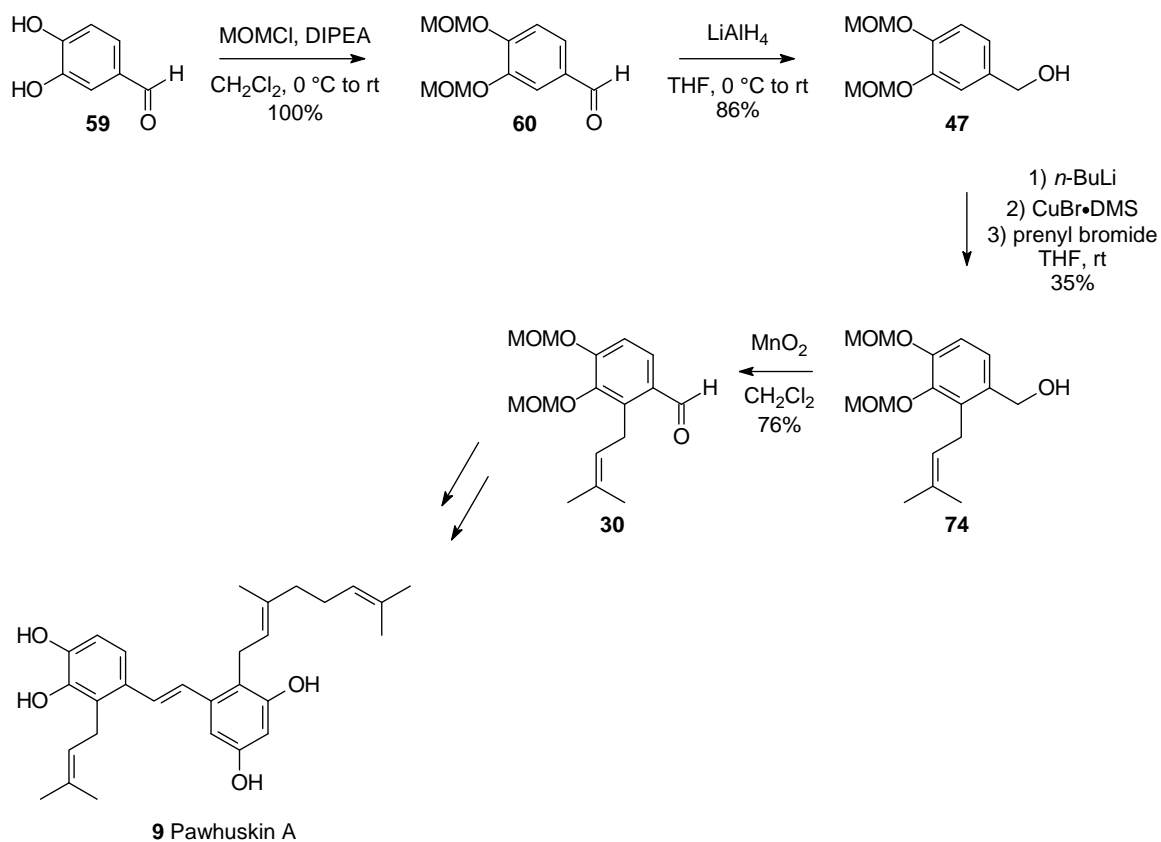


Figure 39. Synthesis of aldehyde **30** toward Pawhuskin A

To begin the synthesis of pawhuskin A relevant analogues (Figure 40), the steps to prepare the prenylated alcohol **74** were repeated. In more recent years, our group has developed DOM and halogen–metal exchange conditions that included the additives TMEDA and CuI, and these modifications were believed to provide more favorable yields of the desired alkylated arenes.² Formation of the dianion of compound **47** with *n*-BuLi, followed by transmetalation in the presence of CuI, and finally alkylation with prenyl bromide provided *both* of the regioisomeric arenes **74** and **61**. After separation by column chromatography, the products were identified in the same manner as in

pawhuskin A: coupling constants in the ^1H NMR spectra within the aromatic doublets clearly showed compound **74** with $J = 8$ Hz and compound **61** with $J = 2$ Hz, respectively, and the products were made approximately in a 1 : 1 ratio (6.51 mmol scale). Repetition of published conditions,⁵⁶ excluding the additive TMEDA and with use of $\text{CuBr}\cdot\text{DMS}$ as opposed to CuI , proved to give the products in a $\sim 1 : 1$ ratio as well (1.31 mmol scale).

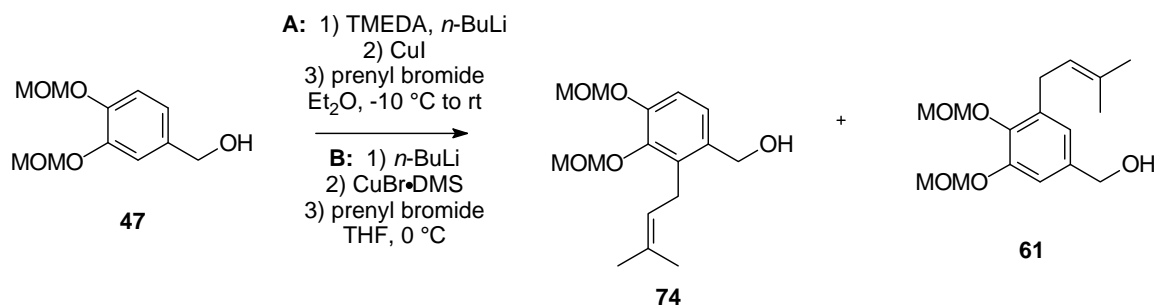


Figure 40. A new regioisomeric product **61** of a published DOM procedure⁵⁶

Two of the most active compounds to date would be constructed from the isomeric products of this DOM reaction sequence. Analogue **79** (Figure 41) was assembled from the prenylated arene **61**, and proved to be considerably selective for the KOP receptor ($\delta/\kappa = >67$, $\mu/\kappa = >67$) with a $K_e = 150$ nM. Likewise, **90** was prepared from prenylated arene **74**, was extremely active at the DOP receptor ($K_e = 25$ nM), and was tremendously selective over the KOP receptor ($\kappa/\delta = >400$).

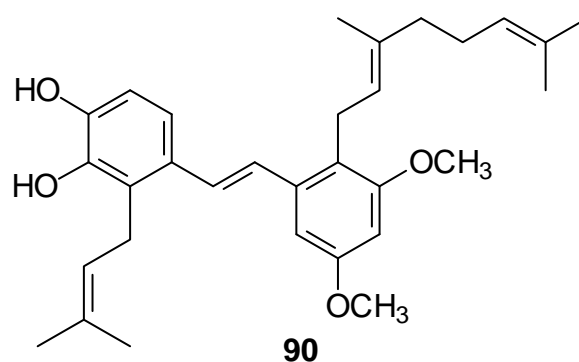
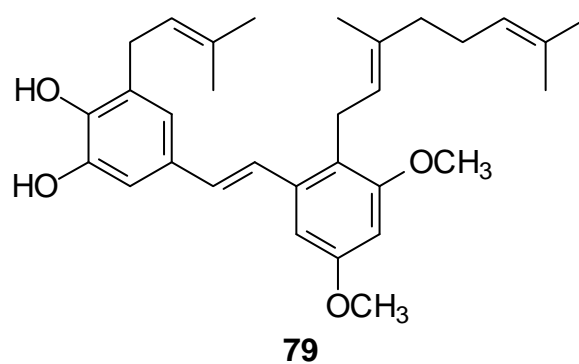


Figure 41. Structures of Pawhuskin A analogues **79** and **90**

There are many variables in a DOM reaction sequence that could alter the product distribution. Our specific application of this strategy entails three potential directing groups, one of which possesses a full negative charge. Because only two regioisomers are formed, and both products consist of alkylation adjacent to the MOM ethers, it is logical to conclude that these ethers are acting as the more effective directing groups. The full negative charge at the benzylic alcohol position might also have a role: a second

anion may be less likely to be formed in close proximity to the first anion due to charge–charge repulsion.

Reactions run at lower temperatures may have a greater tendency to favor formation of the *more* stable dianion intermediate. Indeed, the temperature of the reaction appeared to have an impact on the distribution of products (Table 12). Trials 1–6 are arranged in order of decreasing reaction temperature. Following purification by flash column chromatography, the products were analyzed by ¹H NMR spectroscopy. The *ortho* alkylated product **74** was distinct due to the large coupling within the aromatic hydrogen resonances ($J = 8$ Hz), and the *meta* alkylated product **61** was characteristic of aromatic hydrogen resonances with smaller couplings ($J = 2$ Hz).

Trials 2a and 2b are the most similar to the conditions published previously.⁵⁶ The research notebook conditions of Matt Bueller were followed closely because there was an error in the published procedure (4 L of solvent was not used). Nevertheless the alcohol was treated with excess *n*-BuLi, approximately one equivalent of CuBr•DMS, and 1.2 eq of prenyl bromide in THF at 0 °C (trial 2a, Table 12). Again the regioisomeric products **74** and **61** were formed in a 1 : 1 ratio (1.31 mmol scale). Because clean separation of the regioisomers was difficult, the reaction conditions were repeated on a larger scale of 4.53 mmol (trial 2b). Fortunately, at the larger scale the regioisomers were more easily separable, and a 1.8 : 1 ratio of **74** : **61** was achieved in a combined yield of 51%, the greatest of all of the trials. A parallel reaction (trial 1a) run at ambient temperature gave the *ortho* alkylated product **74** and the *meta* alkylated product **61** in a ratio of 1.1 : 1 on a 0.92 mmol scale. Due to the varying product distribution between trials 2a and 2b, the reaction conditions of trial 1a were repeated on a larger scale (trial 1b). The separation proved to be more successful as demonstrated before, and products **74** and **61** were obtained in a 2.9 : 1 ratio.

Employing the newer reaction conditions,² (trial 3) with both additives TMEDA and CuI in Et₂O and the reagents introduced to the reaction at a temperature of –10 °C,

the alkylated products were obtained in 1 : 1.2 ratio. Decreasing the temperature at introduction of each reagent to $-20\text{ }^{\circ}\text{C}$ (trial 4) and allowing warming to $0\text{ }^{\circ}\text{C}$ between additions, provided compounds **74** and **61** in a $\sim 1 : 2$ ratio. Furthermore, these conditions were repeated on approximately half the amount of material (trial 5). Copper was excluded from the smaller reaction, because of the effect it has on the work-up. The ratio of products **74** : **61** formed under these conditions was 1 : 4. Undoubtedly, at smaller scales the reaction temperature can be more easily controlled. Reaction heat transfer is dependent on two variables, surface area at which the reaction vessel is in contact with the cooling bath, and the volume of the reaction. The described surface area is maximized and the volume of reaction is minimized at smaller reaction scales assuming a constant concentration.

From the data provided in Table 12, it can be surmised that the isolated amount of isomer **61** relative to compound **74** increased with decreasing temperature; the amount of compound **61** was increased and the amount of compound **74** was decreased by a factor of 12 with reaction temperatures ranging from $25\text{ }^{\circ}\text{C}$ to $-20\text{ }^{\circ}\text{C}$, and vice versa. Clean isolation of the products on scales much less than 4 mmol proved to be a challenge. In addition to the challenges with isolation, the reaction yields may suffer at smaller scales because the anions are more easily quenched by adventitious water prior to the addition of prenyl bromide.

Trial	Scale (mmol)	TMEDA (mmol)	<i>n</i>-BuLi (mmol)	CuI (mmol)	CuBr•DMS (mmol)	Prenyl bromide (mmol)	Solvent [conc.]	T	74 : 61
1a	0.92	NA	1.95	NA	1.02	1.11	THF [0.13 M]	rt	1.1 : 1
1b	4.46	NA	9.52	NA	4.91	4.94	THF [0.13 M]	rt	2.9 : 1
2a	1.31	NA	2.75	NA	1.11	1.53	THF [0.13M]	0 °C	1 : 1
2b	4.53	NA	9.52	NA	4.98	4.94	THF [0.13 M]	0 °C	1.8 : 1
3	6.51	14.01	14.25	6.53	NA	7.16	Et ₂ O [0.07 M]	-10 °C to rt	1 : 1.2
4	7.97	16.67	17.50	7.98	NA	11.93	Et ₂ O [0.06 M]	-20 °C to 0 °C to rt	1 : 1.9
5	4.18	8.67	9.20	NA	NA	6.31	Et ₂ O [0.06 M]	-20 °C to 0 °C to rt	1 : 4.0

Table 12. The effect of temperature on product ratio in directed *ortho* metallation

The effect of a bulky protecting group on product distribution also was analyzed. The *meta* alkylated product **130** was expected to be formed almost exclusively, due to the anticipated steric hindrance of the TBS ether in compound **128** (Figure 42). After TBS protection of alcohol **47** provided silyl ether **128**, treatment of compound **128** with TMEDA, *n*-BuLi, and prenyl bromide induced directed *ortho* metallation in Et₂O at -20 °C. The *ortho* alkylated product was not observed under these conditions. However, an interesting dialkylated byproduct **129** was obtained. The structure of compound **129** was confirmed by ¹H and ¹³C NMR spectroscopy, as well as a DEPT experiment and HRMS. The amount formed was 3.6 : 1 of compound **130** to compound **129**. Reducing the amount of *n*-BuLi and prenyl bromide in the reaction might address this issue. However, it should be noted that compounds **130** and **129** were formed in 3% and 1% yield, respectively, and the abysmal yield was due to an overwhelming amount of retro-Brook rearranged product. In addition, a significant amount of unreacted starting material (**128**) was present by TLC analysis. Given these concerns, this strategy was not pursued further.

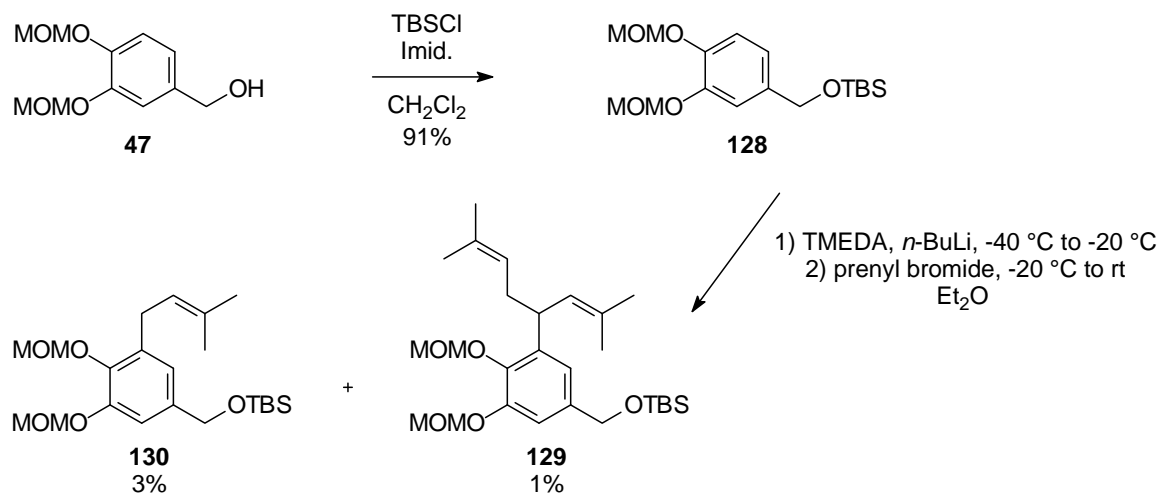


Figure 42. The effect of a bulky protecting group in product distribution

The *meta* alkylated product **130** also was prepared in a manner similar to that described in Figure 38 based on the past synthesis of schweinfurthins F (**5**) and G (**6**).⁸ The TBS ether **126** (Figure 43)⁸ was prepared in 4 steps from the known bromovanillin (**122**) as described. Halogen–metal exchange was carried out in THF. By TLC a substantial amount of retro–Brook rearrangement product and virtually no desired product was formed from the reaction, and thus isolation of these unwanted products was not pursued. Unfortunately, there is no known way to reverse the retro–Brook rearrangement and so this product is not useful.

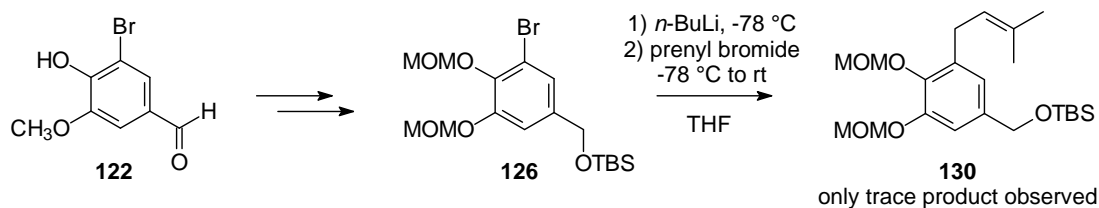


Figure 43. Unsuccessful halogen–metal exchange toward compound **130**

As described in the synthesis of pawhuskin A, the new *ortho* alkylated arene **74** is concisely constructed from commercial 3,4-dihydroxybenzaldehyde via a DOM reaction sequence as shown in Figure 39. Seven years after this publication,⁵⁶ it was discovered that the *meta* alkylated arene **61** also was formed during this reaction. The distribution of products clearly is affected by the temperature at which the reagents are added to the reaction mixture. With decreasing temperature, more of the distant dianion intermediate leading to product **61** is formed, as opposed to the proximal dianion which leads to compound **74**. Further studies in which the temperature is varied even more might be done in order to strengthen this hypothesis. As mentioned above, a reasonable scale must be maintained in order to allow for clean isolation of multiple products. Scales of at least 4 mmol may be optimal for definitive results. Both regioisomers proved to be useful in the synthesis of the most promising pawhuskin analogues, namely compounds **79** and **90**. Relocation of the A–ring prenyl group determines whether the analogue is a potent KOP receptor modulator, or an exceptionally potent DOP receptor modulator. Future analogue design will heavily rely on the products of this directed *ortho* metallation reaction.

The discovery of the second regioisomer is not only beneficial in the context of pawhuskin analogue preparation, but it also could allow more rapid construction of many schweinfurthins. In addition, the concept of utilizing a DOM reaction strategy to assemble the A–ring of schweinfurthin C could be revisited. As described here, the alkyl

group is installed in just 3 steps from the commercial starting material. The current preparation of the schweinfurthins entailed a sequence of 6 steps prior to halogen–metal exchange from vanillin, and required an additional TBS deprotection step. Application of these new findings would allow for more efficient syntheses of *meta* alkylated arenes.

CHAPTER 6
SYNTHESIS OF A NEW CORE LINKAGE: AN EXTENSION OF
PROMISING ANALOGUES

Hydrophobicity can be predicted by the ratio of the total number polar groups to the total number of carbon atoms.⁶⁰ The higher this ratio, the more water-soluble the compound should be. Pawhuskin A is naturally hydrophobic, bearing 29 carbons and only 4 oxygens. This could become problematic in potential clinical applications because drugs that are negligibly water soluble may be deposited before reaching the intended site of action. These deposits can obstruct blood vessels and cause damage to the organs.⁶⁰ To address this inherent property of the pawhuskins, without changing the natural H-bond contacts and steric characteristics of the compounds, we pursued the possibility of altering the central stilbene linkage. The new linkage would have to mimic the spatial arrangement of the *trans* positioned arenes, possess sp² character, and contain a polar group to increase the water solubility. As defined by these parameters, a reasonable stilbene replacement might be an amide linkage. The most active compounds to date are the stilbenes **79** and **90**, and the most promising amides to target would be derivatives of these structures such as compounds **131** and **132** (Figure 44).

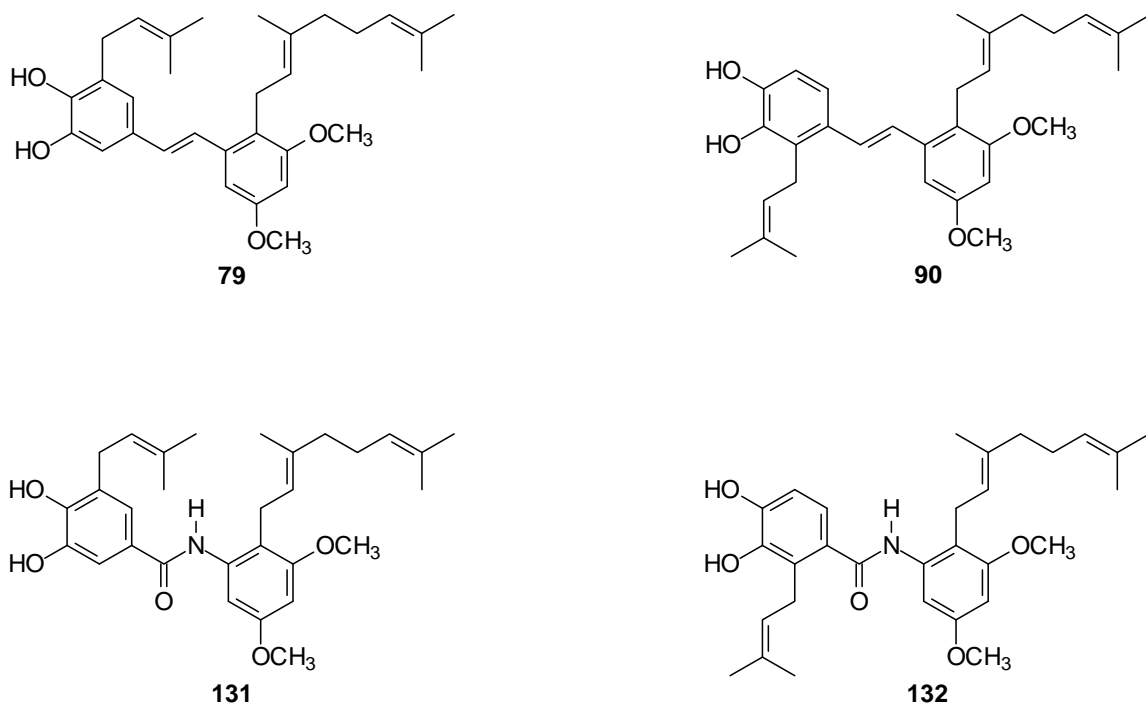


Figure 44. Active stilbenes **79** and **90** and respective target amides

Because a potential drug must pass through a number of membranes consisting of a phospholipid bilayer before reaching its site of action, a balance of hydrophilicity and lipophilicity must be made. The partition coefficient ($\log P$) is a way of predicting a drug's lipophilicity: the greater the $\log P$ value the more lipid-soluble the compound is, and vice versa. $\log P$ is a measure of a drug's solubility between two immiscible layers, octanol and water, and according to Lipinski's rules $\log P$ should be less than 5.⁸² Based on the drug's structure it is possible to calculate an approximate partition coefficient ($\text{clog}P$), and many computer programs including ChemDraw may be used to do so. The $\text{clog}P$ of pawhuskin A (Table 13) was calculated to be 8.17. The addition of two methyl groups, as shown in the structures of **79** and **90**, increases the $\text{clog}P$ value to 9.56. As shown in Table 13, the target amides **131** and **132** are expected to bear decreased $\text{clog}P$

values by a factor of ~100 relative to compounds **79** and **90**. Even though the calculated partition coefficient still would be greater than 5, the approach of introducing drug-like characteristics can be done in a step-wise fashion. If the amide(s) prove to retain opioid receptor activity further modifications can be made in order to reduce the lipophilicity still further.

Compound	clog <i>P</i>
Pawhuskin A	8.17
79	9.56
90	9.56
131	7.04
132	7.04

Table 13. Calculated partition coefficients

Amides **131** and **132** could be prepared via different late-stage convergent fashions, including a carbodiimide coupling and nucleophilic acyl substitution. The generalized amides **133** (Figure 45) could be seen arising from representative acid/acid chloride **134** and amine **135**. The reverse pairing also may be viable, but due to the availability of precursors to compound **134** from previous analogue studies, as well as commercial availability of amines with a 3,5-oxygenated pattern, this strategy was favored for the initial studies.

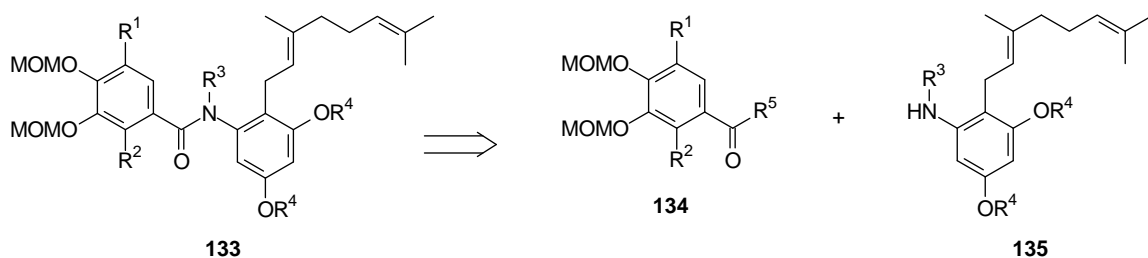


Figure 45. Retrosynthesis of analogues **131** and **132**

Several amine synthons, represented by structure **135**, now have been prepared from commercial 3,5-dimethoxyaniline (**136**, Figure 46). Treatment of amine **136** with NEt_3 and acetic anhydride afforded acetanilide **137** in 91% yield. Electrophilic aromatic substitution was induced upon treatment with geraniol and $\text{BF}_3 \cdot \text{OEt}_2$ to provide the geranylated arene **138** in modest yield. This regiochemistry was expected based on precedent with Friedel-Crafts acylation reactions on 3,5-dimethoxyacetanilide (**137**).⁸³ It was confirmed by analysis of the ^1H NMR spectrum which showed unsymmetrical aromatic resonances. Finally, the ethyl amine **139** and amine **140** were made available by reduction with LiAlH_4 in THF or hydrolysis upon treatment with NaOH in MeOH ,⁸⁴ respectively.

An attempt to prepare amine **140** from amide **138** also was made by treatment of the amide with SOCl_2 in MeOH .⁸⁵ Unfortunately, these conditions were too harsh for the system and an inseparable mixture of material was delivered from the reaction. Even though the ethyl amine **139** was provided in a more modest yield, the reaction time was much shorter in comparison to that in the formation of **140**. Model studies might prove whether the more easily accessible amine **139** would be useful in successive reactions to provide the amide desired as a stilbene analogue.

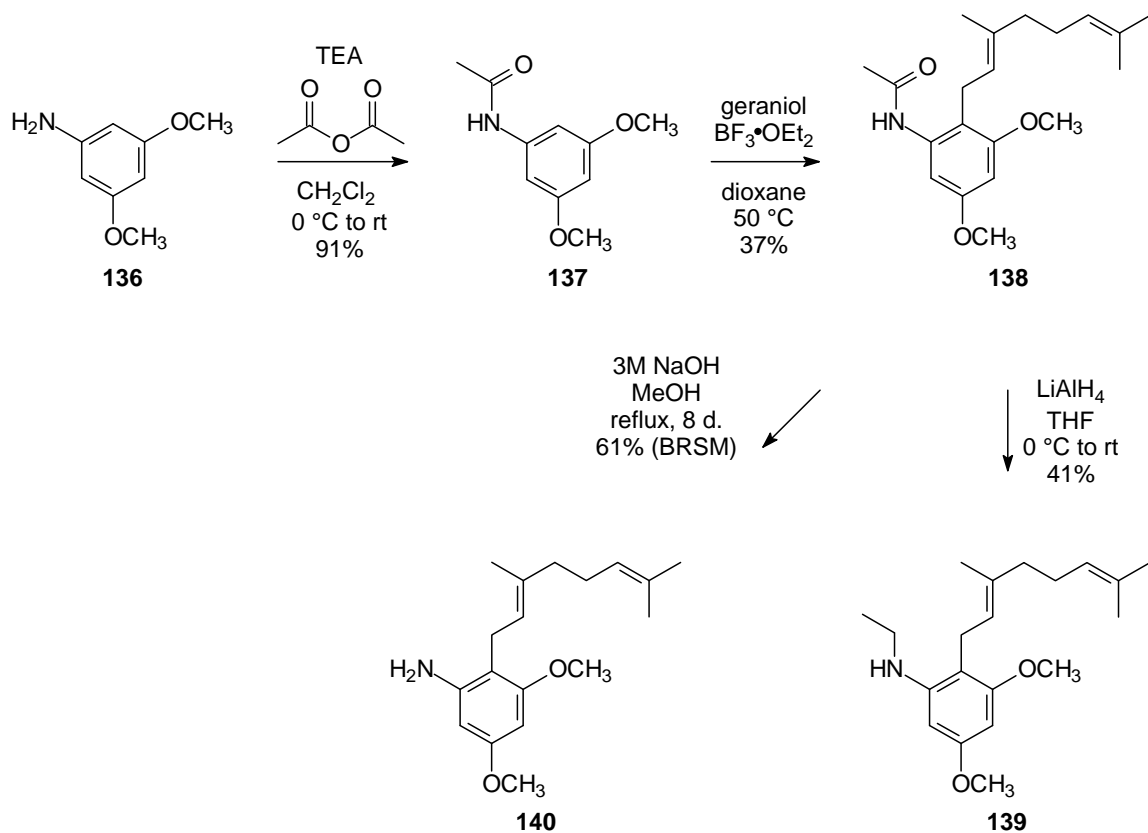


Figure 46. Synthesis of amines **139** and **140**

Prior to discovery of the promising activity of methylated analogues **79** and **90**, preparation of the amide **133** was designed so that it would model the structure of pawhuskin A (**9**), i.e. with the B-ring hydroxyl groups available for H-bond donation to the receptor site. To reach this goal, acetanilide **137** (Figure 47) was treated with aluminum iodide in the presence of TBAI to provide the demethylated compound **141** in reasonable yield.⁸⁶ Similar to the preparation of amide **138**, electrophilic aromatic substitution on compound **141** made available acetamide **142** in modest yield.

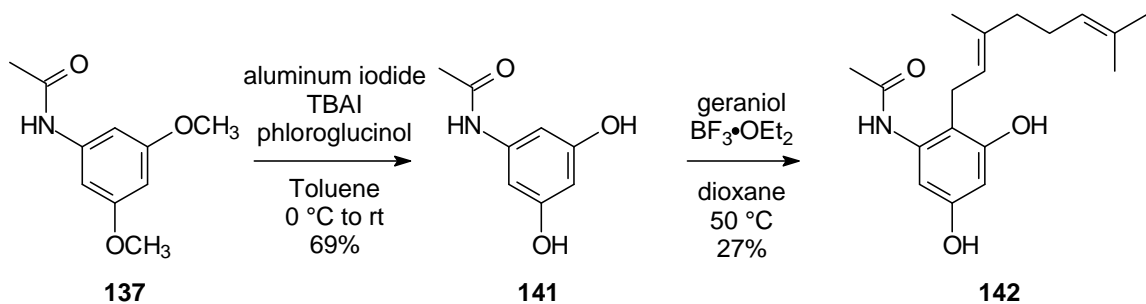


Figure 47. Synthesis of acetanilide **142**

Several model systems were examined before proceeding to the preparation of the representative carboxylic acid **134**. Benzoic acid (**143**, Figure 48) and ethylamine **139** were treated with hydroxybenzotriazole (HOBt) and EDC hydrochloride under standard conditions.⁸⁷ Because 67% of unreacted amine **139** was recovered from this reaction, it was determined that this secondary amine was too sterically hindered for carbodiimide coupling under these conditions. Therefore, a more reactive acid equivalent, benzoyl chloride (**144**), was treated with the ethyl amine **139** in Et₂O. Quantitative conversion to the desired product **145** was observed by ¹H NMR spectroscopy. Likewise, the addition of amine **140** to chloride **144** successfully provided amide **146** as discerned by ¹H and ¹³C NMR spectroscopy.⁸⁸ However the spectra showed a mixture of benzoyl chloride (**144**) and the desired amide **146**. Benzoic acid (**143**) also reacted with 3,5-dimethoxyaniline (**136**) in the presence of DCC. One new spot was observed by TLC, but this was later tentatively identified to be the HOBt ester intermediate **148** rather than the desired amide **147**. Failure of this fourth model system to afford the desired product might be due to the inherently less nucleophilic nature of aniline, and might also be an explanation for the first failed model reaction.

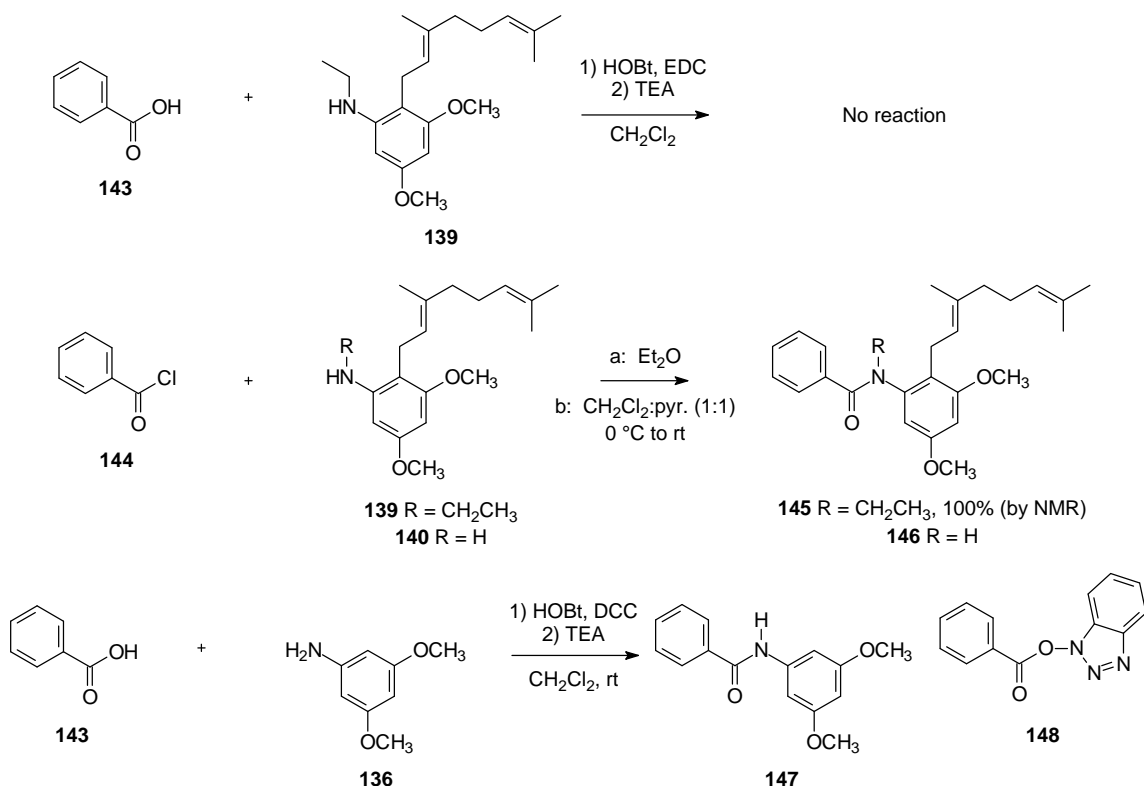


Figure 48. Amide model reactions

As mentioned above, preparation of precursors to the acid or the corresponding acid chloride as represented by compound **134** (Figure 45) have been explained in detail in previous analogue studies. A directed *ortho* metallation reaction with a dianion intermediate gave both regioisomers **61** and **74**, as described in Chapter 5. Direct oxidation of benzyl alcohol **61** (Figure 49) in the presence of PDC was attempted. After seven days a significant amount of starting material still was observed by TLC. Repeated attempts toward target acid **149** from alcohol **61** instead delivered significant amounts of the aldehyde byproduct **150**. This finding encouraged a more step-wise approach. The structure of byproduct **150** was confirmed by both ¹H and ¹³C NMR spectroscopy, in

addition to a DEPT experiment and HRMS. As shown in Figure 49, when treated with MnO_2 the functionalized benzyl alcohols **61** and **74** were oxidized to the corresponding aldehydes **151** and **30**, respectively. Oxidation of aldehyde **151** with PDC was attempted,⁸⁹ but after a reaction time of several days only trace amounts of the carboxylic acid **149** were formed. Attempted oxidation of aldehyde **151** in the presence of ceric ammonium nitrate (CAN) and *t*-BuOOH,⁹⁰ as well as MnO_2 and NaCN ⁹¹ failed to provide the target carboxylic acid **149**. Finally, a Pinnick oxidation would afford the acid **149**.⁹² Likewise, aldehyde **30** underwent Pinnick oxidation to afford acid **152** in quantitative yield, although this transformation required multiple trials. In the first attempts, degradation of product occurred upon acidic work-up and/or purification on acidic media. It wasn't until acid treatment was altogether avoided, and the equivalents of 2-methyl-2-butene were doubled, that the reaction was successful. Excessive amounts of hypochlorous acid generated from the reaction were detrimental to the prenyl chain, as this functionality was not intact upon analysis of the ^1H NMR spectrum of the initial product mixture.

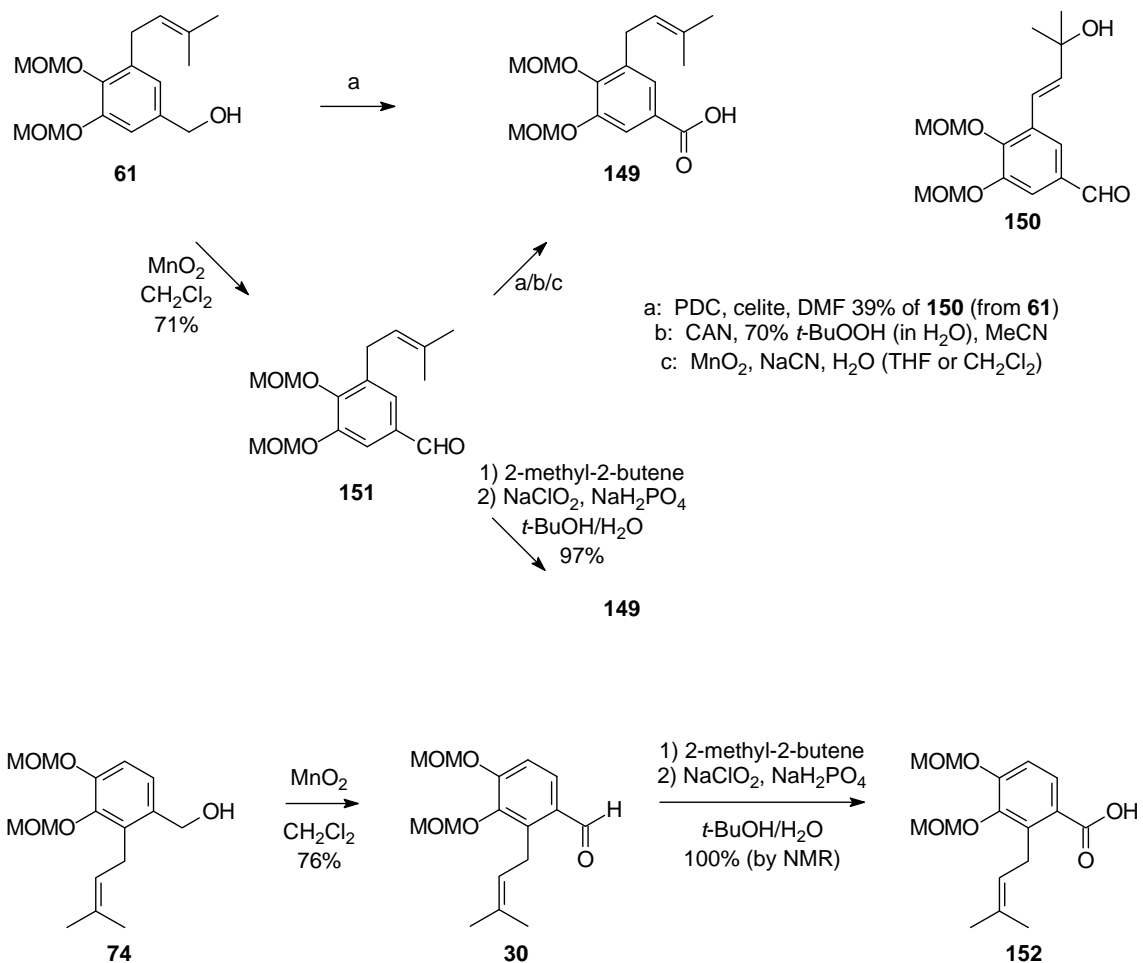


Figure 49. Preparation of carboxylic acids **149** and **152**

Once the carboxylic acid **152** was successfully prepared, several carbodiimide coupling reactions were attempted (Figure 50). Attempted coupling with amine **140** in the presence of EDC hydrochloride and HOBt failed to provide the targeted amide **153**.⁸⁷ Instead, a significant amount of an intermediate in the reaction sequence was isolated. This product proved to be the adduct of the reacting acid and HOBt, which could be viewed as an ester precursor (**154**) to the desired amide **153**. The next step in the reaction

sequence would be addition of the amine **140**. The fact that this transformation did not take place, made clear because much of the starting amine was recovered, encouraged reevaluation of the nucleophilic nature of the substituted aniline **136**. Second, an as yet unidentified byproduct of the EDC reaction was isolated. This compound resembled the starting material **152**, but the prenyl chain was not intact as made apparent by analysis of the ^1H NMR spectrum. The EDC is commercially available as the hydrochloride and, as per previous assessment, acid caused degradation of the isoprenoid unit. To avoid acid-catalyzed decomposition, compounds **152** and **140** were treated with DCC in the presence of HOBt.⁹³ Amide formation with DCC was slightly more successful than the aforementioned EDC coupling reaction. Only the acid-HOBt ester intermediate **154** was isolated and characterized by its ^1H NMR spectrum, but degraded starting material was not observed. Again, the last step of the desired transformation did not occur, and the amine **140** must be a weaker nucleophile than once considered. Carbodiimide couplings are normally moderately successful in forming amides, but the literature does show that yields are lower in the preparation of phenylamides than with alkylamides.⁹³ Additionally, Huczyński and co-workers also have reported isolation of the intermediate HOBt ester in their attempted preparation of a naphthylamide, and the target amide was not observed.⁹³ Characterization of reaction intermediate **154** enabled reassessment of the DCC product observed by TLC from reaction of acid **143** and amine **136** (Figure 48). The ester **148** was likely the new spot visible upon TLC analysis.

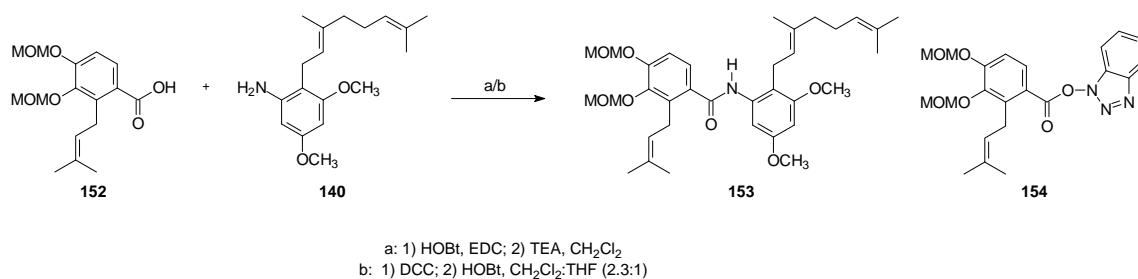


Figure 50. Attempted carbodiimide coupling reactions

As shown in Figure 51, an attempt to recycle ester **154** was made. A mixture of amine **140**, KHMDS, and ester **154** was allowed to react in order to obtain the corresponding amide **153**. The reaction was conducted on a 0.05 mmol scale of ester **154**. Only 4 mg of product was isolated, and the ¹H NMR spectrum showed a 2:1 mixture of amide **153** : acid **152** which had been carried through from the previous step. The presence of the acid **152** was verified by the ¹³C NMR spectrum, in addition to a DEPT experiment, and confirmed by GCMS. Because only a trace amount of amide **153** was obtained, the material was not carried forward.

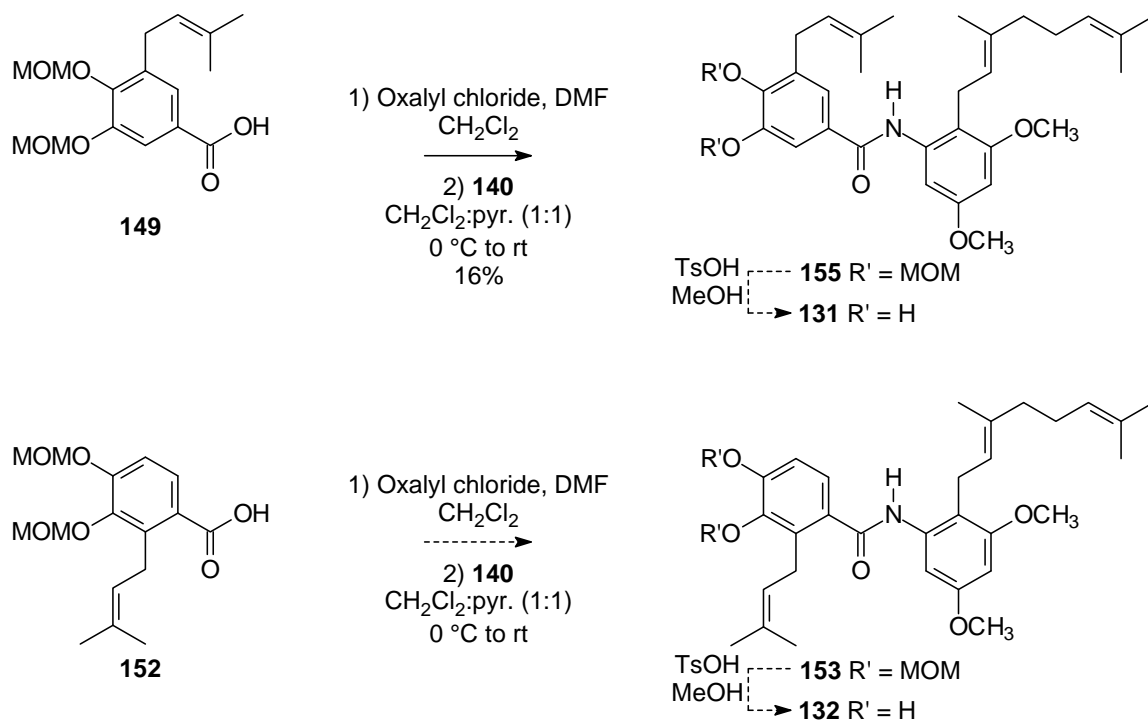


Figure 52. Synthesis of amide **155**

Amides **131** and **132** also might be made from the corresponding imine, a strategy where coupling would be done prior to oxidation. Representative amide **156** (Figure 53) could be envisioned to arise from imine **157** through Pinnick oxidation.⁹⁴ The imine would be provided through condensation of representative aldehyde **158** and amine **140**.⁹⁵

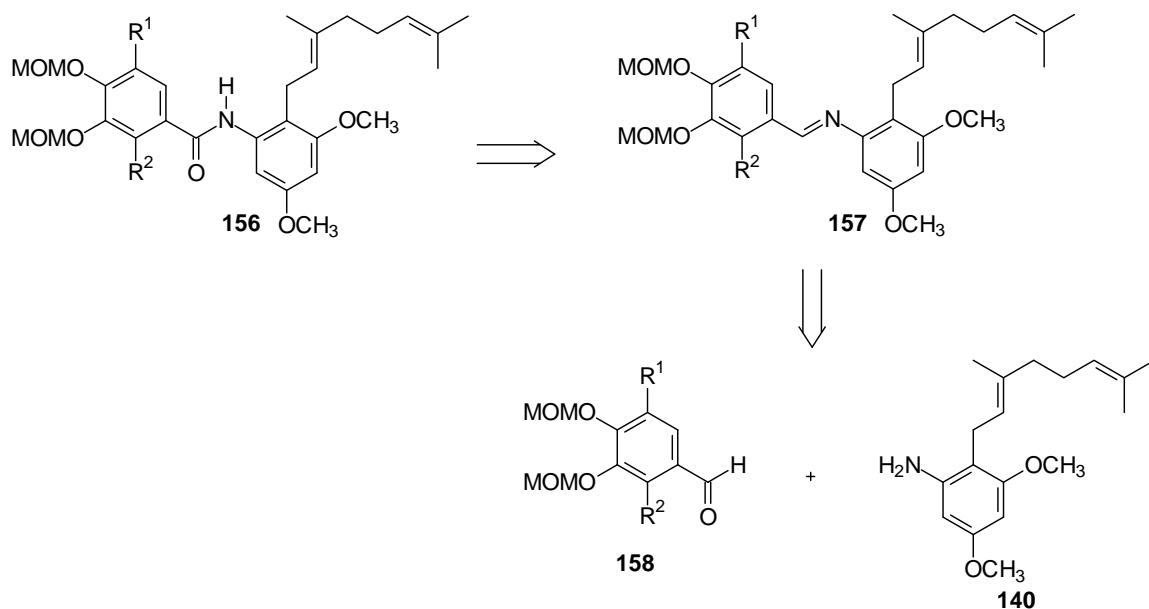


Figure 53. Retrosynthesis of analogues **131** and **132** via imine

As shown in Figure 54, condensation of aldehyde **151** and amine **140** in the presence of NH_4Cl only afforded a trace amount of imine **159**.⁹⁵ Simpler models of this reaction also were attempted, and conversion to the corresponding imine was equally poor. Due to the unsuccessful conversion to the imine **159**, Pinnick oxidation to amide **155** was not pursued. The poorly nucleophilic nature of amine **140** would also serve as an explanation for the low conversion to the imine product. Due to the loss of highly functionalized late-stage intermediates, attention was redirected toward the previously described routes.

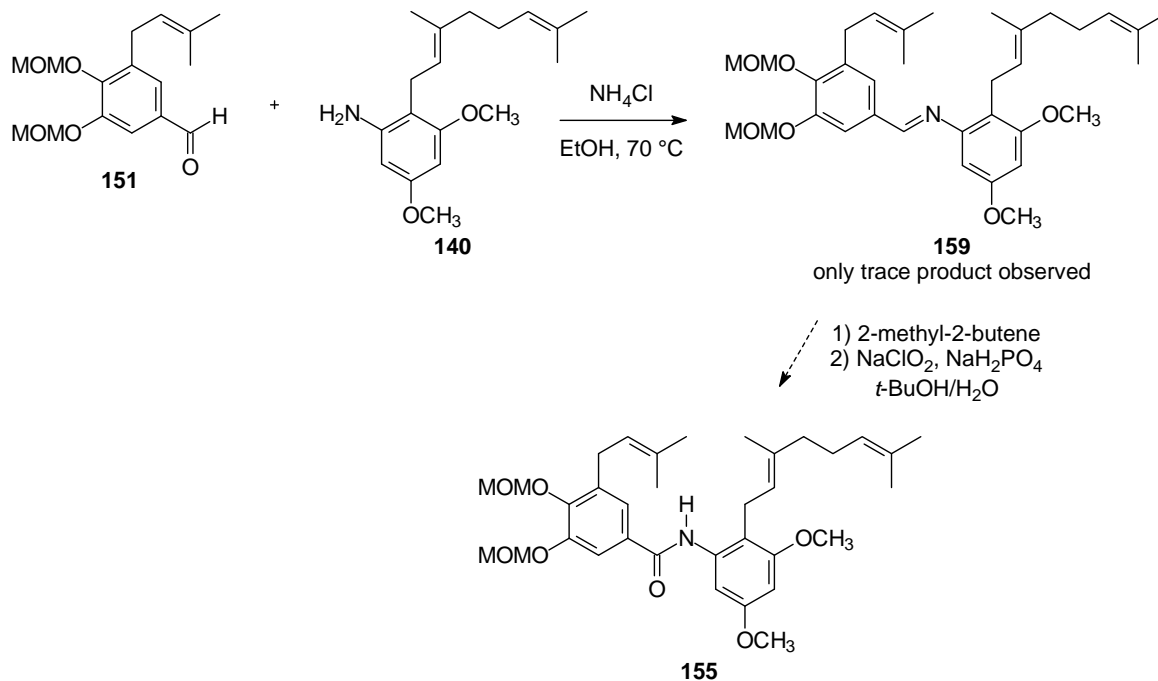


Figure 54. Synthesis of imine **159**

Many obstacles were encountered during these efforts to prepare the amide(s). Preparation of the geranylated amines was not straightforward. Mild conditions and sometimes long reaction times were necessary in reduction/hydrolysis to afford amines **139** and **140** in moderate to good yield. A number of oxidations were unsuccessful in providing carboxylic acids **149** and **152** with an intact prenyl group. Pinnick oxidation showed much better utility in forming the prenylated benzoic acids as long as an excess of 2-methyl-2-butane was added to the reaction vessel. There has been some success in carbodiimide couplings in that the intermediate HOBt ester **154** has been isolated. Reaction of the intermediate with base and amine **140** proved to be minimally effective in providing the MOM protected amide **153**. The difficulty in the coupling is perceived to be due to the weakly nucleophilic nature of the functionalized 3,5-dimethoxyanilines,

such as compound **135**, and not necessarily attributed to steric hindrance as originally thought in the earliest model reaction of compounds **139** and **143** toward amide **145**. For this reason, formation of imine **159** was also difficult. Increasing the electrophilic nature of the left half acid **149** was deemed necessary. Conversion to the acid chloride and treatment with amine **140** was effective in providing the MOM protected amide **155**.

Synthesis of the amide core linkage would introduce more polar groups into the pawhuskin scaffold. The amide shows promise in retaining the overall conformation because it would possess sp^2 character. Because the replacement is internal to the structure, it is likely that the relevant interactions necessary for opioid receptor activity will be maintained. Stilbene replacement in active compounds **79** and **90** should lower the $clogP$ by at least a factor of 100, and thereby more closely fit Lipinski's rules of drug design. Refinement of this synthetic scheme also might prove useful in other applications. Previously reported syntheses of the schweinfurthin stilbenes have been helpful in guiding efficient synthesis of target pawhuskin analogues. Similarly, design of amide analogues for the pawhuskins might be useful in providing potent schweinfurthin amides (**1–6**, Figure 55). This approach also could be applied to combretastatin A-1 (**160**)⁹⁶ and other resveratrol-like (**20**) compounds, as shown below in Figure 55.

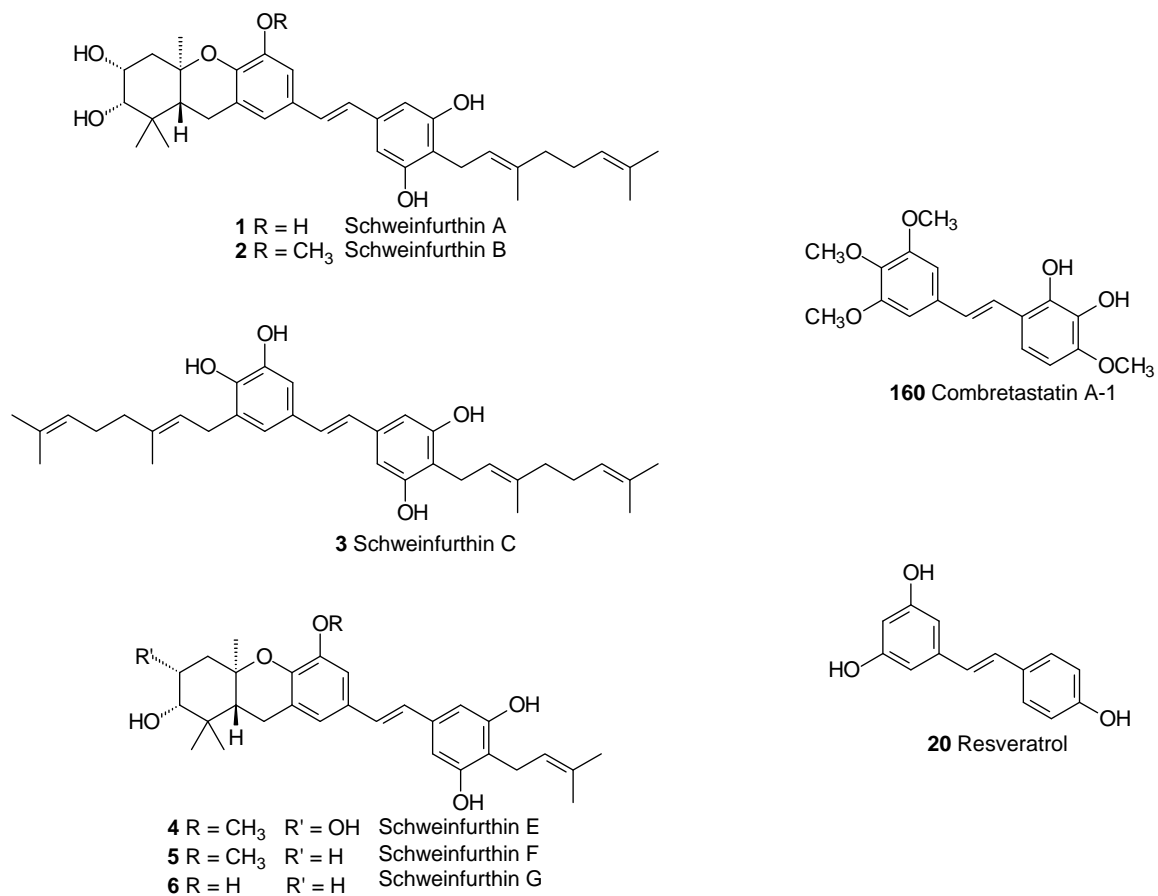


Figure 55. Potential applications of the amide core linkage

CHAPTER 7 SUMMARY AND FUTURE DIRECTIONS

In summary, a class of opioid receptor modulators known as the pawhuskins was first reported in 2004. The biological activity of these compounds is interesting given the absence of the traditional opioid pharmacophore which contains a basic nitrogen. Because of our extensive synthetic studies of prenylated stilbenes, we sought to elucidate the structural features of the non-nitrogenous opioid receptor antagonists that are required for their activity.

The studies reported here encompass the preparation of several compounds reminiscent of the schweinfurthin scaffold. The synthesis of pawhuskin A and C and analogues thereof has provided an understanding of the novel pawhuskin pharmacophores, especially that of pawhuskin A. The A-ring *para* hydrogen bond donation contact and the hydrophobic alkyl chain are necessary in pawhuskin A-opioid receptor binding. The location of the alkyl group, however, determines opioid receptor selectivity. A 3,4,5-pattern results in κ -selectivity, while the isomeric 2,3,4-pattern is far more attractive at the δ receptor. The length of the hydrophobic alkyl chain within the B-ring also appears to be an important factor in opioid receptor activity, while removal of the hydrogen bond donors in this ring does not abrogate the activity. Given the respective κ and δ potency, as well as selectivity, of isomeric structures **79** and **90**, further modifications of these targets are worth pursuing. Additionally, in structures similar to pawhuskin C, MOP receptor selectivity increased with increasing length of the hydrophobic alkyl chain and vice versa. Thus, our findings would support preparation of compounds selective for the κ - or δ - or μ -opioid receptors.

The bioassays conducted have been effective in identifying the potency and selectivity of the pawhuskin analogues to the opioid receptors. Because the assay has provided the K_e at each of the opioid receptors by displacement of the selective agonists, the KOP selectivity of pawhuskin A has been determined, as well as the κ -selectivity of

analogue **79**, the δ -selectivity of analogue **90**, and the μ -selectivity of schweinfurthin J. Given the minor structural changes from parent compounds found in these structures, the assay is an appropriate strategy to provide the necessary preliminary data and to guide future analogue design.

A new regioisomer was discovered in an already published directed *ortho* metallation reaction entailing formation of a dianion. The alkylated arene is prepared in just 3 steps from commercial 3,4-dihydroxybenzaldehyde while preparation of a similar schweinfurthin arene was done in 6 steps from commercial vanillin. Both isomers have proven useful, as target compounds **79** and **90** demonstrated the greatest affinity for the opioid receptors. The temperature at which directed *ortho* metallation was conducted had an effect on product distribution. In addition, a large protecting group proved to have an effect on distribution of products, albeit a retro-Brook rearrangement was a competing mechanism.

The synthesis of the pawhuskin amide posed many challenges. Deacylation/hydrolysis of the acetanilide afforded the amine in modest yields and sometimes required substantial reaction duration. Many oxidations were ineffective in providing the target carboxylic acid, but a carefully planned Pinnick oxidation showed great utility in forming the product without alkenyl chain degradation. Success was minimal in carbodiimide couplings and condensation to the imine. Nevertheless, a useful HOBt ester intermediate was isolated and this material was recycled providing a trace amount of the target amide. The difficulty in forming the amide and imine was perceived to be due to the weakly nucleophilic nature of the functionalized aniline employed. However, compensation for the weak nucleophile was achieved by formation of a more reactive acid chloride electrophile, and preparation of an amide analogue of pawhuskin A was accomplished.

Since the onset of these studies, the crystal structure of the human κ -opioid receptor has been published⁹⁷ in a complex with the antagonist JD₁Tic (**161**, Figure 56).

However, the structure of the piperidine-containing compound **161** varies considerably from the pawhuskin scaffold, and it is difficult to make assumptions on pawhuskin–KOP receptor binding from the available data. Until more structural information on the κ -opioid receptor is available, further investigations of the biological activity of pawhuskin analogues will have to proceed through synthesis and bioassay. The research described in this thesis provides a firm foundation for such studies.

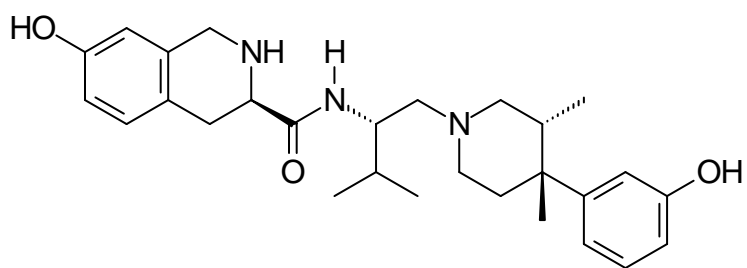


Figure 56. Selective KOP receptor antagonist JDTic (**161**)

CHAPTER 8 EXPERIMENTAL PROCEDURES

General experimental conditions. Both tetrahydrofuran (THF) and diethyl ether (Et₂O) were freshly distilled from sodium and benzophenone. Both methylene chloride (CH₂Cl₂) and triethylamine (Et₃N) were distilled from calcium hydride prior to use. Solutions of *n*-BuLi were purchased from a commercial source and titrated with diphenylacetic acid prior to use. All other reagents and solvents were purchased from commercial sources and used without further purification. All reactions in nonaqueous solvents were conducted in flame-dried glassware under a positive pressure of Ar and with magnetic stirring. NMR spectra were obtained at 300–600 MHz for ¹H and 75–150 MHz for ¹³C with CDCl₃ or CD₃OD as solvent and (CH₃)₄Si (¹H, 0.00 ppm) or CDCl₃ (¹³C, 77.0 ppm) or CD₃OD (¹H of CHD₂OD at 4.78 ppm, ¹³C, 49.0 ppm) as internal standards unless otherwise noted. The ³¹P NMR chemical shifts were reported in ppm downfield relative to 85% H₃PO₄ (external standard). High-resolution mass spectra were obtained at the University of Iowa Mass Spectrometry Facility. Silica gel (60 Å, 0.040–0.063 mm) was used for flash chromatography. Bioassays were conducted according to the procedure as previously described.¹⁶

Alcohol 36. To a stirred solution of ester **35** (9.03 g, 53.7 mmol) in CH₂Cl₂ (250 mL) at 0 °C was added DIPEA (28.1 mL, 161 mmol), followed by dropwise addition of MOMCl (9.38 mL, 123.5 mmol). After stirring for 17 h, the reaction was quenched by addition of NH₄Cl, extracted with CH₂Cl₂, washed with 2M NaOH, dried (MgSO₄), filtered, and concentrated *in vacuo* to afford the bis(methoxymethyl) acetal (13.8 g, 95%) as a yellow oil. The ¹H NMR spectrum matched known data.⁵⁶ To a stirred solution of bis(methoxymethyl) acetal (5.02 g, 19.6 mmol) in THF (125 mL) at 0 °C was added LiAlH₄ (1.53 g, 40.2 mmol) in portions. The reaction was allowed to stir for 17 h, and then was diluted with EtOAc and slowly quenched by addition of H₂O and 1M HCl. The

resulting mixture was extracted with EtOAc, dried (MgSO₄), filtered, and concentrated *in vacuo*. Final purification by flash column chromatography (30% EtOAc in hexanes) provided benzyl alcohol **36** (3.53 g, 79%) as a pale yellow oil. The ¹H NMR spectrum matched known data.⁵⁴

THP acetal 37. To a stirred solution of alcohol **36** (3.53 g, 15.5 mmol) in CHCl₃ (250 mL) at room temperature was added NBS (2.76 g, 15.5 mmol) in small portions. The reaction was allowed to stir for 2 h, and then was quenched by addition of NaHCO₃. After addition of aqueous Na₂S₂O₃, the mixture was extracted with CHCl₃. The combined organic extracts were washed with brine, dried (MgSO₄), filtered, and concentrated *in vacuo* to afford the aryl bromide (4.76 g, 100%) as a golden oil. The ¹H NMR spectrum matched known data.⁹⁸ The PPTS (40 mg, 1.6 mmol) was added to a stirred solution of bromide (4.76 g, 15.5 mmol) and DHP (4.25 mL, 46.9 mmol) in CH₂Cl₂ (30 mL) under an argon atmosphere. The reaction was allowed to stir overnight, and then quenched by addition of NaHCO₃. The mixture was extracted with Et₂O, dried (NaSO₄), filtered, and concentrated *in vacuo*. The desired tetrahydropyran acetal **37** was obtained as a yellow oil (5.99 g, 86%): ¹H NMR (500 MHz, CDCl₃) δ 6.95 (d, *J* = 2.7 Hz, 1H), 6.81(d, *J* = 2.8 Hz, 1H), 5.22 (s, 2H), 5.16 (d, *J* = 1.1 Hz, 2H), 4.80–4.77 (m, 2H), 4.57 (d, *J* = 13.6 Hz, 1H), 3.95–3.90 (m, 1H), 3.58–3.54 (m, 1H), 3.51 (s, 3H), 3.47 (s, 3H), 1.94–1.54 (m, 6H); ¹³C NMR (125 MHz, CDCl₃) δ 157.1, 154.2, 139.9, 109.7, 104.9, 103.7, 98.3, 95.1, 94.5, 68.5, 62.0, 56.3, 56.0, 30.4, 25.3, 19.2; HRMS (EI) *m/z* calcd for C₁₆H₂₃O₆Br (M)⁺ 390.0678, found 390.0670.

Geranylated arene 38. To a solution of *n*-BuLi (2.4 M in hexanes, 1.3 mL, 3.1 mmol) in Et₂O (30 mL) at –10 °C was added bromide **37** (1.01 g, 2.6 mmol) dissolved in Et₂O (2 mL) dropwise. After the reaction was allowed to stir for 15 min, the geranyl bromide (0.7 mL, 3.5 mmol) was added over 7 min. Once allowed to stir overnight, the reaction

was quenched by addition of NH_4Cl . The mixture was extracted with EtOAc, and then the combined organic extracts were washed with brine, dried (MgSO_4), filtered, and concentrated *in vacuo*. Final purification by flash column chromatography afforded geranylated compound **38** (562 mg, 49%) as a yellow oil: ^1H NMR (300 MHz, CDCl_3) δ 6.81 (s, 1H), 6.77 (s, 1H), 5.16 (s, 2H), 5.14 (s, 2H), 5.09–5.06 (m, 2H), 4.77–4.71 (m, 2H), 4.46 (d, $J = 12$ Hz, 1H), 3.91 (t, $J = 8.7$ Hz, 1H), 3.56–3.52 (m, 1H), 3.47 (s, 3H), 3.45 (s, 3H), 3.37 (d, $J = 6.0$ Hz, 2H), 2.22–1.80 (m, 5H), 1.77 (s, 3H), 1.64 (s, 3H), 1.51 (s, 3H); ^{13}C NMR (75 MHz, CDCl_3) δ 155.9, 155.7, 138.0, 134.3, 131.1, 124.2, 123.1, 122.9, 109.5, 102.6, 97.8, 94.4 (2C), 66.7, 61.9, 55.8 (2C), 39.6, 30.4, 26.5, 25.5, 25.4, 24.3, 19.2, 17.5, 16.0; HRMS (ESI) m/z calcd for $\text{C}_{26}\text{H}_{40}\text{O}_6\text{Na}$, $(\text{M} + \text{Na})^+$ 471.2723, found 471.2733.

Benzylic alcohol 39. To a solution of the THP acetal **38** (500 mg, 1.1 mmol) in MeOH (20 mL) at 0 °C was added TsOH (234 mg, 1.1 eq). The reaction was monitored at 5 to 10 min intervals via TLC analysis. After 80 min the reaction was quenched by addition of NaHCO_3 , and the mixture was extracted with EtOAc. The combined organic extracts were washed with brine, dried (MgSO_4), filtered, and concentrated by rotary evaporation. Final purification by flash column chromatography (20% EtOAc in hexanes) provided alcohol **39** (27 mg, 66%) as a yellow oil. The ^1H NMR spectrum matched published data.⁵⁶

Aldehyde 34. Activated MnO_2 (644 mg, 5.0 mmol) was added to a solution of alcohol **39** (267 mg, 0.7 mmol) in CH_2Cl_2 (15 mL) at room temperature, and the mixture was stirred overnight. The mixture was filtered, and the filtrate was concentrated *in vacuo*. Final purification by flash column chromatography (50% EtOAc in hexanes) afforded aldehyde **34** (256 mg, 96%) as a yellow oil: ^1H NMR (300 MHz, CDCl_3) δ 10.26 (s, 1H), 7.21 (d, $J = 2.7$ Hz, 1H), 7.04 (d, $J = 2.2$ Hz, 1H), 5.21 (s, 2H), 5.19 (s, 2H), 5.14–5.10

(m, 1H), 5.05–5.00 (m, 1H), 3.73 (d, $J = 6.5$ Hz, 2H), 3.48 (s, 6H), 2.08–1.93 (m, 4H), 1.86 (s, 3H), 1.73 (s, 3H), 1.65 (s, 3H); ^{13}C NMR (125 MHz, CDCl_3) δ 191.6, 156.3, 156.2, 135.3 (2C), 131.5, 128.1, 124.1, 123.2, 109.3, 108.7, 94.7, 94.5, 56.2, 56.1, 39.6, 26.6, 25.6, 22.9, 17.6, 16.3; HRMS (ESI) m/z calcd for $\text{C}_{21}\text{H}_{30}\text{O}_5\text{Na}$ ($\text{M} + \text{Na}$) $^+$ 385.1991, found 385.1983.¹⁶

Stilbene 45. To a solution of phosphonate **44**¹⁶ (44 mg, 0.011 mmol) and aldehyde **34** (34 mg, 0.09 mmol) in THF (1.5 mL) was added potassium hexamethyldisilazane (KHMDS) (0.5 M as a solution in toluene, 0.86 mL, 0.430 mmol). After the reaction stirred for 20 h, it was quenched by addition of NH_4Cl . The resulting mixture was extracted with EtOAc, washed with brine, dried (MgSO_4), filtered, and concentrated *in vacuo*. Final purification by flash column chromatography (1% EtOAc in hexanes) provided stilbene **45** (38 mg, 68%) as a yellow oil: ^1H NMR (300 MHz, CDCl_3) δ 7.31 (d, $J = 8.7$ Hz, 1H), 7.09 (s, 2H), 6.93 (d, $J = 2.2$ Hz, 1H), 6.79 (d, $J = 9.1$ Hz, 1H), 6.74 (d, $J = 2.2$ Hz, 1H), 5.18–5.08 (m, 9H), 3.85 (s, 3H), 3.60–3.55 (m, 5H), 3.49–3.44 (m, 8H), 2.05–1.94 (m, 4H), 1.79 (s, 6H), 1.68 (s, 3H), 1.62 (s, 3H), 1.55 (s, 3H); ^{13}C NMR (75 MHz, CDCl_3) δ 156.1, 155.8, 151.8, 143.8, 138.7, 134.5, 134.3, 131.5, 131.3, 130.6, 128.4, 126.7, 124.3, 123.4, 123.3, 123.2, 122.8, 121.9, 110.1, 106.5, 102.7, 99.0, 94.7, 57.6, 56.0 (2C), 55.7, 39.7, 26.7, 25.8, 25.6 (2C), 24.7, 18.1, 17.6, 16.3; HRMS (EI) m/z calcd for $\text{C}_{36}\text{H}_{50}\text{O}_7$ (M) $^+$ 594.3557, found 594.3569.

Analogue 46. After TsOH (36 mg, 0.19 mmol) was added to a solution of stilbene **45** (19 mg, 0.03) in MeOH (3 mL), the reaction was allowed to stir for 23.5 h and then it was quenched by addition of NaHCO_3 . The resulting mixture was extracted with EtOAc, dried (MgSO_4), filtered, and concentrated *in vacuo*. Final purification by preparative TLC (30% EtOAc in hexanes) delivered phenol **46** (6 mg, 41%) as a yellow oil: ^1H NMR (500 MHz, CD_3OD) δ 6.98–6.89 (m, 3H), 6.68 (d, $J = 8.6$ Hz, 1H), 6.44 (d, $J = 2.4$

Hz, 1H), 6.14 (d, $J = 2.3$ Hz, 1H), 5.05–4.99 (m, 2H), 4.95–4.92 (m, 1H), 3.77 (s, 3H), 3.38 (d, $J = 6.8$ Hz, 2H), 3.27 (d, $J = 6.9$ Hz, 2H), 1.96–1.85 (m, 4H), 1.70 (s, 3H), 1.66 (s, 3H), 1.57 (s, 3H), 1.47 (s, 3H), 1.41 (s, 3H); ^{13}C NMR (125 MHz, CD_3OD) δ 157.0, 156.8, 148.2, 145.0, 140.1, 134.4, 132.1, 131.8 (2C), 128.8, 128.1, 127.5, 125.9, 125.4, 124.5, 119.2, 117.8, 109.9, 104.6, 102.7, 56.4, 40.9, 27.8, 26.0 (2C), 25.8, 25.1, 18.2, 17.7, 16.5; HRMS (EI) m/z calcd for $\text{C}_{30}\text{H}_{38}\text{O}_4$ (M) $^+$ 462.2770, found 462.2785.

Phosphonate 48. Triethylamine (0.81 mL, 5.8 mmol) was added to a solution of alcohol **47** (875 mg, 3.8 mmol) in THF (7 mL) at 0 °C. After dropwise addition of methanesulfonyl chloride (0.39 mL, 5.0 mmol), the reaction was allowed to stir for 30 min and lithium bromide (502 mg, 5.8 mmol) in THF (4 mL) was added. After it was stirred for 3.5 h, the reaction mixture was diluted with EtOAc, washed with brine, dried (MgSO_4), filtered, and concentrated *in vacuo*. Triethyl phosphite (2 mL, 11.7 mmol) was added, and the solution was heated to 89 °C. The reaction was allowed to stir for 17 h, cooled, and concentrated *in vacuo* at 60 °C overnight. Final purification by flash column chromatography (90% EtOAc in hexanes) afforded phosphonate **48** (312 mg, 23%) as a yellow oil. The ^1H NMR spectrum matched that of the known compound.⁹⁹

Phosphonate 50. To a solution of alcohol **49** (958 mg, 5.7 mmol) in THF (30 mL) at 0 °C was added triethylamine (1.20 mL, 8.5 mmol), and then methanesulfonyl chloride (0.57 mL, 7.4 mmol) was added dropwise. After it was stirred for 60 min, LiBr (746 mg, 8.6 mmol) in THF (3 mL) was added and the reaction was allowed to stir for 19 h. The resulting mixture was diluted with EtOAc, washed with brine, dried (Na_2SO_4), filtered through basic alumina, and concentrated *in vacuo*. Triethyl phosphite (3.0 mL, 17.5 mmol) was added to the neat oil, the reaction was heated to 90 °C, and then allowed to stir for 20 h. The mixture was concentrated *in vacuo* at 60 °C overnight. Final purification by flash column chromatography (1% EtOH in CH_2Cl_2) afforded

phosphonate **50** (507 mg, 31%) as a yellow oil. The ^1H NMR spectrum was identical to literature data.¹⁰⁰

Phosphonate 52. Triethylamine (1.25 mL, 8.9 mmol) was added to a solution of **51** (1.00 g, 6.0 mmol) in THF (45 mL) at 0 °C and then methanesulfonyl chloride (0.60 mL, 7.7 mmol) was added dropwise. After 45 min of stirring, LiBr (777 mg, 9.0 mmol) in THF (4 mL) was added. The reaction was allowed to stir for 2 h, washed with brine, dried (MgSO_4), filtered, and concentrated *in vacuo*. To the resulting mixture was added triethyl phosphite (2 mL, 11.7 mmol). The reaction was heated to 90 °C, allowed to stir for 15 h, and then concentrated *in vacuo* at 60 °C overnight. Final purification by flash column chromatography (1% EtOH in CH_2Cl_2) provided phosphonate **52** (1.57 g, 92%) as a yellow oil. Both the ^1H and ^{31}P NMR spectra match known data.⁵

Stilbene 53. To a solution of KHMDS (0.5 M solution in toluene, 2.3 mL, 1.16 mmol) in THF (1.5 mL) were added phosphonate **48** (46 mg, 0.13 mmol) and aldehyde **34** (35 mg, 0.10 mmol). After the solution was stirred for 4 h, the reaction was quenched by addition of NH_4Cl . The resulting mixture was extracted with EtOAc, washed with brine, dried (MgSO_4), filtered, and concentrated *in vacuo*. Final purification by flash column chromatography (7% EtOAc in hexanes) provided stilbene **53** (46 mg, 86%) as a yellow oil: ^1H NMR (500 MHz, CDCl_3) δ 7.31–7.11 (m, 4H), 6.96 (s, 1H), 6.88 (d, $J = 15.7$ Hz, 1H), 6.74 (s, 1H), 5.27–5.05 (m, 10H), 3.54–3.48 (m, 14H), 2.04–1.97 (m, 4H), 1.82 (s, 3H), 1.61 (s, 3H), 1.54 (s, 3H); ^{13}C NMR (125 MHz, CDCl_3) δ 156.1, 155.8, 147.4, 146.9, 138.2, 134.5, 132.4, 131.3, 130.1, 125.5, 124.2, 123.3, 122.8, 120.9, 116.7, 114.8, 106.2, 102.9, 95.5, 95.4, 94.6 (2C), 56.2 (2C), 56.0 (2C), 39.7, 26.7, 25.6, 24.7, 17.6, 16.2; HRMS (EI) m/z calcd for $\text{C}_{32}\text{H}_{44}\text{O}_8$ (M)⁺ 556.3036, found 556.3056.¹⁶

Analogue 54. To a solution of stilbene **53** (23 mg, 0.04 mmol) in MeOH (4 mL) was added TsOH (63 mg, 0.33 mmol). The solution was stirred for 24 h, and the reaction was quenched by addition of NaHCO₃. The resulting mixture was extracted with EtOAc, dried (MgSO₄), filtered, and concentrated in vacuo. Final purification by preparative TLC (30% EtOAc in hexanes) afforded stilbene **54** (6 mg, 38%) as a yellow oil: ¹H NMR (500 MHz, CD₃OD) δ 6.96 (d, *J* = 16 Hz, 1H), 6.85 (d, *J* = 2.3 Hz, 1H), 6.71 (d, *J* = 2 Hz, 1H), 6.70 (d, *J* = 1.7 Hz, 1H), 6.65 (d, *J* = 15.8 Hz, 1H), 6.63 (d, *J* = 8.3 Hz, 1H), 6.44 (d, *J* = 2.1 Hz, 1H), 6.13 (d, *J* = 2.3 Hz, 1H), 5.01–5.00 (m, 1H), 4.95–4.92 (m, 1H), 3.27 (d, *J* = 6.6 Hz, 2H), 1.97–1.92 (m, 2H), 1.88–1.85 (m, 2H), 1.70 (s, 3H), 1.47 (s, 3H), 1.42 (s, 3H); ¹³C NMR (125 MHz, CD₃OD) δ 157.0, 156.7, 146.5, 146.4, 139.8, 134.5, 132.1, 131.6, 130.7, 125.8, 125.4 (2C), 120.0, 119.1, 116.4, 114.0, 104.3, 102.6, 40.8, 27.8, 25.8, 25.1, 17.7, 16.5; HRMS (EI) *m/z* calcd for C₂₄H₂₈O₄ (M)⁺ 380.1988, found 380.2014.¹⁶

Stilbene 55. Aldehyde **34** (34 mg, 0.09 mmol) and phosphonate **50** (51 mg, 0.18 mmol) were added to a solution of KHMDS (0.5 M solution in toluene, 2.25 mL, 1.13 mmol) in THF (1.5 mL). After it was stirred for 4 h, the reaction was quenched by addition of NH₄Cl. The resulting mixture was extracted with EtOAc, washed with brine, dried (MgSO₄), filtered, and concentrated *in vacuo*. Final purification by flash column chromatography (7% EtOAc in hexanes) made available stilbene **55** (34 mg, 73%) as a yellow oil: ¹H NMR (300 MHz, CDCl₃) δ 7.42 (d, *J* = 8.3 Hz, 2H), 7.20 (d, *J* = 16.1 Hz, 1H), 7.02 (d, *J* = 8.4 Hz, 2H), 6.97–6.88 (m, 2H), 6.74 (d, *J* = 2.2 Hz, 1H), 5.23–5.03 (m, 8H), 3.50–3.45 (m, 11H), 2.05–1.95 (m, 4H), 1.80 (s, 3H), 1.61 (s, 3H), 1.54 (s, 3H); ¹³C NMR (75 MHz, CDCl₃) δ 156.9, 156.1, 155.8, 138.4, 134.5, 131.6, 131.3, 130.0, 127.7 (2C), 127.4, 125.0, 124.2, 123.4, 122.8, 116.4 (2C), 106.2, 102.8, 94.7, 94.4, 56.0 (3C), 39.7, 26.7, 25.6, 24.7, 17.6, 16.3; HRMS (EI) *m/z* calcd for C₃₀H₄₀O₆ (M)⁺ 496.2825, found 496.2824.

Analogue 56. To a solution of stilbene **55** (17 mg, 0.03 mmol) in MeOH (2.5 mL) was added TsOH (39 mg, 0.21 mmol). After the reaction stirred for 2 d at rt, it was quenched by addition of NaHCO₃. The mixture was extracted with EtOAc, and the combined organic extracts were dried (MgSO₄), filtered, and concentrated *in vacuo*. Final purification by preparative TLC (30% EtOAc in hexanes) delivered phenol **56** (19 mg, 50%) as a yellow oil: ¹H NMR spectrum matched known data¹⁰¹; ¹³C NMR (125 MHz, CDCl₃) δ 155.6, 155.4, 154.5, 138.8, 137.5, 131.9, 130.6, 130.4, 128.0 (2C), 124.4, 123.8, 122.4, 117.7, 115.6 (2C), 105.2, 102.6, 39.6, 26.5, 25.6, 25.0, 17.7, 16.3; HRMS (EI) *m/z* calcd for C₂₄H₂₈O₃ (M)⁺ 364.2038, found 364.2037.

Stilbene 57. To a solution of KHMDS (0.5 M solution in toluene, 2.6 mL, 1.30 mmol) in THF (1.5 mL) was added phosphonate **52** (51 mg, 0.18 mmol) and aldehyde **34** (40 mg, 0.11 mmol). After it was stirred for 3.5 h, the reaction was quenched by addition of NH₄Cl. The resultant mixture was extracted with EtOAc, washed with brine, dried (MgSO₄), filtered, and concentrated *in vacuo*. Final purification by flash column chromatography (10% EtOAc in hexanes) yielded product **57** (53 mg, 96%) as a yellow oil: ¹H NMR (500 MHz, CDCl₃) δ 7.33–7.25 (m, 2H), 7.16–7.14 (m, 2H), 6.97–6.91 (m, 3H), 6.76 (s, 1H), 5.20–5.19 (m, 6H), 5.13 (t, *J* = 6 Hz, 1H), 5.05 (t, *J* = 6.1 Hz, 1H), 3.50–3.46 (m, 11H), 2.05–1.96 (m, 4H), 1.81 (s, 3H), 1.61 (s, 3H), 1.54 (s, 3H); ¹³C NMR (125 MHz, CDCl₃) δ 157.6, 156.1, 155.8, 139.1, 138.0, 134.6, 131.3, 130.4, 129.6, 127.1, 124.2, 123.3, 123.0, 120.3, 115.5, 114.3, 106.4, 103.1, 94.7 (2C), 94.4, 56.0 (2C), 55.9, 39.7, 26.7, 25.6, 24.7, 17.6, 16.3; HRMS (EI) *m/z* calcd for C₃₀H₄₀O₆ (M)⁺ 496.2825, found 496.2847.

Analogue 58. To a solution of **57** (27 mg, 0.05 mmol) in MeOH (10 mL) was added TsOH (96 mg, 0.51 mmol). The reaction was allowed to stir for 24 h, and then was

quenched by addition of NaHCO₃. The organic materials were extracted with EtOAc, dried (MgSO₄), filtered, and concentrated *in vacuo*. Final purification of the residue by flash column chromatography (10% EtOAc in hexanes) provided phenol **58** (11 mg, 56%) as a yellow oil: ¹H NMR (400 MHz, CD₃OD) δ 7.15 (d, *J* = 16.2 Hz, 1H), 7.04 (t, *J* = 7.8 Hz, 1H), 6.85–6.83 (m, 1H), 6.82–6.81 (m, 1H), 6.72 (d, *J* = 16.1 Hz, 1H), 6.57 (ddd, *J* = 8.1 Hz, 2.6 Hz, 1.1 Hz, 1H), 6.47 (d, *J* = 2.3 Hz, 1H), 6.18 (d, *J* = 2.2 Hz, 1H), 5.04–5.00 (m, 1H), 4.95–4.91 (m, 1H), 3.29 (d, *J* = 6.9 Hz, 2H), 1.97–1.84 (m, 4H), 1.70 (s, 3H), 1.46 (s, 3H), 1.41 (s, 3H); ¹³C NMR (100 MHz, CD₃OD) δ 158.8, 157.1, 156.8, 140.7, 139.3, 134.6, 132.1, 130.6, 128.3, 125.8, 125.4, 119.5, 119.1, 115.5, 114.0, 104.5, 103.0, 101.4, 40.8, 27.7, 25.8, 25.1, 17.7, 16.5; HRMS (EI) *m/z* calcd for C₂₄H₂₈O₃ (M)⁺ 364.2038, found 364.2044.

Aldehyde 60. To a solution of **59** (151 mg, 1.1 mmol) and DIPEA (0.57 mL, 3.3 mmol) in CH₂Cl₂ (10 mL) at 0 °C was added MOMCl (0.30 mL, 4.0 mmol). The reaction was allowed to stir for 21 h, and then it was quenched by addition of NH₄Cl and extracted with CH₂Cl₂. The extracts were washed with 2M NaOH, dried (MgSO₄), filtered, and concentrated *in vacuo*. Bis(methoxymethyl) ether **60** (252 mg, 100% by ¹H NMR) was obtained as a yellow oil, with ¹H NMR data that matched the literature spectrum.⁵⁴

Alcohol 47. To a solution of aldehyde **60** (3.13 g, 13.8 mmol) in THF (150 mL) at 0 °C was added LiAlH₄ (1.58 g, 41.5 mmol). The reaction was allowed to stir for 23 h and then quenched by the slow addition of 1M HCl. The resulting mixture was extracted with EtOAc, and the extracts were washed with brine, dried (MgSO₄), filtered, and concentrated *in vacuo* to afford alcohol **47** (2.70 g, 86%) as a pale yellow oil. The ¹H NMR spectrum matched known data.⁵⁶

Prenylated arene 61. Alcohol **47** (719 mg, 3.2 mmol) in Et₂O (4 mL) was added dropwise to a solution of *n*-BuLi (2.4 M solution in hexanes, 2.9 mL, 7.0 mmol) and TMEDA (1.0 mL, 6.7 mmol) in Et₂O (50 mL) at -10 °C. The mixture was allowed to stir for 15 min and then solid CuI (600 mg, 3.2 mmol) was added. Once the reaction turned a dark gray color (10 min) prenyl bromide (0.40 mL, 3.4 mmol) in Et₂O (5 mL) was added dropwise (~7 min). The reaction was allowed to warm from -10 °C to rt and stir at rt for 17 h and then quenched by the addition of H₂O, extracted with Et₂O, dried (MgSO₄), and filtered, and the filtrate was concentrated *in vacuo*. Final purification by flash column chromatography (10% EtOAc in hexanes) afforded prenylated compound **61** (254 mg, 27%) as a light yellow oil: ¹H NMR (500 MHz, CDCl₃) δ 7.01 (d, *J* = 2.0 Hz, 1H), 6.83 (d, *J* = 1.8 Hz, 1H), 5.31–5.28 (m, 1H), 5.19 (s, 2H), 5.10 (s, 2H), 4.59 (d, *J* = 3.4 Hz, 2H), 3.60 (s, 3H), 3.50 (s, 3H), 3.41 (d, *J* = 7.3 Hz, 2H), 1.74 (s, 3H), 1.72 (s, 3H); ¹³C NMR (75 MHz, CDCl₃) δ 149.6, 143.8, 137.0, 136.0, 132.5, 122.5, 121.4, 112.6, 98.9, 94.9, 64.8, 57.3, 56.1, 28.4, 25.6, 17.7; HRMS (ESI) *m/z* calcd for C₁₆H₂₄O₅Na (M + Na)⁺ 319.1521, found 319.1523.

Phosphonate 62. To a solution of alcohol **61** (920 mg, 3.1 mmol) in THF (30 mL) at 0 °C was added TEA (0.65 mL, 4.6 mmol), then MsCl (0.31 mL, 4.0 mmol). The mixture was allowed to stir for 2.75 h, and due to incomplete conversion to the mesylate, additional TEA (0.65 mL, 4.6 mmol) and MsCl (0.31 mL, 4.0 mmol) were added. After the reaction was allowed to stir for 50 min, dilute LiBr (404 mg, 4.7 mmol) in THF (4 mL) was added. The reaction was stirred for 16 h, and then was diluted with EtOAc. The resulting mixture was washed with brine. The combined organics were dried (Na₂SO₄), filtered, and concentrated *in vacuo*. Triethyl phosphite (2 mL, 11.7 mmol) was added to the neat oil, the reaction was heated to 90 °C, and the reaction was allowed to stir overnight (~22 h). The mixture was concentrated *in vacuo* at 60 °C overnight. Final purification of the residue by flash column chromatography (1% EtOH in CH₂Cl₂)

provided phosphonate **62** (911 mg, 70%) as a pale yellow oil: ^1H NMR (500 MHz, CDCl_3) δ 6.93 (t, $J = 2.4$ Hz, 1H), 6.75 (t, $J = 2.4$ Hz, 1H), 5.30–5.26 (m, 1H), 5.17 (s, 2H), 5.08 (s, 2H), 4.05–3.99 (m, 4H), 3.59 (s, 3H), 3.49 (s, 3H), 3.38 (d, $J = 7.2$ Hz, 2H), 3.06 (d, $J_{\text{HP}} = 21.3$ Hz, 2H), 1.73 (s, 3H), 1.71 (s, 3H), 1.26 (t, $J = 7.0$ Hz, 6H); ^{13}C NMR (125 MHz, CDCl_3) δ 149.6 (d, $J_{\text{CP}} = 3.3$ Hz), 143.7 (d, $J_{\text{CP}} = 3.9$ Hz), 136.0 (d, $J_{\text{CP}} = 3.1$ Hz), 132.6, 127.4 (d, $J_{\text{CP}} = 9.2$ Hz), 124.4 (d, $J_{\text{CP}} = 6.8$ Hz), 122.6, 115.6 (d, $J_{\text{CP}} = 6.2$ Hz), 99.1 (d, $J_{\text{CP}} = 2.1$ Hz), 95.2, 62.0 (d, $J_{\text{CP}} = 6.8$ Hz), 57.4, 56.2, 33.9, 32.8, 28.4, 25.7, 17.8, 16.3 (2C); HRMS (ESI) m/z calcd for $\text{C}_{20}\text{H}_{33}\text{O}_7\text{NaP}$ ($\text{M} + \text{Na}$) $^+$ 439.1862, found 439.1862.

Stilbene 63. To a stirred solution of aldehyde **34** (31 mg, 0.09 mmol) and phosphonate **62** (59 mg, 0.14 mmol) in THF (1.7 mL) at 0 °C was added KHMDS (1.0 M in THF, 0.60 mL, 0.6 mmol). The reaction was stirred for 19 h, and then was quenched by addition of saturated aqueous NH_4Cl . The resultant mixture was extracted with EtOAc. The combined organics were washed with brine, dried (MgSO_4), filtered, and concentrated *in vacuo*. Final purification by preparative TLC (15% EtOAc in hexanes) provided stilbene **63** (24 mg, 45%) as a yellow oil: ^1H NMR (500 MHz, CDCl_3) δ 7.17 (d, $J = 16.0$ Hz, 1H), 7.13 (d, $J = 1.8$ Hz, 1H), 6.97 (d, $J = 1.8$ Hz, 1H), 6.94 (d, $J = 2.2$ Hz, 1H), 6.86 (d, $J = 15.9$ Hz, 1H), 6.74 (d, $J = 2.1$ Hz, 1H), 5.34–5.30 (m, 1H), 5.21 (s, 2H), 5.20–5.17 (m, 5H), 5.12 (s, 2H), 5.06–5.03 (m, 1H), 3.60 (s, 3H), 3.52 (s, 3H), 3.50 (s, 3H), 3.48 (s, 3H), 3.45 (d, $J = 6.8$ Hz, 2H), 3.42 (d, $J = 7.3$ Hz, 2H), 2.06–2.01 (m, 2H), 1.98–1.95 (m, 2H), 1.81 (s, 3H), 1.76 (s, 3H), 1.74 (s, 3H), 1.60 (s, 3H), 1.53 (s, 3H); ^{13}C NMR (125 MHz, CDCl_3) δ 156.1, 155.8, 150.0, 144.5, 138.3, 136.1, 134.4, 133.9, 132.7, 131.3, 130.4, 125.9, 124.2, 123.4, 122.9, 122.6, 121.6, 112.1, 106.3, 102.9, 99.1, 95.2, 94.7 (2C), 57.5, 56.2, 56.1 (2C), 39.7, 28.6, 26.7, 25.8, 25.6, 24.7, 17.9, 17.6, 16.3; HRMS (ESI) m/z calcd for $\text{C}_{37}\text{H}_{53}\text{O}_8$ ($\text{M} + \text{H}$) $^+$ 625.3740, found 625.3742.

Analogue 64. To a solution of MOM ether **63** (23 mg, 0.04 mmol) in MeOH (3.7 mL) was added TsOH (57 mg, 0.30 mmol). The reaction was allowed to stir for 24 h, then the reaction was quenched by the addition of saturated aqueous NaHCO₃, and the resultant mixture was extracted with EtOAc. The combined organics were dried (MgSO₄), filtered, and concentrated *in vacuo*. Final purification by preparative TLC (30% EtOAc in hexanes) afforded phenol **64** (8 mg of 1 : 1 mixture with diethyl phosphate; 6 mg of product alone, 35%) as a golden yellow oil: ¹H NMR (500 MHz, CDCl₃) δ 7.09 (d, *J* = 15.7 Hz, 1H), 6.93 (s, 1H), 6.78–6.74 (m, 2H), 6.64 (s, 1H), 6.36 (s, 1H), 5.34 (t, *J* = 6.7 Hz, 1H), 5.18 (t, *J* = 6.4 Hz, 1H), 5.05 (t, *J* = 6.4 Hz, 1H), 3.41 (d, *J* = 6.3 Hz, 2H), 3.37 (d, *J* = 7.1 Hz, 2H), 2.09–2.06 (m, 2H), 2.04–2.01 (m, 2H), 1.82 (s, 3H), 1.79 (s, 3H), 1.78 (s, 3H), 1.65 (s, 3H), 1.57 (s, 3H); ¹³C NMR (125 MHz, CDCl₃) δ 155.6, 154.7, 144.2, 142.1, 138.7, 137.2, 134.8, 131.8, 130.8, 130.3, 127.5, 124.6, 123.9, 122.6, 121.8, 120.3, 117.6, 111.1, 105.1, 102.6, 39.7, 29.7, 26.5, 25.8, 25.6, 24.9, 17.9, 17.7, 16.3; HRMS (ESI) *m/z* calcd for C₂₉H₃₇O₄ (M + H)⁺ 449.2692, found 449.2691.

Benzylic alcohol 67. To a solution of **35** (5.00 g, 29.6 mmol) in acetone (125 mL) at room temperature was added K₂CO₃ (12.3 g, 89.3 mmol). After 3 min, iodomethane (4.7 mL, 74.5 mmol) was added to the mixture. The reaction was heated at reflux, allowed to stir overnight, and then was quenched by addition of H₂O, and acidified with 1M HCl. The resulting mixture was extracted with EtOAc. The combined organic extracts were washed with 2M NaOH, dried (MgSO₄), filtered, and concentrated *in vacuo*. The dimethylated compound (5.84 g, 100%) was obtained as a yellow oil without additional purification. The ¹H NMR spectrum matched known data.¹⁰² The LiAlH₄ (2.26 g, 59.6 mmol) was added in portions to a solution of the ester (5.84 g, 29.8 mmol) in THF (250 mL) at 0 °C. The reaction was allowed to warm to room temperature while stirring overnight. The reaction mixture was slowly diluted with EtOAc, and then was quenched by the dropwise addition of H₂O. The resulting mixture was extracted with EtOAc, and

the combined organic extracts were dried (MgSO_4), filtered, and concentrated *in vacuo*. Final purification by flash column chromatography (30% EtOAc in hexanes) afforded benzylic alcohol **67** (4.05 g, 81%) as a white solid. The ^1H NMR spectrum matched the known data.¹⁰³

Bromide 68. To a stirred solution of compound **67** (562 mg, 3.3 mmol) in CHCl_3 at room temperature was added NBS (597 mg, 3.4 mmol) in small portions. The reaction was allowed to stir for 2 h, and then it was quenched by addition of saturated aqueous NaHCO_3 . After the addition of saturated aqueous $\text{Na}_2\text{S}_2\text{O}_3$, the resulting mixture was extracted with CHCl_3 . The combined organic extracts were washed with brine, dried (MgSO_4), filtered, and concentrated *in vacuo*. The aryl bromide **68** (776 mg, 94%) was obtained as an orange oil.⁷²

THP acetal 69. To a stirred solution of benzylic alcohol **68** (2.78 g, 11.3 mmol) and DHP (3.1 mL, 33.8 mmol) in CH_2Cl_2 (30 mL) was added PPTS (313 mg, 12.4 mmol). After the reaction was allowed to stir overnight, it was quenched by addition of saturated aqueous NaHCO_3 . The mixture was extracted with Et_2O , dried (Na_2SO_4), filtered, and concentrated *in vacuo*. Final purification by flash column chromatography (~12% EtOAc in hexanes) afforded THP acetal **69** (2.57 g, 69%) as a white solid. The ^1H NMR spectrum matched known data.⁷³

Geranylated arene 70. To a stirred solution of TMEDA (0.58 mL, 3.9 mmol) and *n*-BuLi (2.47 M solution in hexanes, 1.5 mL, 3.6 mmol) in Et_2O (20 mL) at $-10\text{ }^\circ\text{C}$ was added the bromide **69** (979 mg, 3.0 mmol) dissolved in Et_2O (4 mL). After 45 min of stirring, CuI (742 mg, 3.9 mmol) was added and then geranyl bromide (840 mg, 3.9 mmol) was added slowly over 8 min to the reaction. After the mixture was stirred overnight, the reaction was quenched by addition of saturated aqueous NH_4Cl . The

resulting mixture was extracted with EtOAc, and the combined organic extracts were washed with brine, dried (MgSO₄), filtered, and concentrated *in vacuo*. Final purification by flash column chromatography (4% EtOAc in hexanes) afforded compound **70** (364 mg, 32%) as a yellow oil: ¹H NMR (500 MHz, CDCl₃) δ 6.61 (d, *J* = 2.4 Hz, 1H), 6.42 (d, *J* = 2.5 Hz, 1H), 5.07–5.04 (m, 2H), 4.74 (d, *J* = 12.2 Hz, 1H), 4.70 (t, *J* = 3.7 Hz, 1H), 4.48 (d, *J* = 12.1 Hz, 1H), 3.94–3.90 (m, 1H), 3.80 (s, 3H), 3.79 (s, 3H), 3.37–3.29 (m, 2H), 2.06–1.80 (m, 5H), 1.80–1.54 (m, 5H), 1.75 (s, 3H), 1.65 (s, 3H), 1.57 (s, 3H); ¹³C NMR (125 MHz, CDCl₃) δ 158.6, 158.4, 138.0, 134.5, 131.2, 124.4, 123.3, 121.3, 105.0, 98.0 (2C), 66.9, 62.2, 55.7, 55.3, 39.8, 30.7, 26.8, 25.7, 25.5, 24.1, 19.5, 17.7, 16.1; HRMS (ESI) *m/z* calcd for C₂₄H₃₆O₄Na (M + Na)⁺ 411.2511, found 411.2495.¹⁶

Benzylic alcohol 71. To a solution of the THP acetal **70** (364 mg, 0.9 mmol) in MeOH (8 mL) at room temperature was added TsOH (356 mg, 1.9 mmol). The solution was stirred for 2.5 h and quenched by addition of NaHCO₃. The mixture was extracted with EtOAc, and the combined organic extracts were dried (MgSO₄), filtered, and concentrated *in vacuo* to afford the benzylic alcohol **71** as a yellow oil. This material was used in further reactions without additional purification: ¹H NMR (300 MHz, CDCl₃) δ 6.59 (d, *J* = 2.4 Hz, 1H), 6.43 (d, *J* = 2.2 Hz, 1H), 5.09–5.02 (m, 2H) 4.64 (d, *J* = 3.9 Hz, 2H), 3.81 (s, 3H), 3.80 (s, 3H), 3.35 (d, *J* = 6.8 Hz, 2H), 2.10–1.94 (m, 4H), 1.76 (s, 3H), 1.65 (s, 3H), 1.57 (s, 3H); ¹³C NMR (75 MHz, CDCl₃) δ 158.7, 158.3, 140.6, 135.0, 131.4, 124.1, 123.5, 120.3, 104.0, 97.9, 63.3, 55.6, 55.3, 39.6, 26.6, 25.6, 23.7, 17.6, 16.1; HRMS (EI) *m/z* calcd for C₁₉H₂₈O₃ (M)⁺ 304.2038, found 304.2044.¹⁶

Aldehyde 66. To a stirred solution of the benzylic alcohol **71** (285 mg, 0.9 mmol, assuming 100% conversion in the previous step) in CH₂Cl₂ (15 mL) was added activated MnO₂ (815 mg, 9.4 mmol). The mixture was stirred overnight and subsequently was filtered and concentrated *in vacuo*. Final purification by flash column chromatography

(12% EtOAc in hexanes) afforded aldehyde **66** (146 mg, 52% from **70**) as a yellow oil: $^1\text{H NMR}$ (300 MHz, CDCl_3) δ 10.3 (s, 1H), 6.98 (d, $J = 2.2$ Hz, 1H), 6.68 (d, $J = 1.9$ Hz, 1H), 5.13–5.07 (m, 1H), 5.05–5.00 (m, 1H), 3.82 (s, 6H), 3.70 (d, $J = 6.5$ Hz, 2H), 2.24–1.90 (m, 4H), 1.76 (s, 3H), 1.64 (s, 3H), 1.56 (s, 3H); $^{13}\text{CNMR}$ (75 MHz, CDCl_3) δ 191.8, 158.8, 158.6, 135.2, 134.9, 131.4, 127.3, 124.0, 123.4, 104.8, 101.9, 55.8, 55.5, 39.5, 26.5, 25.6, 22.5, 17.6, 16.2; HRMS (ESI) m/z calcd for $\text{C}_{19}\text{H}_{26}\text{O}_3\text{Na}$ ($\text{M} + \text{Na}$) $^+$ 325.1780, found 325.1783.¹⁶

Phenol 72. To a stirred solution of MOM ether **44** (103 mg, 0.3 mmol) in EtOH (2.5 mL) was added TsOH (152 mg, 0.8 mmol). The solution was stirred overnight, quenched by addition of saturated aqueous NH_4Cl , and extracted with EtOAc. The combined organic extracts were washed with brine, dried (MgSO_4), and concentrated *in vacuo* to afford the phenol **72** as a yellow oil,¹⁶ and the material was moved forward without additional purification: $^1\text{H NMR}$ (300 MHz, CDCl_3) δ 6.96 (dd, $J = 8.7$ Hz, $J_{\text{HP}} = 3.2$ Hz, 1H), 6.68 (d, $J = 8.8$ Hz, 1H), 4.96 (t, $J = 6.5$ Hz, 1H), 3.99–3.86 (m, 4H), 3.79 (s, 3H), 3.70 (s, 3H), 3.42 (d, $J = 6.5$ Hz, 2H), 3.04 (d, $J_{\text{HP}} = 21$ Hz, 2H), 1.72 (s, 3H), 1.61 (s, 3H), 1.18 (td, $J = 7.5$ Hz, $J_{\text{HP}} = 3.7$ Hz, 6H).

Methyl ether 73. To a stirred solution of the phenol (88 mg, 0.3 mmol) in acetone (6 mL) were added K_2CO_3 (242 mg, 1.8 mmol) and MeI (0.1 mL, 1.6 mmol). After the mixture was heated to reflux and stirred overnight, it was quenched by addition of H_2O , and the mixture was extracted with EtOAc. The organic extracts were washed with 2 M NaOH, dried (MgSO_4), and concentrated *in vacuo*. Without additional purification, methyl ether **73** (56 mg, 59%, 2 steps) was obtained as a yellow oil: $^1\text{H NMR}$ (300 MHz, CDCl_3) δ 6.96 (dd, $J = 8.7$ Hz, $J_{\text{HP}} = 3.2$ Hz, 1H), 6.68 (d, $J = 8.8$ Hz, 1H), 4.96 (t, $J = 6.5$ Hz, 1H), 3.99–3.86 (m, 4H), 3.79 (s, 3H), 3.70 (s, 3H), 3.42 (d, $J = 6.5$ Hz, 2H), 3.04 (d, $J_{\text{HP}} = 21$ Hz, 2H), 1.72 (s, 3H), 1.61 (s, 3H), 1.18 (td, $J = 7.5$ Hz, $J_{\text{HP}} = 3.7$ Hz, 6H).¹⁶

Prenylated arene 74. To a solution of alcohol **47** (1.02 g, 4.5 mmol) in THF (35 mL) at rt was added *n*-BuLi (2.38 M solution in hexanes, 4.0 mL, 9.5 mmol) dropwise over 6 min. After the solution was allowed to stir for 30 min, CuBr•DMS (1.01 g, 4.9 mmol) was added to the reaction. The mixture was allowed to stir for an additional 30 min, and then prenyl bromide (0.6 mL, 4.9 mmol) was added dropwise (13 min) to the reaction. Once the reaction was allowed to stir at rt for 2 h it was quenched by addition of NH₄Cl. The mixture was extracted with Et₂O, and the organic extracts were dried (MgSO₄), filtered, and concentrated *in vacuo*. Final purification by flash column chromatography (8% EtOAc in hexanes) afforded the prenylated arene **74** (467 mg, 35%) as a golden oil. The ¹H NMR spectrum was identical to the known data.⁵⁶

Phosphonate 75. To a solution of compound **74** (324 mg, 1.1 mmol) in THF (11 mL) at 0 °C was added TEA (0.23 mL, 1.6 mmol) and then MsCl (0.11 mL, 1.4 mmol) was added to the reaction vessel. After 1 h of stirring an additional amount of TEA (0.23 mL, 1.6 mmol) and MsCl (0.11 mL, 1.4 mmol) was added to the reaction. The reaction was allowed to stir for 1 h before LiBr (145 mg, 1.7 mmol) in THF (4 mL) was added. The reaction stirred for 17 h while warming to rt, and then was diluted with EtOAc. The resultant mixture was washed with brine. The combined organics were dried (Na₂SO₄), filtered, and concentrated *in vacuo*. Triethyl phosphite (2 mL, 11.8 mmol) was added to the neat oil, the reaction was heated to 90 °C, and was allowed to stir for 20.5 h. The mixture was concentrated at 60 °C under reduced pressure overnight. Final purification of the resulting oil by flash column chromatography (1% EtOH in CH₂Cl₂) provided phosphonate **75** (234 mg, 51%) as a yellow oil: ¹H NMR (500 MHz, CDCl₃) δ 7.02 (dd, *J* = 8.7 Hz, 3.0 Hz, 1H), 6.97 (d, *J* = 8.5 Hz, 1H), 5.17 (s, 2H), 5.08 (s, 2H), 5.07–5.03 (m, 1H), 4.04–3.96 (m, 4H), 3.58 (s, 3H), 3.55 (d, *J* = 6.3 Hz, 2H), 3.49 (s, 3H), 3.10 (d, *J* = 21.5 Hz, 2H), 1.79 (s, 3H), 1.69 (s, 3H), 1.24 (t, *J* = 7.2 Hz, 6H); ¹³C NMR (125 MHz,

CDCl_3) δ 148.9 (d, J_{CP} = 3.8 Hz), 144.9 (d, J_{CP} = 3.3 Hz), 135.5 (d, J_{CP} = 7.1 Hz), 131.9, 129.0, 128.2, 126.7 (d, J_{CP} = 5.5 Hz), 124.7 (d, J_{CP} = 9.3 Hz), 122.7, 114.0 (d, J_{CP} = 3.6 Hz), 62.0 (d, J_{CP} = 6.7 Hz, 2C), 57.5, 56.2, 30.0 (d, J_{CP} = 138.5 Hz), 25.8, 25.6, 18.0, 16.4 (d, J_{CP} = 6.1 Hz, 2C); ^{31}P NMR (202 MHz, CDCl_3) δ 27.1; HRMS (ESI) m/z calcd for $\text{C}_{20}\text{H}_{33}\text{O}_7\text{NaP}$ ($\text{M} + \text{Na}$) $^+$ 439.1862, found 439.1873.

Stilbene 78. To a stirred solution of aldehyde **66** (21 mg, 0.07 mmol) and phosphonate **62** (51 mg, 0.12 mmol) in THF (1.4 mL) at 0 °C was added KHMDS (0.5 M in toluene, 0.69 mL, 0.35 mmol). The solution was stirred for 22 h at rt, and the reaction was quenched with NH_4Cl . The resultant mixture was extracted with EtOAc, and the combined organic extracts were washed with brine, dried (MgSO_4), filtered, and concentrated *in vacuo*. Final purification by preparative TLC (30% EtOAc in hexanes) gave stilbene **78** (36 mg, 92%) as a yellow oil: ^1H NMR (500 MHz, CDCl_3) δ 7.20 (d, J = 16.0 Hz, 1H), 7.14 (d, J = 1.8 Hz, 1H), 6.98 (d, J = 2.1 Hz, 1H), 6.87 (d, J = 15.7 Hz, 1H), 6.72 (d, J = 2.4 Hz, 1H), 6.41 (d, J = 2.6 Hz, 1H), 5.34–5.31 (m, 1H), 5.22 (s, 2H), 5.12 (s, 2H), 5.06–5.03 (m, 1H), 3.85 (s, 3H), 3.81 (s, 3H), 3.61 (s, 3H), 3.52 (s, 3H), 3.44–3.41 (m, 4H), 2.06–2.02 (m, 2H), 1.98–1.95 (m, 2H), 1.81 (s, 3H), 1.76 (s, 3H), 1.74 (s, 3H), 1.60 (s, 3H), 1.53 (s, 3H); ^{13}C NMR (125 MHz, CDCl_3) δ 158.5, 158.4, 150.0, 144.4, 137.9, 136.1, 134.2, 133.9, 132.7, 131.2, 130.1, 126.3, 124.3, 123.5, 122.6, 121.5, 121.2, 112.1, 101.4, 99.1, 98.1, 95.2, 57.5, 56.2, 55.7, 55.4, 39.7, 28.6, 26.7, 25.8, 25.6, 24.4, 17.9, 17.6, 16.2; HRMS (ESI) m/z calcd for $\text{C}_{35}\text{H}_{49}\text{O}_6$ ($\text{M} + \text{H}$) $^+$ 565.3529, found 565.3524.¹⁶

Analogue 79. To a solution of bis-MOM acetal **78** (36 mg, 0.06 mmol) in MeOH (6.4 mL) was added TsOH (49 mg, 0.26 mmol). After the solution was stirred for 19.5 h at rt, additional TsOH (25 mg, 0.13 mmol) was added due to incomplete conversion to product. After the solution was stirred for an additional 22.5 h, the reaction was quenched

by addition of NaHCO₃. The resultant mixture was extracted with EtOAc, and the combined organic extracts were dried (MgSO₄), filtered, and concentrated *in vacuo*. Final purification by preparative TLC (35% EtOAc in hexanes) provided stilbene **79** (14 mg, 47%) as a yellow oil: ¹H NMR (500 MHz, CDCl₃) δ 7.37 (d, *J* = 15.6 Hz, 1H), 6.94 (s, 1H), 6.84–6.80 (m, 2H), 6.71 (d, *J* = 2.1 Hz, 1H), 6.40 (d, *J* = 2.0 Hz, 1H), 5.45 (br s, 1H), 5.34 (t, *J* = 6.1 Hz, 1H), 5.11 (t, *J* = 6.7 Hz, 1H), 5.06–5.04 (m, 1H), 3.84 (s, 3H), 3.80 (s, 3H), 3.42 (d, *J* = 6.5 Hz, 2H), 3.37 (d, *J* = 7.1 Hz, 2H), 2.07–2.03 (m, 2H), 1.98–1.95 (m, 2H), 1.81–1.79 (m, 9H), 1.61 (s, 3H), 1.54 (s, 3H); ¹³C NMR (125 MHz, CDCl₃) δ 158.5, 158.4, 144.2, 141.9, 138.0, 135.3, 134.4, 131.3, 130.6, 130.1, 127.3, 125.2, 124.3, 123.6, 121.6, 121.1, 120.5, 110.9, 101.5, 97.9, 55.7, 55.4, 39.7, 29.9, 26.8, 25.8, 25.6, 24.4, 17.9, 17.6, 16.3; HRMS (ESI) *m/z* calcd for C₃₁H₄₁O₄ (M)⁺ 477.3005, found 477.2994.¹⁶

Stilbene 80. To a stirred suspension of NaH (60% dispersion in mineral oil, washed with hexanes, 28 mg, 0.7 mmol) in THF (2.5 mL) were added aldehyde **66** (35 mg, 0.1 mmol), phosphonate **48** (49 mg, 0.1 mmol), and 15-crown-5 (3 drops). The mixture was stirred for 2 h and quenched with saturated aqueous NH₄Cl. The resultant mixture was extracted with EtOAc, and the combined organic extracts were washed with brine, dried (MgSO₄), filtered, and concentrated *in vacuo*. Final purification of the residue by flash column chromatography (10% EtOAc in hexanes) gave stilbene **80** (38 mg, 67%) as a yellow oil: ¹H NMR (300 MHz, CDCl₃) δ 7.32 (d, *J* = 1.6 Hz, 1H), 7.21 (d, *J* = 16.1 Hz, 1H), 7.15 (d, *J* = 8.4 Hz, 1H), 7.10 (dd, *J* = 8.5 Hz, 1.7 Hz, 1H), 6.89 (d, *J* = 16.2 Hz, 1H), 6.72 (d, *J* = 2.2 Hz, 1H), 6.42 (d, *J* = 2.1 Hz, 1H), 5.28 (s, 2H), 5.26 (s, 2H), 5.14–5.03 (m, 2H), 3.85 (s, 3H), 3.81 (s, 3H), 3.54 (s, 3H), 3.53 (s, 3H), 3.43 (d, *J* = 6.7 Hz, 2H), 2.08–1.95 (m, 4H), 1.81 (s, 3H), 1.61 (s, 3H), 1.54 (s, 3H); ¹³C NMR (75 MHz, CDCl₃) δ 158.5, 158.3, 147.3, 146.8, 137.8, 134.3, 132.4, 131.2, 129.7, 125.8, 124.3, 123.5, 121.1, 120.8,

116.5, 114.6, 101.2, 98.0, 95.4, 95.3, 56.2 (2C), 55.6, 55.3, 39.7, 26.7, 25.6, 24.3, 17.6, 16.2; HRMS (ESI) m/z calcd for $C_{30}H_{41}O_6$ ($M + H$)⁺ 497.2903, found 497.2918.¹⁶

Analogue 81. To a solution of bis(methoxymethyl) ether **80** (18 mg, 0.04 mmol) in MeOH (2 mL) was added TsOH (29 mg, 0.15 mmol). After the solution was stirred overnight, the reaction was quenched by addition of saturated aqueous $NaHCO_3$. The resultant mixture was extracted with EtOAc, and the combined organic extracts were dried ($MgSO_4$), filtered, and concentrated *in vacuo*. Final purification of a portion (25%) of the residual oil by preparative TLC (25% EtOAc in hexanes) afforded the stilbene **81** (5 mg, 100% by NMR) as a yellow oil; the remaining material (75%) was moved forward without additional purification. For compound **81**: 1H NMR (300 MHz, $CDCl_3$) δ 7.20–6.82 (m, 5H), 6.71 (m, 1H), 6.42 (m, 1H), 5.19–4.98 (m, 2H), 3.86 (s, 3H), 3.81 (s, 3H), 3.42 (d, $J = 5.9$ Hz, 2H), 2.07–1.97 (m, 4H), 1.80 (s, 3H), 1.62 (s, 3H), 1.55 (s, 3H); ^{13}C NMR (75 MHz, $CDCl_3$) δ 158.5, 158.4, 143.8, 143.5, 137.9, 134.5, 131.3, 129.9, 125.1, 124.3, 123.5, 121.1, 119.9, 115.5, 113.1, 110.9, 101.4, 97.9, 55.7, 55.4, 39.7, 26.7, 25.6, 24.3, 17.7, 16.3; HRMS (ESI) m/z calcd for $C_{26}H_{33}O_4$ ($M + H$)⁺ 409.2379, found 409.2374.¹⁶

Stilbene 82. To a solution of phosphonate **50** (47 mg, 0.16 mmol) and aldehyde **66** (41 mg, 0.14 mmol) in THF (1.5 mL) was added KHMDS (0.5 M solution in toluene, 3.25 mL, 1.63 mmol). After the reaction stirred for 3.5 h, it was quenched by addition of NH_4Cl and extracted with EtOAc, and the combined extracts were washed with brine, dried ($MgSO_4$), filtered, and concentrated *in vacuo*. Final purification by flash column chromatography (8% EtOAc in hexanes) provided stilbene **82** (19 mg, 32%) as a yellow oil: 1H NMR (500 MHz, $CDCl_3$) δ 7.42 (d, $J = 7.8$ Hz, 2H), 7.23 (d, $J = 15.9$ Hz, 1H), 7.02 (d, $J = 7.6$ Hz, 2H), 6.91 (d, $J = 16.1$ Hz, 1H), 6.73 (s, 1H), 6.41 (s, 1H), 5.19 (s, 2H), 5.12–5.05 (m, 2H), 3.85 (s, 3H), 3.81 (s, 3H), 3.49 (s, 3H), 3.43 (d, $J = 6.7$ Hz, 2H),

2.05–1.96 (m, 4H), 1.79 (s, 3H), 1.61 (s, 3H), 1.54 (s, 3H); ^{13}C NMR (125 MHz, CDCl_3) δ 158.6, 158.4, 156.8, 138.0, 134.4, 131.6, 131.2, 129.7, 127.7 (2C), 125.4, 124.3, 123.6, 121.1, 116.4 (2C), 101.5, 98.0, 94.4, 56.0, 55.7, 55.3, 39.7, 26.7, 25.6, 24.4, 17.6, 16.2; HRMS (EI) m/z calcd for $\text{C}_{28}\text{H}_{36}\text{O}_4$ (M) $^+$ 436.2614, found 436.2606.

Analogue 83. To a solution of compound **82** (19 mg, 0.04 mmol) in MeOH (2 mL) was added TsOH (25 mg, 0.13 mmol) and the reaction was allowed to stir for 12 h. The reaction was quenched by addition of NaHCO_3 and extracted with EtOAc, and the combined extracts were dried (MgSO_4), filtered, and concentrated *in vacuo*. Final purification by preparative TLC (30% EtOAc in hexanes) delivered phenol **83** (5 mg, 33%) as a yellow oil: ^1H NMR (500 MHz, CDCl_3) δ 7.38 (d, J = 8.5 Hz, 2H), 7.19 (d, J = 16 Hz, 1H), 6.90 (d, J = 15.9 Hz, 1H), 6.83 (d, J = 8.5 Hz, 2H), 6.72 (d, J = 2.2 Hz, 1H), 6.41 (d, J = 2.4 Hz, 1H), 5.13–5.04 (m, 2H), 3.85 (s, 3H), 3.81 (s, 3H), 3.43 (d, J = 6.6 Hz, 2H), 2.07–1.95 (m, 4H), 1.79 (s, 3H), 1.62 (s, 3H), 1.54 (s, 3H); ^{13}C NMR (125 MHz, CDCl_3) δ 158.5, 158.4, 155.3, 138.1, 134.4, 131.3, 130.6, 129.8 (2C), 127.9, 125.0, 124.3, 123.6, 121.0, 115.6 (2C), 101.5, 97.9, 55.7, 55.4, 39.7, 26.7, 25.6, 24.4, 17.6, 16.2; HRMS (EI) m/z calcd for $\text{C}_{26}\text{H}_{32}\text{O}_3$ (M) $^+$ 392.2351, found 392.2366.

Stilbene 84. A solution of KHMDS (0.5 M in toluene, 0.95 mL, 0.48 mmol) was added to a solution of aldehyde **66** (12 mg, 0.04 mmol) and phosphonate **52** (45 mg, 0.20 mmol) in THF (1.5 mL) at rt. After the reaction was stirred for 4.5 h, it was quenched by addition of NH_4Cl and extracted with EtOAc, and the combined extracts were washed with brine, dried (MgSO_4), filtered, and concentrated *in vacuo*. Final purification by preparative TLC (15% EtOAc in hexanes) yielded stilbene **84** (7 mg, 41%) as a colorless oil: ^1H NMR (500 MHz, CDCl_3) δ 7.35–7.25 (m, 2H), 7.17–7.14 (m, 2H), 6.95–6.91 (m, 2H), 6.73 (d, J = 2.0 Hz, 1H), 6.43 (d, J = 1.9 Hz, 1H), 5.20 (s, 2H), 5.11 (t, J = 5.8 Hz, 1H), 5.05 (t, J = 6.4 Hz, 1H), 3.85 (s, 3H), 3.81 (s, 3H), 3.50 (s, 3H), 3.43 (d, J = 6.4 Hz,

2H), 2.05–1.95 (m, 4H), 1.80 (s, 3H), 1.61 (s, 3H), 1.54 (s, 3H); ^{13}C NMR (125 MHz, CDCl_3) δ 158.6, 158.4, 157.6, 139.2, 137.7, 134.5, 131.2, 130.1, 129.6, 127.5, 124.3, 123.5, 121.4, 120.3, 115.5, 114.3, 101.6, 98.3, 94.4, 56.0, 55.7, 55.4, 39.7, 26.7, 25.6, 24.4, 17.6, 16.2; HRMS (EI) m/z calcd for $\text{C}_{28}\text{H}_{36}\text{O}_4$ (M) $^+$ 436.2614, found 436.2619.

Analogue 85. To a solution of compound **84** (7 mg, 0.02 mmol) in MeOH:THF (1:1 mL) was added TsOH (7 mg, 0.04 mmol). The reaction was allowed to stir for 20.5 h, then additional TsOH was added due to incomplete conversion to product. After stirring for an additional 22 h at rt, the reaction was quenched by addition of NaHCO_3 and extracted with EtOAc. The combined extracts were dried (MgSO_4), filtered, and concentrated *in vacuo*. Final purification by preparative TLC (15% EtOAc in hexanes) provided phenol **85** (4 mg, 67%) as a yellow oil: ^1H NMR (500 MHz, CDCl_3) δ 7.33 (d, J = 16.2 Hz, 1H), 7.22 (t, J = 7.8 Hz, 1H), 7.07 (d, J = 7.5 Hz, 1H), 6.97–6.96 (m, 1H), 6.90 (d, J = 16.1 Hz, 1H), 6.75–6.72 (m, 2H), 6.43 (d, J = 2.4 Hz, 1H), 5.13–5.10 (m, 1H), 5.06–5.03 (m, 1H), 3.85 (s, 3H), 3.81 (s, 3H), 3.44 (d, J = 6.6 Hz, 2H), 3.35 (s, 1H), 2.07–2.03 (m, 2H), 1.99–1.96 (m, 2H), 1.80 (s, 3H), 1.61 (s, 3H), 1.55 (s, 3H); ^{13}C NMR (125 MHz, CDCl_3) δ 158.6, 158.4, 155.8, 139.4, 137.6, 134.5, 131.3, 130.0, 129.8, 127.6, 124.3, 123.5, 121.4, 119.4, 114.6, 113.1, 101.7, 98.3, 55.7, 55.4, 39.7, 29.7, 26.7, 25.6, 17.7, 16.3; HRMS (ESI) m/z calcd for $\text{C}_{26}\text{H}_{33}\text{O}_3$ ($\text{M} + \text{H}$) $^+$ 393.2430, found 393.2427.

Analogue 86. To a stirred suspension of NaH (60% dispersion in mineral oil, washed with hexanes, 33 mg, 0.8 mmol) in THF (2.5 mL) were added phosphonate **73** (56 mg, 0.2 mmol), aldehyde **66** (39 mg, 0.1 mmol), and 15-crown-5 (3 drops). The mixture was stirred for 2 h and quenched by addition of saturated aqueous NH_4Cl . The resulting mixture was extracted with EtOAc, and the combined organic extracts were washed with brine, dried (MgSO_4), filtered, and concentrated *in vacuo*. Final purification by flash column chromatography (10% EtOAc in hexanes) afforded stilbene **86** (20 mg, 31%) as a

yellow oil: ^1H NMR (500 MHz, CDCl_3) δ 7.32 (d, $J = 8.7$ Hz, 1H), 7.12 (s, 2H), 6.80 (d, $J = 8.8$ Hz, 1H), 6.71 (d, $J = 2.5$ Hz, 1H), 6.21 (d, $J = 2.5$ Hz, 1H), 5.16–5.11 (m, 2H), 5.07–5.04 (m, 1H), 3.88 (s, 3H), 3.84 (s, 3H), 3.81 (s, 3H), 3.81 (s, 3H), 3.52–3.50 (m, 2H), 3.42 (d, $J = 6.7$ Hz, 2H), 2.07–2.03 (m, 2H), 1.98–1.92 (m, 2H), 1.81 (s, 3H), 1.78 (s, 3H), 1.67 (s, 3H), 1.62 (s, 3H), 1.55 (s, 3H); ^{13}C NMR (125 MHz, CDCl_3) δ 158.5, 158.4, 152.3, 146.9, 138.4, 134.4, 134.0, 131.4, 131.2, 130.4, 128.0, 127.0, 124.4, 123.5, 123.3, 121.6, 121.1, 110.2, 101.6, 97.9, 60.7, 55.7 (2C), 55.3, 39.7, 26.8, 25.7, 25.6, 25.5, 24.3, 18.1, 17.6, 16.3; HRMS (EI) m/z calcd for $\text{C}_{33}\text{H}_{44}\text{O}_4$ (M) $^+$ 504.3240, found 504.3237.¹⁶

Stilbene 87. To a stirred solution of aldehyde **66** (27 mg, 0.1 mmol) and **44** (51 mg, 0.1 mmol) in THF (1.5 mL) at room temperature were added NaH (60% dispersion in mineral oil, 22 mg, 0.6 mmol) and 15-crown-5 (2 drops). After the mixture was stirred overnight, the reaction was quenched by addition of NH_4Cl . The resulting mixture was extracted with EtOAc, and then the combined organic extracts were dried (MgSO_4), filtered, and concentrated *in vacuo*. Final purification by flash column chromatography (10% EtOAc in hexanes) provided **87** (18 mg) in 38% yield as a yellow oil: ^1H NMR (300 MHz, CDCl_3) δ 7.33 (d, $J = 8.7$ Hz, 1H), 7.11 (m, 2H), 6.80 (d, $J = 8.6$ Hz, 1H), 6.70 (d, $J = 2.3$ Hz, 1H), 6.41 (d, $J = 2.5$ Hz, 1H), 5.16–5.03 (m, 3H), 5.09 (s, 2H), 3.86 (s, 3H), 3.83 (s, 3H), 3.81 (s, 3H), 3.60 (s, 3H), 3.57 (d, $J = 6.6$ Hz, 2H), 3.42 (d, $J = 6.7$ Hz, 2H), 2.05–1.96 (m, 4H), 1.80 (s, 3H), 1.78 (s, 3H), 1.68 (s, 3H), 1.62 (s, 3H), 1.55 (s, 3H); ^{13}C NMR (75 MHz, CDCl_3) δ 158.8, 158.7, 152.1, 144.1, 138.7, 134.8, 134.5, 131.6 (2C), 130.9, 128.4, 127.3, 124.7, 123.8, 123.6, 122.2, 121.4, 110.4, 101.8, 99.4, 98.2, 58.0, 56.1, 56.0, 55.6, 40.1, 30.0, 27.1, 26.1, 26.0 (2C), 24.7, 18.5, 18.0, 16.6; HRMS (EI) m/z calcd for $\text{C}_{34}\text{H}_{46}\text{O}_5$ (M) $^+$ 534.3345, found 534.3330.¹⁶

Analogue 88. To a stirred solution of MOM ether **87** (27 mg, 0.1 mmol) in MeOH (2.5 mL) was added TsOH (40 mg, 0.2 mmol). The solution was stirred overnight, and the reaction was quenched by addition of saturated aqueous NaHCO₃. The resulting mixture was extracted with EtOAc, and the organic extracts were dried (MgSO₄), filtered, and concentrated *in vacuo*. Stilbene **88** (22 mg, 88%) was obtained as a yellow oil: ¹H NMR (300 MHz, CDCl₃) δ 7.14 (m, 2H), 7.10 (m, 1H), 6.76 (m, 1H), 6.73 (d, *J* = 2.4 Hz, 1H), 6.42 (d, *J* = 2.2 Hz, 1H), 5.21–5.04 (m, 3H), 3.90 (s, 3H), 3.84 (s, 3H), 3.81 (s, 3H), 3.52 (d, *J* = 6.5 Hz, 2H), 3.43 (d, *J* = 6.4 Hz, 2H), 2.09–1.96 (m, 4H), 1.82 (s, 3H), 1.78 (s, 3H), 1.68 (s, 3H), 1.62 (s, 3H), 1.55 (s, 3H); ¹³C NMR (75 MHz, CDCl₃) δ 158.9, 158.1, 146.2, 143.6, 138.7, 134.7, 131.9, 131.5, 131.0, 128.5, 127.5, 126.1, 124.7, 123.9, 123.0, 121.5, 117.5, 108.8, 101.9, 98.3, 56.0, 55.7, 55.3, 39.8, 26.8, 25.7, 25.6, 25.1, 24.4, 18.1, 17.6, 16.3; HRMS (EI) *m/z* calcd for C₃₂H₄₂O₄ (M + H)⁺ 490.3083, found 490.3087.¹⁶

Analogue 86. To a solution of stilbene **88** (11 mg, 0.02 mmol) in THF (3 mL) were added NaH (60% dispersion in mineral oil, 6 mg, 0.2 mmol) and MeI (2 drops). The mixture was stirred for 5 h, and the reaction was quenched by addition of H₂O. The resultant mixture was extracted with EtOAc, and the combined organic extracts were washed with 2 M NaOH, dried (MgSO₄), filtered, and concentrated *in vacuo*. Stilbene **86** (6 mg, 55%) was obtained as a yellow oil, with ¹H NMR data that were identical to the data given above.

Stilbene 89. To a solution of aldehyde **66** (26 mg, 0.09 mmol) and phosphonate **75** (63 mg, 0.15 mmol) in THF (1.7 mL) at 0 °C was added KHMDS (1.0 M solution in THF, 0.43 mL, 0.43 mmol). The reaction was allowed to warm to rt while stirring for 18 h. It was then quenched by the addition of NH₄Cl, and the resultant mixture was extracted with EtOAc. The combined organic extracts were washed with brine, dried (MgSO₄), filtered, and concentrated *in vacuo*. Final purification by preparative TLC (30% EtOAc

in hexanes) provided stilbene **89** (34 mg, 69%) as a yellow oil: ^1H NMR (500 MHz, CDCl_3) δ 7.30 (d, $J = 8.4$ Hz, 1H), 7.12–7.11 (m, 2H), 7.02 (d, $J = 8.7$ Hz, 1H), 6.70 (d, $J = 2.6$ Hz, 1H), 6.42 (d, $J = 2.3$ Hz, 1H), 5.21 (s, 2H), 5.18–5.12 (m, 1H), 5.12–5.10 (m, 3H), 5.07–5.04 (m, 1H), 3.83 (s, 3H), 3.81 (s, 3H), 3.60 (s, 3H), 3.56 (d, $J = 6.5$ Hz, 2H), 3.51 (s, 3H), 3.42 (d, $J = 6.3$ Hz, 2H), 2.07–2.02 (m, 2H), 1.98–1.95 (m, 2H), 1.80 (s, 3H), 1.78 (s, 3H), 1.68 (s, 3H), 1.61 (s, 3H), 1.55 (s, 3H); ^{13}C NMR (125 MHz, CDCl_3) δ 158.5, 158.4, 149.3, 144.6, 138.3, 134.5, 134.3, 131.9, 131.4, 131.2, 128.0, 127.4, 124.3, 123.5, 123.3, 122.0, 121.2, 114.2, 101.6, 99.2, 98.0, 95.1, 57.6, 56.2, 55.7, 55.3, 39.7, 26.8, 25.8, 25.6, 25.6, 24.3, 18.2, 17.6, 16.3; HRMS (ESI) m/z calcd for $\text{C}_{35}\text{H}_{49}\text{O}_6$ ($\text{M} + \text{H}$) $^+$ 565.3529, found 565.3541.

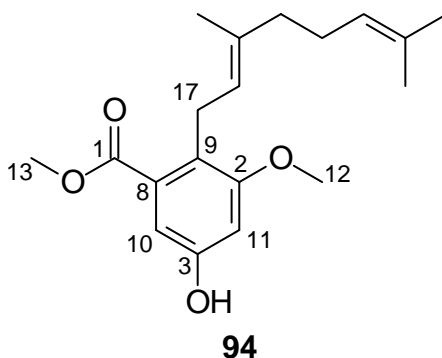
Analogue 90. To a solution of the bis(methoxymethyl) ether **89** (33 mg, 0.06 mmol) in MeOH (5.8 mL) was added TsOH (46 mg, 0.24 mmol). The reaction was allowed to stir for 3 d, and was quenched by the addition of NaHCO_3 . The resultant mixture was extracted with EtOAc, and the combined organic extracts were dried (MgSO_4), filtered, and concentrated *in vacuo*. Phenol **90** (6 mg, 21%) was obtained as a yellow oil after final purification by preparative TLC (30% EtOAc in hexanes): ^1H NMR (500 MHz, CDCl_3) δ 7.14–7.06 (m, 3H), 6.77 (d, $J = 8.7$ Hz, 1H), 6.71 (d, $J = 2.7$ Hz, 1H), 6.42 (d, $J = 2.0$ Hz, 1H), 5.44 (br s, 2H), 5.24–5.21 (m, 1H), 5.12–5.10 (m, 1H), 5.06–5.03 (m, 1H), 3.84 (s, 3H), 3.31 (s, 3H), 3.51 (d, $J = 6.5$ Hz, 2H), 3.41 (d, $J = 7.0$ Hz, 2H), 2.06–2.02 (m, 2H), 1.97–1.94 (m, 2H), 1.84 (s, 3H), 1.76–1.74 (m, 6H), 1.62 (s, 3H), 1.55 (s, 3H); ^{13}C NMR (125 MHz, CDCl_3) δ 158.6, 158.5, 143.6, 142.0, 138.4, 134.6, 134.4, 131.3, 130.1, 128.2, 127.7, 125.9, 124.4, 123.5, 121.9, 121.2, 118.8, 113.2, 101.9, 97.9, 55.7, 55.3, 39.7, 26.8, 25.9, 25.7, 25.6, 24.4, 18.1, 17.6, 16.2; HRMS (ESI) m/z calcd for $\text{C}_{31}\text{H}_{41}\text{O}_4$ ($\text{M} + \text{H}$) $^+$ 477.3005, found 477.3017.

Analogue 91. To a stirred solution of stilbene **81** in acetone (3 mL) was added K_2CO_3 (35 mg, 0.25 mmol) followed by MeI (38 μ L, 0.61 mmol). The mixture was stirred for 2 days, and the reaction was quenched with H_2O . The resulting mixture was extracted with EtOAc, and the combined organic extracts were washed with brine, dried ($MgSO_4$), filtered, and concentrated *in vacuo*. Final purification by flash column chromatography (gradient of hexanes to 40% EtOAc in hexanes) provided stilbene **91** (4 mg, 27%) as a yellow oil: 1H NMR (300 MHz, $CDCl_3$) δ 7.27–7.18 (m, 1H), 7.06–7.04 (m, 2H), 6.94–6.85 (m, 2H), 6.75 (d, $J = 2.7$ Hz, 1H), 6.43 (d, $J = 2.4$ Hz, 1H), 5.14 (t, $J = 7.5$ Hz, 1H), 5.06 (t, $J = 7.5$ Hz, 1H), 3.94 (s, 3H), 3.91 (s, 3H), 3.86 (s, 3H), 3.83 (s, 3H), 3.46–3.44 (m, 2H), 2.05–1.95 (m, 4H), 1.82 (s, 3H), 1.62 (s, 3H), 1.55 (s, 3H); ^{13}C NMR (75 MHz, $CDCl_3$) δ 158.9, 149.1, 138.0, 134.2, 131.3, 130.8, 130.1, 125.2, 124.2, 123.4, 121.1, 119.9, 111.3, 108.8, 107.1, 105.8, 101.4, 97.9, 56.0, 55.8, 55.7, 55.4, 39.7, 26.8, 25.6, 24.4, 17.6, 16.3; HRMS (EI) m/z calcd for $C_{28}H_{36}O_4$ (M)⁺ 436.2614, found 436.2606.¹⁶

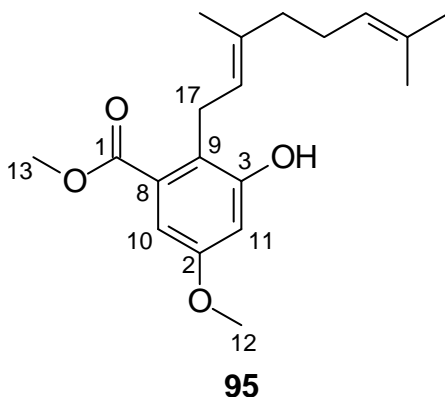
Geranylated arene 92. To a solution of compound **35** (4.06 g, 24.1 mmol) in dioxane (100 mL) was added $BF_3 \cdot OEt_2$ (1.2 mL, 9.7 mmol). The reaction mixture was heated to 50 $^\circ C$, then geraniol (2.1 mL, 12.1 mmol) dissolved in dioxane (25 mL) was added dropwise over 60 min and the reaction was allowed to stir for 2.5 h. The reaction was quenched by addition of H_2O and extracted with Et_2O . The combined extracts were washed with brine, dried ($MgSO_4$), filtered, and concentrated *in vacuo*. Final purification (15% EtOAc in hexanes) provided geranylated compound **92** (871 mg, 24%). The 1H NMR data matched the literature.⁵⁶

Methylated products 93–95. To a stirred solution of K_2CO_3 (1.09 g, 7.9 mmol) and compound **92** (1.85 g, 6.1 mmol) in DMF (60 mL) was added iodomethane (0.49 mL, 7.9 mmol) over 2 min. After the reaction was stirred for 1.5 h, it was quenched by addition

of NH_4Cl . The resulting mixture was extracted with Et_2O , and the combined organics were dried (MgSO_4), filtered, and concentrated *in vacuo*. Final purification by flash column chromatography (4% EtOAc in hexanes) afforded compounds **94** (370 mg, 19%), **95** (205 mg, 11%), and **93** (304 mg, 15%) as yellow oils.



For compound **94**: ^1H NMR (600 MHz, CDCl_3) δ 6.84 (s, 1H), 6.55 (s, 1H), 5.13–5.10 (m, 1H), 5.08–5.04 (m, 1H), 3.85 (s, 3H), 3.76 (s, 3H), 3.54 (d, $J = 6.4$ Hz, 2H), 2.06–2.01 (m, 2H), 1.97–1.92 (m, 2H), 1.72 (s, 3H), 1.64 (s, 3H), 1.56 (s, 3H); ^{13}C NMR (150 MHz, CDCl_3) δ 169.2 (C-1), 159.2 (C-2), 154.7 (C-3), 135.1 (C-4), 131.9 (C-5), 124.2 (C-6), 123.6 (C-7), 123.5 (2C, C-8, C-9), 108.2 (C-10), 102.2 (C-11), 55.6 (C-12), 52.1 (C-13); 39.8 (C-14), 26.5 (C-15), 25.7 (C-16), 25.0 (C-17), 17.8 (C-18), 15.9 (C-19); HMBC data, H-17 \rightarrow C-9, C-2; H-13 \rightarrow C-1; H-12 \rightarrow C-2; H-11 \rightarrow C-10, C-9, C-3, C-2; H-10 \rightarrow C-11, C-8, C-3, C-1; HRMS (EI) m/z calcd for $\text{C}_{19}\text{H}_{26}\text{O}_4$ (M) $^+$ 318.1831, found 318.1847.



For compound **95**: ^1H NMR (600 MHz, CDCl_3) δ 6.89 (d, $J = 2.2$ Hz, 1H), 6.57 (d, $J = 2.2$ Hz, 1H), 6.44 (br s, 1H), 5.21–5.19 (m, 1H), 5.04–5.03 (m, 1H), 3.87 (s, 3H), 3.74 (s, 3H), 3.61 (d, $J = 6.2$ Hz, 2H), 2.08–2.05 (m, 2H), 2.02–1.99 (m, 2H), 1.76 (s, 3H), 1.65 (s, 3H), 1.57 (s, 3H); ^{13}C NMR (150 MHz, CDCl_3) δ 168.9 (C-1), 158.1 (C-2), 156.3 (C-3), 136.9 (C-4), 131.8 (C-5), 124.1 (C-6), 122.7 (C-7), 121.3 (C-8), 120.8 (C-9), 107.2 (C-10), 105.8 (C-11), 55.6 (C-12), 52.3 (C-13), 39.8 (C-14), 26.6 (C-15), 25.9 (C-16), 25.6 (C-17), 17.8 (C-18), 16.2 (C-19); HMBC data H-17 \rightarrow C-9, C-3; H-13 \rightarrow C-1; H-12 \rightarrow C-2; H-11 \rightarrow C-10, C-9, C-3, C-2; H-10 \rightarrow C-11, C-8, C-2, C-1; HRMS (EI) m/z calcd for $\text{C}_{19}\text{H}_{26}\text{O}_4$ (M) $^+$ 318.1831, found 318.1827.

For compound **93**: ^1H NMR (400 MHz, CDCl_3) δ 6.85 (d, $J = 2.1$ Hz, 1H), 6.57 (d, $J = 2.1$ Hz, 1H), 5.16–5.11 (m, 1H), 5.09–5.03 (m, 1H), 3.86 (s, 3H), 3.79 (s, 6H), 3.57 (d, $J = 5.1$ Hz, 2H), 2.08–2.01 (m, 2H), 1.97–1.92 (m, 2H), 1.73 (s, 3H), 1.64 (s, 3H), 1.56 (s, 3H); ^{13}C NMR (100 MHz, CDCl_3) δ 168.6, 158.7, 158.1, 134.5, 131.8, 130.9, 124.3, 124.1, 123.3, 104.8, 102.0, 55.6, 55.3, 51.9, 39.7, 26.6, 25.5, 24.9, 17.5, 16.0; HRMS (EI) m/z calcd for $\text{C}_{20}\text{H}_{28}\text{O}_4$ (M) $^+$ 332.1988, found 332.1988.

Silyl ether 105. To a stirred solution of alcohol **36** (3.19 g, 14.0 mmol) and imidazole (5.04 g, 74.1 mmol) in CH₂Cl₂ (125 mL) at room temperature was added TBSCl (2.95 g, 19.6 mmol). After the reaction was allowed to stir for 21 h, it was quenched by addition of NH₄Cl and water. The mixture was extracted with CH₂Cl₂, dried (MgSO₄), filtered, and concentrated *in vacuo*. Final purification by flash column chromatography (15% EtOAc in hexanes) afforded silyl ether **105** (5.09 g, 100% by NMR) as a pale yellow oil. The ¹H NMR spectrum matched literature data.⁵⁴

Prenylated arene 106. To a stirred solution of TMEDA (0.57 mL, 3.8 mmol) and *n*-BuLi (2.4 M in hexanes, 1.5 mL, 3.6 mmol) in Et₂O (30 mL) at -10 °C was added silyl ether **105** (1.01 g, 2.9 mmol) dissolved in Et₂O (4 mL). After stirring 30 min, CuI (725 mg, 3.8 mmol) was added, followed by addition of a solution of prenyl bromide (0.41 mL, 3.5 mmol) in Et₂O (4 mL) over 20 min. The reaction was allowed to stir for 90 min, quenched by addition of NH₄Cl, extracted with EtOAc, washed with brine, dried (MgSO₄), filtered, and concentrated *in vacuo*. Final purification by flash column chromatography (7% EtOAc in hexanes) provided prenylated compound **106** (240 mg, 20%) as a yellow oil. The ¹H NMR spectrum matched known data.⁶⁶

Benzylic alcohol 107. To a solution of compound **106** (240 mg, 0.58 mmol) in THF (5 mL) was added TBAF (1 M solution in THF, 0.76 mL, 0.76 mmol). The reaction was allowed to stir for 23 h and then quenched by addition of NH₄Cl. The resulting mixture was extracted with EtOAc, washed with brine, dried (MgSO₄), filtered, and concentrated *in vacuo*. Final purification by flash column chromatography (30% EtOAc in hexanes) afforded benzyl alcohol **107** (99 mg, 57%) as a yellow oil. The ¹H NMR spectrum matched known data.⁹

Stilbene 109. To a solution of KHMDS (0.5 M solution in toluene, 2.12 mL, 1.06 mmol) in THF (1.5 mL) were added phosphonate **104**^{8,9} (46 mg, 0.11 mmol) and aldehyde **108** (20 mg, 0.09 mmol). After the solution was stirred for 2 h, the reaction was quenched by addition of NH₄Cl. The resulting mixture was extracted with EtOAc, washed with brine, dried (MgSO₄), filtered, and concentrated *in vacuo*. Final purification by flash column chromatography provided stilbene **109** (25 mg, 58%) as a yellow oil: ¹H NMR (500 MHz, CDCl₃) δ 7.32 (d, *J* = 1.9 Hz, 1H), 7.14–7.09 (m, 2H), 6.98–6.89 (m, 4H), 5.29 (s, 2H), 5.25–5.21 (m, 7H), 3.56 (s, 3H), 3.53 (s, 3H), 3.50 (s, 6H), 3.39 (d, *J* = 7.2 Hz, 2H), 1.79 (s, 3H), 1.66 (s, 3H); ¹³C NMR (125 MHz, CDCl₃) δ 155.8 (2C), 147.4, 146.8, 136.4, 132.1, 131.0, 127.7 (2C), 122.7, 121.0, 119.7, 116.6, 114.3, 106.0 (2C), 95.4 (2C), 94.5 (2C), 56.2 (2C), 56.0 (2C), 25.7, 22.7, 17.7; HRMS (EI) *m/z* calcd for C₂₇H₃₆O₈ (M)⁺ 488.2410, found 488.2416.¹⁶

Analogue 110. After TsOH (40 mg, 0.21 mmol) was added to a solution of stilbene **109** (13 mg, 0.03 mmol) in MeOH (2.5 mL), the solution was stirred for 24 h. The reaction was quenched by addition of NaHCO₃, and the resulting mixture was extracted with EtOAc, dried (MgSO₄), filtered, and concentrated *in vacuo*. Final purification by preparative TLC (30% EtOAc in hexanes) gave stilbene **110** (4 mg, 50%) as a yellow oil. The ¹H and ¹³C NMR spectra matched published data.^{16,78,79}

Stilbene 112. To a solution of KHMDS (0.5 M solution in toluene, 4.62 mL, 2.31 mmol) in THF (1.5 mL) were added phosphonate **104** (99 mg, 0.24 mmol) and aldehyde **111** (32 mg, 0.19 mmol). After the solution was stirred for 3 h, the reaction was quenched by addition of NH₄Cl. The resulting mixture was extracted with EtOAc, washed with brine, dried (MgSO₄), filtered, and concentrated *in vacuo*. Final purification of the residue by flash column chromatography (4% EtOAc in hexanes) provided stilbene **112** (33 mg, 40%) as a yellow oil: ¹H NMR (500 MHz, CDCl₃) δ 7.44 (t, *J* = 2.7 Hz, 1H), 7.42 (t, *J* =

1.9 Hz, 1H), 7.03–7.01 (m, 2H), 6.98–6.95 (m, 1H), 6.92–6.90 (m, 1H), 6.92 (s, 2H), 5.24–5.19 (m, 5H), 5.19 (s, 2H), 3.50 (s, 6H), 3.49 (s, 3H), 3.39 (d, $J = 7.2$ Hz, 2H), 1.79 (s, 3H), 1.66 (s, 3H); ^{13}C NMR (125 MHz, CDCl_3) δ 156.8, 155.8 (2C), 136.6, 131.3, 131.0, 127.7, 127.6 (2C), 127.2, 122.7, 119.6, 116.4 (2C), 106.0 (2C), 94.5 (2C), 94.4, 56.0 (3C), 25.8, 22.8, 17.8; HRMS (EI) m/z calcd for $\text{C}_{25}\text{H}_{32}\text{O}_6$ (M) $^+$ 428.2199, found 428.2191.¹⁶

Analogue 113. To a solution of compound **112** (17 mg, 0.04 mmol) in MeOH (5 mL) was added TsOH (46 mg, 0.24 mmol). After the solution was stirred for 24 h, the reaction was quenched with NaHCO_3 . The resulting mixture was extracted with EtOAc, dried (MgSO_4), filtered, and concentrated *in vacuo*. Final purification by flash column chromatography (12% EtOAc in hexanes) provided stilbene **113** (12 mg, 100%) as a yellow oil. Both the ^1H and ^{13}C data matched those of the known compound.^{16,78,79}

Aldehyde 30. To a stirred solution of alcohol **74** (208 mg, 0.7 mmol) in CH_2Cl_2 (12 mL) was added activated MnO_2 (306 mg, 3.5 mmol). After the mixture was allowed to stir for 7 days, it was filtered and concentrated *in vacuo*. Final purification by flash column chromatography (12% EtOAc in hexanes) provided aldehyde **30** (158 mg, 76%) as a pink oil. The ^1H NMR spectrum matched the known data.⁵⁶

Directed *ortho* metallation procedures: The procedures described above in the preparation of compounds **61** or **74**⁵⁶ were followed with temperature variations as indicated in Table 12, Chapter 5.

Silyl ether 128. To a stirred solution of alcohol **47** (824 mg, 3.6 mmol) in CH_2Cl_2 (35 mL) at rt was added imidazole (1.23 g, 18.1 mmol) and TBSCl (713 mg, 4.7 mmol). After the reaction was allowed to stir for 18.5 h, it was quenched by addition of NH_4Cl .

The resultant mixture was extracted with CH₂Cl₂, and the combined extracts were dried (MgSO₄), filtered, and concentrated *in vacuo*. Final purification by flash column chromatography (10% EtOAc in hexanes) afforded silyl ether **128** (1.12 g, 91%) as a pale yellow oil: ¹H NMR (500 MHz, CDCl₃) δ 7.16 (d, *J* = 2.7 Hz, 1H), 7.11 (d, *J* = 8.1 Hz, 1H), 6.92–6.90 (m, 1H), 5.22 (s, 2H), 5.21 (s, 2H), 4.67 (s, 2H), 3.51 (s, 6H), 0.94 (s, 9H), 0.90 (s, 6H); ¹³C NMR (75 MHz, CDCl₃) δ 147.2, 146.1, 136.0, 119.9, 116.7, 114.9, 95.6, 95.4, 64.5, 56.1, 56.0, 25.9 (3C), 18.3, –5.3 (2C); HRMS (ESI) *m/z* calcd for C₁₇H₃₀O₅NaSi (M + Na)⁺ 365.1760, found 365.1768.

Prenylated compounds 129 and 130. To a solution of TMEDA (0.60 mL, 4.0 mmol) in Et₂O (50 mL) at –35 °C was added *n*-BuLi (1.75 M solution in hexanes, 2.10 mL, 3.7 mmol). The solution was allowed to warm to –20 °C, and then a solution of silyl ether **128** (1.06 g, 3.1 mmol) in Et₂O (4 mL) was added to the reaction over 9 min. After the reaction warmed to 0 °C over the course of an hour, it was cooled to –20 °C, and a solution of prenyl bromide (0.6 mL, 5.1 mmol) was added over 16 min. After the reaction mixture stirred for 18 h while warming to rt, the reaction was quenched by addition of NH₄Cl. The resultant mixture was extracted with Et₂O, and the combined organic layers were dried (MgSO₄), filtered, and concentrated *in vacuo*. Final purification by flash column chromatography (5% EtOAc in hexanes) followed by a second purification by flash column chromatography (2% Et OAc in hexanes) provided compound **129** (11 mg, 1%) as a yellow oil and compound **130** (34 mg, 3%) as a yellow oil: For compound **129**: ¹H NMR (500 MHz, CDCl₃) δ 6.98 (d, *J* = 1.8 Hz, 1H), 6.91 (d, *J* = 1.8 Hz, 1H), 5.30 (dt, *J* = 9.6 Hz, 1.1 Hz, 1H), 5.21 (s, 2H), 5.10 (dd, *J* = 7.6 Hz, 3.8 Hz, 2H), 5.12–5.08 (m, 1H), 4.69 (s, 2H), 4.05 (dt, *J* = 8.9 Hz, 5.9 Hz, 1H), 3.64 (s, 3H), 3.52 (s, 3H), 2.39–2.33 (m, 1H), 2.30–2.24 (m, 1H), 1.72 (s, 3H), 1.68 (s, 6H), 1.60 (s, 3H), 0.97 (s, 9H), 0.12 (s, 6H); ¹³C NMR (125 MHz, CDCl₃) δ 149.7, 142.7, 140.0, 137.5, 132.1, 131.9, 128.3, 122.8, 118.7, 111.5, 99.2, 95.2, 64.8, 57.4, 56.1, 37.3, 35.6,

25.9 (4C), 25.8, 18.4, 18.2, 17.9, -5.2 (2C); HRMS (ESI) m/z calcd for $C_{27}H_{46}O_5NaSi$ ($M + Na$)⁺ 501.3012, found 501.3018.

For compound **130**: ¹H NMR (500 MHz, CDCl₃) δ 7.00 (d, $J = 2.0$ Hz, 1H), 6.84–6.83 (m, 1H), 5.36–5.31 (m, 1H), 5.21 (s, 2H), 5.12 (s, 2H), 4.68 (s, 2H), 3.63 (s, 3H), 3.52 (s, 3H), 3.44 (d, $J = 7.2$ Hz, 2H), 1.78 (s, 3H), 1.74 (s, 3H), 0.97 (s, 9H), 0.12 (s, 6H); ¹³C NMR (125 MHz, CDCl₃) δ 149.6, 143.5, 137.5, 135.6, 132.6, 122.7, 120.4, 112.0, 99.1, 95.2, 64.6, 57.4, 56.1, 28.5, 25.9 (3C), 25.7, 18.4, 17.8, -5.3 (2C); HRMS (ESI) m/z calcd for $C_{22}H_{38}O_5NaSi$ ($M + Na$)⁺ 433.2386, found 433.2385.

Acetamide 137. To a stirred solution of 3,5-dimethoxyaniline **136** (5.02 g, 32.7 mmol) in CH₂Cl₂ (100 mL) at 0 °C was added TEA (5.8 mL, 40.2 mmol), and then acetic anhydride (4.0 mL, 42.5 mmol) was added to the solution. The reaction was allowed to stir for 24 h, and then was quenched by addition of H₂O. The resultant mixture was extracted with CH₂Cl₂, and the combined organics were washed with brine, dried (MgSO₄), filtered, and concentrated *in vacuo* to make available acetamide **137** (5.83 g, 91%) as a light brown solid. The ¹H NMR matched the known data.¹⁰⁴

Geranylated compound 138. To a solution of acetamide **137** (5.59 g, 28.7 mmol) in dioxane (150 mL) was added BF₃•OEt₂ (2.8 mL, 22.7 mmol). The mixture was heated to 50 °C, and then geraniol (2.5 mL, 14.4 mmol) in dioxane (32 mL) was added drop wise over 1 h to the reaction. The reaction was allowed to stir for 2 h at 50 °C before it was quenched by addition of H₂O. The resultant mixture was extracted with Et₂O, and the combined organic extracts were dried (MgSO₄), filtered, and concentrated *in vacuo*. Final purification by flash column chromatography (25% EtOAc in hexanes) provided geranylated compound **138** (1.77 g, 37%) as a white solid: ¹H NMR (500 MHz, CD₃OD) δ 6.47 (d, $J = 2.4$ Hz, 1H), 6.36 (d, $J = 2.3$ Hz, 1H), 5.01–4.94 (m, 2H), 3.72 (s, 3H), 3.69

(s, 3H), 3.19 (d, $J = 7.0$ Hz, 2H), 2.04 (s, 3H), 2.01–1.95 (m, 2H), 1.91–1.85 (m, 2H), 1.66 (s, 3H), 1.56 (s, 3H), 1.50 (s, 3H); ^{13}C NMR (125 MHz, CD_3OD) δ 172.2, 160.1, 160.0, 137.6, 135.6, 132.1, 125.4, 124.1, 119.1, 104.5, 98.0, 56.2, 55.8, 40.8, 27.7, 25.9, 24.2, 23.2, 17.7, 16.3; HRMS (ESI) m/z calcd for $\text{C}_{20}\text{H}_{30}\text{NO}_3$ ($\text{M} + \text{H}$) $^+$ 332.2226, found 332.2218.

Ethyl amine 139. To a solution of LiAlH_4 (172 mg, 4.5 mmol) in THF (15 mL) at 0 °C was added compound **138** (500 mg, 1.5 mmol). The reaction was allowed to stir for 18 h, and then it was quenched by addition of 1M HCl, and then slow addition of H_2O . The resultant mixture was extracted with EtOAc, and the combined organic layers were washed with brine, dried (MgSO_4), filtered, and concentrated *in vacuo*. Final purification by flash column chromatography (8% EtOAc in hexanes) delivered ethyl amine **139** (197 mg, 41%) as a yellow oil: ^1H NMR (500 MHz, CD_3OD) δ 5.91 (d, $J = 2.6$ Hz, 1H), 5.84 (d, $J = 2.3$ Hz, 1H), 5.01–4.98 (m, 1H), 4.95–4.92 (m, 1H), 3.67 (s, 6H), 3.15 (d, $J = 7.0$ Hz, 2H), 3.01 (q, $J = 7.2$ Hz, 2H), 2.03–1.98 (m, 2H), 1.93–1.90 (m, 2H), 1.70 (s, 3H), 1.57 (s, 3H), 1.50 (s, 3H), 1.14 (t, $J = 7.1$ Hz, 3H); ^{13}C NMR (125 MHz, CD_3OD) δ 161.1, 159.3, 149.4, 136.2, 132.2, 125.2, 124.6, 107.5, 91.7, 89.0, 56.1, 55.5, 40.8, 39.7, 27.7, 25.9, 23.0, 17.8, 16.2, 15.2; HRMS (ESI) m/z calcd for $\text{C}_{20}\text{H}_{32}\text{NO}_2$ ($\text{M} + \text{H}$) $^+$ 318.2433, found 318.2433.

Amine 140. To a solution of acetamide **137** (110 mg, 0.3 mmol) in MeOH (0.6 mL) was added NaOH (3M solution in MeOH, 0.86 mL, 2.6 mmol), and then the reaction was heated to 50 °C. After stirring for 8 d, the reaction was concentrated and then quenched by addition of H_2O and diluted with CH_2Cl_2 . The resultant mixture was extracted with CH_2Cl_2 , and the combined organics were dried (Na_2SO_4), filtered, and concentrated *in vacuo*. Final purification by flash column chromatography (6% EtOAc in hexanes), and after a second purification by flash column chromatography (3% EtOAc in hexanes),

gave amine **140** (46 mg, 61% BRSM) as an orange–red solid: ^1H NMR (500 MHz, CDCl_3) δ 5.98 (d, $J = 2.2$ Hz, 1H), 5.90 (d, $J = 2.2$ Hz, 1H), 5.09–5.03 (m, 2H), 3.77 (s, 3H), 3.75 (s, 3H), 3.67 (br s, 2H), 3.25 (d, $J = 6.2$ Hz, 2H), 2.10–2.03 (m, 2H), 2.03–1.97 (m, 2H), 1.77 (s, 3H), 1.66 (s, 3H), 1.58 (s, 3H); ^{13}C NMR (125 MHz, CDCl_3) δ 159.2, 158.6, 146.5, 136.0, 131.4, 124.2, 122.7, 107.1, 93.5, 89.5, 55.6, 55.1, 39.6, 26.6, 25.7, 22.4, 17.7, 16.0; HRMS (ESI) m/z calcd for $\text{C}_{18}\text{H}_{28}\text{NO}_2$ ($\text{M} + \text{H}$) $^+$ 290.2120, found 290.2110.

Dihydroxy compound 141.⁸⁶ To a stirred solution of aluminum iodide (4.89 g, 11.9 mmol) in toluene (30 mL) at 0 °C was added TBAI (38 mg, 0.1 mmol) and phloroglucinol (619 mg, 4.9 mmol) followed by addition of amide **137** (200 mg, 1.0 mmol). After 30 min the reaction was quenched by addition of saturated sodium thiosulfate. The mixture was extracted with EtOAc, and the combined organics were washed with brine, dried (MgSO_4), filtered, and concentrated *in vacuo*. Final purification by flash column chromatography (80% EtOAc in hexanes) afforded compound **141** (118 mg, 69%) as a white solid. The ^1H NMR spectrum matched the known data.⁸⁶

Geranylated compound 142. To a stirred solution of amide **141** (551 mg, 3.3 mmol) in dioxane (150 mL) was added $\text{BF}_3 \cdot \text{OEt}_2$ (0.17 mL, 1.4 mmol). The reaction mixture was heated to 50 °C and geraniol (0.25 mL, 1.4 mmol) in dioxane (10 mL) was added dropwise over 60 min. After stirring for an additional 1.3 h, the reaction was quenched by addition of H_2O . The resulting mixture was extracted with Et_2O . Then the combined organics were washed with brine, dried (MgSO_4), filtered, and concentrated *in vacuo*. Purification by flash column chromatography (30% EtOAc in hexanes) afforded geranylated product **142** (118 mg, 27%) as a yellow oil: ^1H NMR (300 MHz, CD_3OD) δ 6.21 (d, $J = 2.5$ Hz, 1H), 6.07 (d, $J = 2.4$ Hz, 1H), 4.95–4.88 (m, 2H), 3.08 (d, $J = 6.7$ Hz, 2H), 1.93–1.85 (m, 5H), 1.81–1.76 (m, 2H), 1.57 (s, 3H), 1.48 (s, 3H), 1.41 (s, 3H); ^{13}C

NMR (125 MHz, CD₃OD) δ 172.0, 157.5, 156.9, 137.8, 135.3, 132.2, 125.4, 124.6, 116.2, 106.0, 101.9, 40.9, 27.8, 25.9, 24.2, 23.2, 17.7, 16.3; HRMS (ESI) m/z calcd for C₁₈H₂₆NO₃ (M + H)⁺ 304.1913, found 304.1917.

Amide 145. To a stirred solution of amine **139** (46 mg, 0.07 mmol) in Et₂O (1 mL) was added benzoyl chloride (**144**, 8 μ L, 0.15 mmol). After the reaction was allowed to stir for 17 h, the mixture was washed with 1M NaOH (x2), and then 1M HCl. The combined organics were washed with brine, dried (Na₂SO₄), filtered, and concentrated *in vacuo*. Final purification by preparative TLC (15% EtOAc in hexanes) afforded amide **145** (32 mg, 100% by NMR) as a yellow oil: ¹H NMR (500 MHz, CDCl₃) δ 7.31–7.29 (m, 2H), 7.20 (t, J = 7.2 Hz, 1H), 7.12 (t, J = 7.5 Hz, 2H), 6.32 (d, J = 2.0 Hz, 1H), 6.05 (d, J = 2.0 Hz, 1H), 5.07–5.04 (m, 1H), 5.00 (t, J = 6.2 Hz, 1H), 4.29 (dq, J = 14.2 Hz, 7.2 Hz, 1H), 3.76 (s, 3H), 3.63 (s, 3H), 3.38 (dq, J = 14.1 Hz, 7.2 Hz, 1H), 3.22–1.99 (m, 2H), 2.06–1.99 (m, 2H), 1.96–1.94 (m, 2H), 1.71 (s, 3H), 1.65 (s, 3H), 1.58 (s, 3H), 1.22 (t, J = 7.2 Hz, 3H); ¹³C NMR (125 MHz, CDCl₃) δ 170.2, 159.4, 158.3, 142.5, 136.3, 135.4, 131.2, 129.4, 128.1 (2C), 127.5 (2C), 124.3, 122.2, 120.2, 106.4, 97.9, 55.5, 55.4, 45.0, 39.7, 26.6, 25.7, 24.6, 17.6, 16.2, 12.5; HRMS (ESI) m/z calcd for C₂₇H₃₅NO₃Na (M + Na)⁺ 444.2515, found 444.2522.

Aldehyde 150. To a stirred mixture of alcohol **61** (371 mg, 1.3 mmol) and celite (685 mg) in DMF (4 mL) was added PDC (1.41 g, 3.8 mmol). The reaction was stirred for 8 d, and then it was diluted with CH₂Cl₂, filtered, and concentrated *in vacuo*. The resulting material was diluted with Et₂O and H₂O was added. The resultant mixture was extracted with Et₂O, and the combined organics were dried (MgSO₄), filtered, and concentrated *in vacuo*. Final purification by flash column chromatography (35% EtOAc in hexanes) afforded compound **150** (36 mg, 39%) as a yellow oil: ¹H NMR (500 MHz, CDCl₃) δ 9.90 (s, 1H), 7.69 (d, J = 1.5 Hz, 1H), 7.55 (d, J = 1.8 Hz, 1H), 7.01 (d, J = 16.1 Hz, 1H),

6.47 (d, $J = 16.4$ Hz, 1H), 5.26 (s, 2H), 5.23 (s, 2H), 3.60 (s, 3H), 3.51 (s, 3H), 1.45 (s, 6H); ^{13}C (125 MHz, CDCl_3) δ 191.2, 150.5, 149.4, 140.6, 132.6, 132.5, 122.6, 120.3, 114.6, 99.1, 95.1, 71.2, 57.8, 56.4, 29.9 (2C); HRMS (ESI) m/z calcd for $\text{C}_{16}\text{H}_{22}\text{O}_6^{23}\text{Na}$ ($\text{M} + \text{Na}$) $^+$ 333.1314, found 333.1326.

Aldehyde 151. To a stirred solution of alcohol **61** (320 mg, 1.1 mmol) in CH_2Cl_2 (18 mL) at room temperature was added MnO_2 (469 mg, 5.4 mmol). The reaction was allowed to stir for 18 h, and then the mixture was filtered, and the filtrate was concentrated *in vacuo*. Final purification by flash column chromatography (8% EtOAc in hexanes) afforded aldehyde **151** (225 mg, 71%) as a yellow oil. The ^1H NMR spectrum matched known data⁵⁶; ^{13}C NMR (125 MHz, CDCl_3) δ 191.3, 150.1, 136.7, 133.8, 132.5, 125.9, 121.6, 113.9, 99.0, 95.1, 57.7, 56.5, 28.5, 25.8, 17.9; HRMS (ESI) m/z calcd for $\text{C}_{16}\text{H}_{22}\text{O}_5\text{Na}$ ($\text{M} + \text{Na}$) $^+$ 317.1365, found 317.1384.

Acid 149.⁹² To a solution of aldehyde **151** (40 mg, 0.1 mmol) in 2-methyl-2-butene (4.0 mL, 37.8 mmol) and *t*-BuOH (1.2 mL) was added a solution of NaClO_2 (129 mg, 1.4 mmol) and NaH_2PO_4 (104 mg, 0.9 mmol) in H_2O (0.5 mL) over 7 min. After the reaction was allowed to stir for 4.5 h, the reaction was extracted with Et_2O . The combined organic layers were dried (Na_2SO_4), filtered, and concentrated *in vacuo*. The material was moved forward without additional purification. Analysis of the ^1H NMR spectrum showed a 3.3 : 1 mixture of acid **149** : aldehyde **151** (or 41 mg of the acid (97%) in the 51 mg mixture) as a light yellow solid from the reaction. For the acid: ^1H NMR (500 MHz, CDCl_3) δ 7.72 (d, $J = 2.2$ Hz, 1H), 7.64 (d, $J = 2.0$ Hz, 1H), 5.33–5.29 (m, 1H), 5.24 (s, 2H), 5.22 (s, 2H), 3.60 (s, 3H), 3.52 (s, 3H), 3.45 (d, $J = 7.5$ Hz, 2H), 1.76 (s, 3H), 1.73 (s, 3H); ^{13}C NMR (125 MHz, CDCl_3) δ 171.3, 149.6, 149.3, 136.1, 133.4, 125.5, 121.8 (2C), 115.7, 98.9, 95.2, 57.6, 56.4, 28.5, 25.7, 17.8; HRMS (ESI) m/z calcd for $\text{C}_{16}\text{H}_{22}\text{O}_6\text{Na}$ ($\text{M} + \text{Na}$) $^+$ 333.1314, found 333.1320.

Acid 152.⁹² To a stirred solution of aldehyde **30** (43 mg, 0.1 mmol) in 2-methyl-2-butene (4.2 mL, 39.7 mmol) and *t*-BuOH (1.2 mL) was added NaClO₂ (137 mg, 1.5 mmol) and NaH₂PO₄ (112 mg, 0.9 mmol) in H₂O (0.5 mL) over 11 min. The reaction was allowed to stir for 3.5 h, and then was extracted with Et₂O. The combined organic layers were dried (MgSO₄), filtered, and concentrated *in vacuo* to afford acid **152** (54 mg, 100% by NMR) as a white solid: ¹H NMR (500 MHz, CDCl₃) δ 7.81(d, *J* = 8.7 Hz, 1H), 7.05 (d, *J* = 8.9 Hz, 1H), 5.26 (s, 2H), 5.18–5.15 (m, 1H), 5.10 (s, 2H), 3.89 (d, *J* = 6.4 Hz, 2H), 3.62 (s, 3H), 3.51 (s, 3H), 1.77 (s, 3H), 1.67 (s, 3H); ¹³C NMR (125 MHz, CDCl₃) δ 172.3, 153.7, 144.9, 139.7, 131.7, 128.8, 123.2, 122.8, 112.5, 99.2, 94.6, 57.7, 56.4, 26.2, 25.7, 18.1; HRMS (ESI) *m/z* calcd for C₁₆H₂₂O₆Na (M + Na)⁺ 333.1314, found 333.1323.

HOBt ester 154.⁸⁷ a) To a stirred solution of acid **152** (31 mg, 0.1 mmol) and *N*-ethyl-*N'*-(3-dimethylaminopropyl)carbodiimide hydrochloride (**EDC**, 21 mg, 0.1 mmol) in CH₂Cl₂ (10 mL) was added HOBt (15 mg, 0.1 mmol). The mixture was allowed to stir for 15 min, and then a solution of amine **140** (30 mg, 0.1 mmol) in triethylamine (20 μL, 0.1 mmol) in CH₂Cl₂ (3 mL) was added dropwise over 8 min. After 22 h of stirring, incomplete conversion to product was observed, and so an additional portion of EDC (22 mg, 0.1 mmol) and triethylamine (20 μL, 0.1 mmol) was added. The reaction was allowed to stir for an additional 5 h, and then was quenched by addition of H₂O. The resultant mixture was extracted with CH₂Cl₂, and the combined organic fractions were washed with brine, dried (MgSO₄), filtered, and concentrated *in vacuo*. Final purification by preparative TLC (20% EtOAc in hexanes) afforded HOBt ester **154** (20 mg, 47%) as a yellow oil.

HOBt ester 154.⁹³ b) To a stirred solution of acid **152** (18 mg, 0.06 mmol) and amine **140** (22 mg, 0.07 mmol) in CH₂Cl₂ (2.0 mL) was added *N,N'*-dicyclohexylcarbodiimide (DCC, 20 mg, 0.10 mmol). The reaction was cooled to 0 °C and a solution of HOBt (9 mg, 0.07 mmol) in THF (0.87 mL) was added. The reaction was allowed to warm to room temperature and stirred for 26 h, and then was concentrated *in vacuo*. Final purification by preparative TLC (20% EtOAc in hexanes) provided HOBt ester **154** (8 mg, 32%) as a yellow oil: ¹H NMR (500 MHz, CDCl₃) δ 8.12–8.09 (m, 2H), 7.56–7.53 (m, 1H), 7.45–7.42 (m, 2H), 7.20 (d, *J* = 8.8 Hz, 1H), 5.33 (s, 2H), 5.16–5.13 (m, 1H), 5.15 (s, 2H), 3.86 (d, *J* = 6.4 Hz, 2H), 3.63 (s, 3H), 3.54 (s, 3H), 1.68 (s, 3H), 1.66 (s, 3H).

Amide 155.⁸⁸ To a stirred solution of acid **149** (41 mg, 0.13 mmol) in CH₂Cl₂ (0.7 mL) was added oxalyl chloride (12 μL, 0.14 mmol) and then DMF (2 drops). The reaction was allowed to stir at rt for 2.5 h and was then concentrated *in vacuo*. The acid chloride in CH₂Cl₂ (0.7 mL) was added over 3 min to a stirred solution of amine **140** (36 mg, 0.12 mmol) in pyridine (0.7 mL) at 0 °C. The reaction mixture stirred for 18 h and then concentrated *in vacuo*. Final purification by flash column chromatography (8% EtOAc in hexanes) provided amide **155** (11 mg, 16%) as a golden oil: ¹H NMR (500 MHz, CDCl₃) δ 7.87 (br s, 1H), 7.51 (d, *J* = 2.3 Hz, 1H), 7.45–7.42 (m, 1H), 7.22 (d, *J* = 1.7 Hz, 1H), 6.83 (d, *J* = 2.5 Hz, 1H), 5.28–5.25 (m, 1H), 5.22 (s, 2H), 5.18 (s, 2H), 5.13–5.11 (m, 1H), 5.03–5.00 (m, 1H), 3.82 (s, 3H), 3.81 (s, 3H), 3.59 (s, 3H), 3.50 (s, 3H), 3.45 (d, *J* = 6.9 Hz, 2H), 3.37 (d, *J* = 6.8 Hz, 2H), 1.74 (s, 3H), 1.72 (s, 3H), 1.66 (s, 3H), 1.61 (s, 3H), 1.52 (s, 3H); ¹³C NMR (125 MHz, CDCl₃) δ 165.3, 158.9, 157.8, 149.8, 148.0, 137.8, 137.4, 136.4, 133.2, 131.7, 131.2, 123.8, 122.1, 122.0, 121.4, 113.6, 99.0, 95.9, 95.3, 57.6, 56.5, 55.8, 55.4, 39.5, 28.9, 26.6, 25.7, 25.6, 22.7, 17.9, 17.6, 16.5; HRMS (ESI) *m/z* calcd for C₃₄H₄₈NO₇ (M + H)⁺ 582.3431, found 582.3438.

APPENDIX:
SELECTED NMR SPECTRA

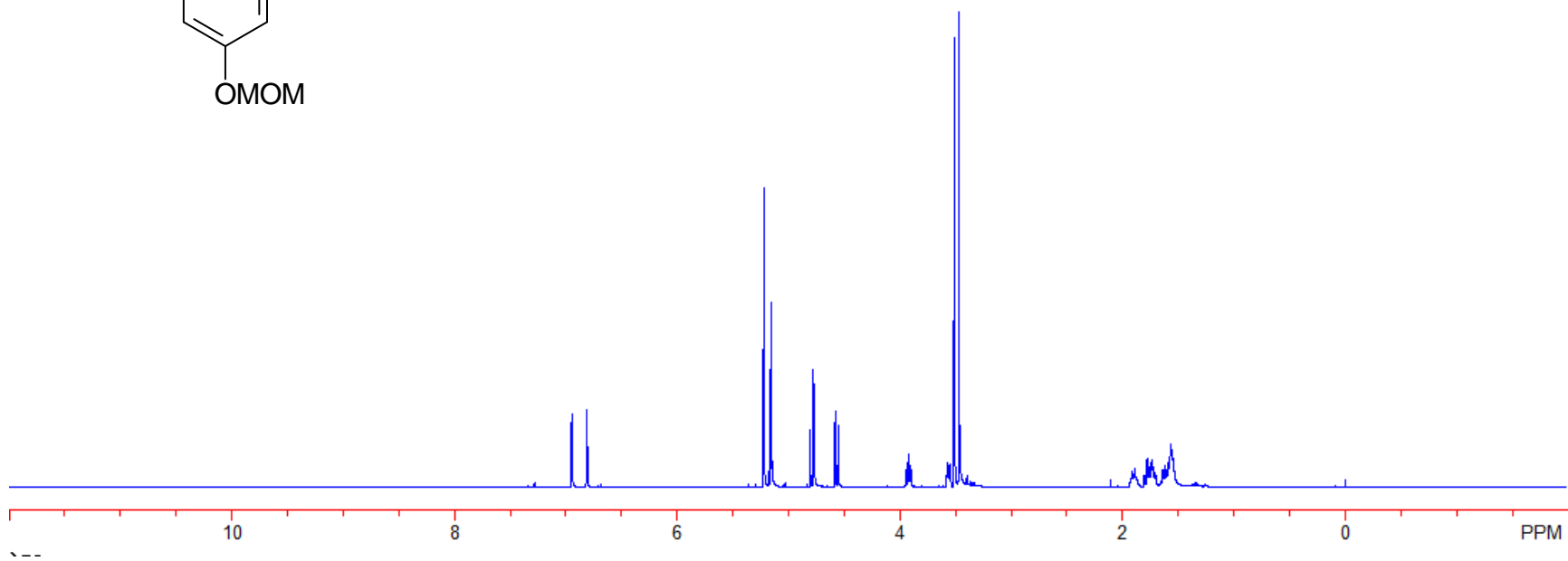
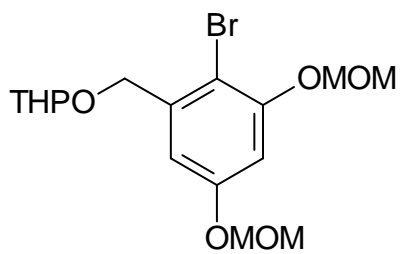


Figure A-1. ^1H NMR spectrum of compound 37

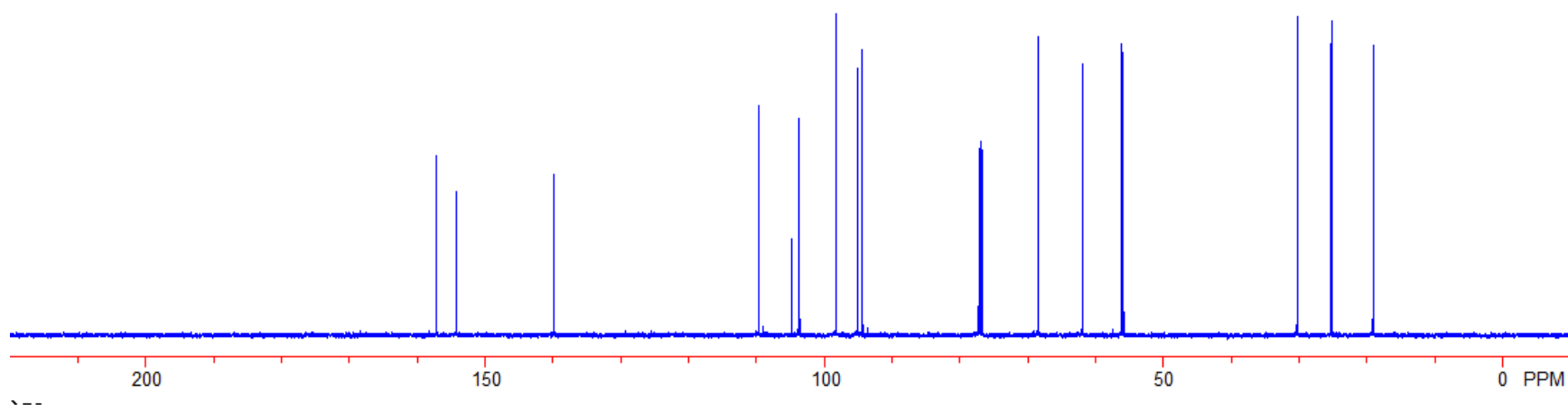
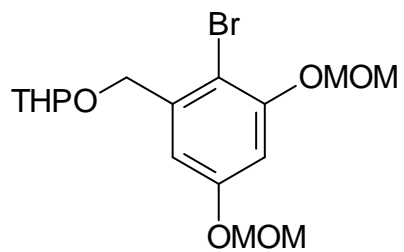


Figure A-2. ^{13}C NMR spectrum of compound 37

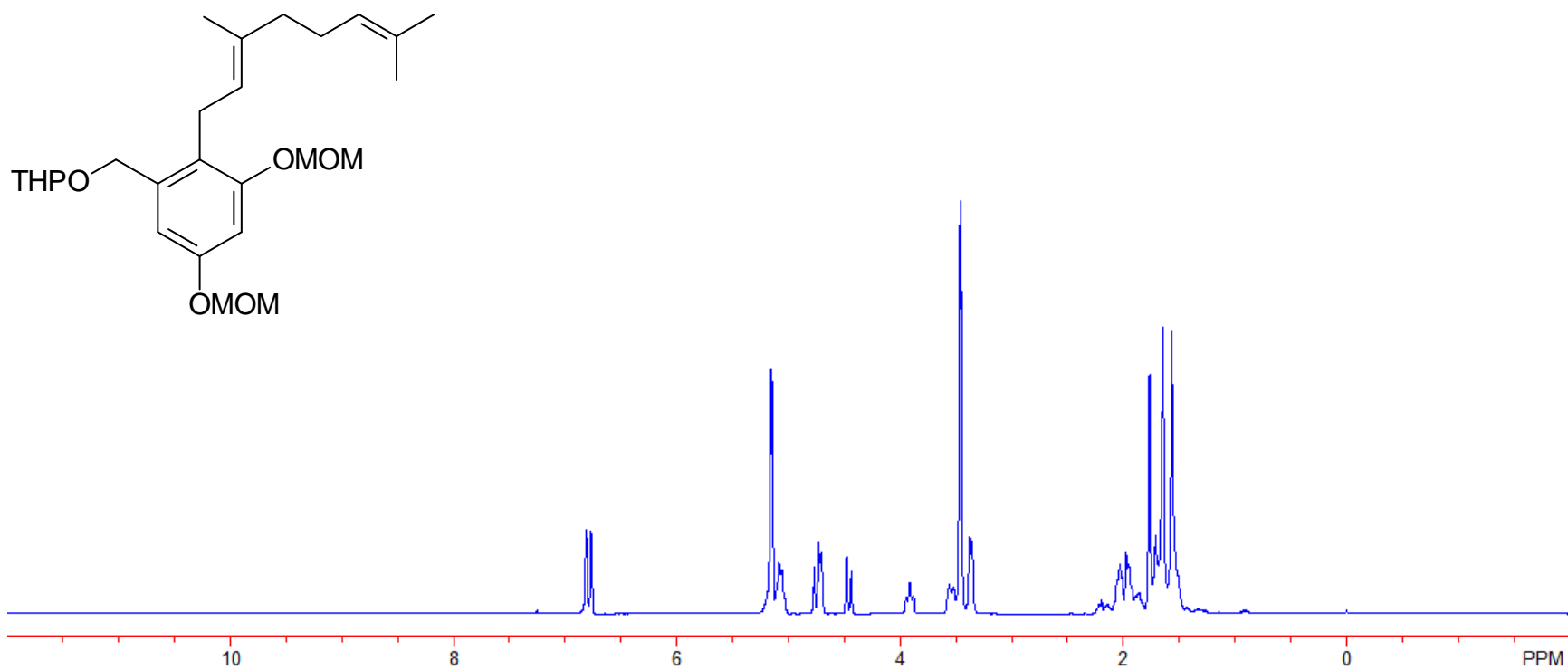


Figure A-3. ¹H NMR spectrum of compound 38

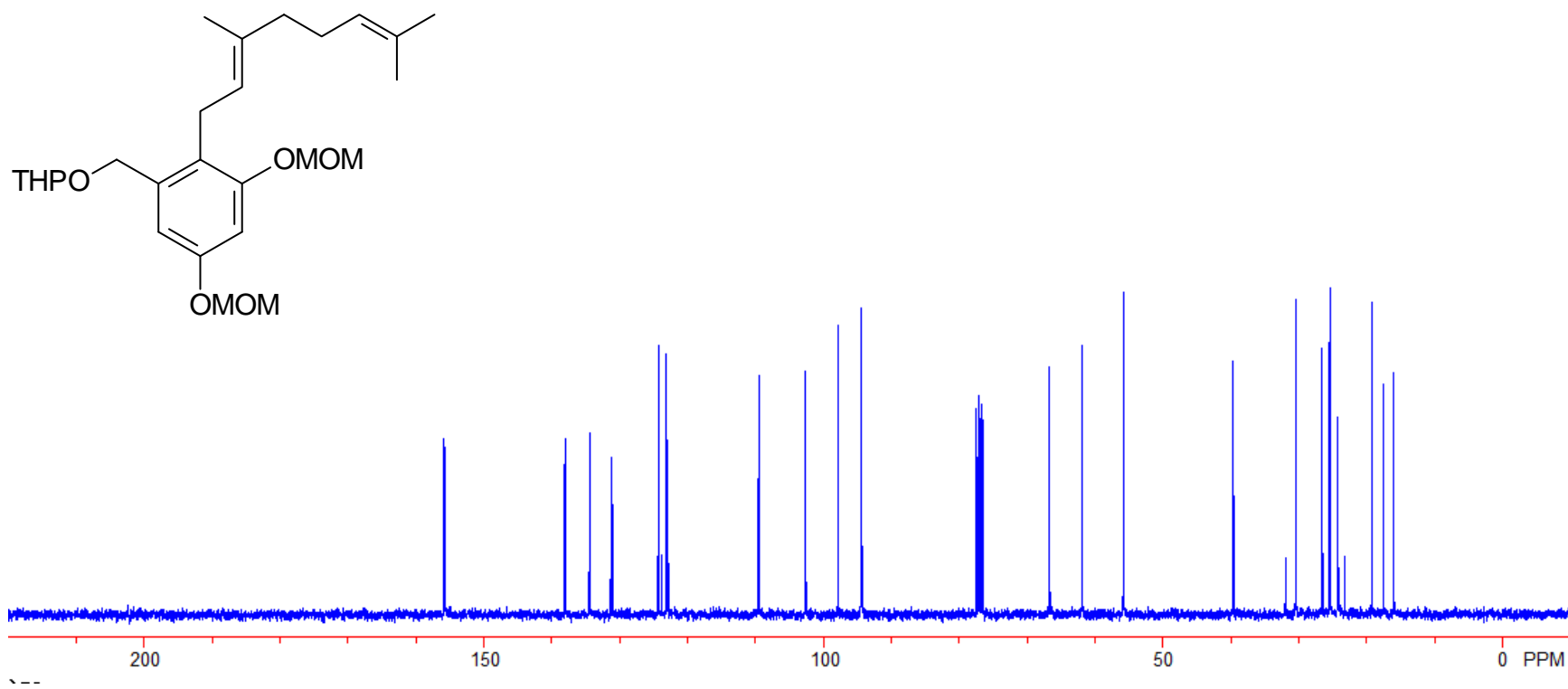


Figure A-4. ¹³C NMR spectrum of compound 38

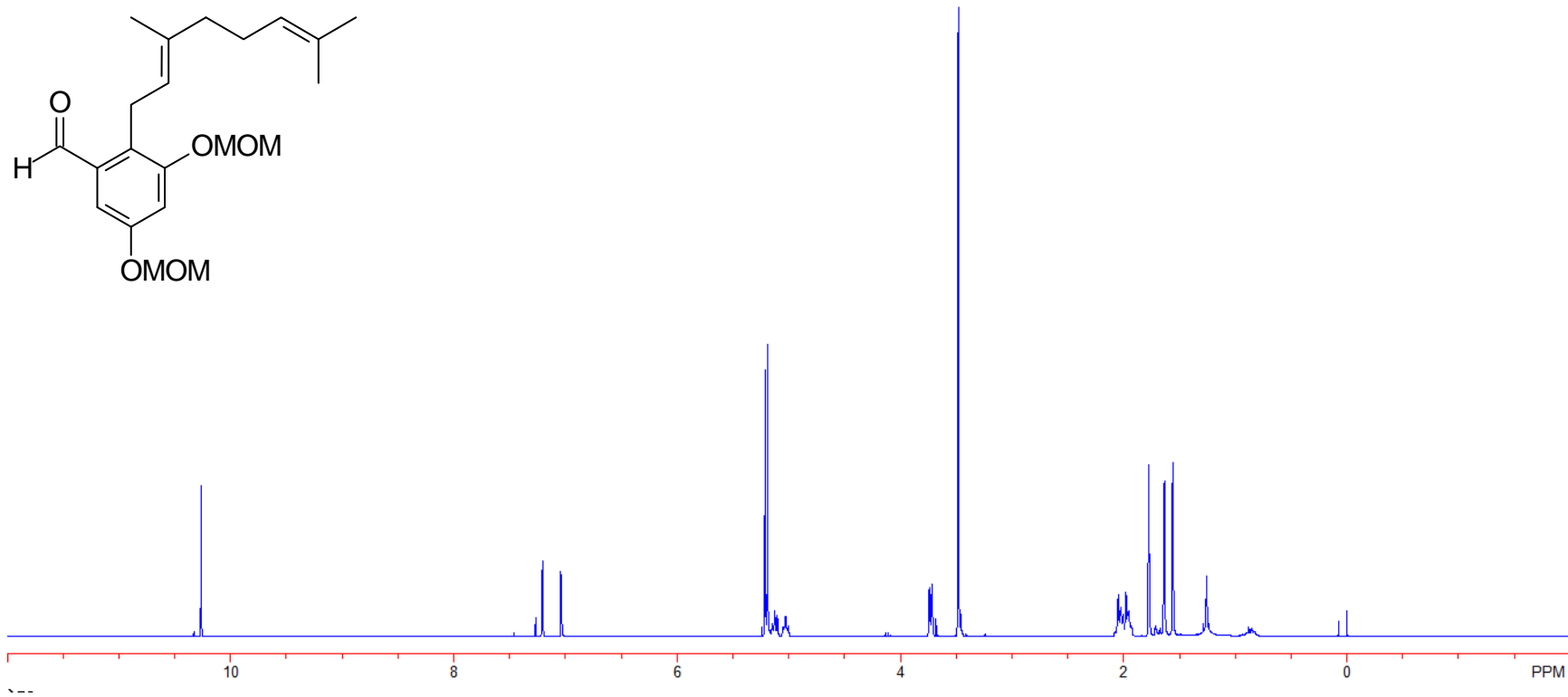


Figure A-5. ^1H NMR spectrum of compound 34

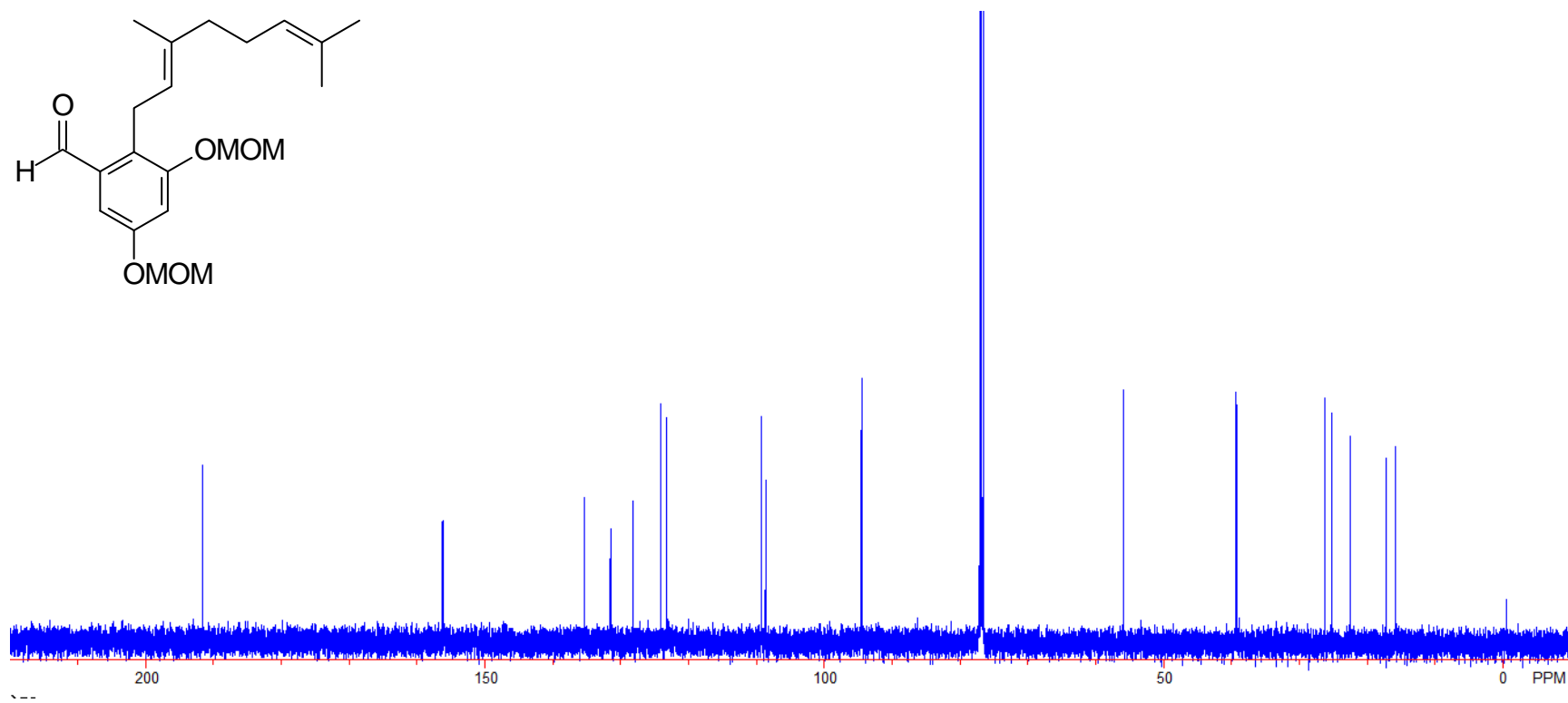
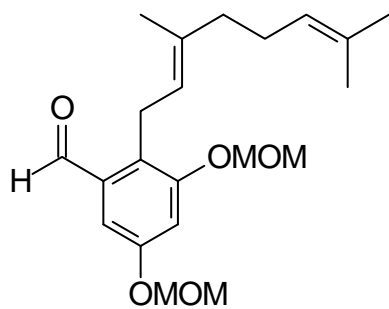


Figure A-6. ^{13}C NMR spectrum of compound 34

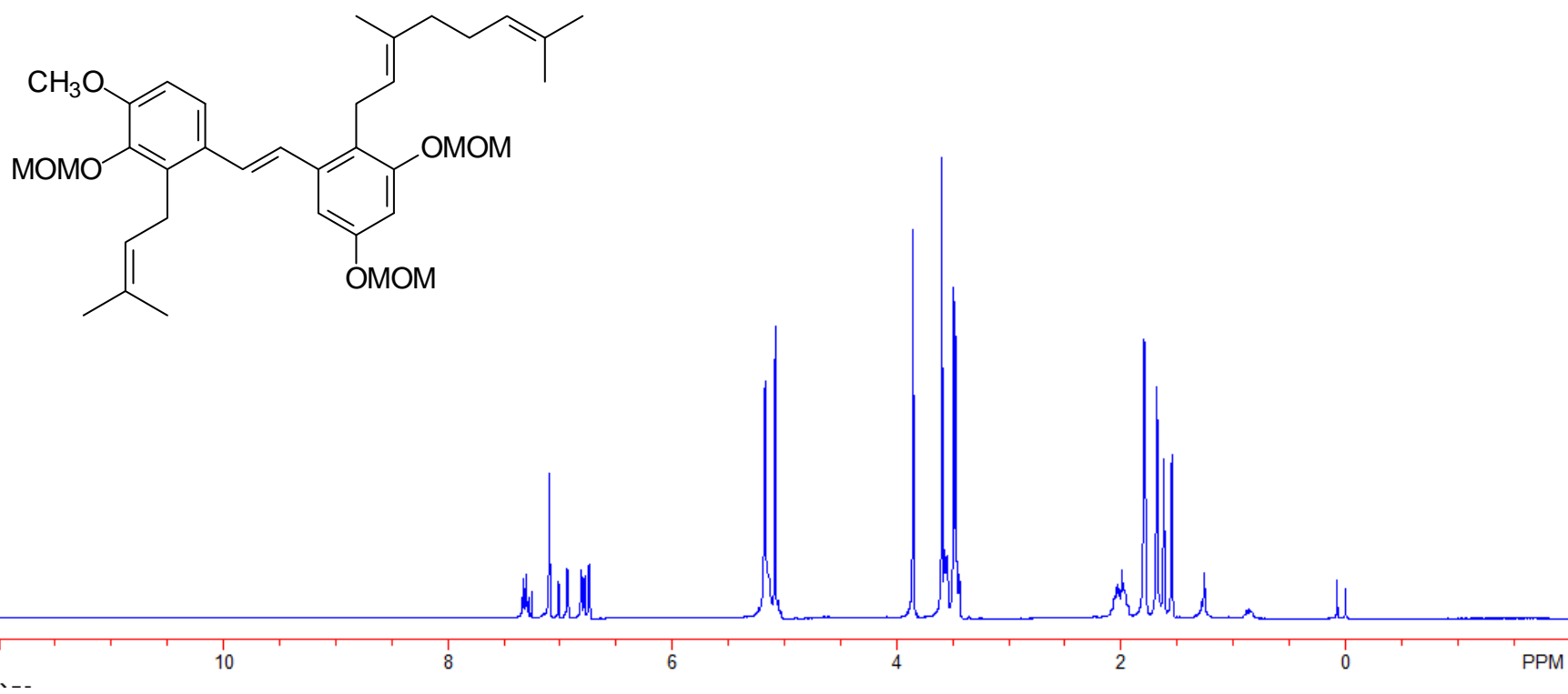


Figure A-7. ¹H NMR spectrum of compound 45

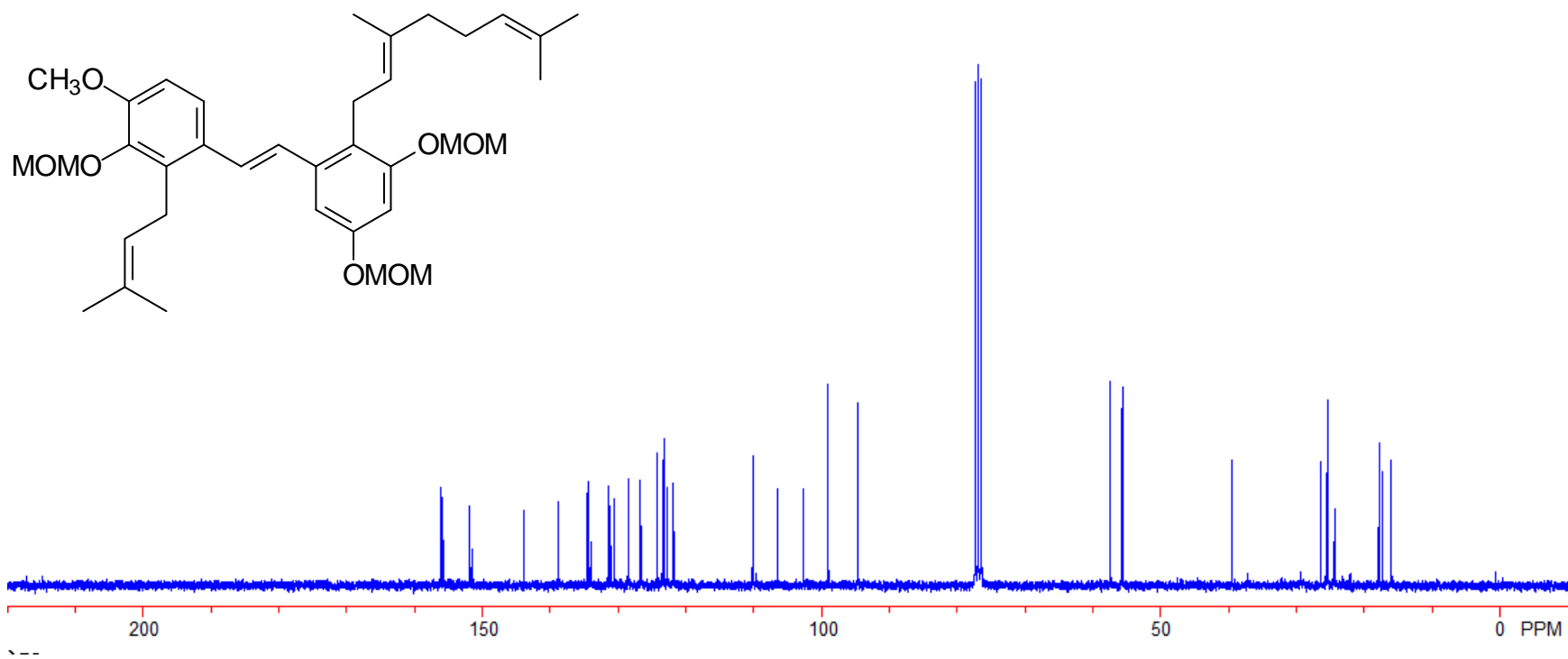


Figure A-8. ^{13}C NMR spectrum of compound 45

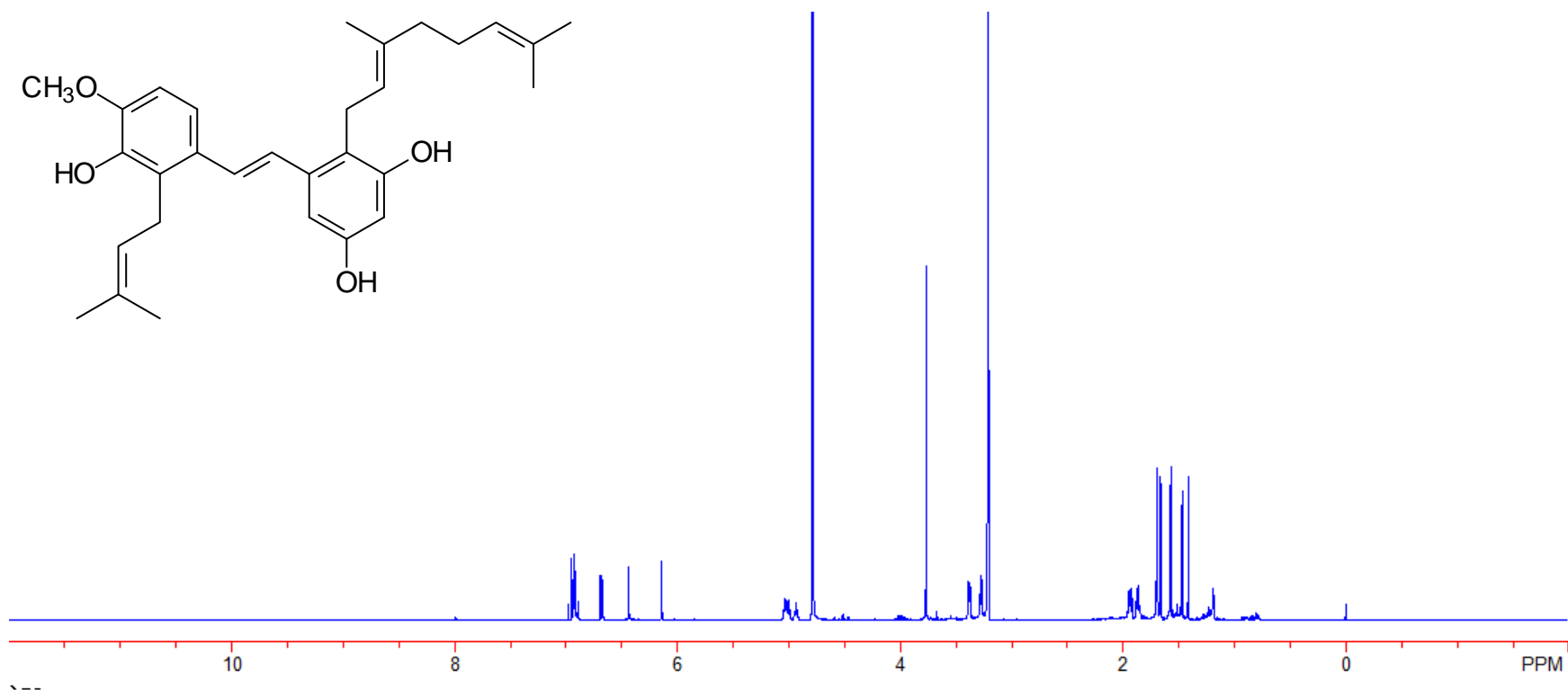


Figure A-9. ¹H NMR spectrum of compound **46**

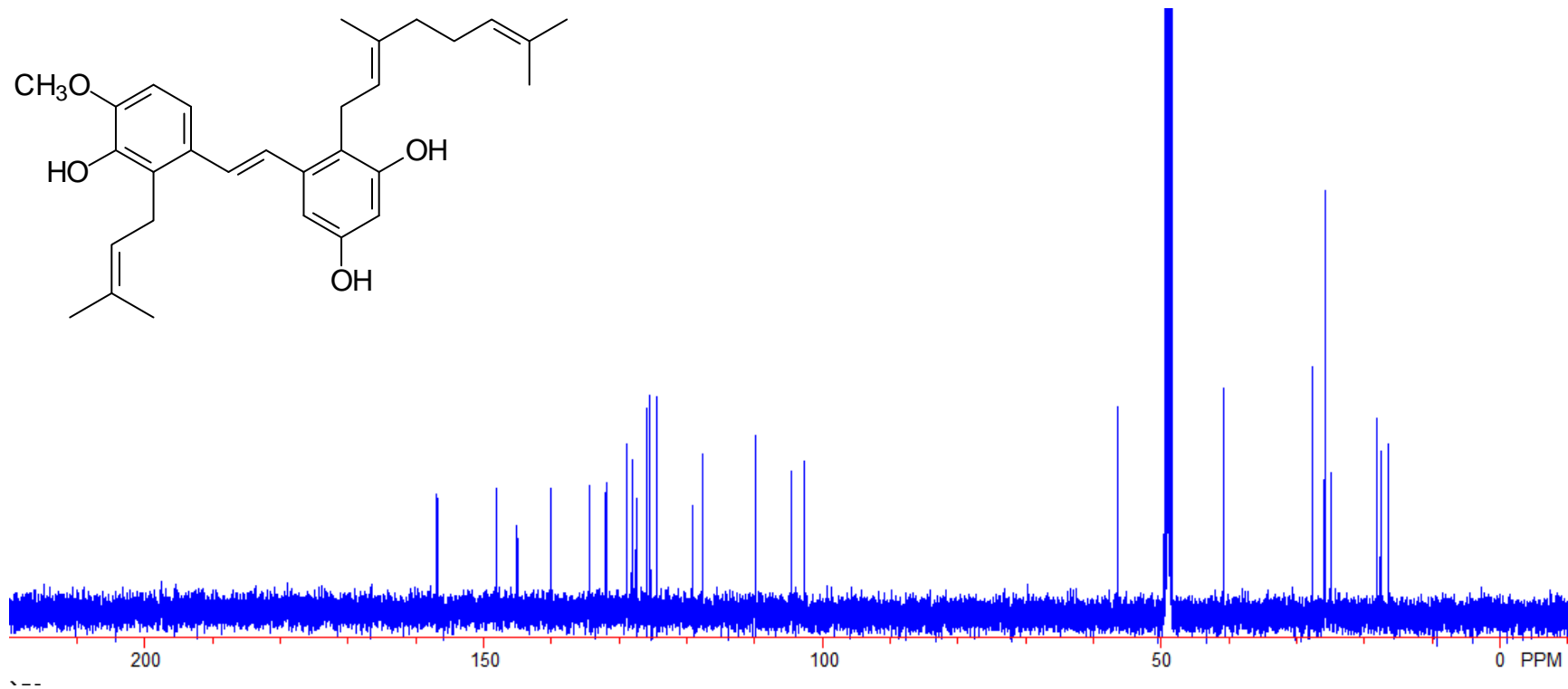


Figure A-10. ^{13}C NMR spectrum of compound **46**

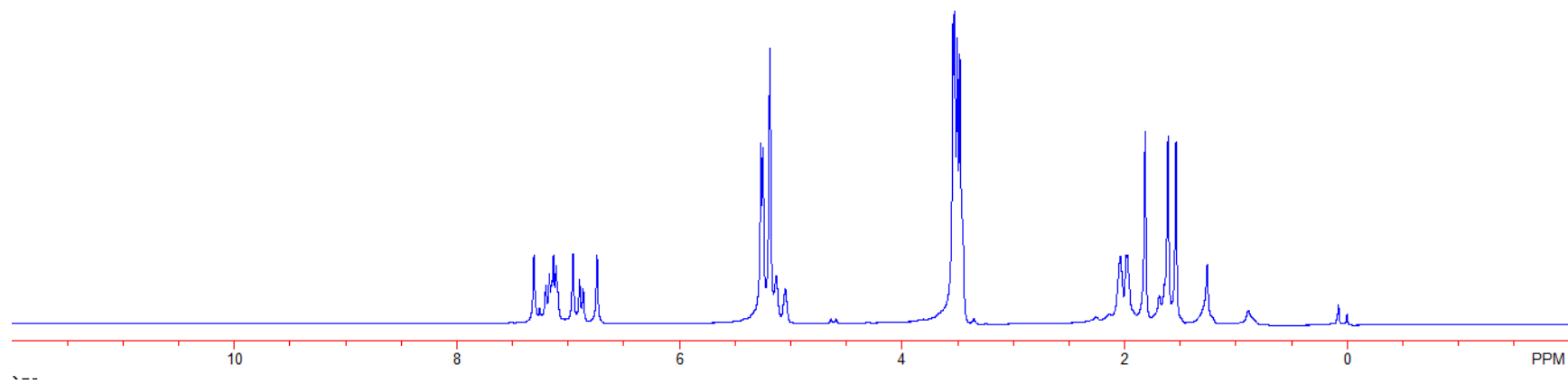
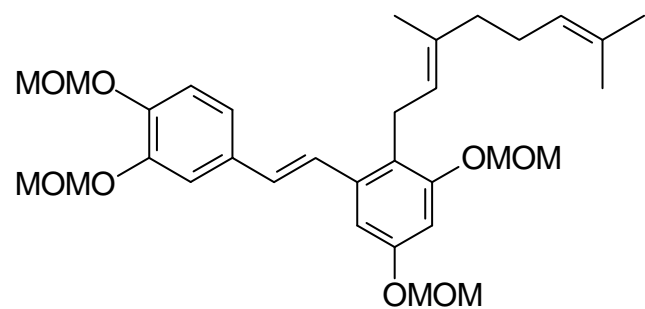


Figure A-11. ¹H NMR spectrum of compound **53**

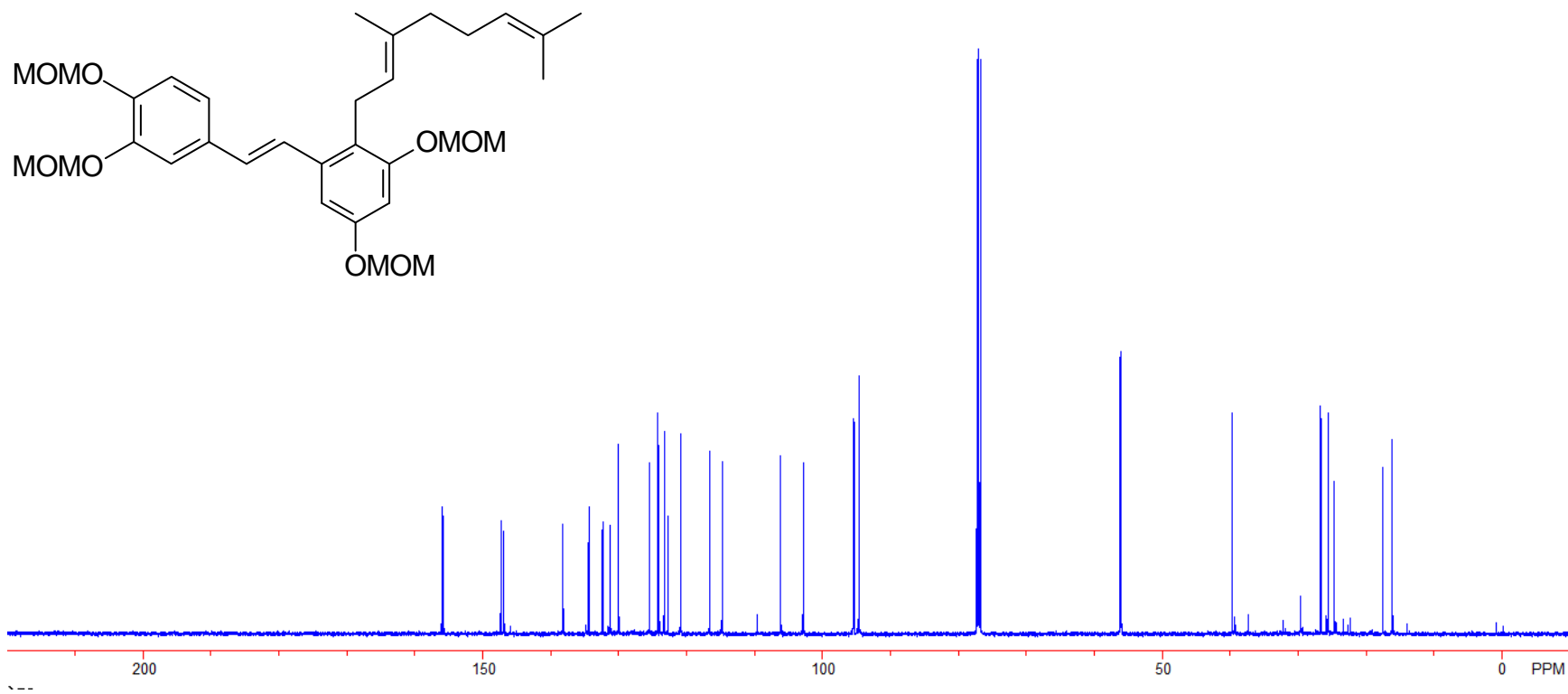


Figure A-12. ^{13}C NMR spectrum of compound **53**

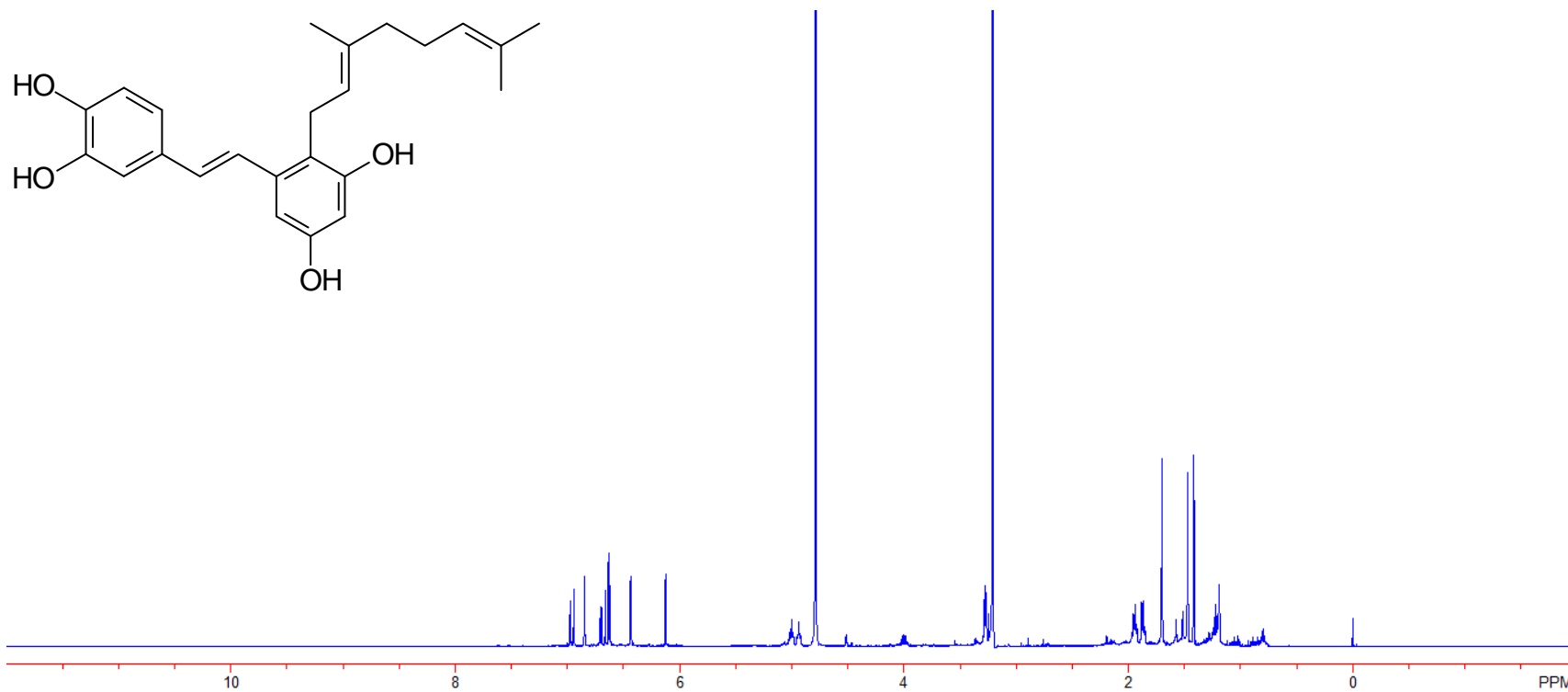


Figure A-13. ¹H NMR spectrum of compound 54

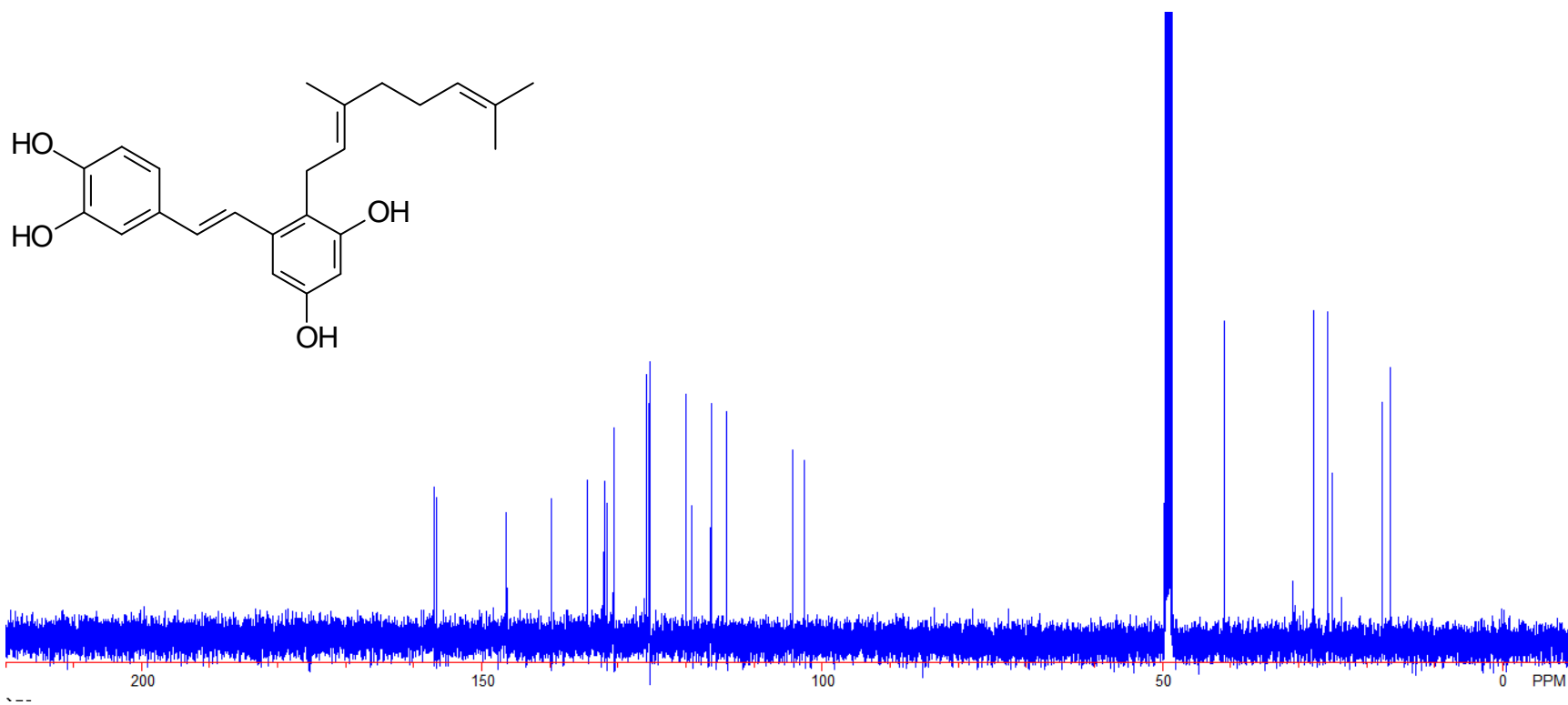


Figure A-14. ^{13}C NMR spectrum of compound **54**

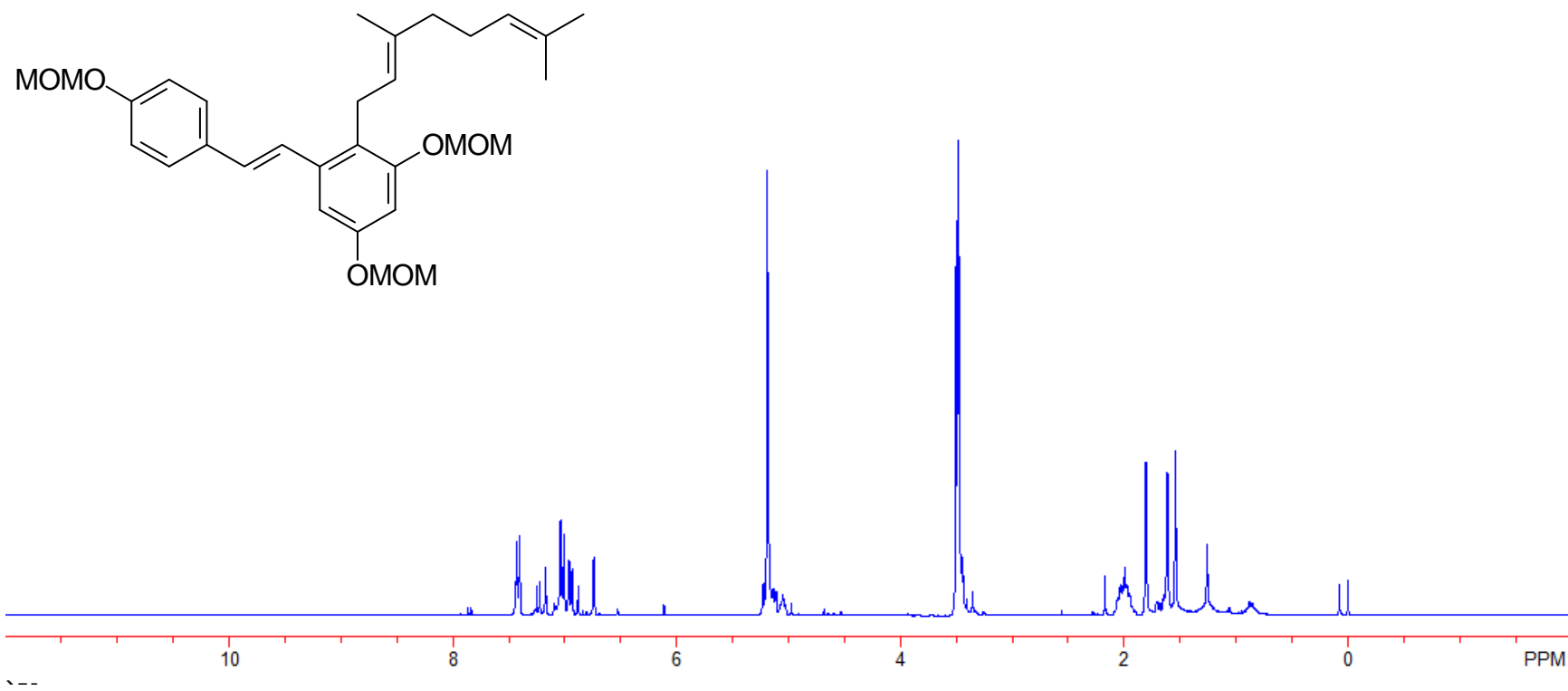


Figure A-15. ¹H NMR spectrum of compound 55

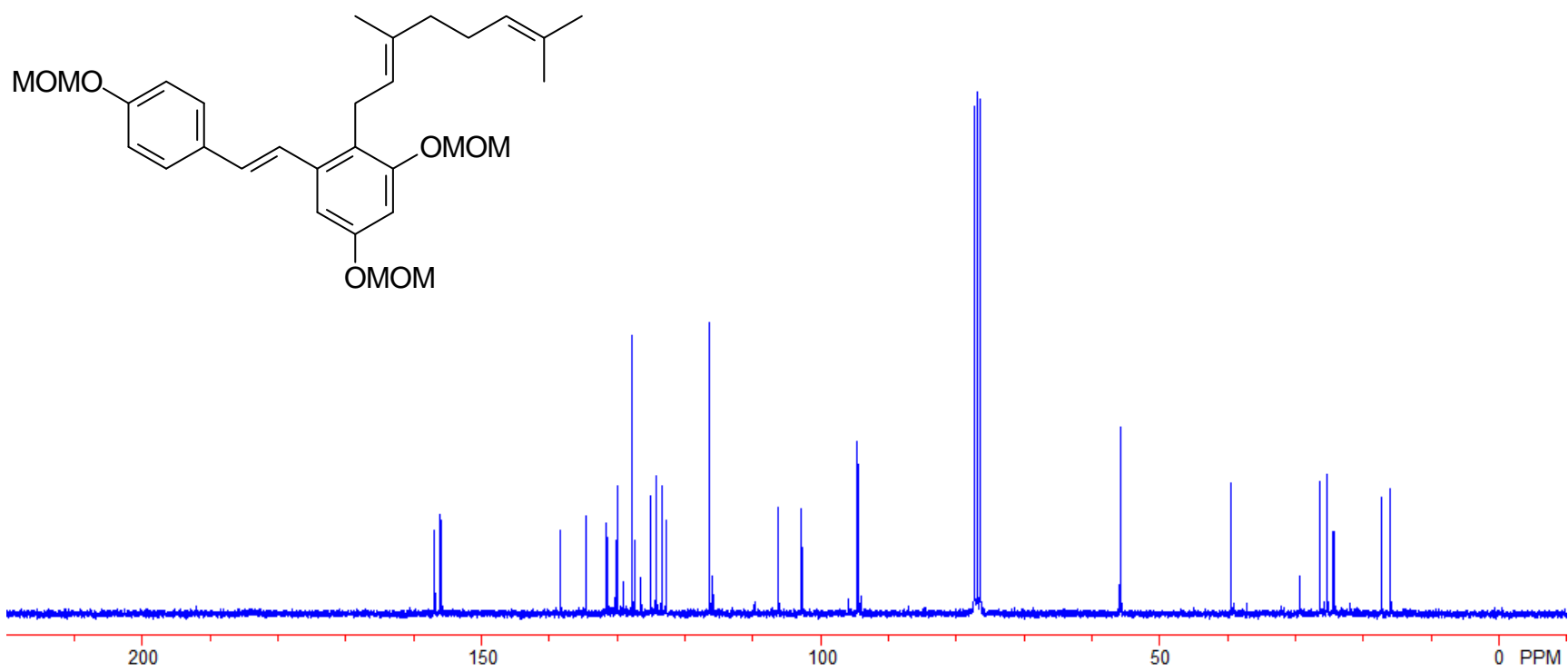


Figure A-16. ¹³C NMR spectrum of compound 55

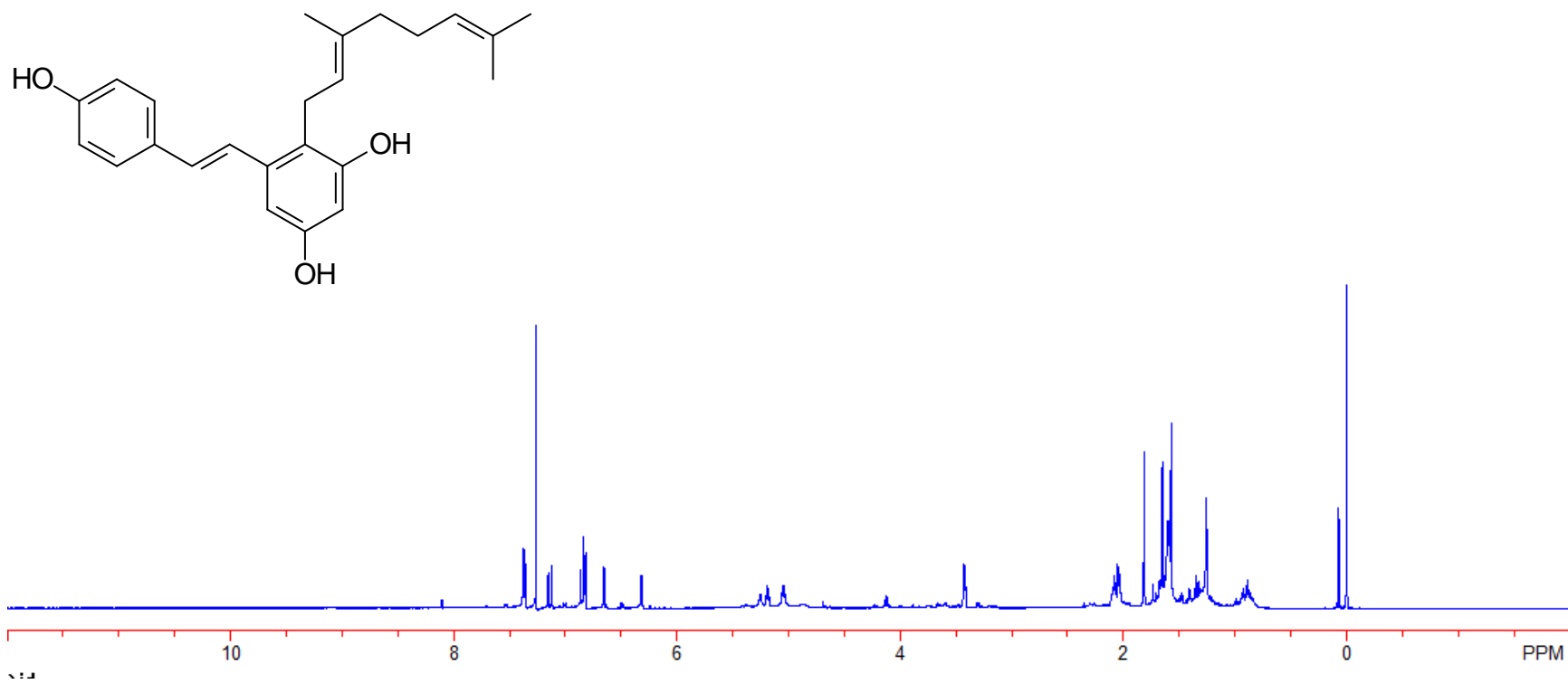


Figure A-17. ^1H NMR spectrum of compound **56**

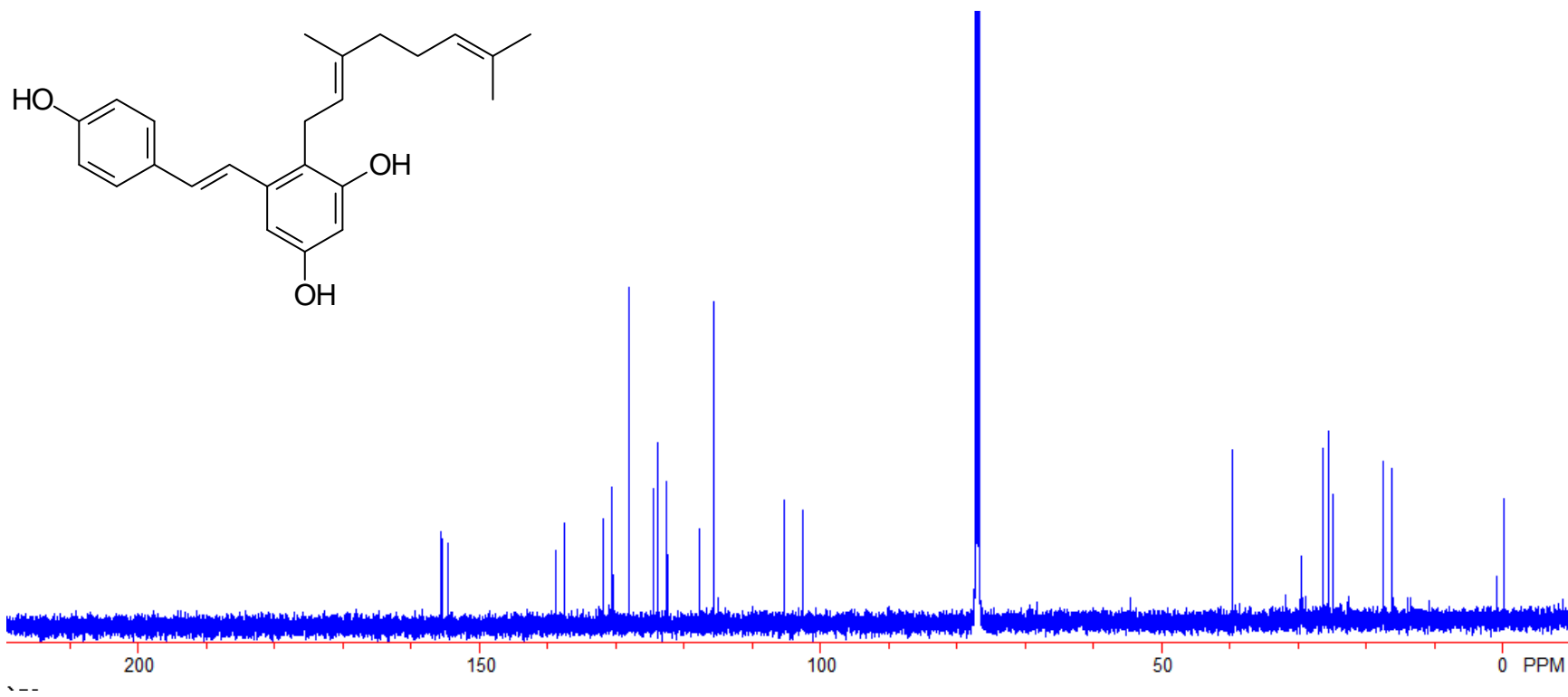


Figure A-18. ^{13}C NMR spectrum of compound **56**

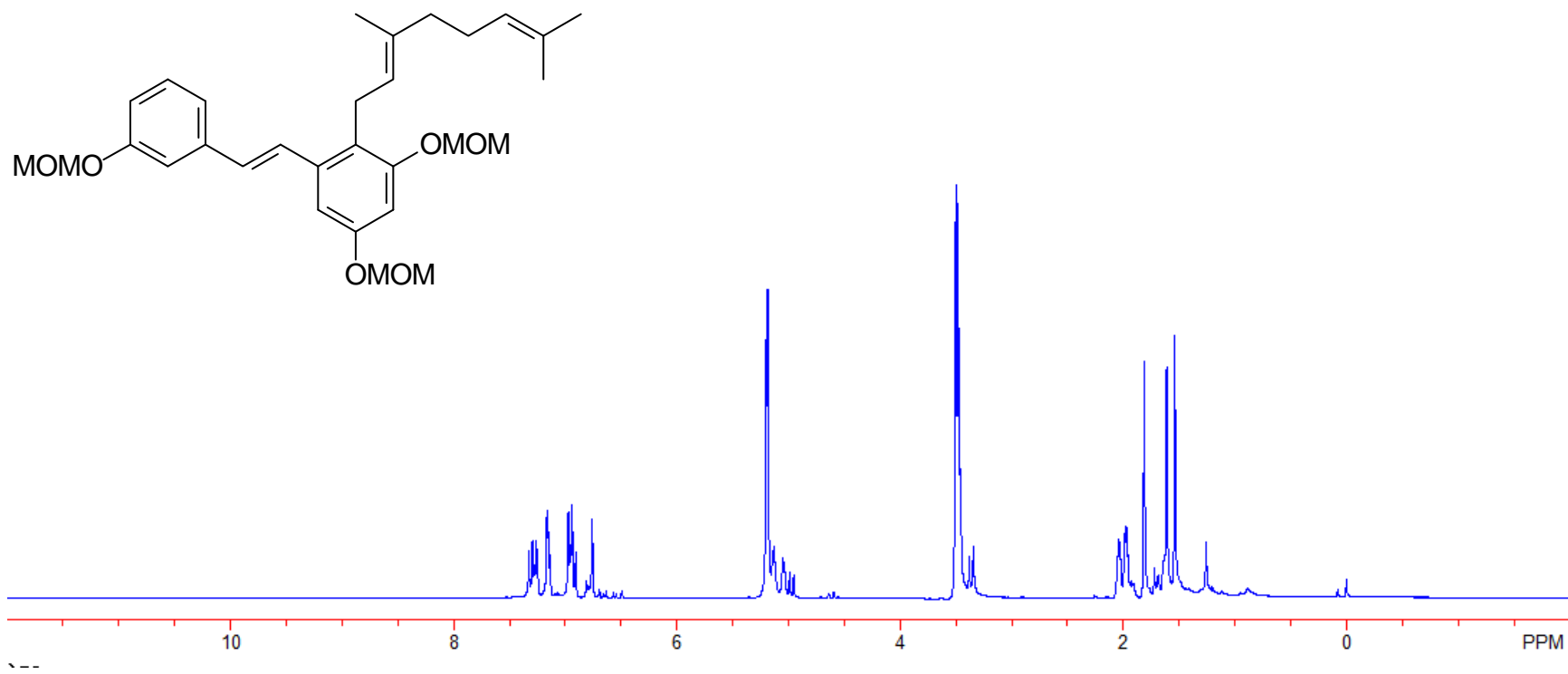


Figure A-19. ^1H NMR spectrum of compound **57**

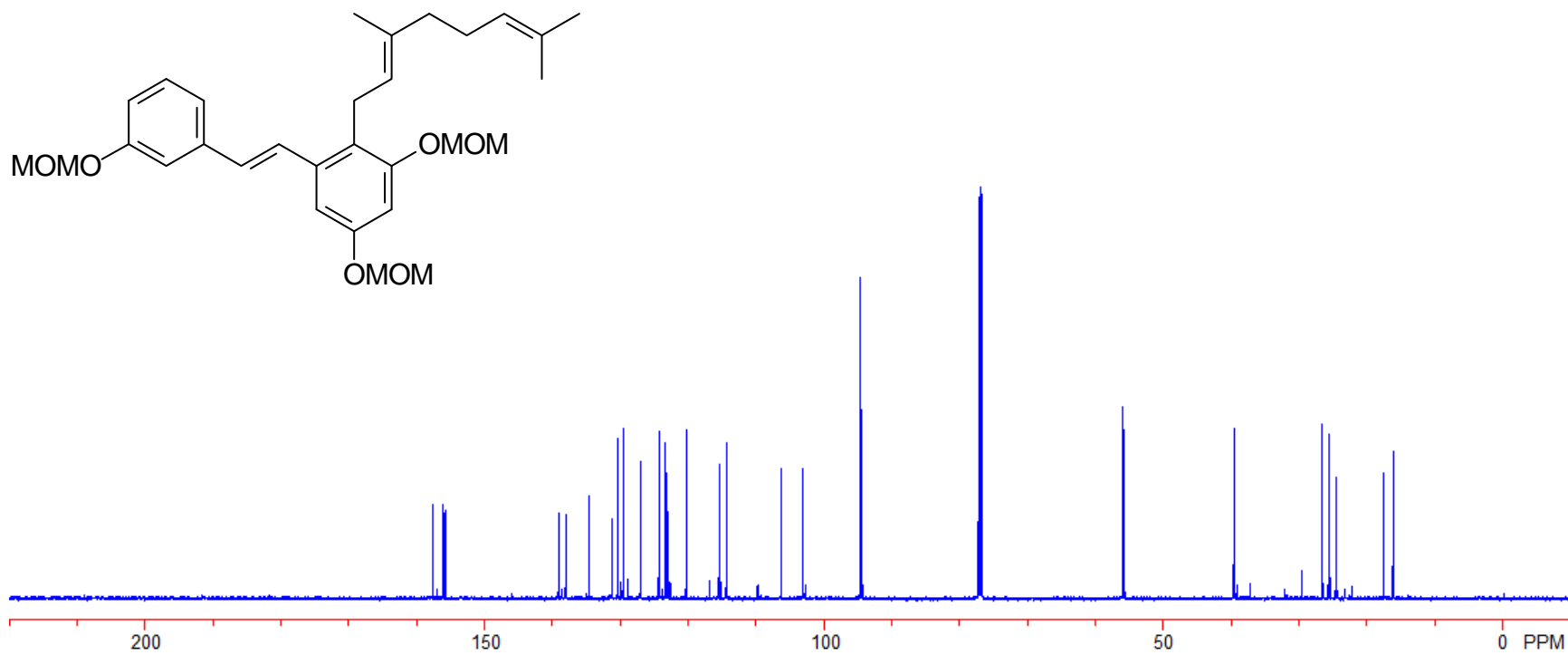


Figure A-20. ^{13}C NMR spectrum of compound **57**

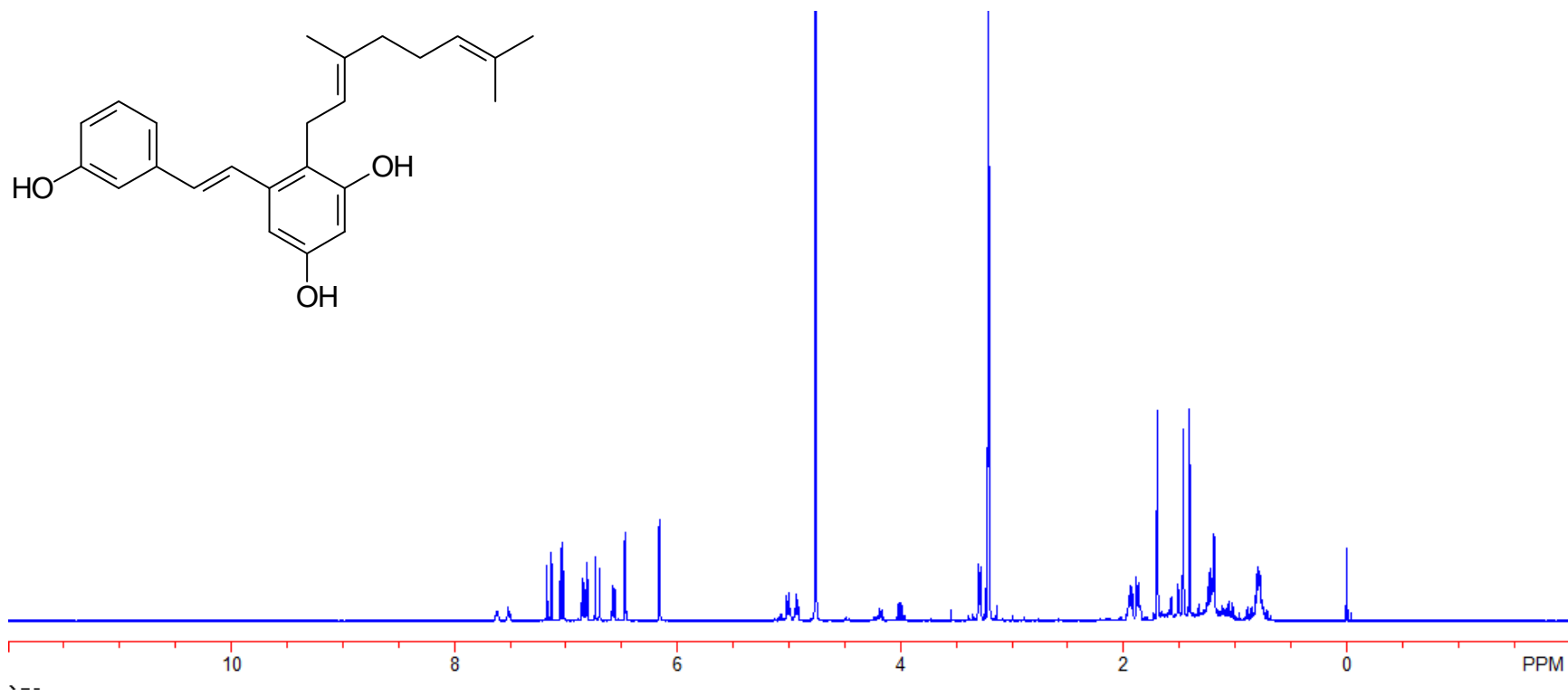


Figure A-21. ^1H NMR spectrum of compound **58**

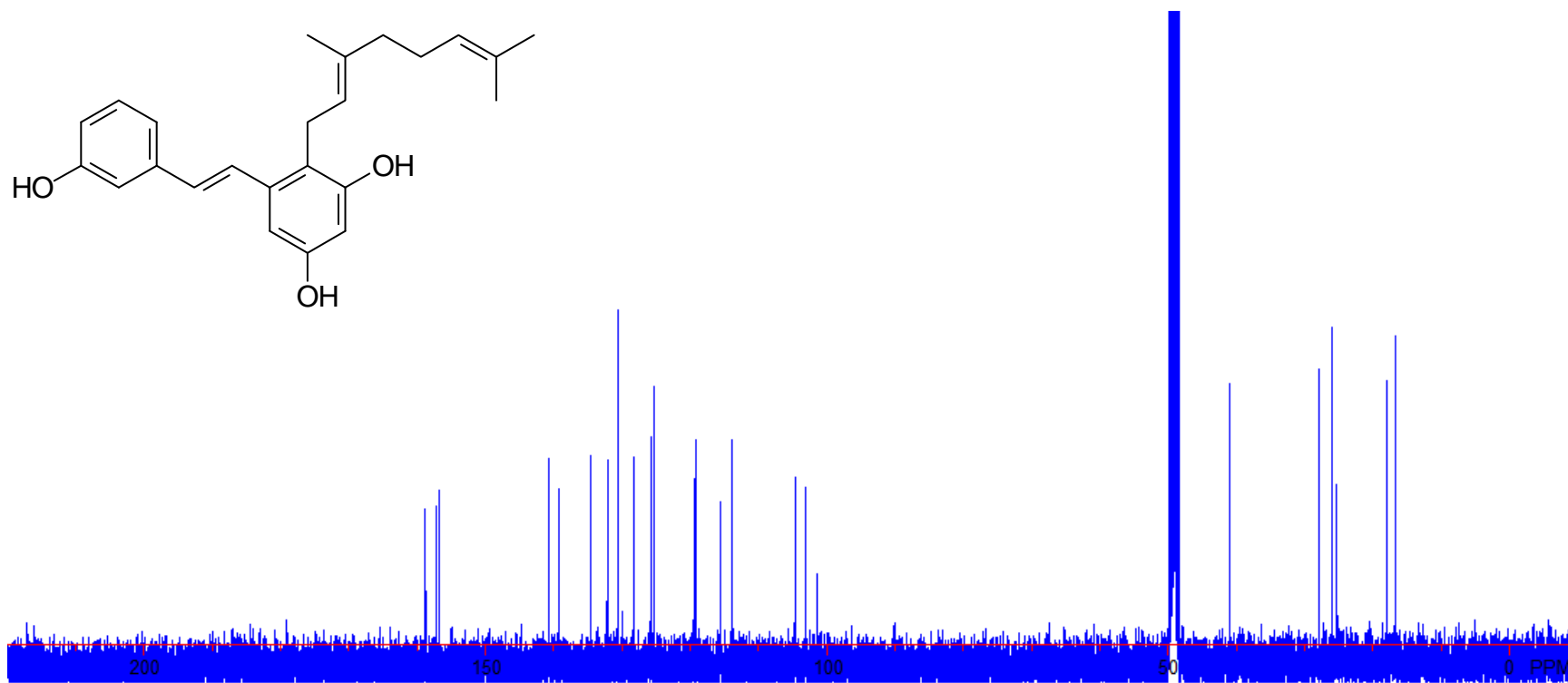


Figure A-22. ^{13}C NMR spectrum of compound **58**

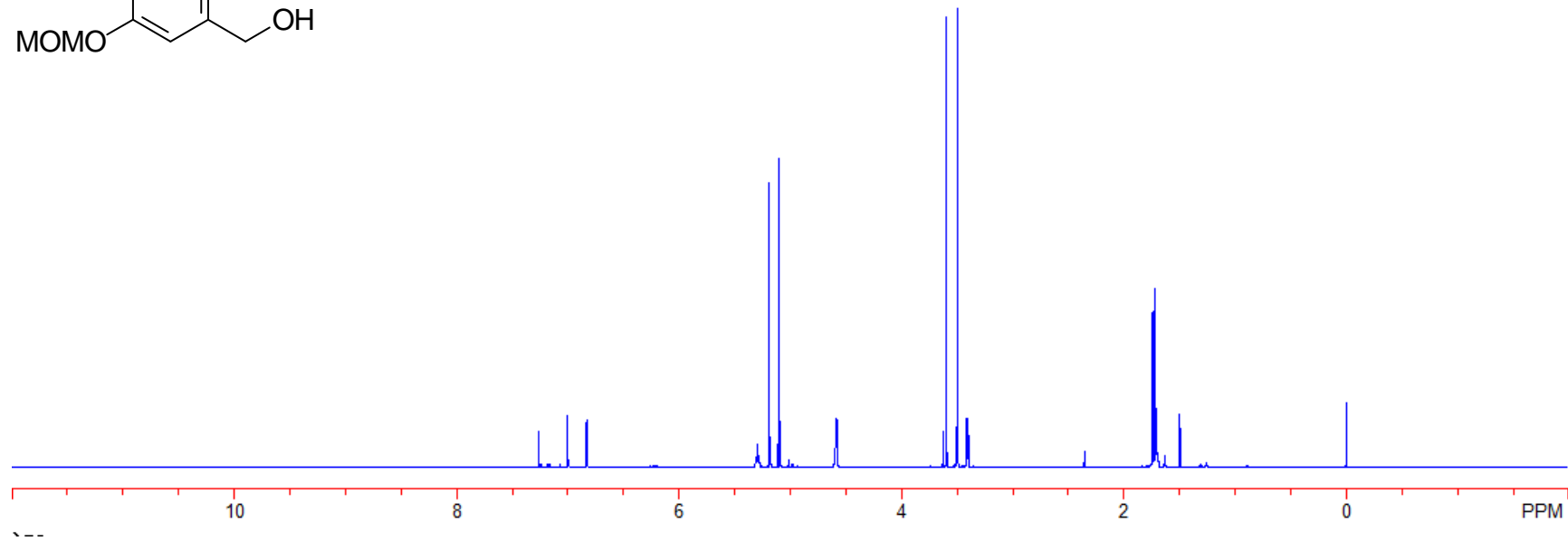
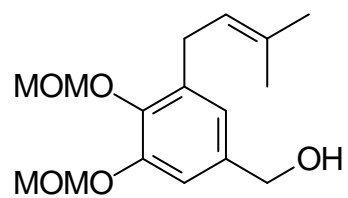


Figure A-23. ^1H NMR spectrum of compound **61**

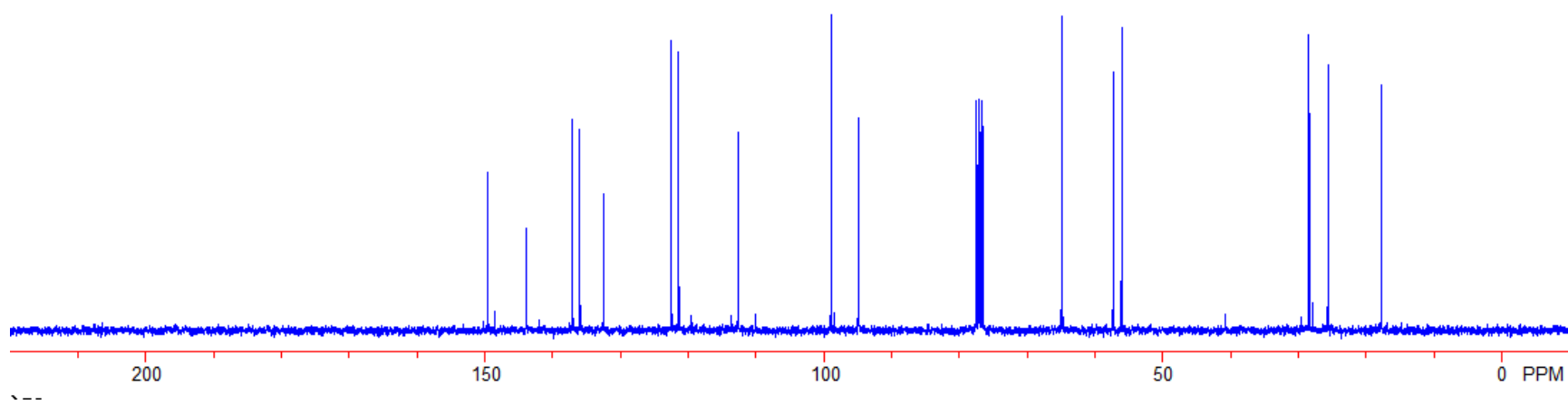
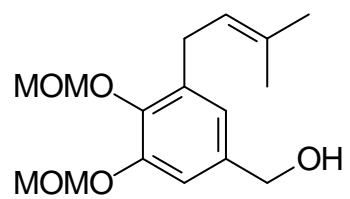


Figure A-24. ^{13}C NMR spectrum of compound **61**

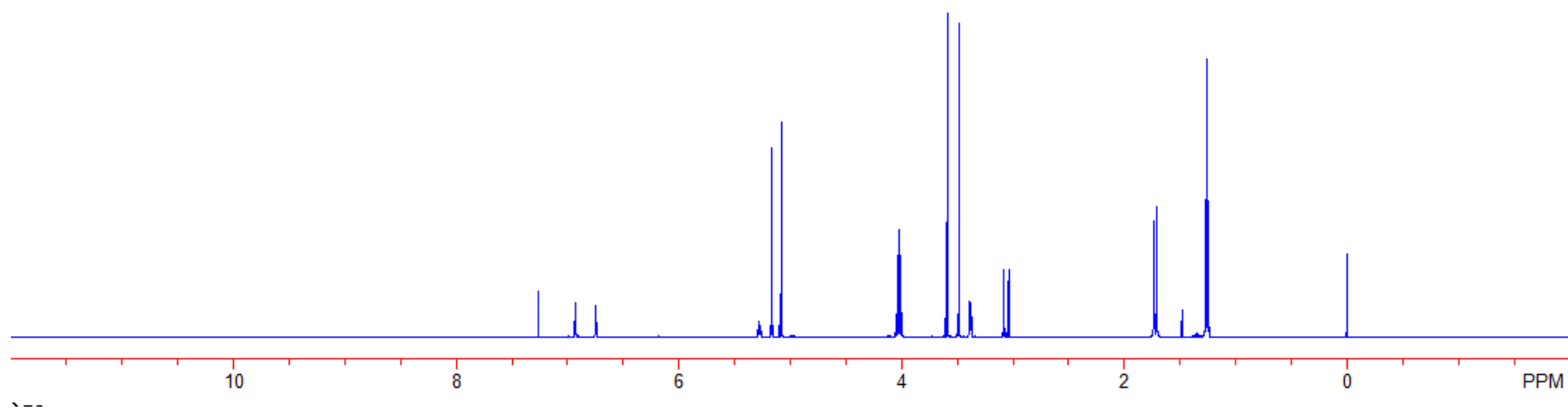
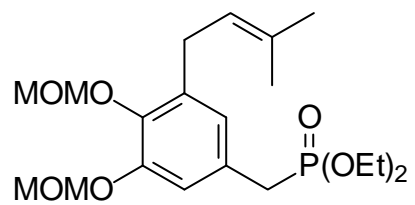


Figure A-25. ¹H NMR spectrum of compound **62**

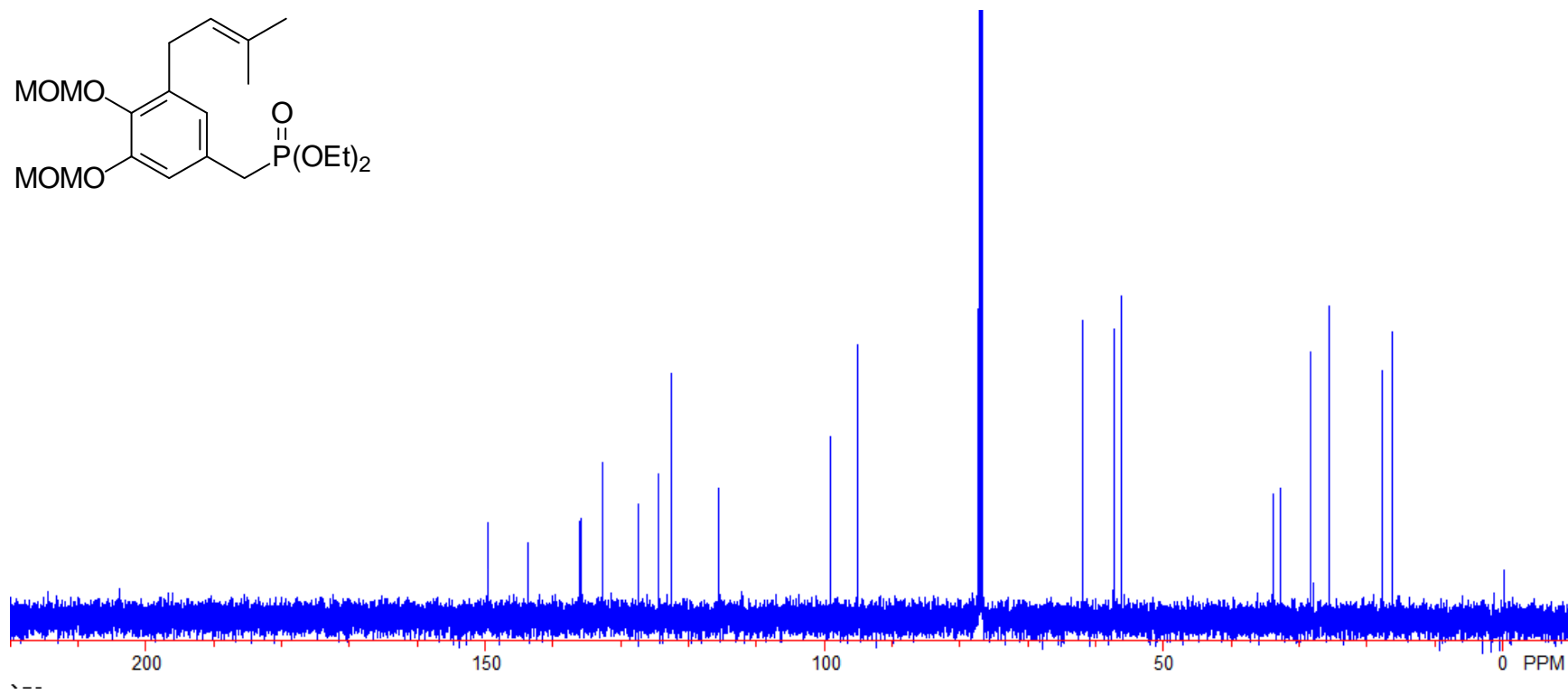
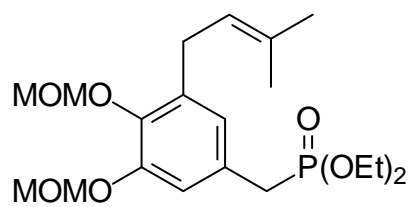


Figure A-26. ^{13}C NMR spectrum of compound 62

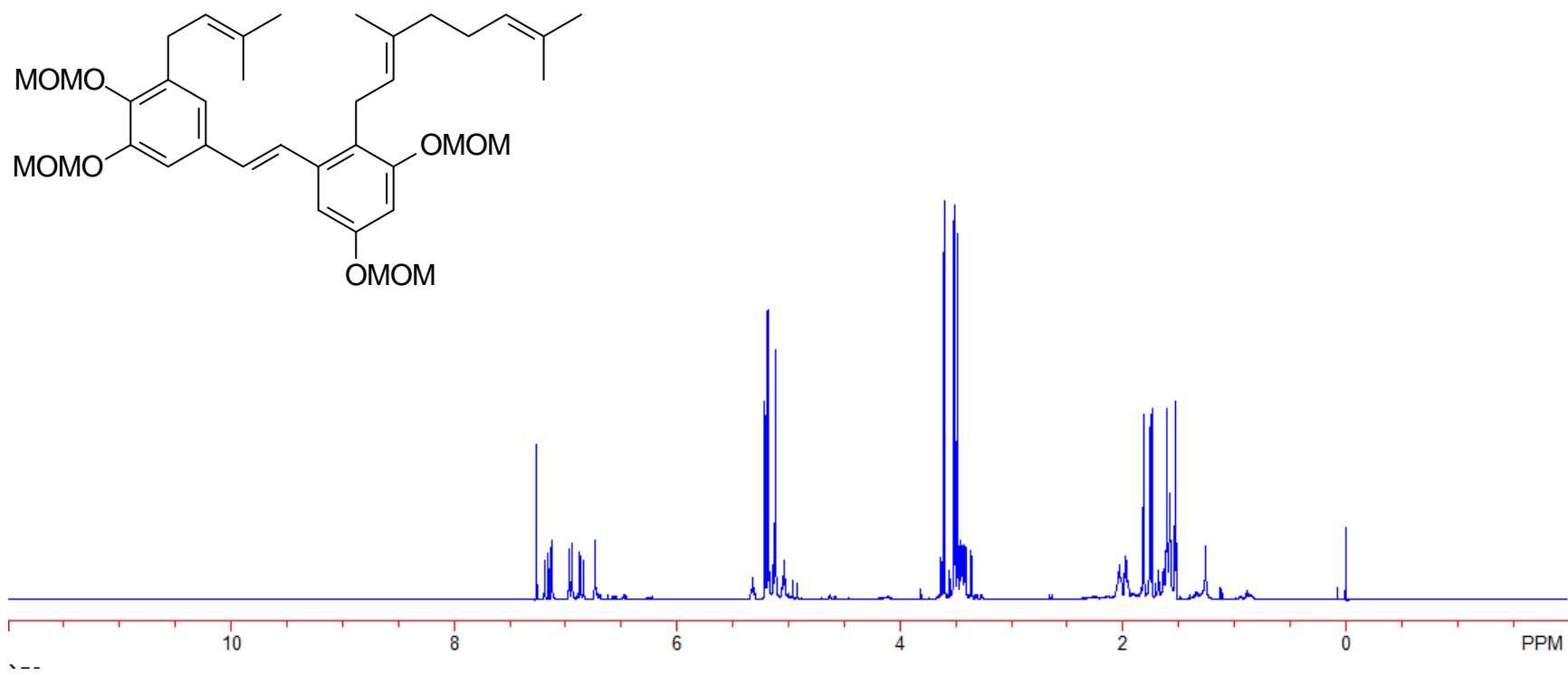


Figure A-27. ^1H NMR spectrum of compound **63**

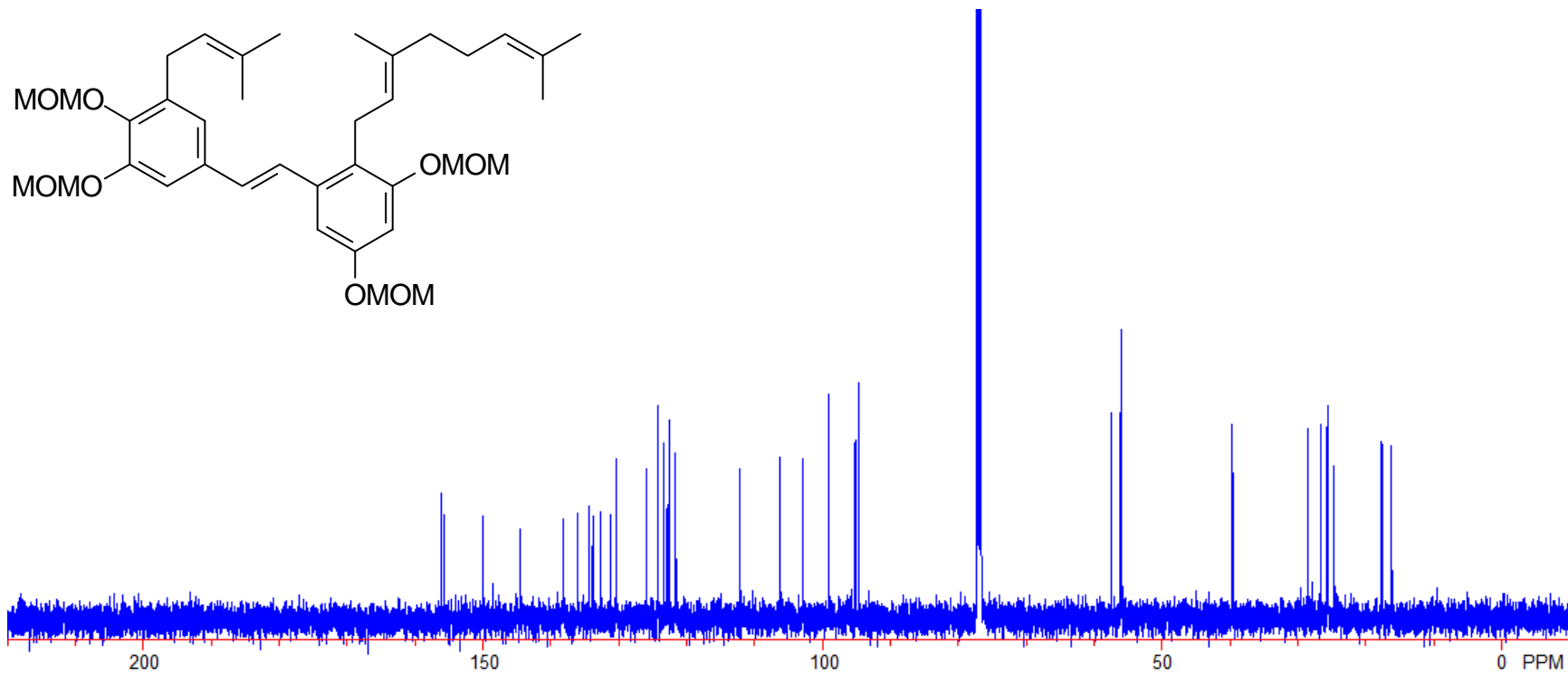


Figure A-28. ^{13}C NMR spectrum of compound **63**

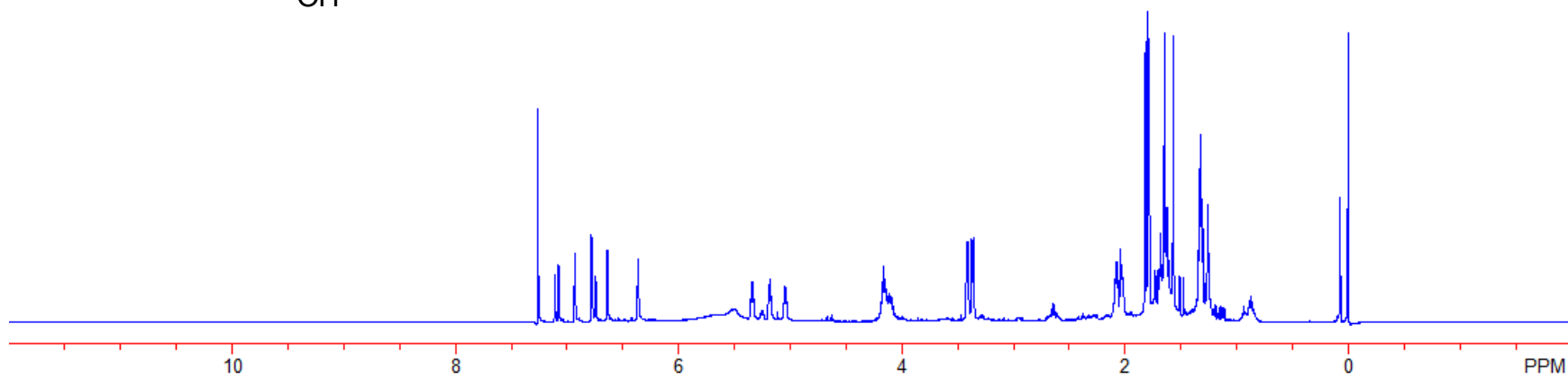
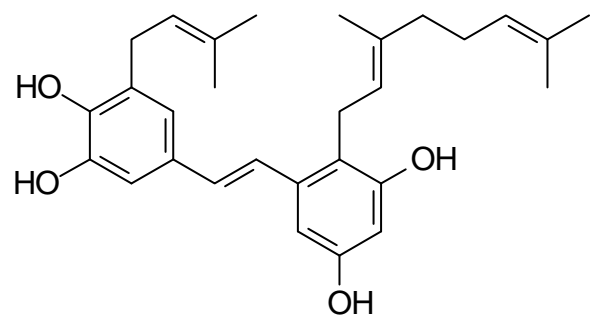


Figure A-29. ^1H NMR spectrum of compound **64**

Please note, it has been taken into account there is a 1:1 ratio of compound **64** to diethyl phosphate.

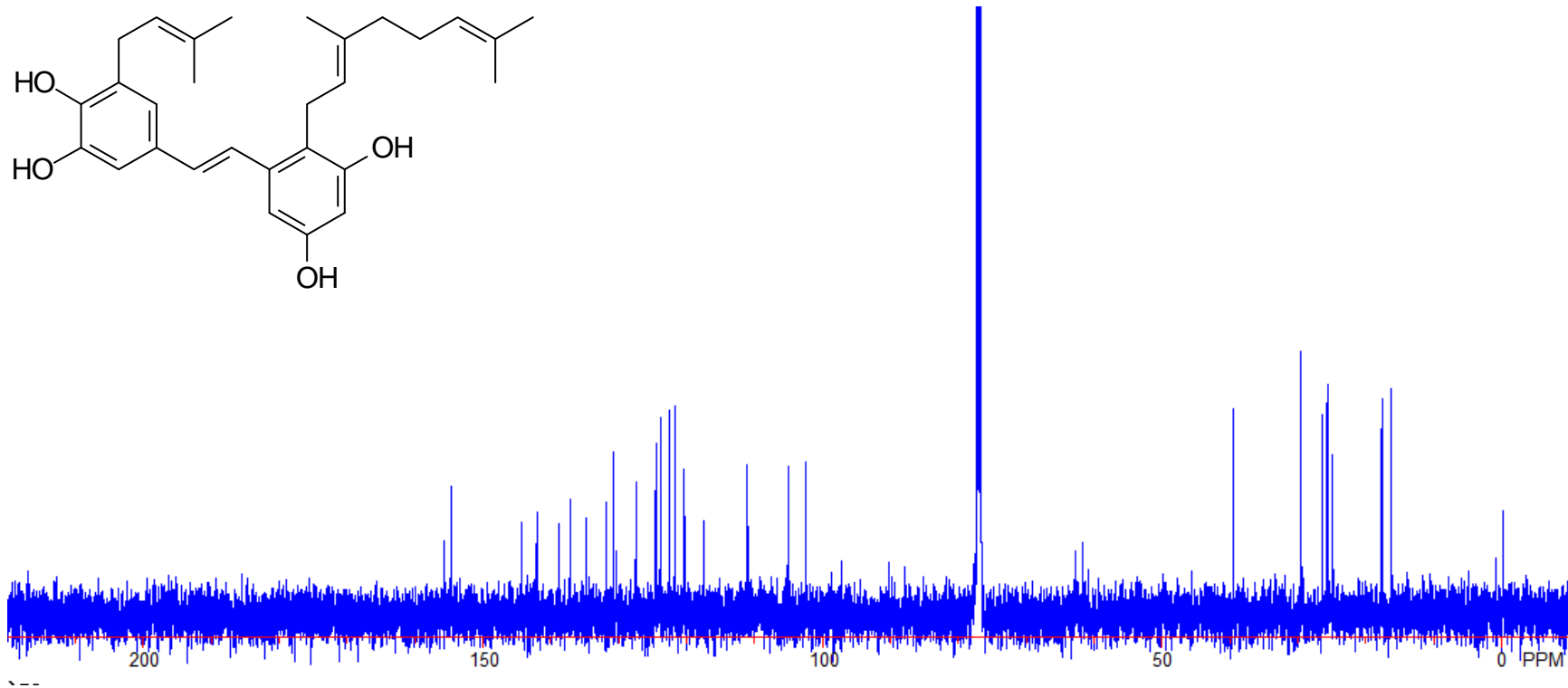


Figure A-30. ^{13}C NMR spectrum of compound **64**

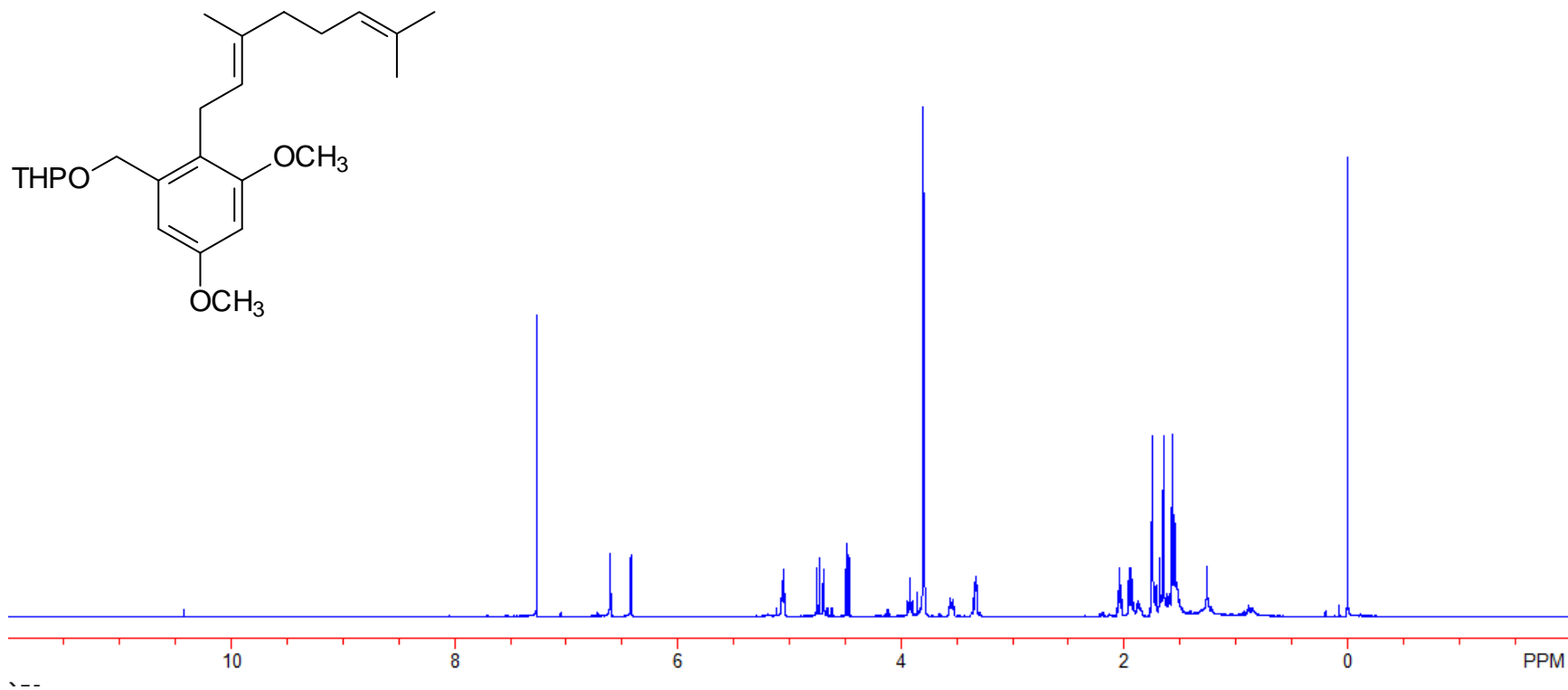


Figure A-31. ^1H NMR spectrum of compound **70**

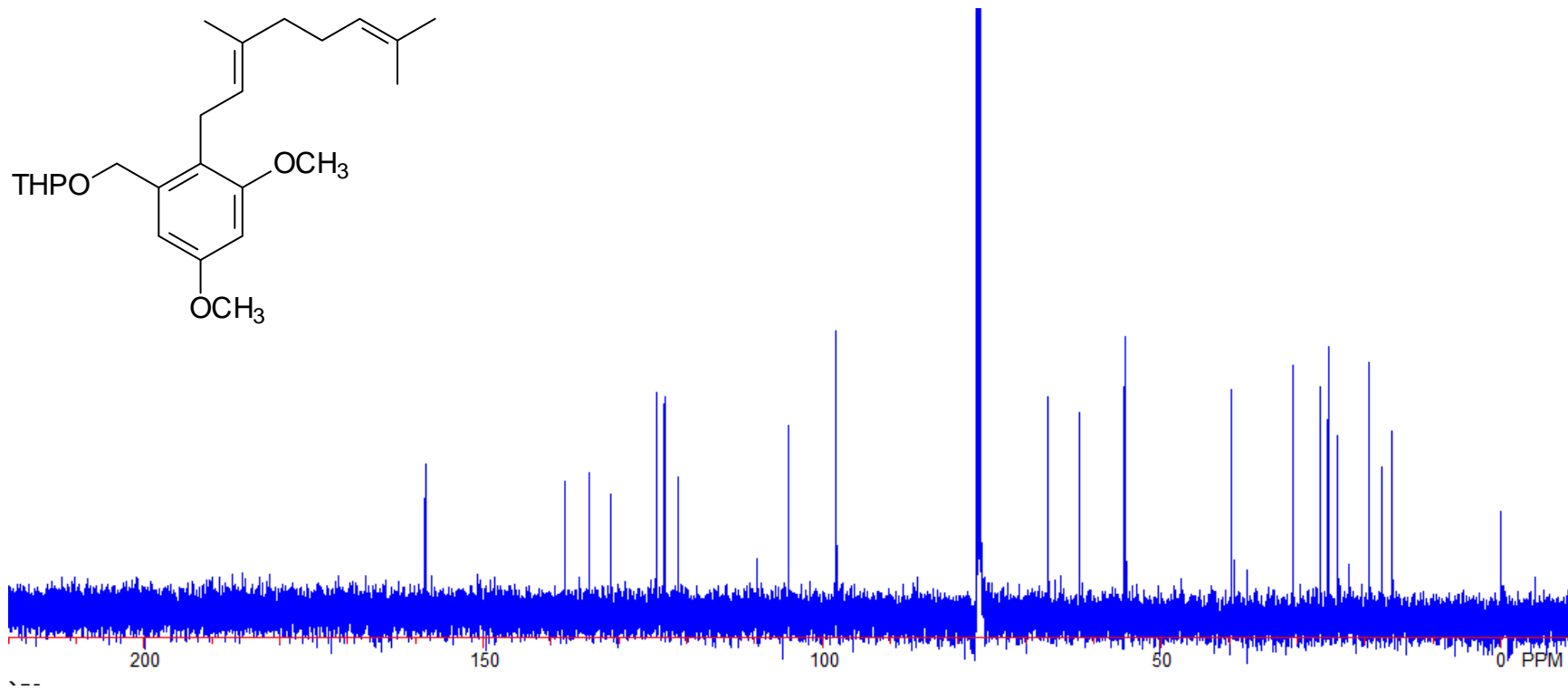
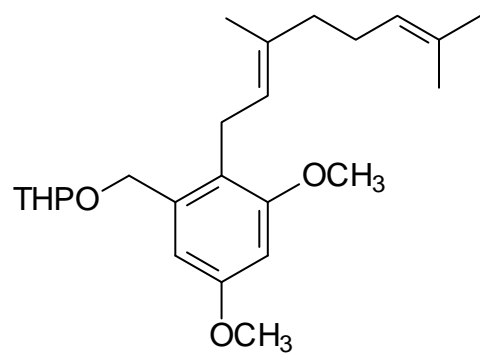


Figure A-32. ¹³C NMR spectrum of compound 70

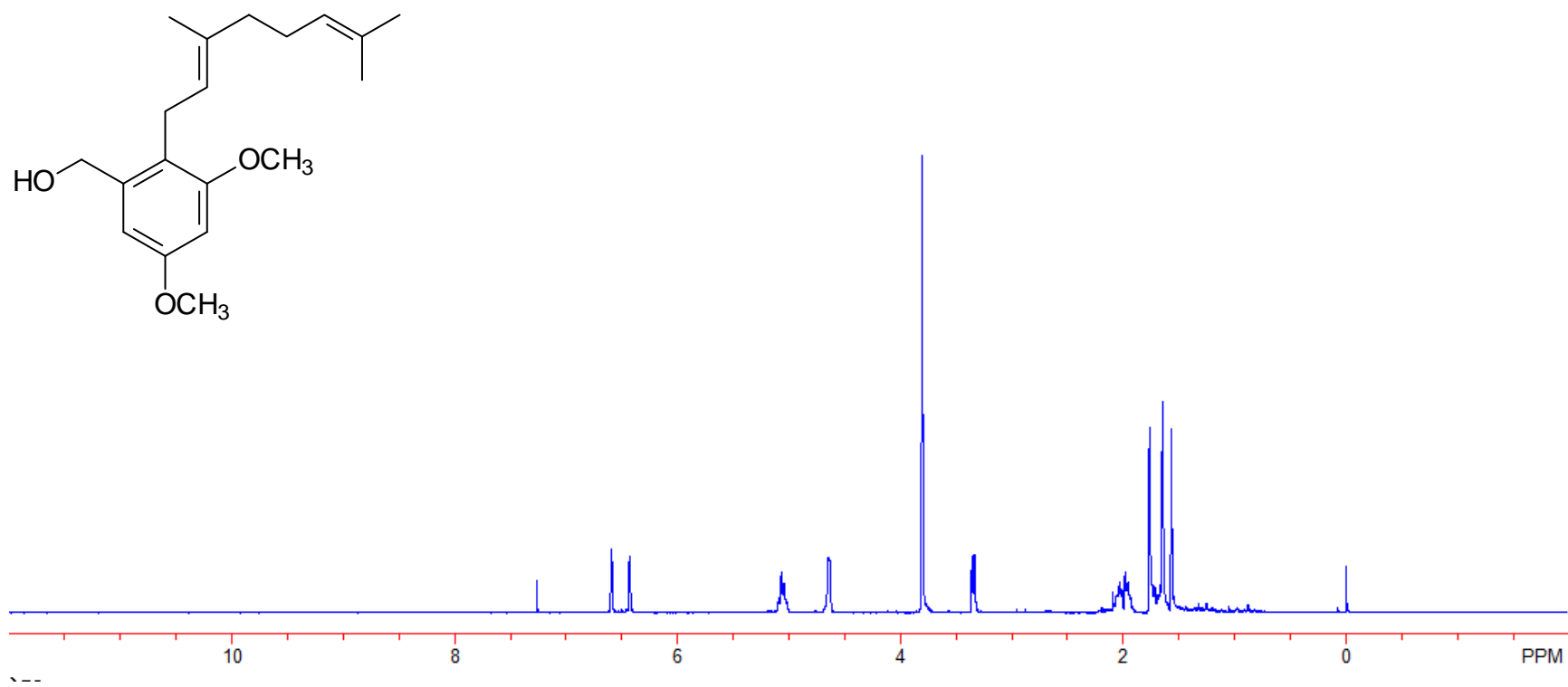


Figure A-33. ¹H NMR spectrum of compound **71**

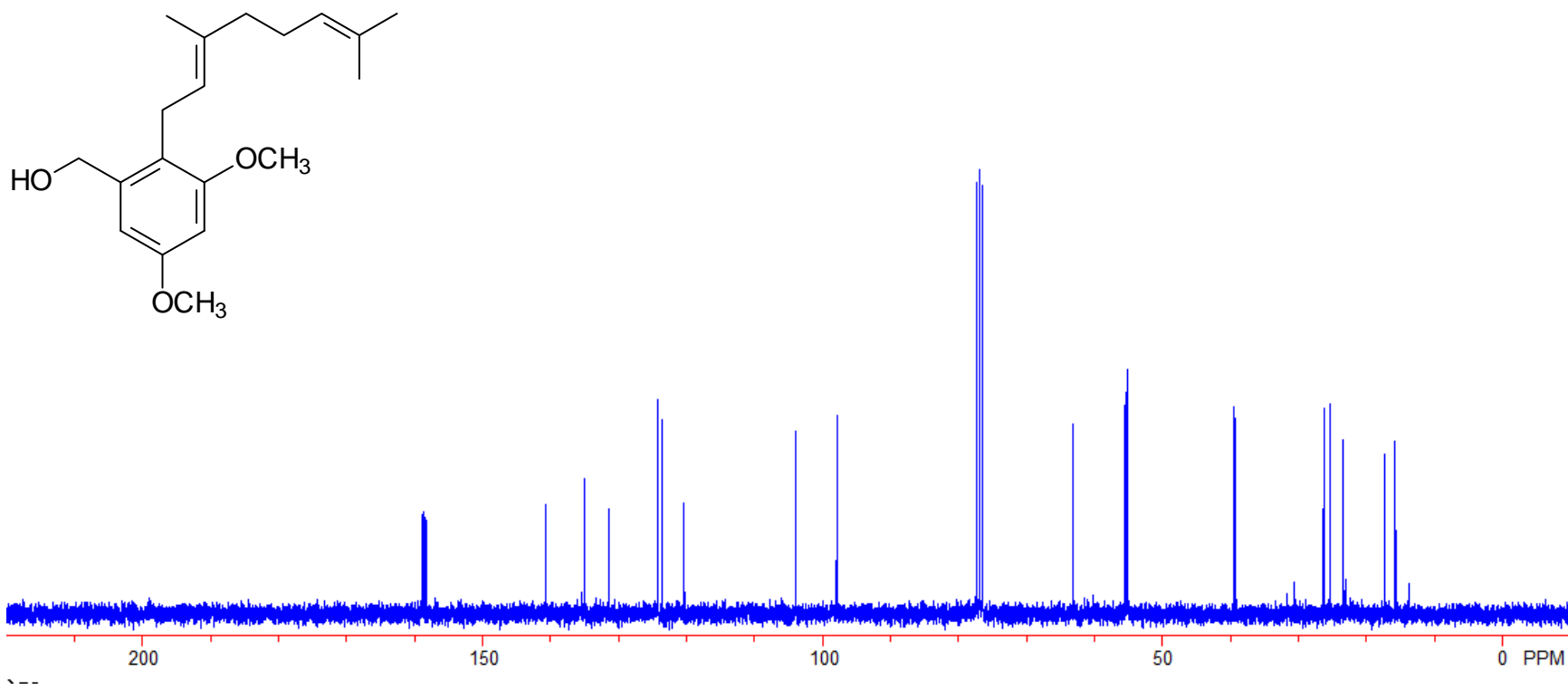


Figure A-34. ^{13}C NMR spectrum of compound **71**

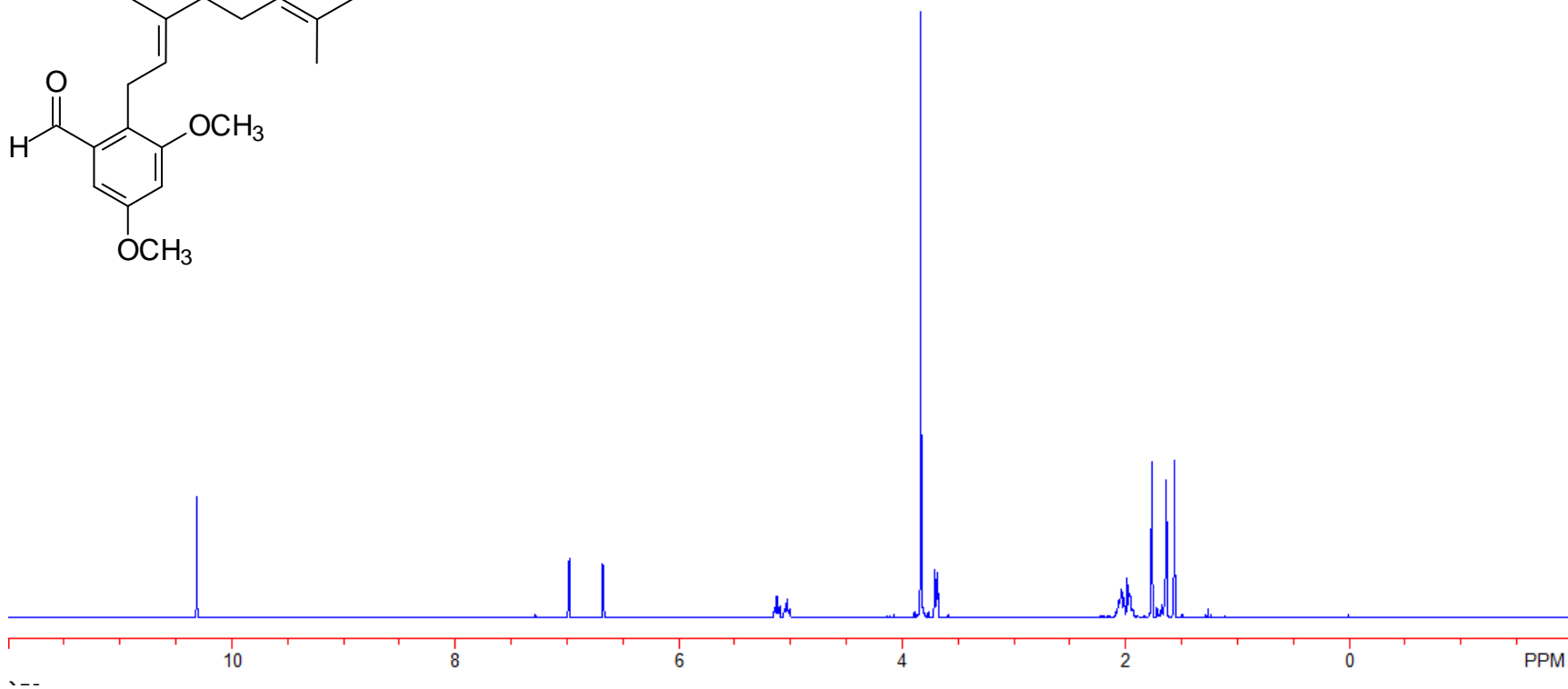
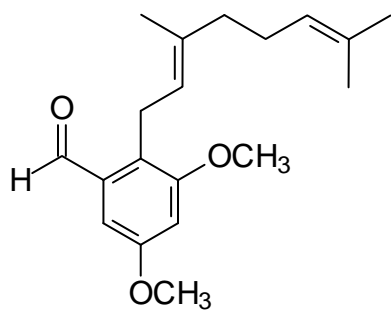


Figure A-35. ¹H NMR spectrum of compound **66**

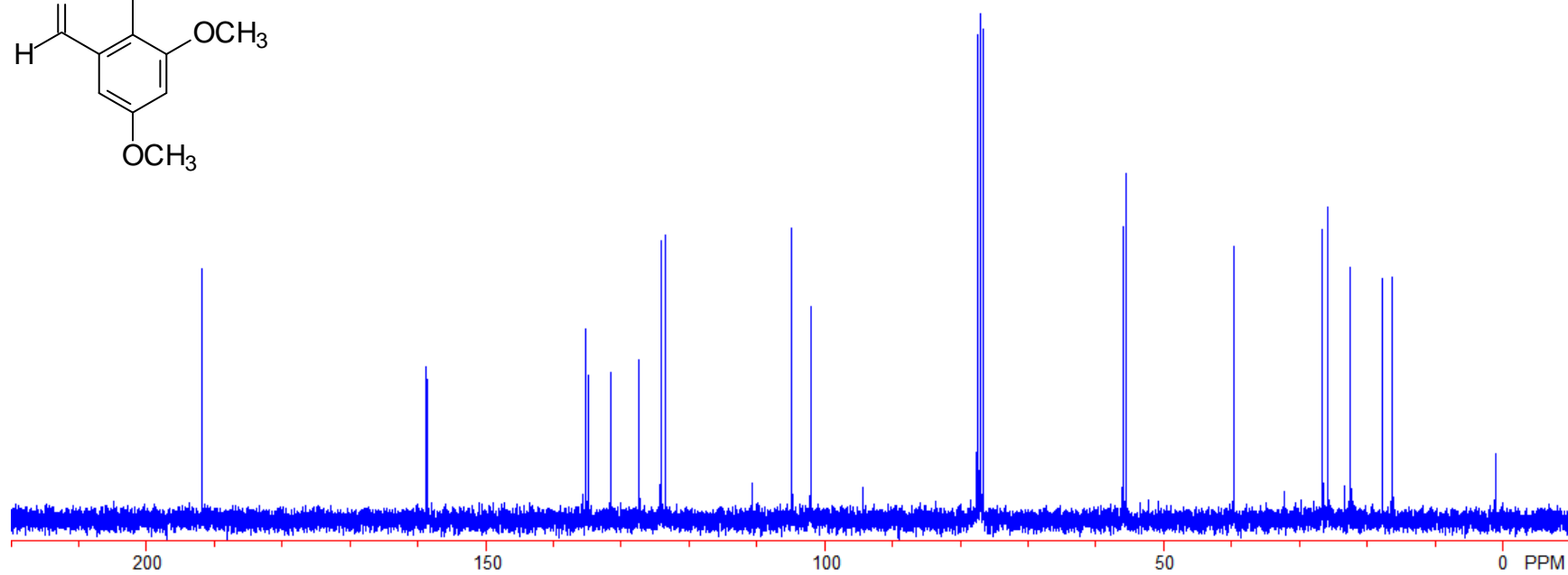
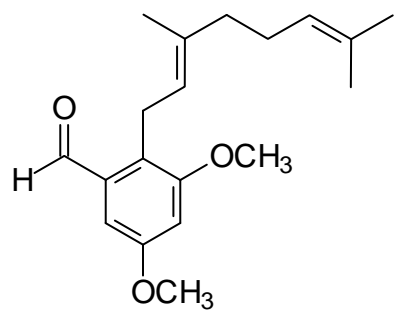


Figure A-36. ^{13}C NMR spectrum of compound **66**

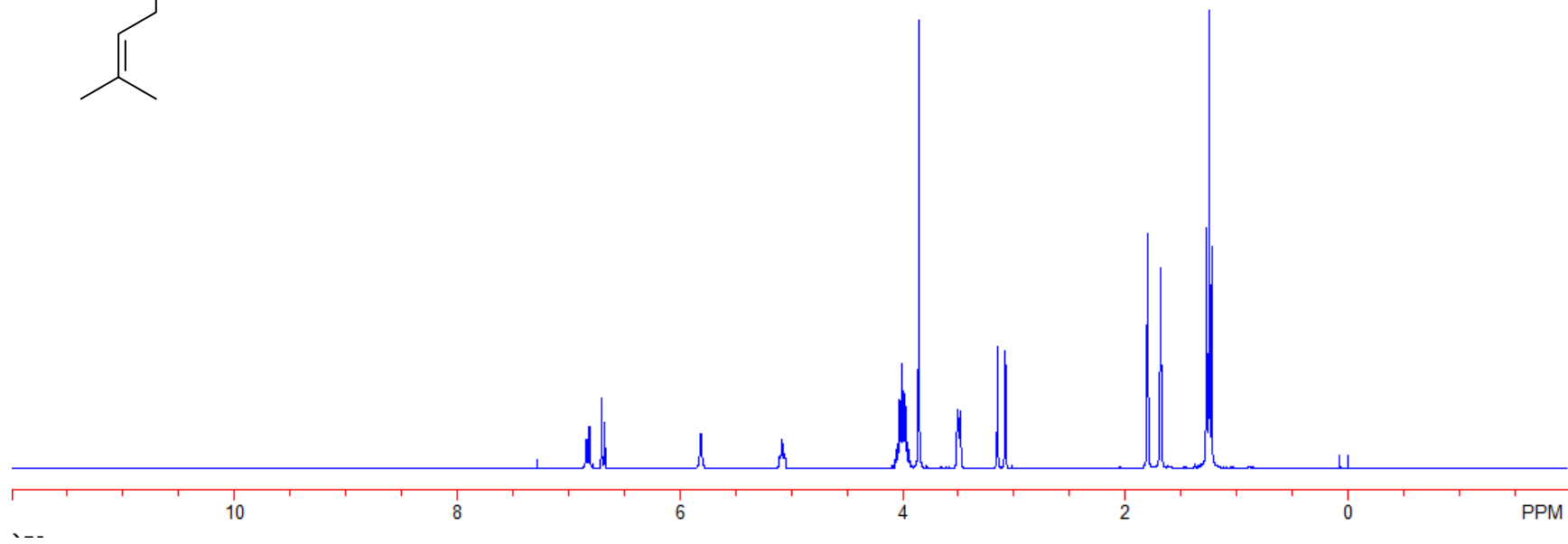
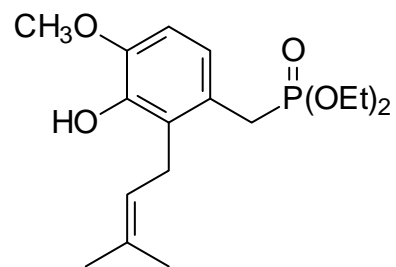


Figure A-37. ¹H NMR spectrum of compound **72**

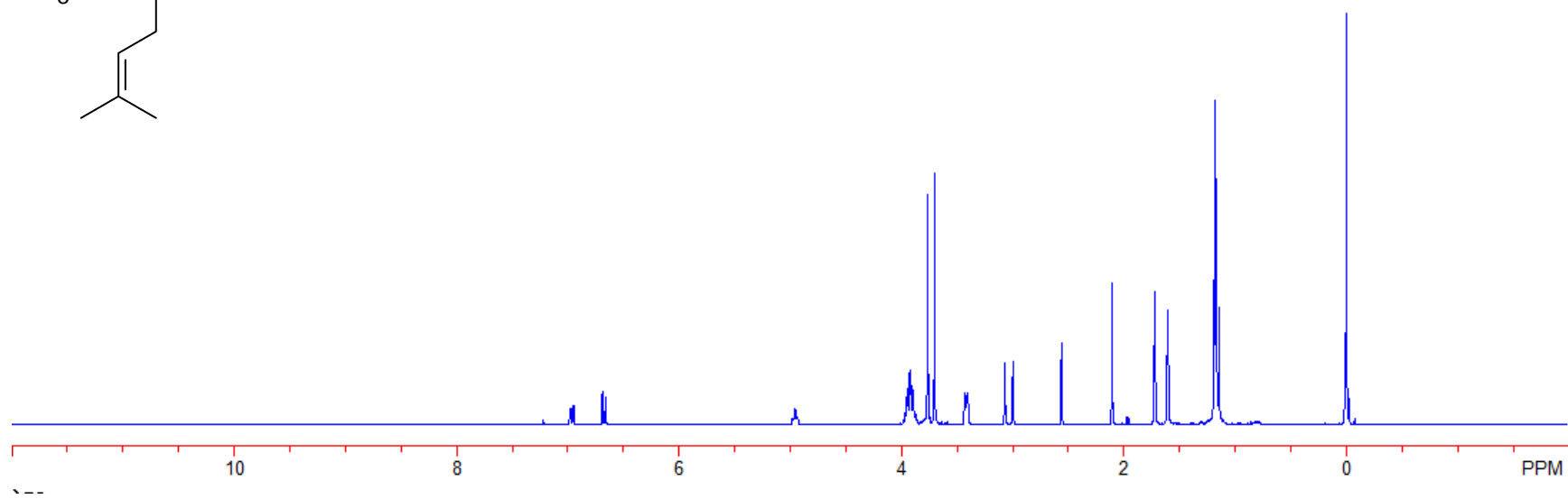
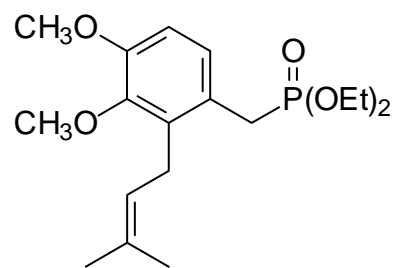


Figure A-38. ¹H NMR spectrum of compound **73**

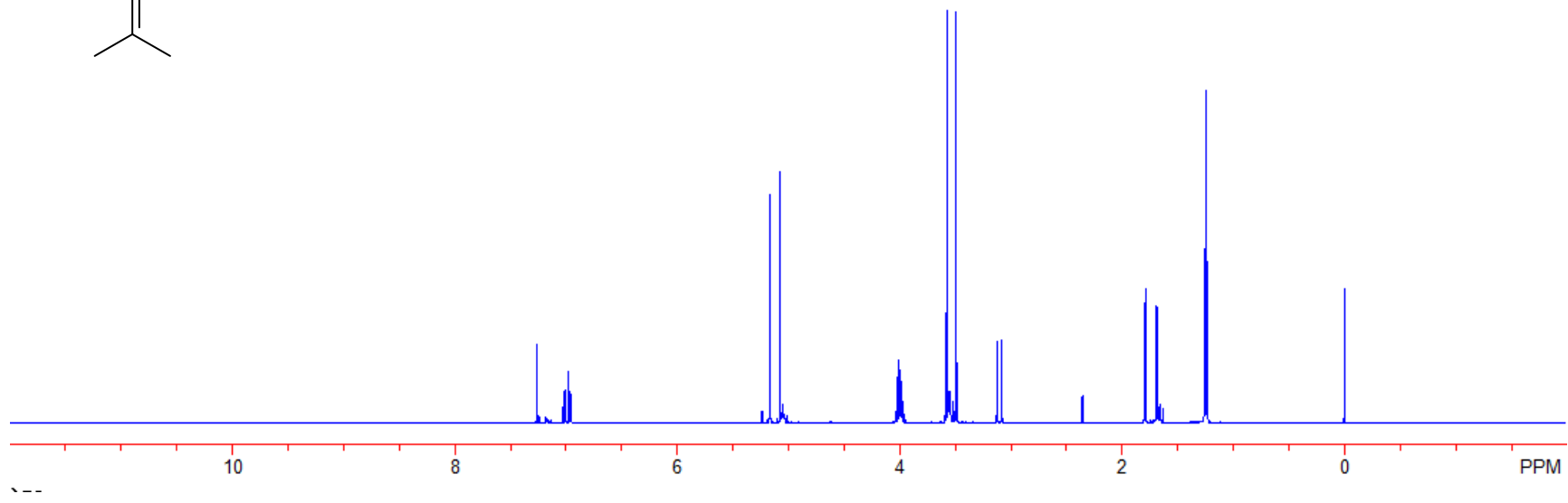
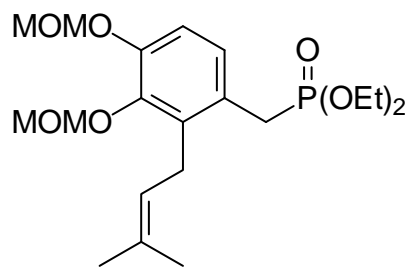


Figure A-39. ¹H NMR spectrum of compound 75

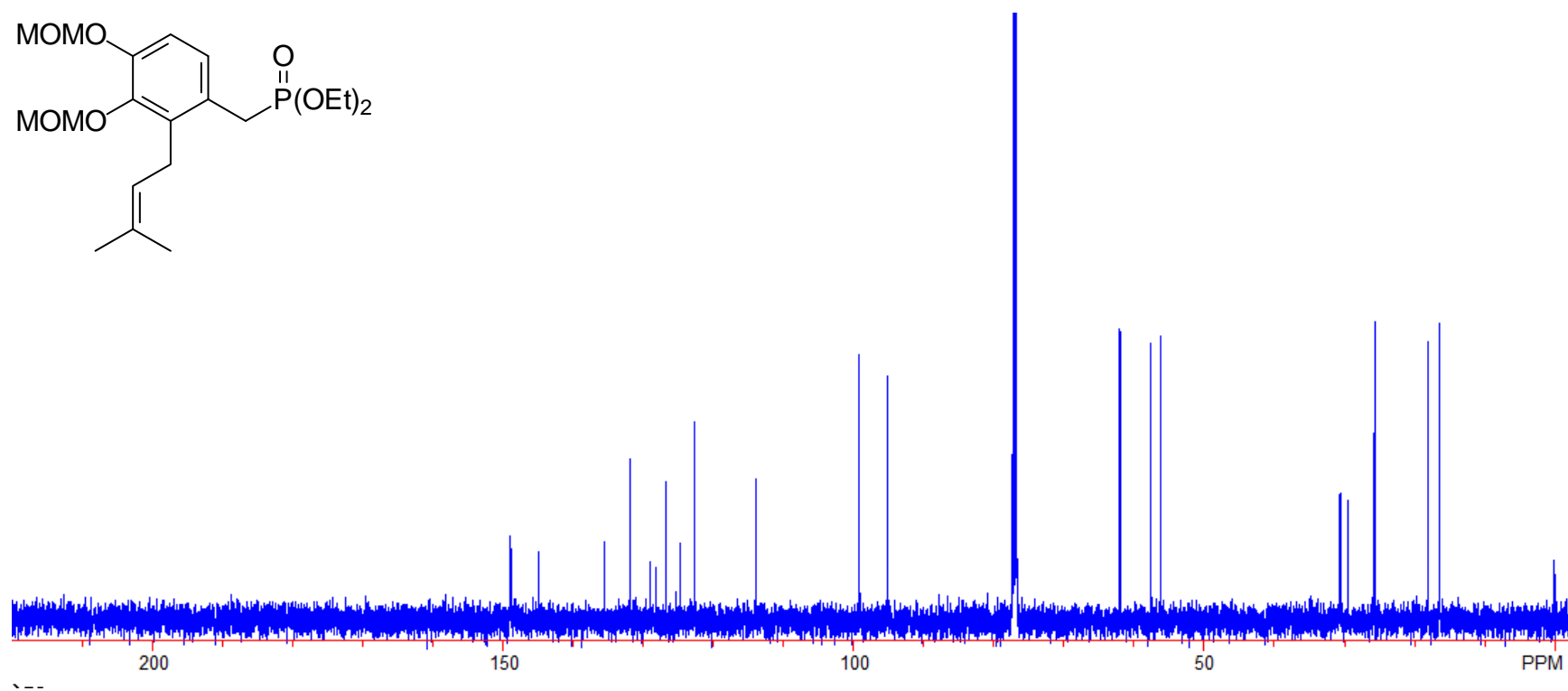
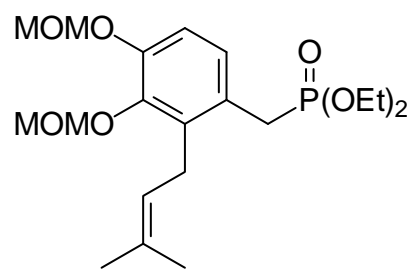


Figure A-40. ^{13}C NMR spectrum of compound 75

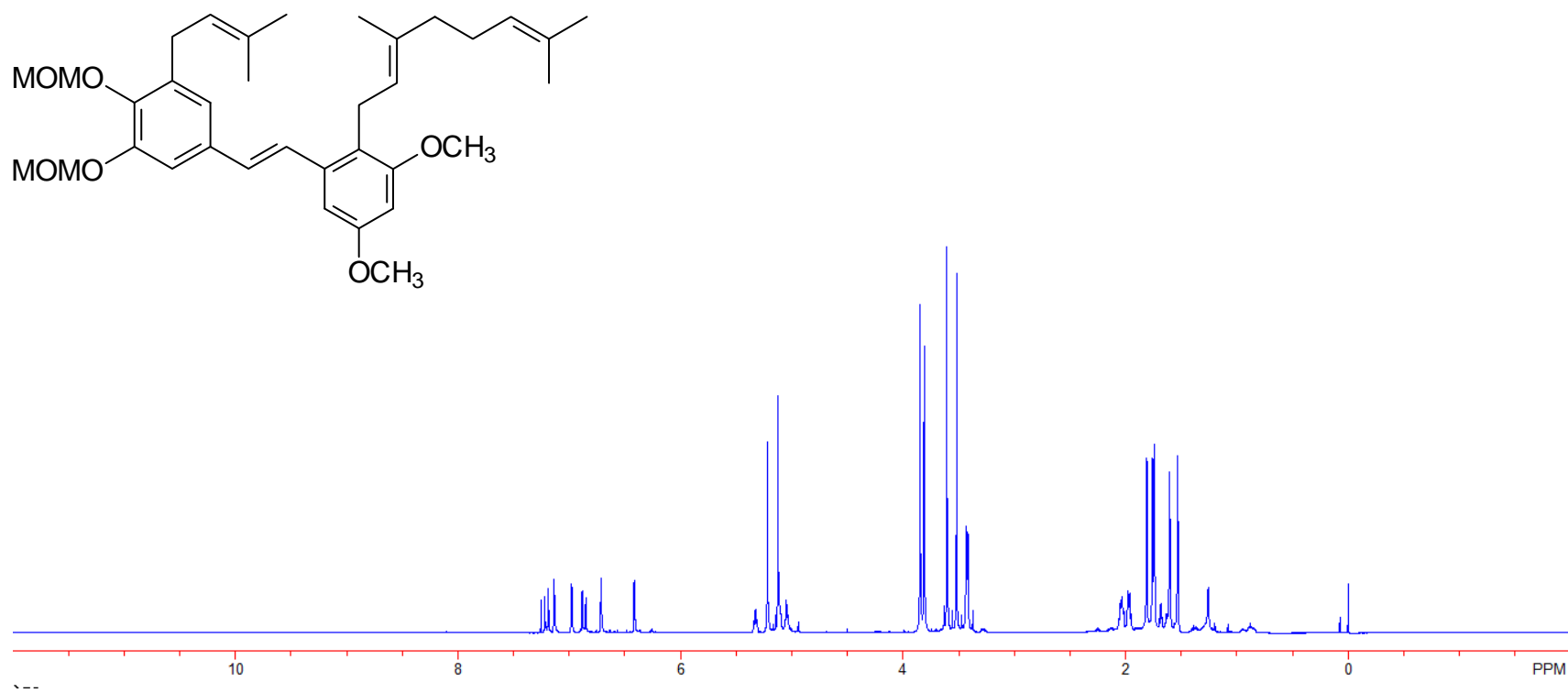


Figure A-41. ^1H NMR spectrum of compound **78**

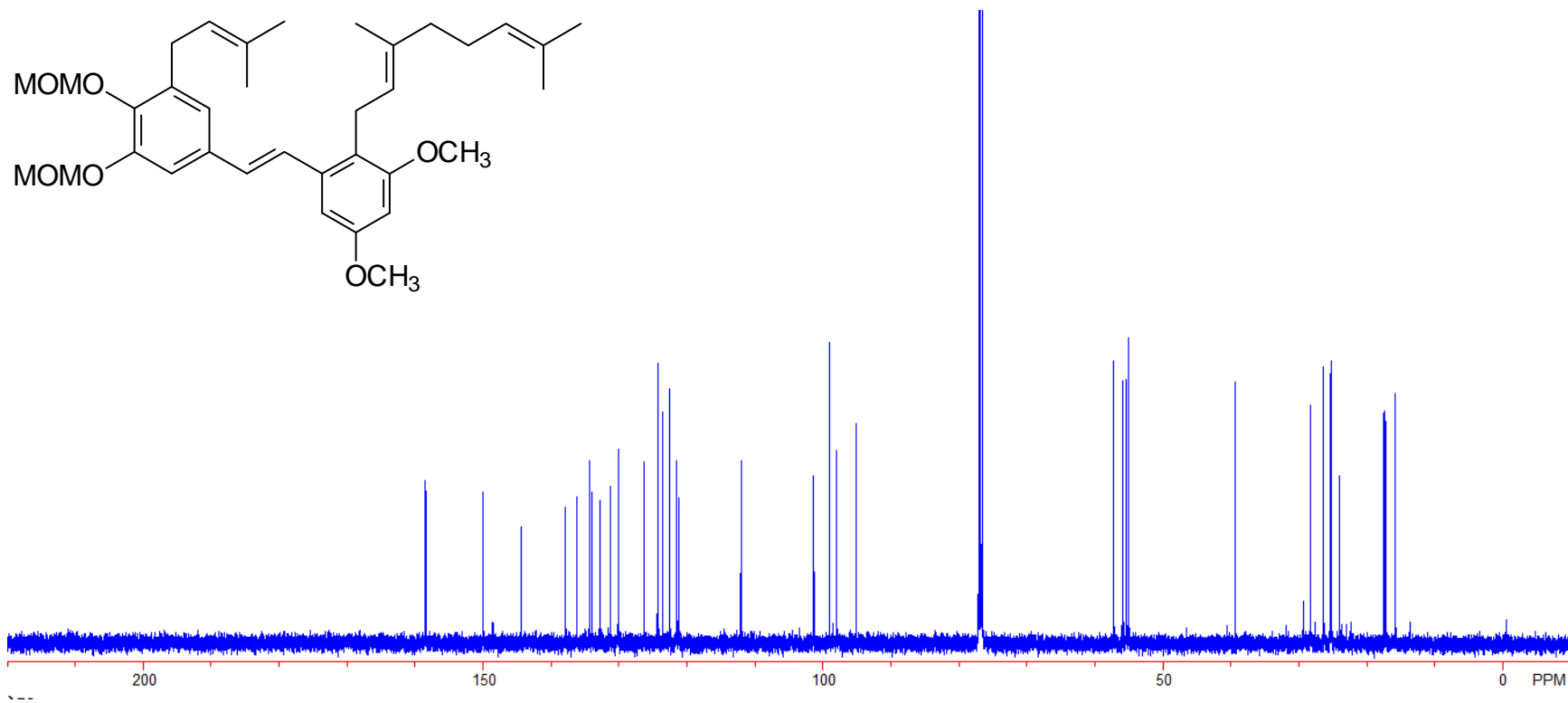


Figure A-42. ^{13}C NMR spectrum of compound **78**

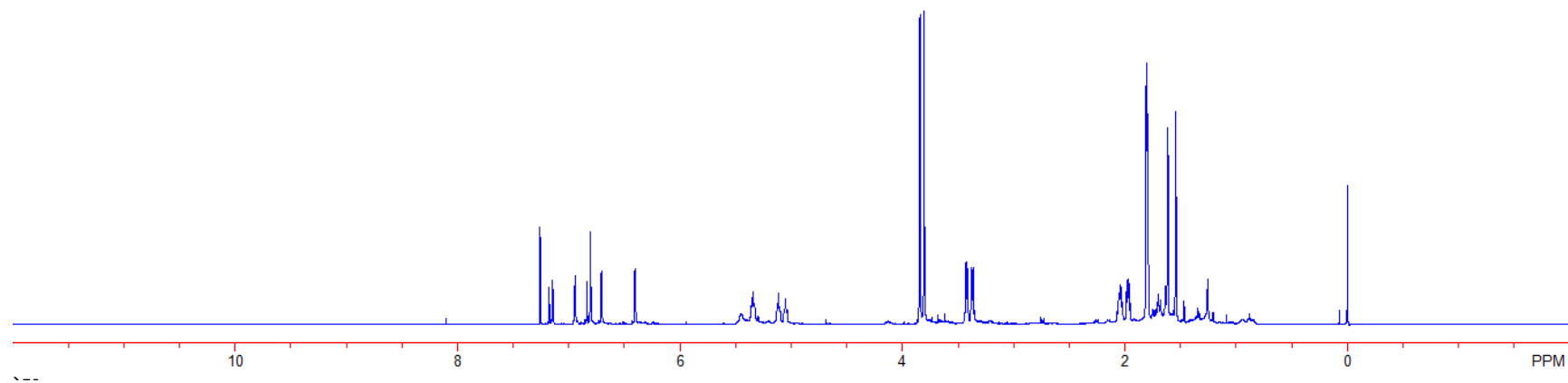
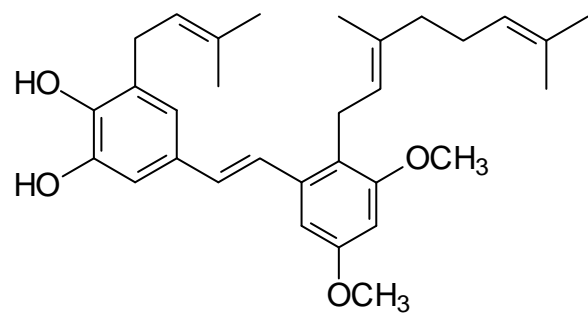


Figure A-43. ¹H NMR spectrum of compound **79**

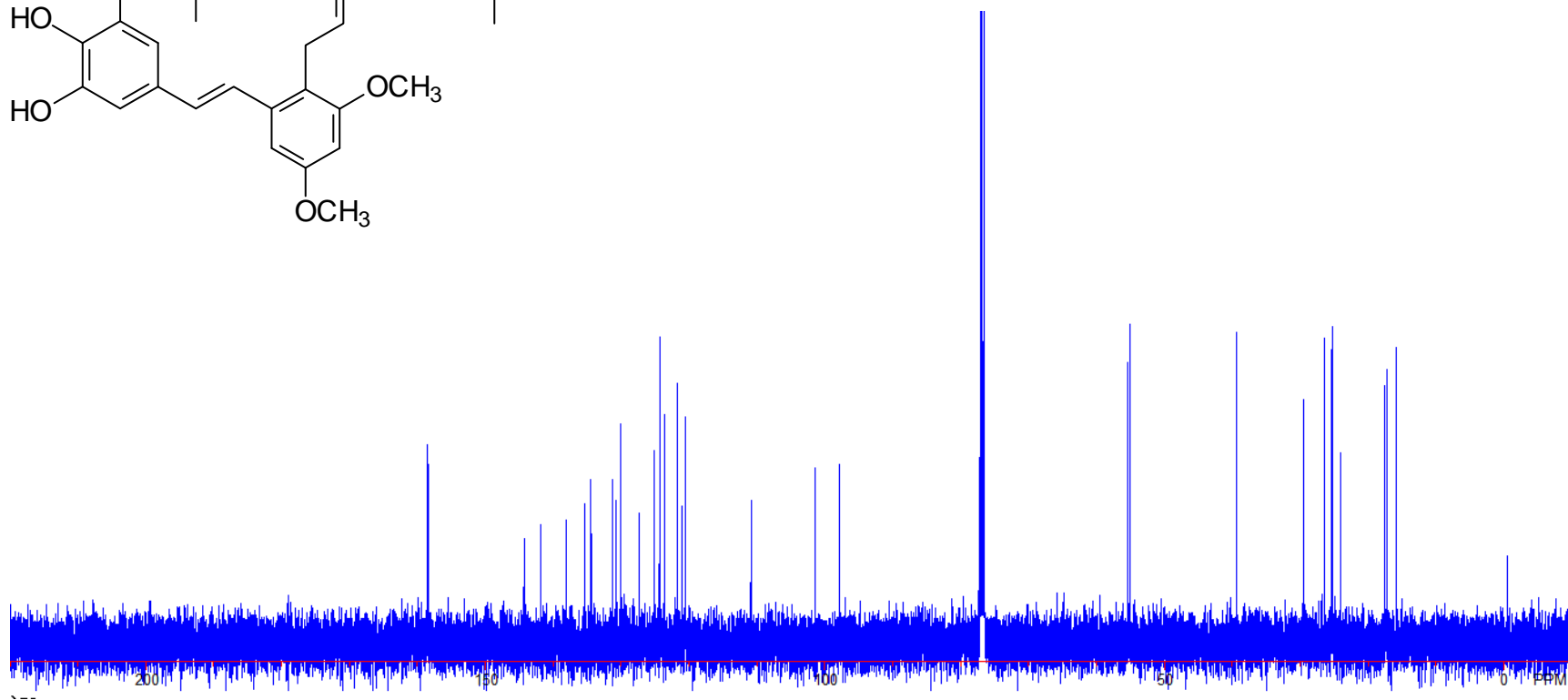
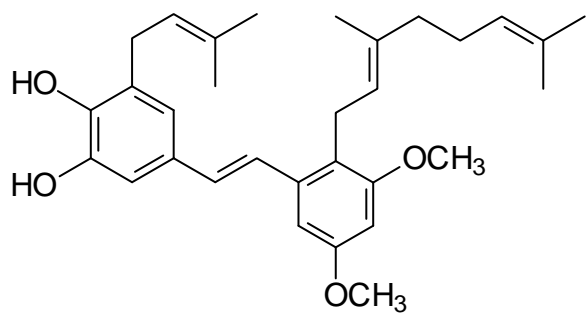


Figure A-44. ¹³C NMR spectrum of compound **79**

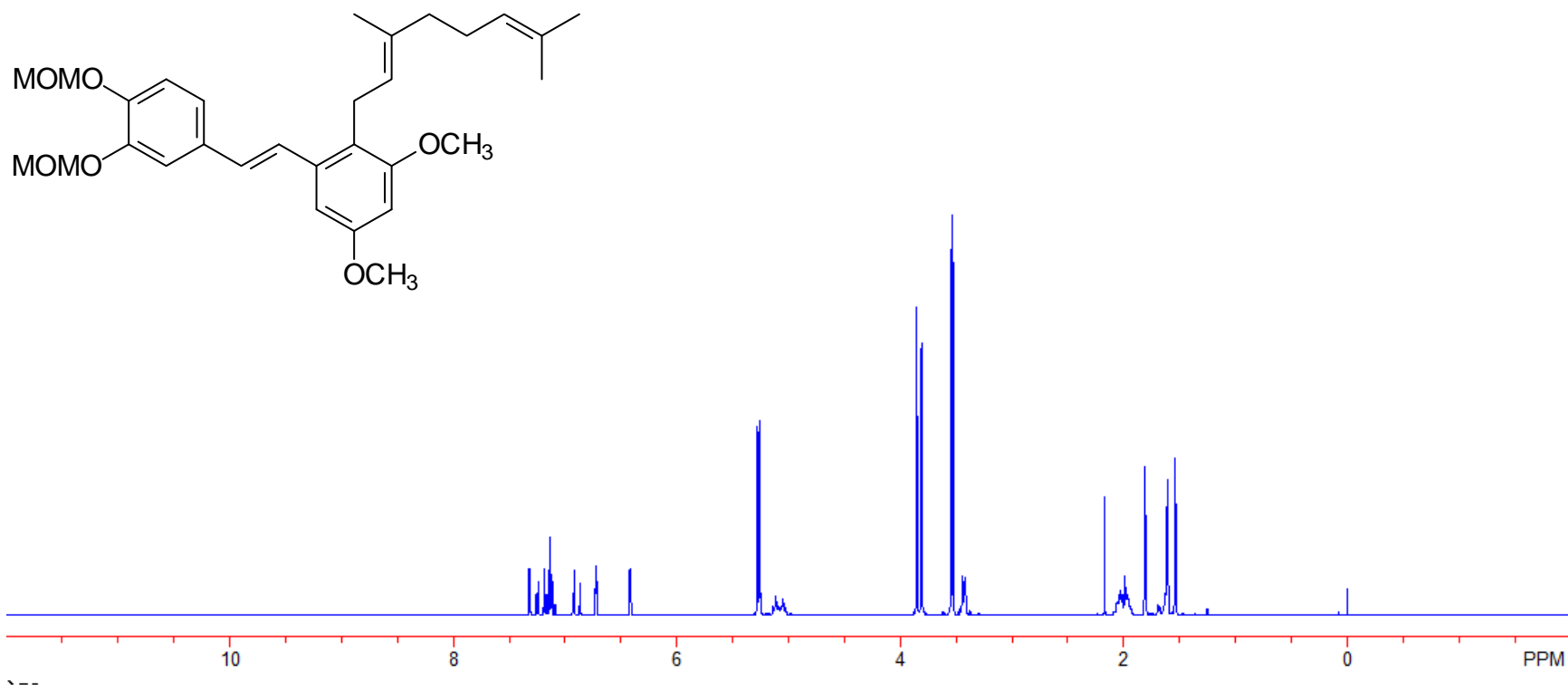


Figure A-45. ¹H NMR spectrum of compound **80**

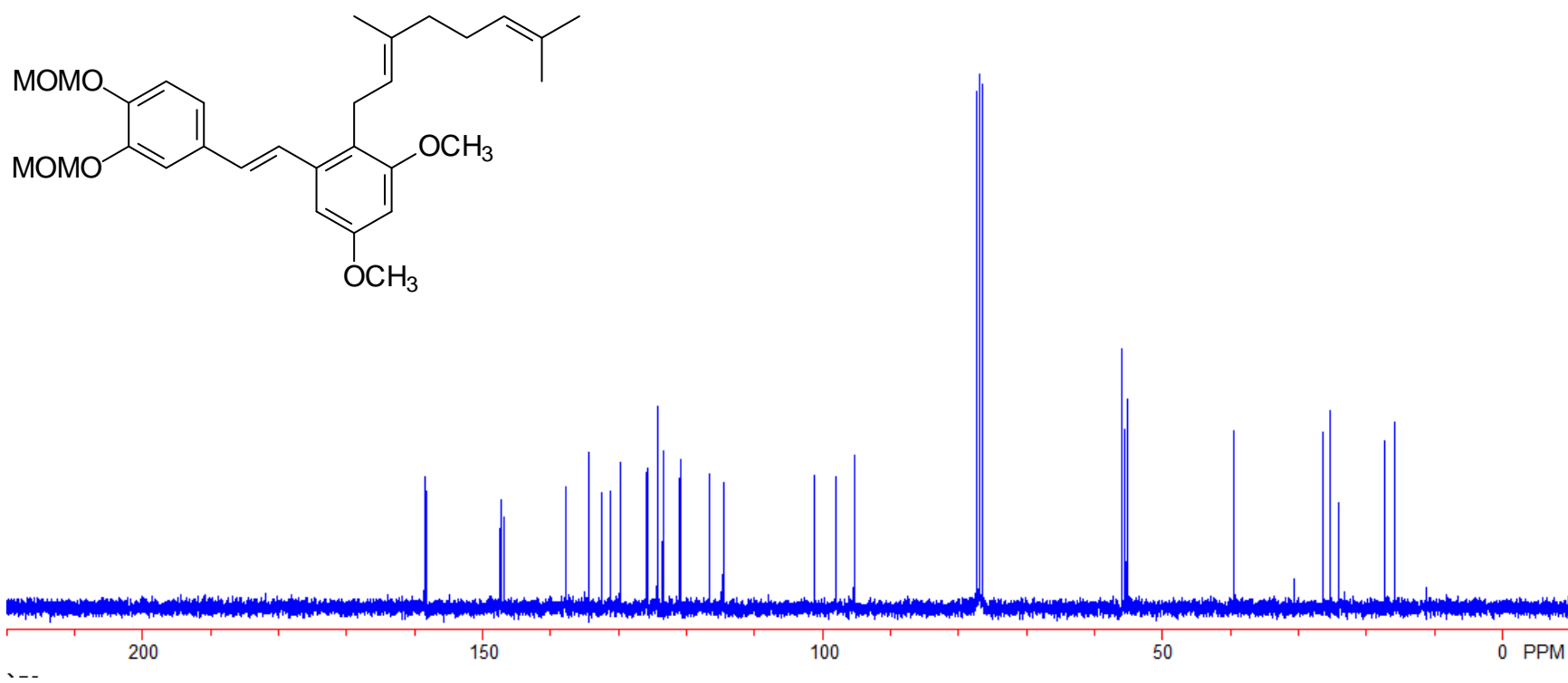


Figure A-46. ^{13}C NMR spectrum of compound **80**

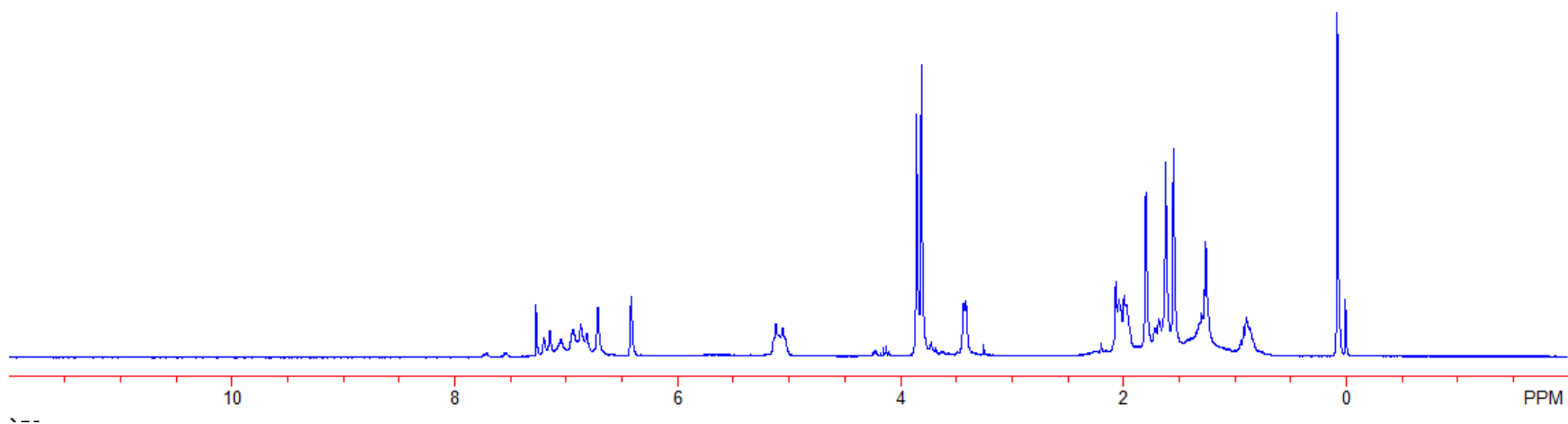
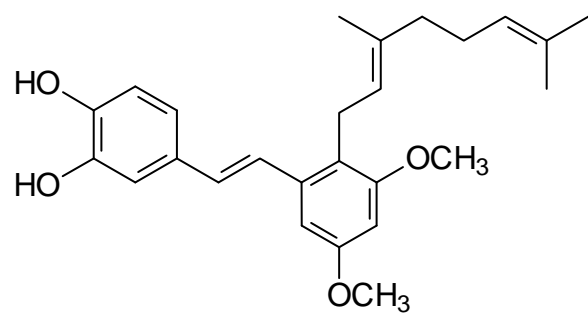


Figure A-47. ¹H NMR spectrum of compound **81**

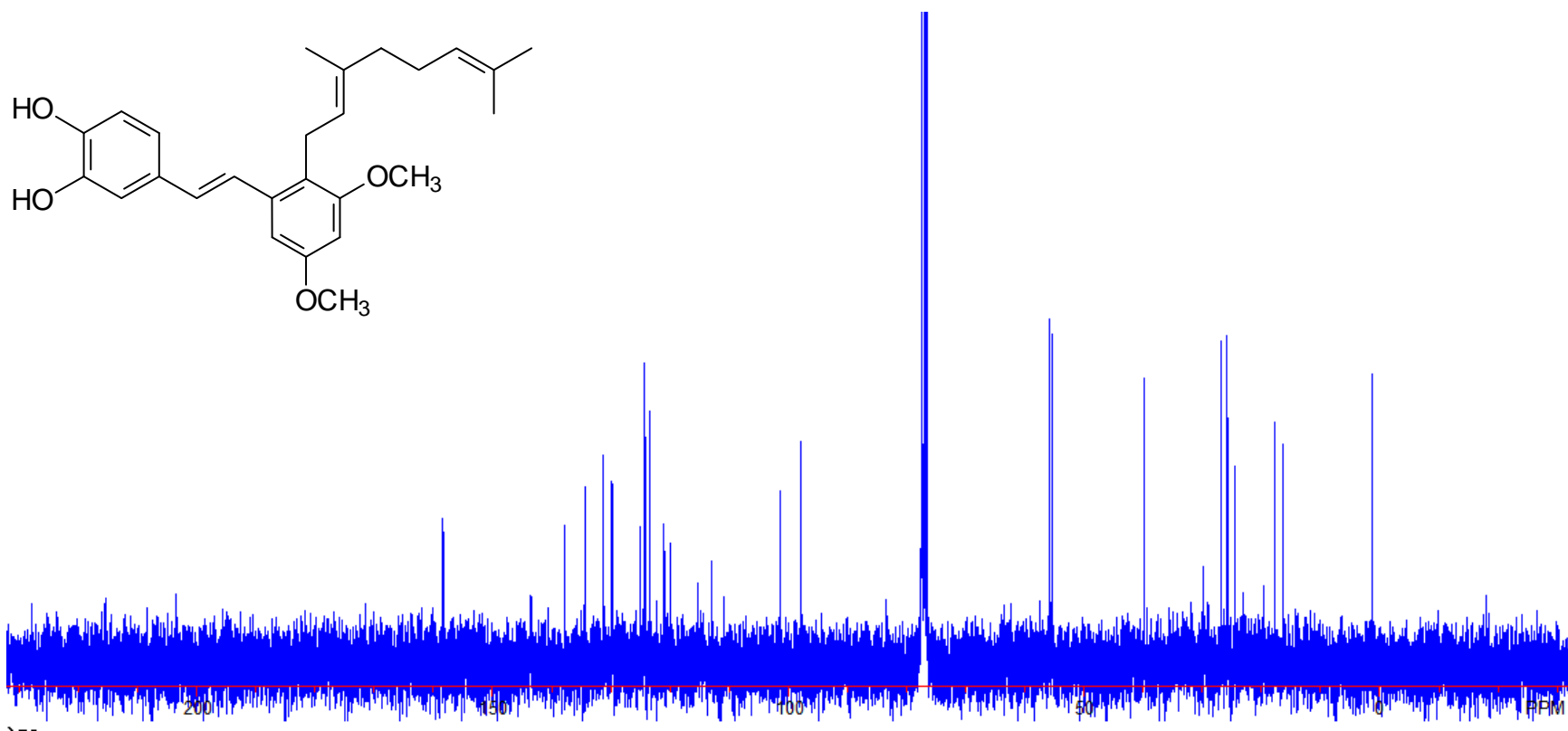


Figure A-48. ^{13}C NMR spectrum of compound **81**

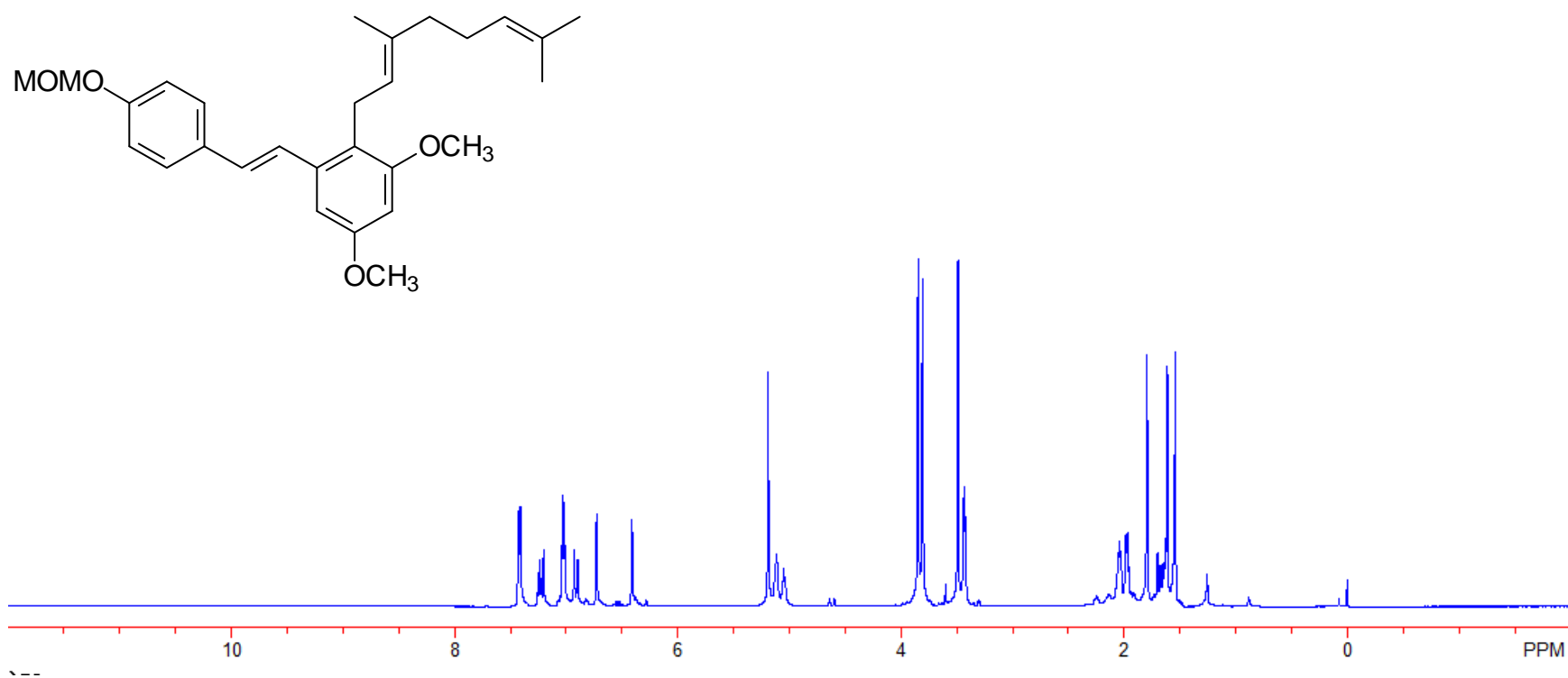


Figure A-49. ^1H NMR spectrum of compound **82**

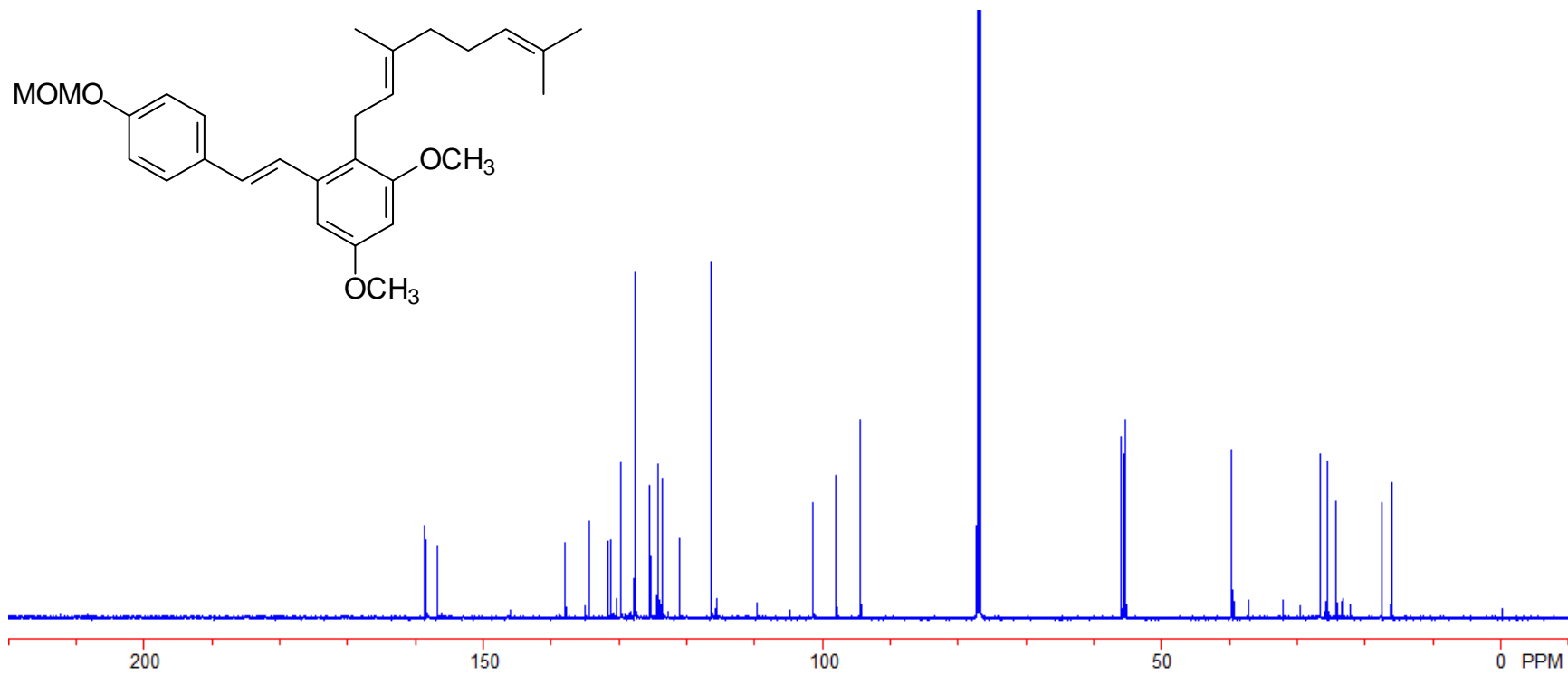


Figure A-50. ^{13}C NMR spectrum of compound **82**

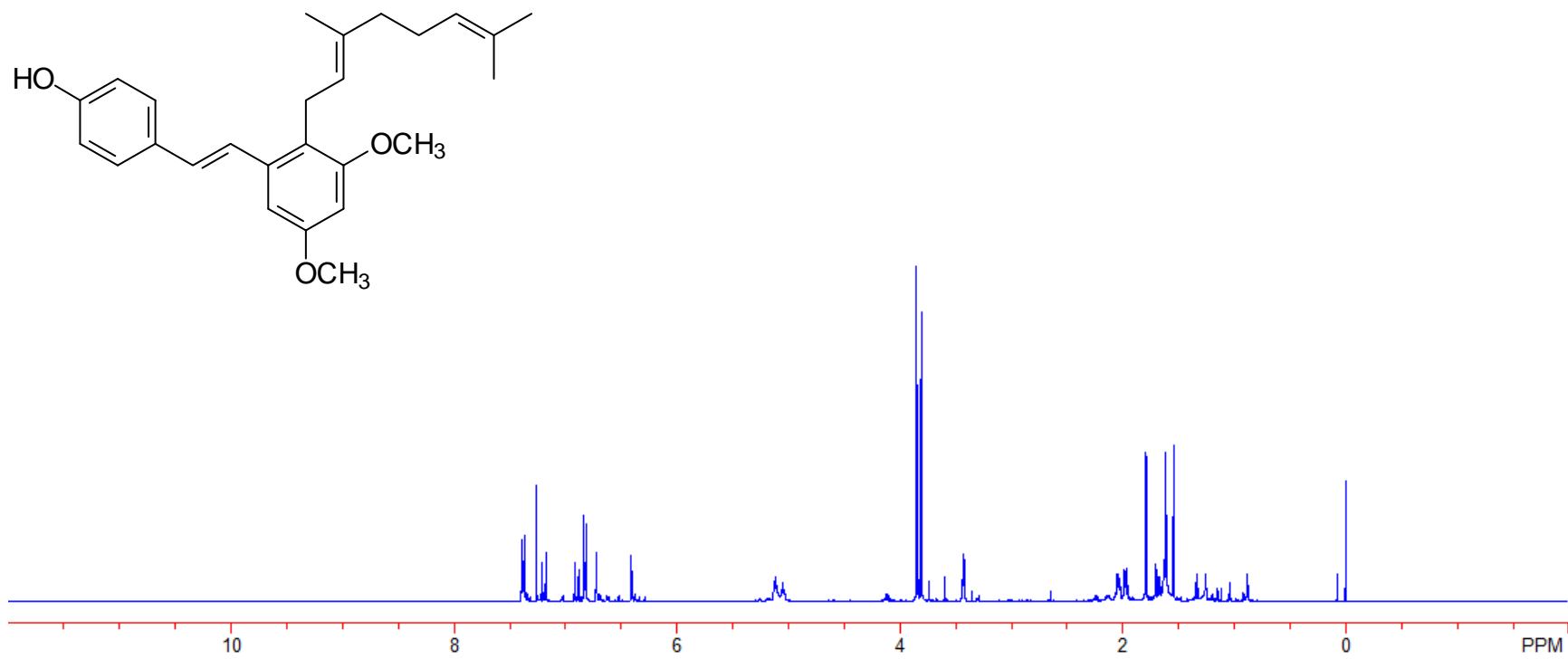


Figure A-51. ^1H NMR spectrum of compound **83**

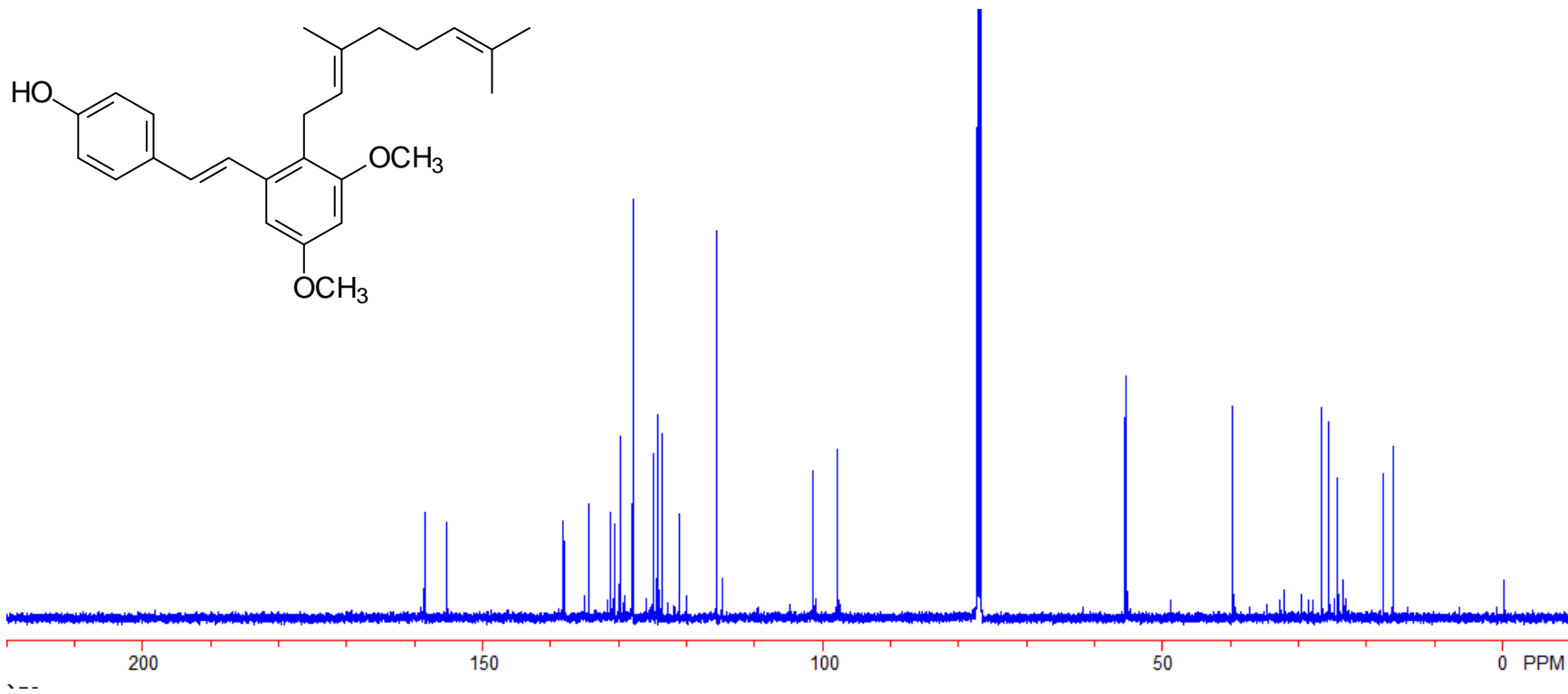


Figure A-52. ^{13}C NMR spectrum of compound **83**

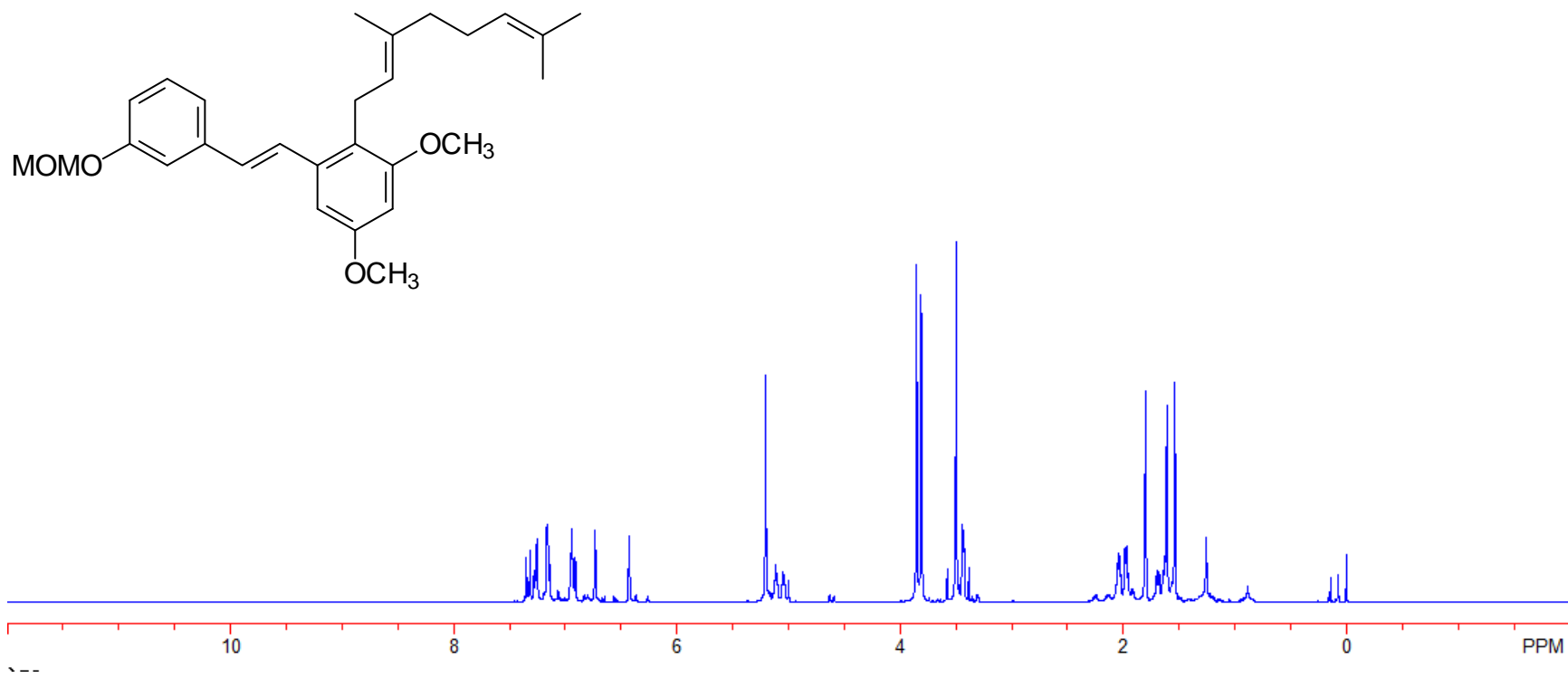


Figure A-53. ¹H NMR spectrum of compound **84**

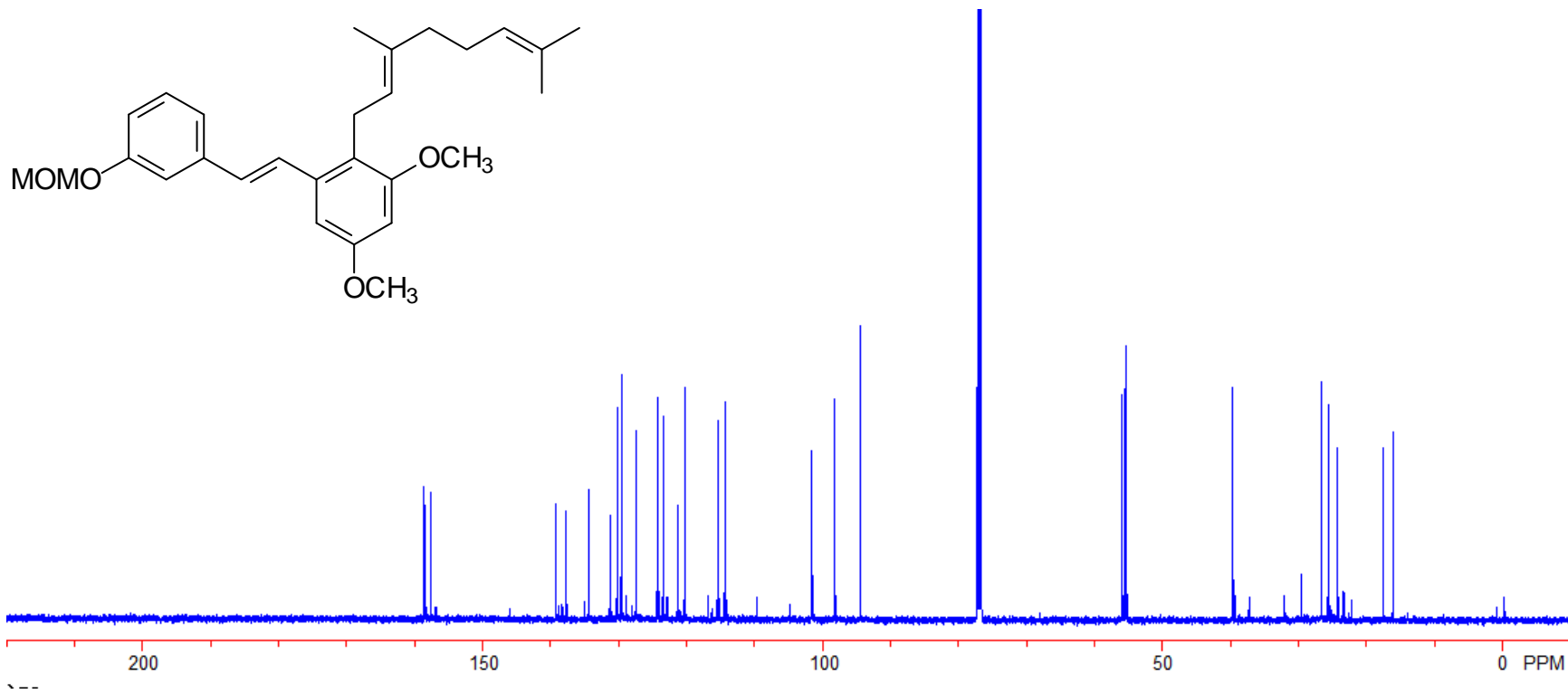


Figure A-54. ^{13}C NMR spectrum of compound **84**

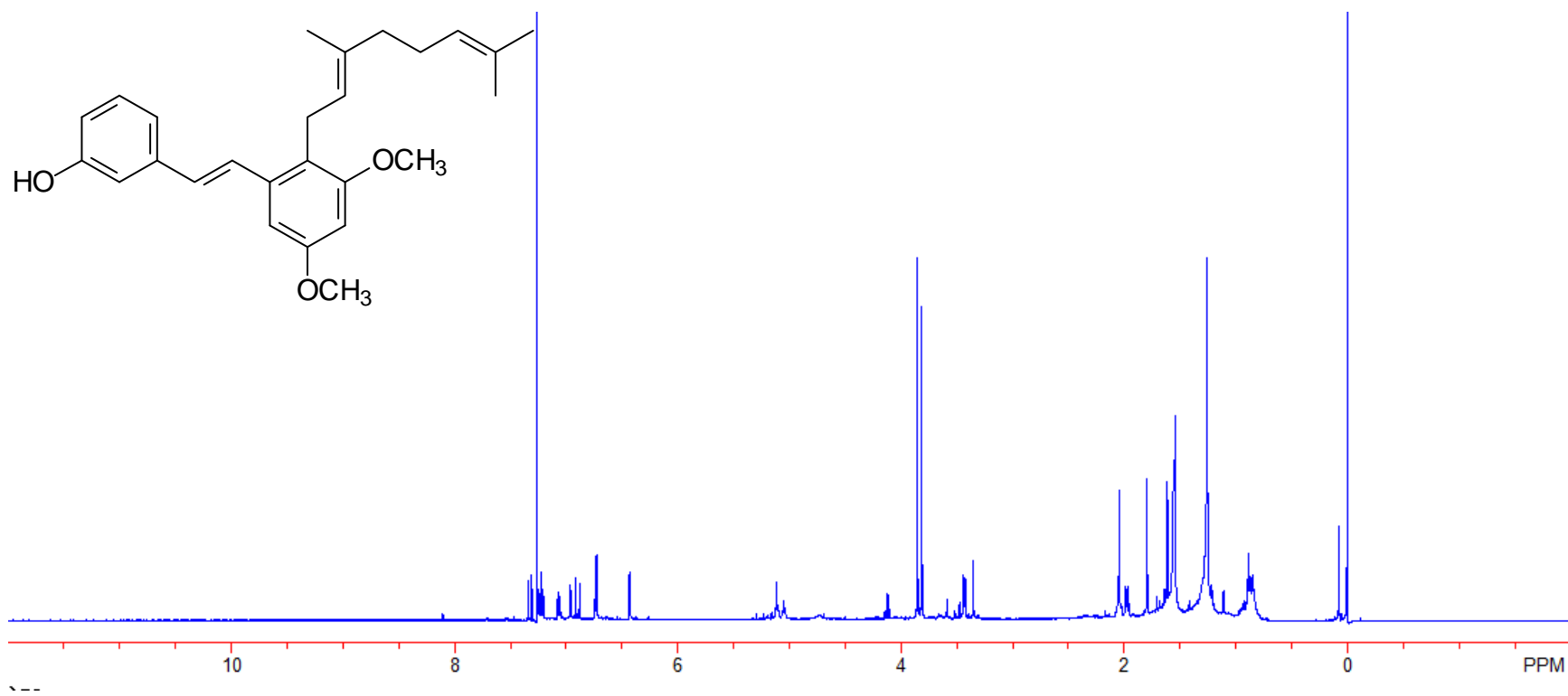


Figure A-55. ¹H NMR spectrum of compound **85**

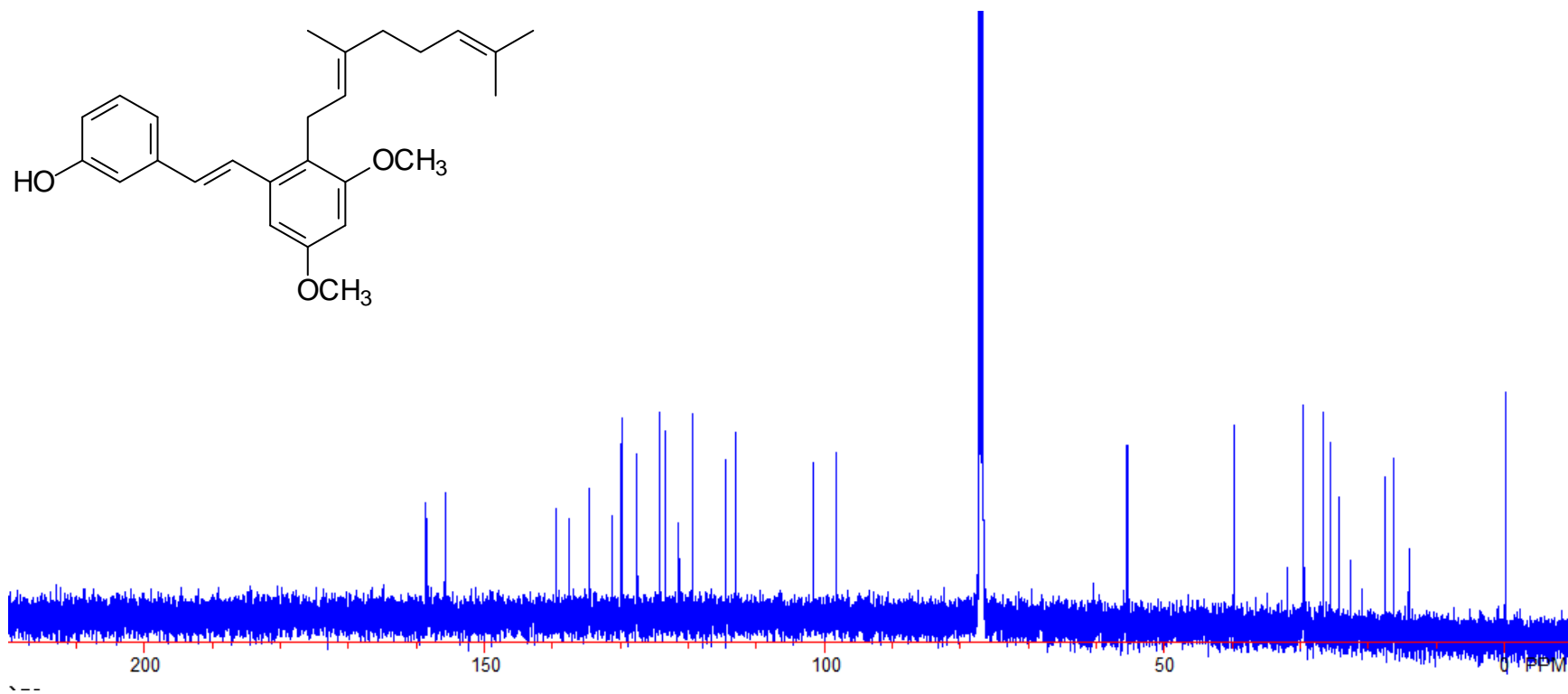


Figure A-56. ^{13}C NMR spectrum of compound **85**

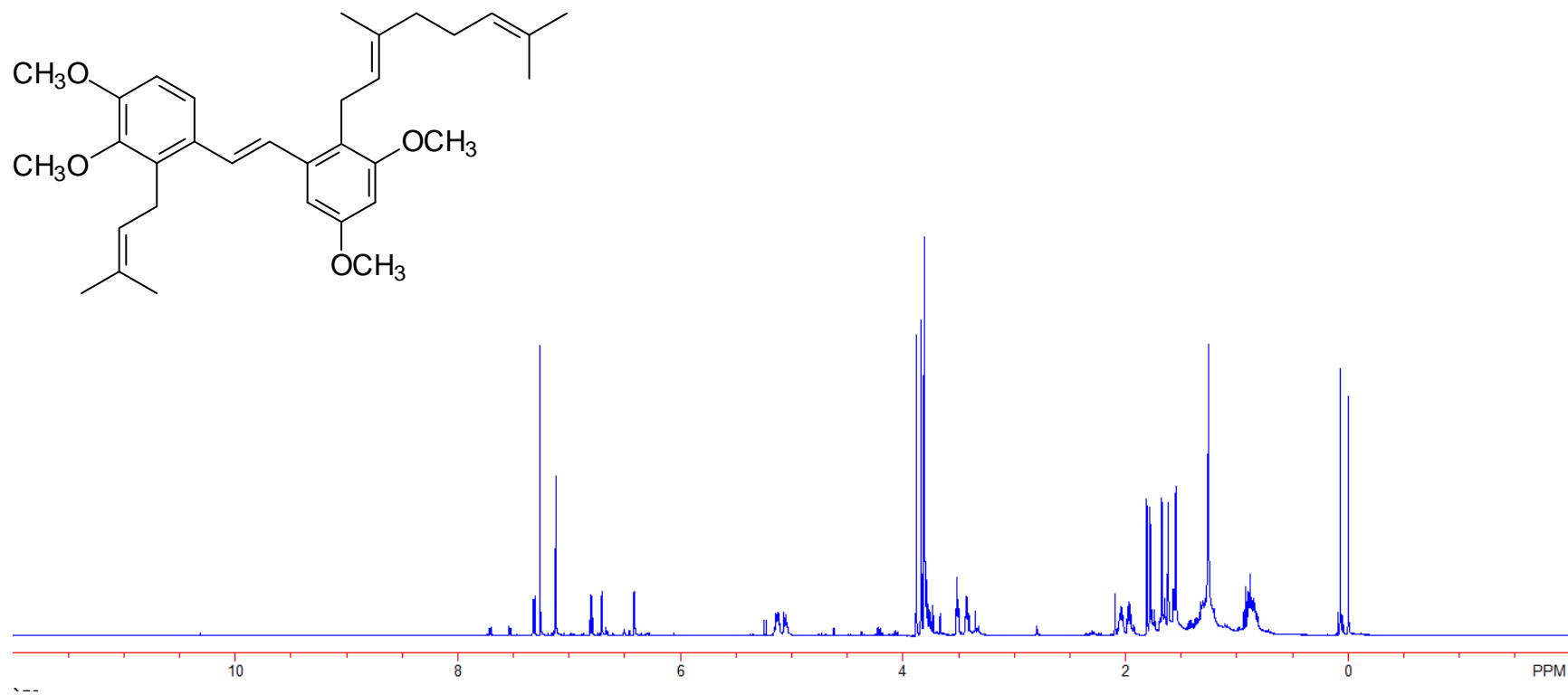


Figure A-57. ¹H NMR spectrum of compound **86**

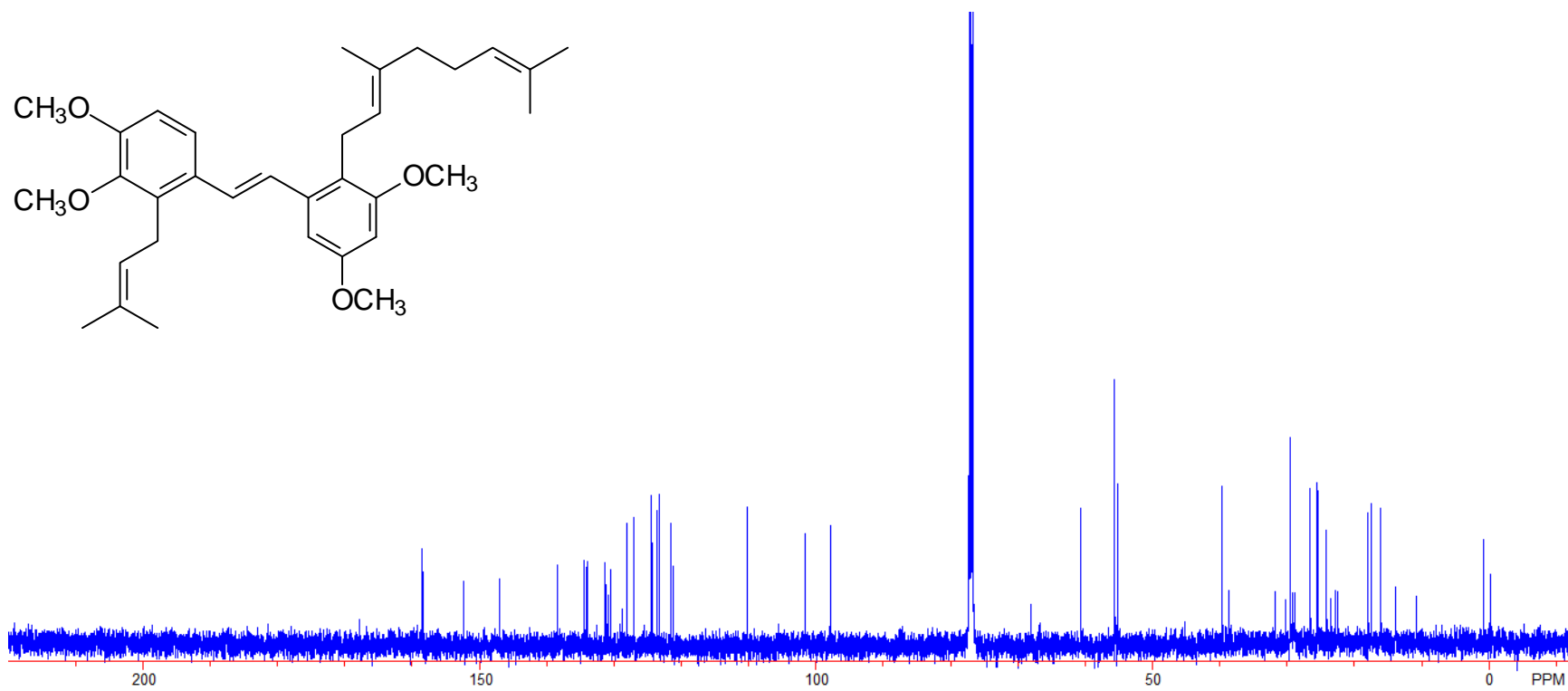


Figure A-58. ^{13}C NMR spectrum of compound **86**

Please note, the resonance at 29.7 ppm is indicative of silica oil.

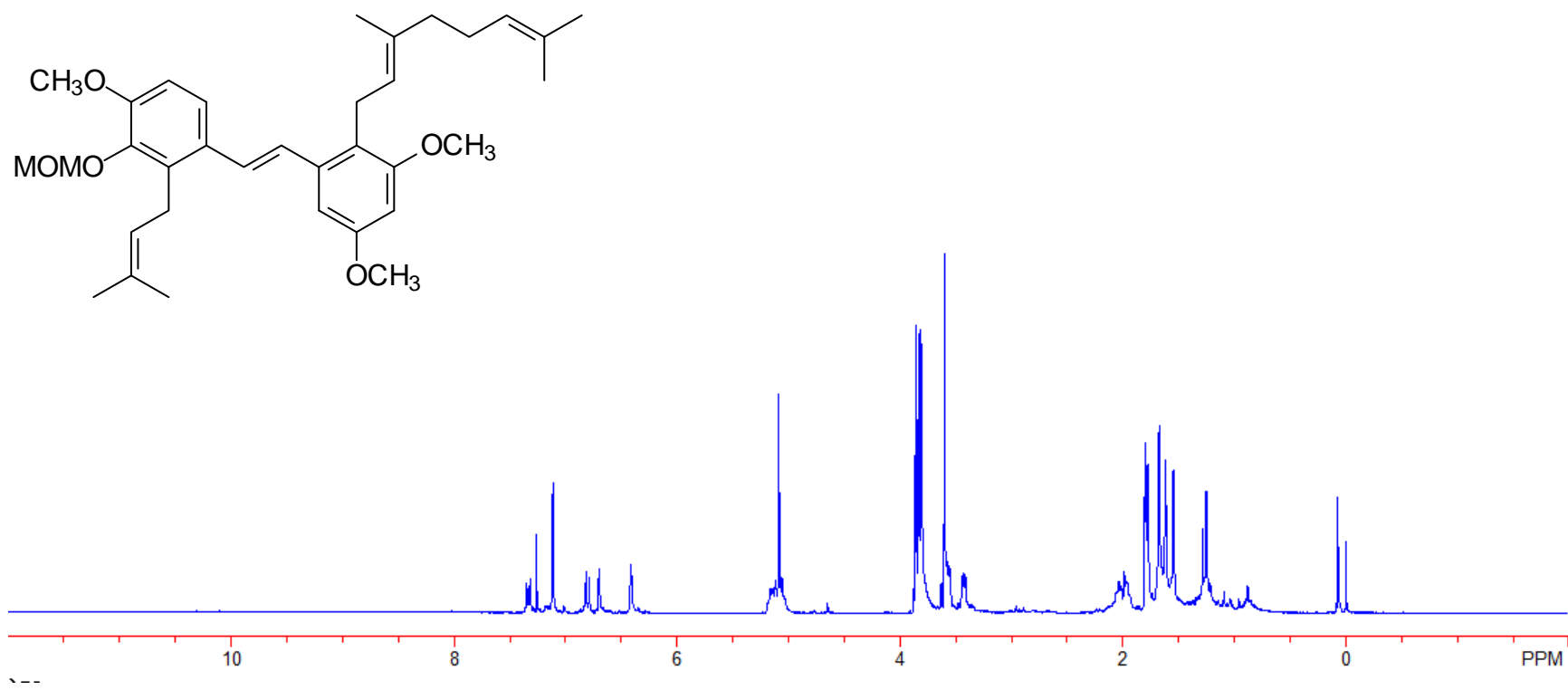


Figure A-59. ^1H NMR spectrum of compound **87**

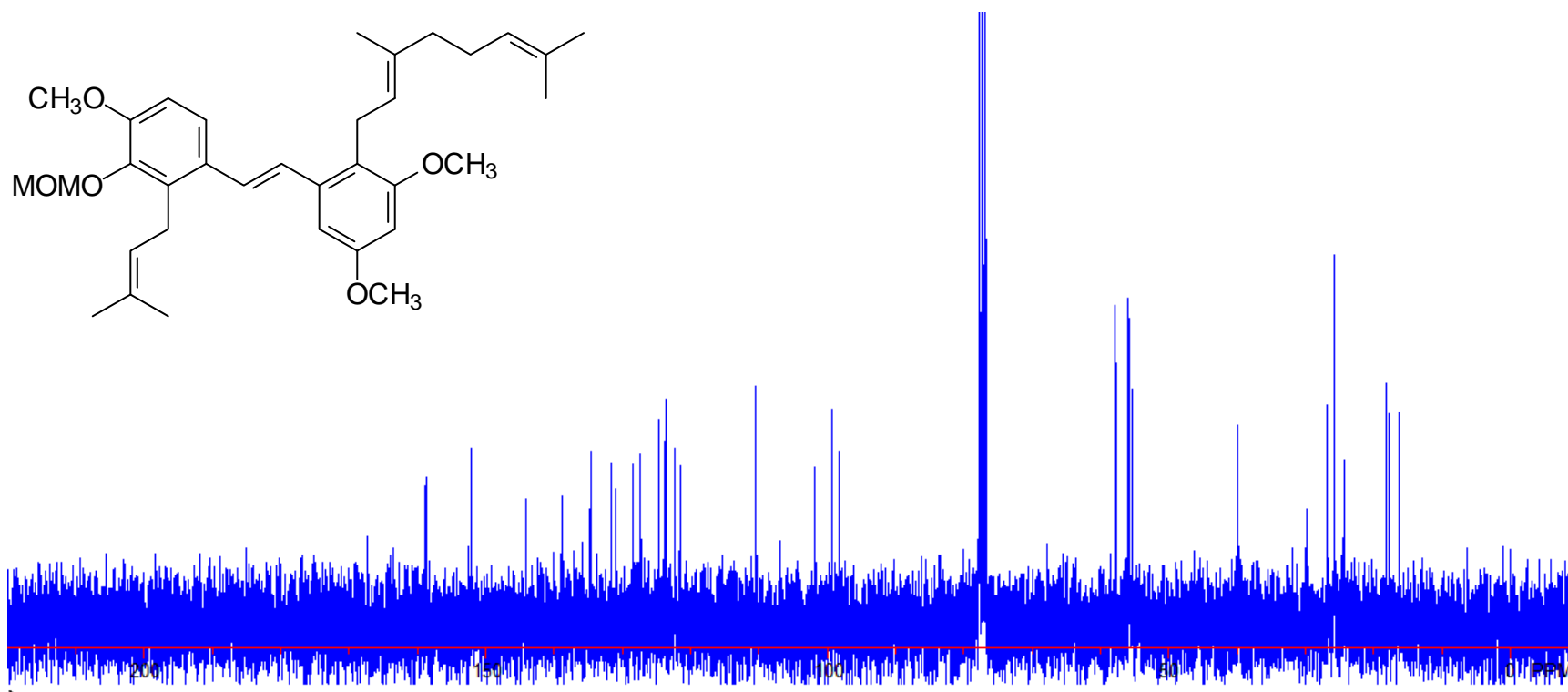


Figure A-60. ^{13}C NMR spectrum of compound **87**

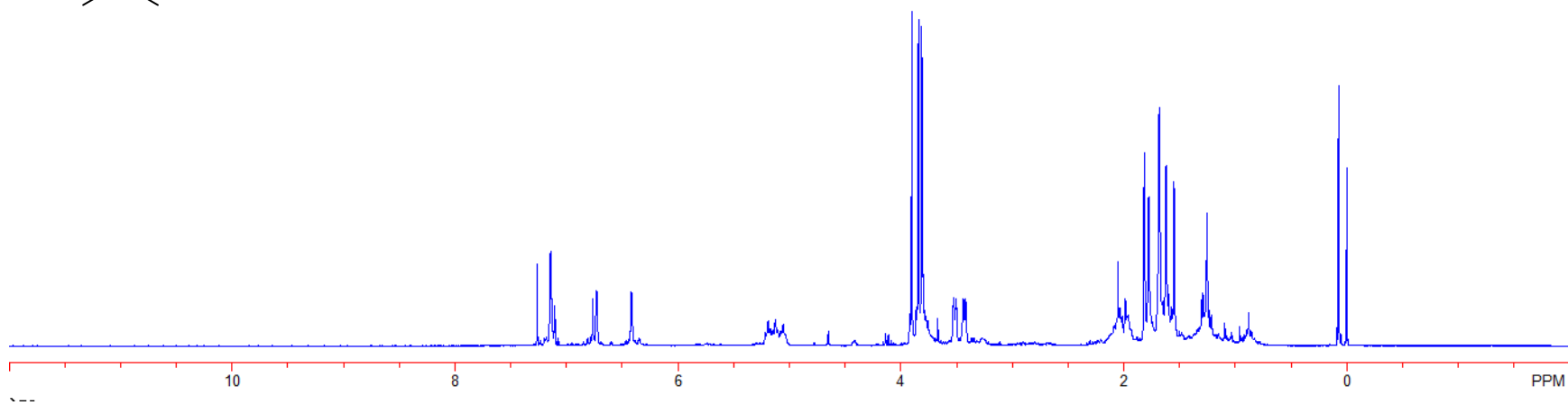
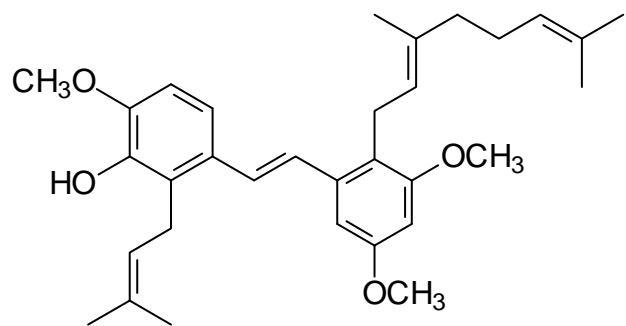


Figure A-61. ¹H NMR spectrum of compound **88**

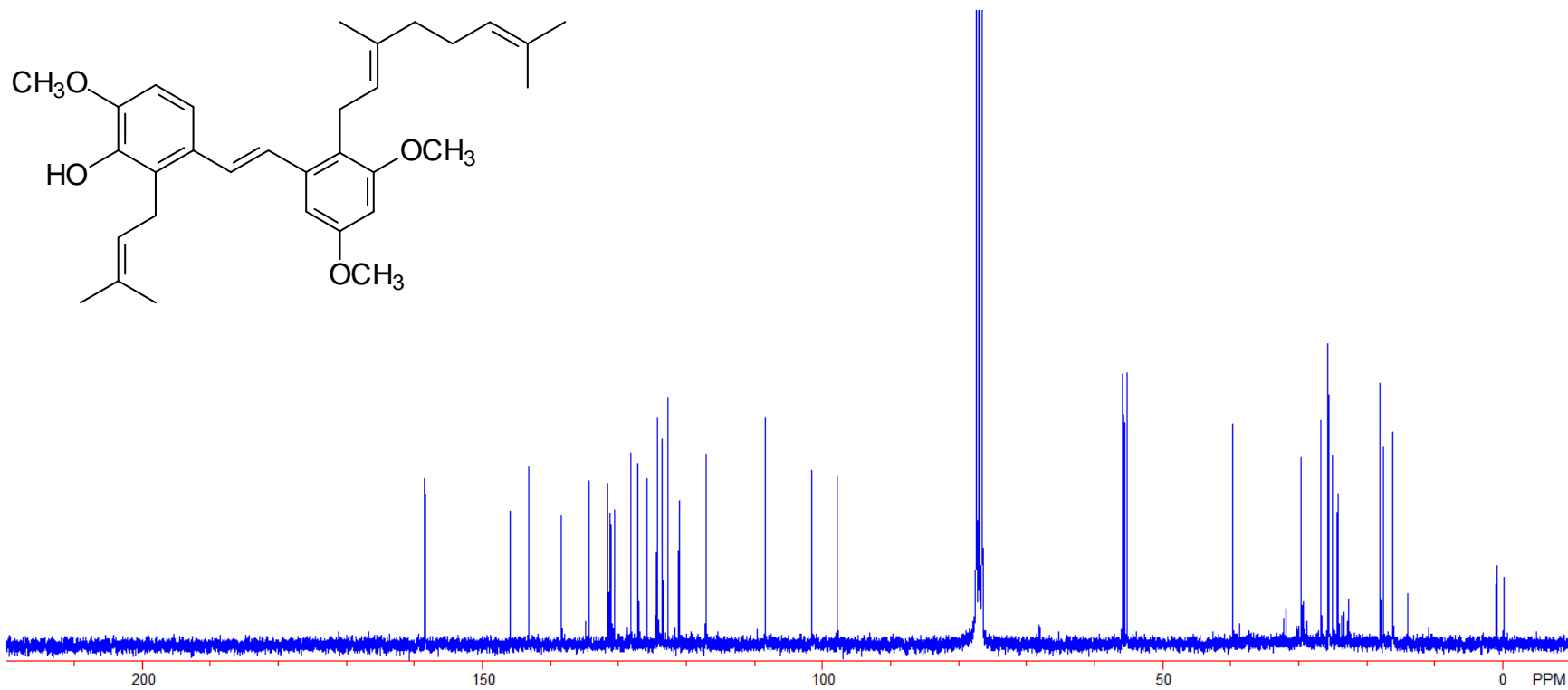


Figure A-62. ^{13}C NMR spectrum of compound **88**

Please note, the resonance at 29.7 ppm is indicative of silica oil.

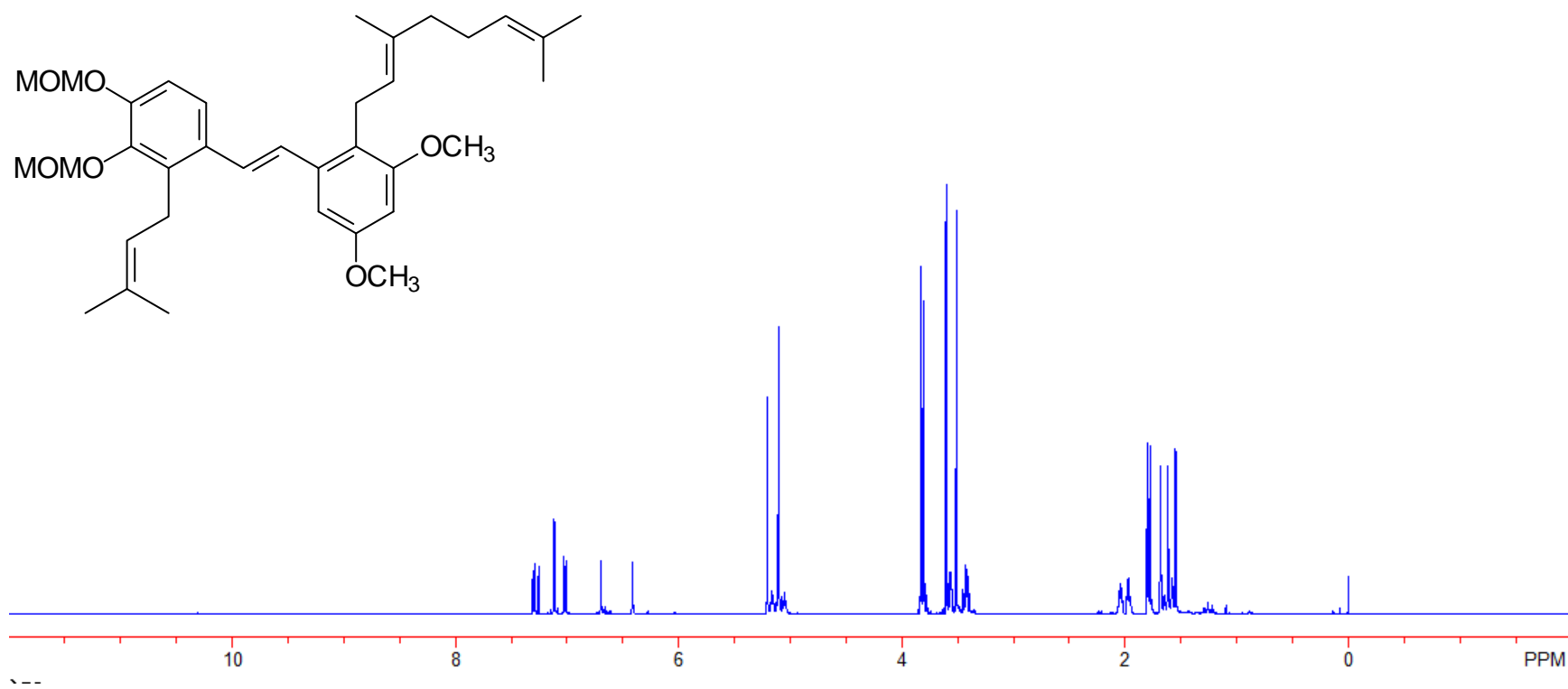


Figure A-63. ^1H NMR spectrum of compound **89**

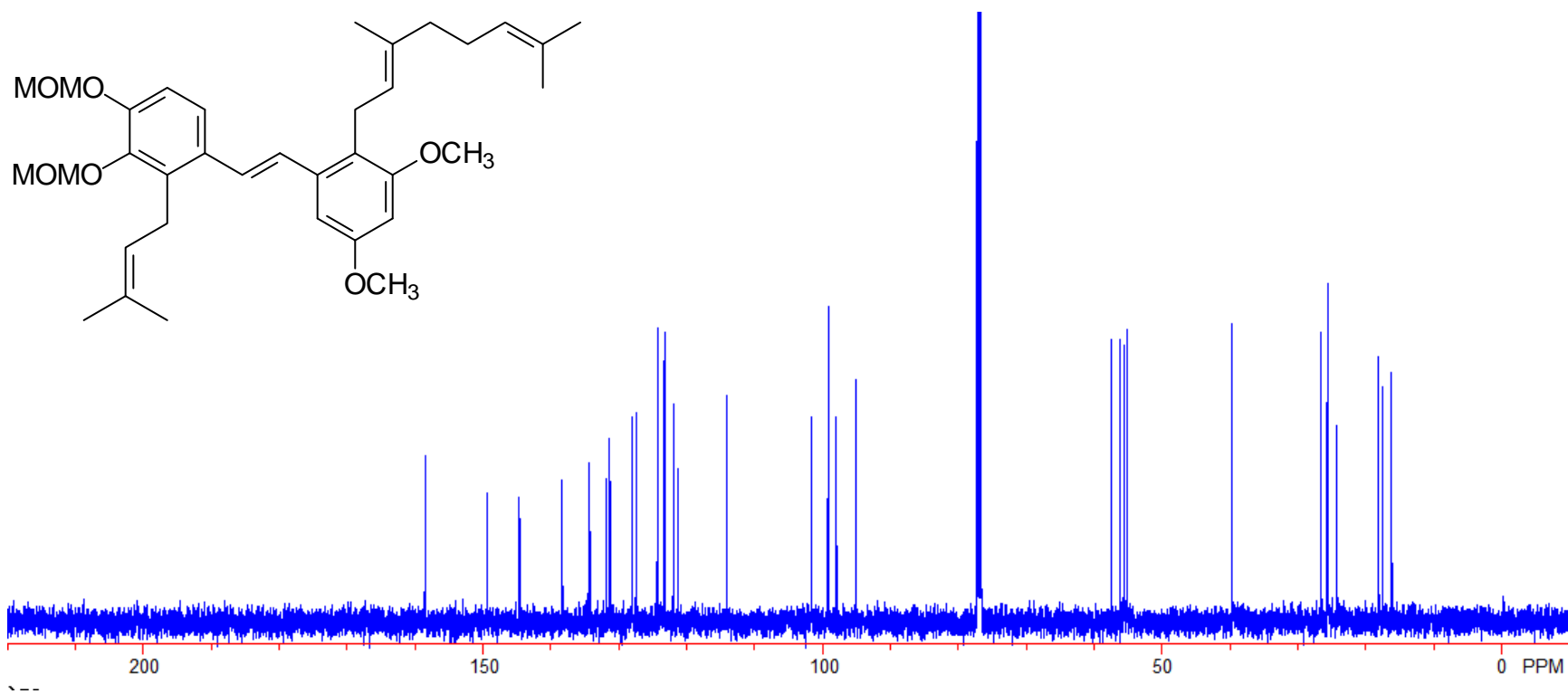


Figure A-64. ^{13}C NMR spectrum of compound **89**

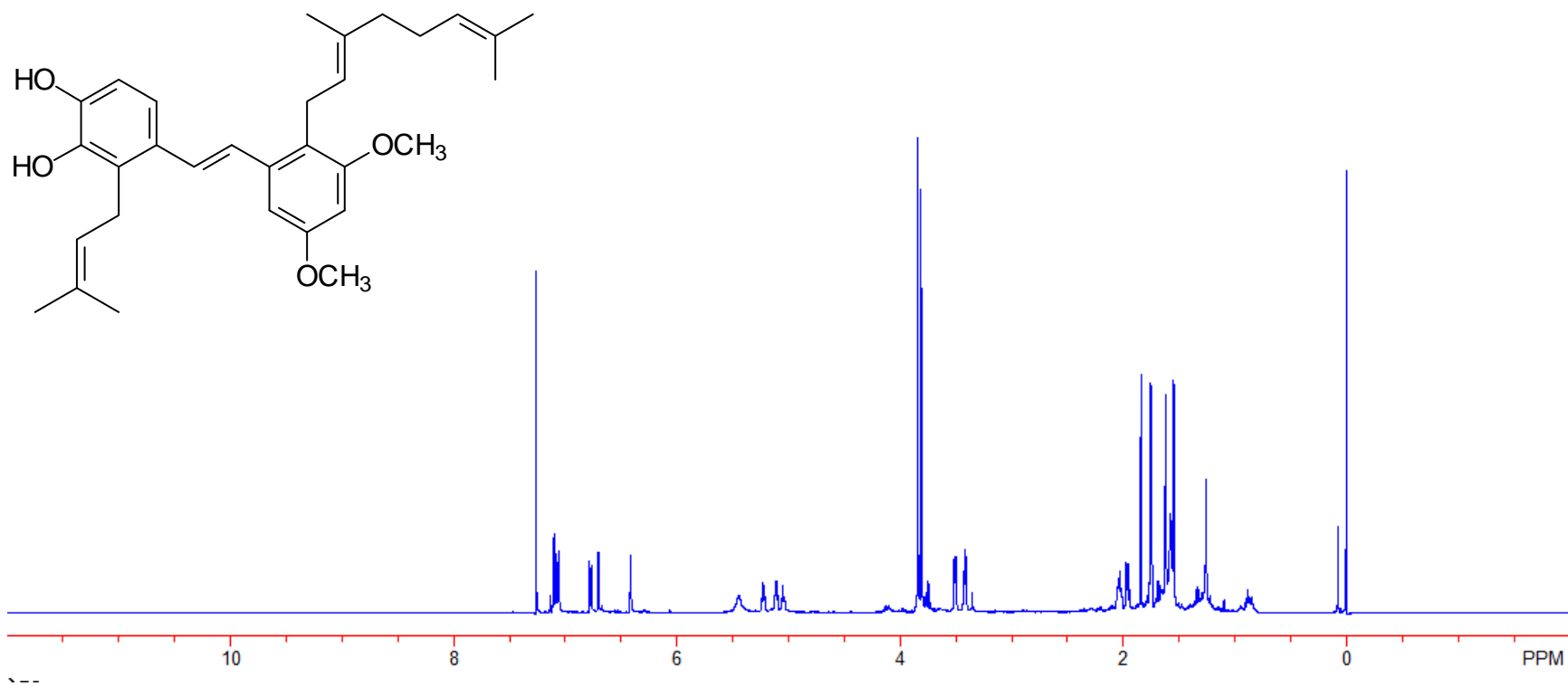


Figure A-65. ¹H NMR spectrum of compound **90**

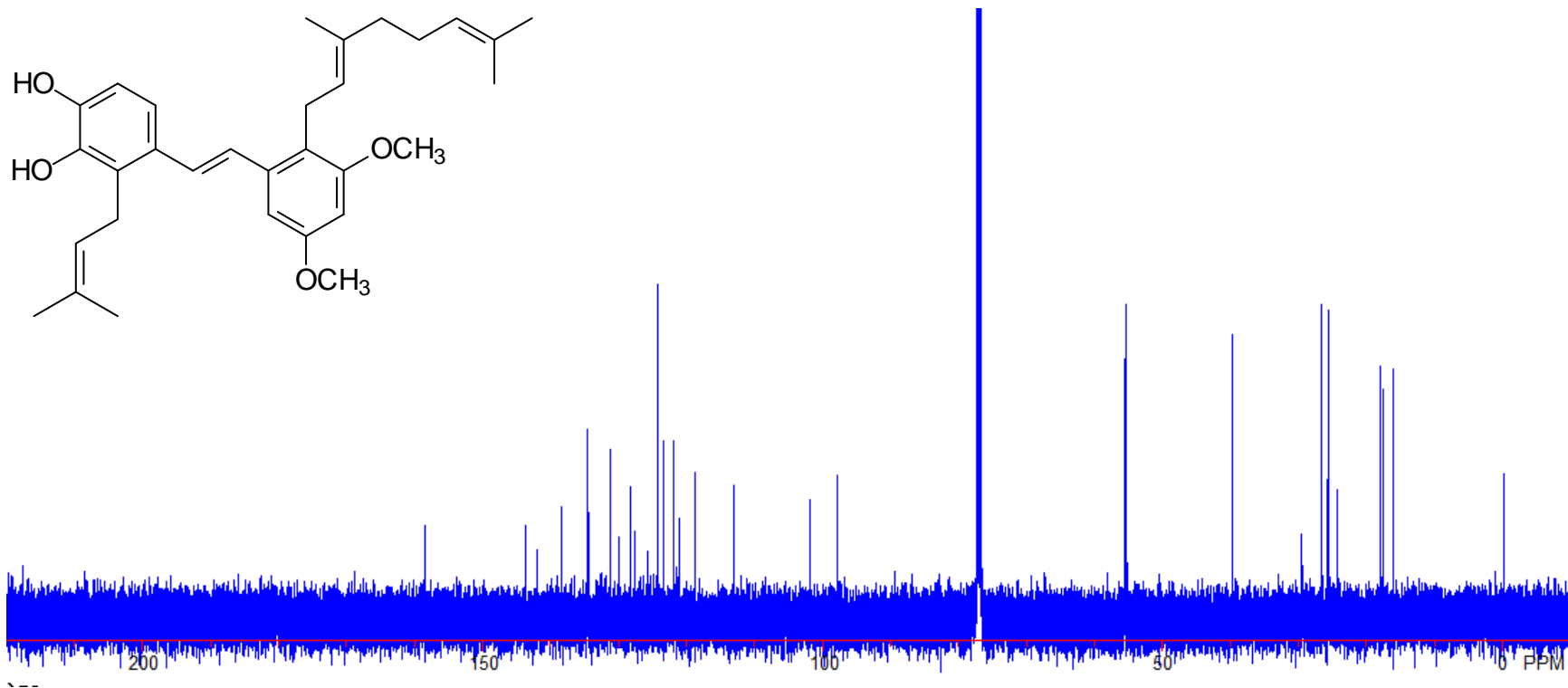


Figure A-66. ^{13}C NMR spectrum of compound **90**

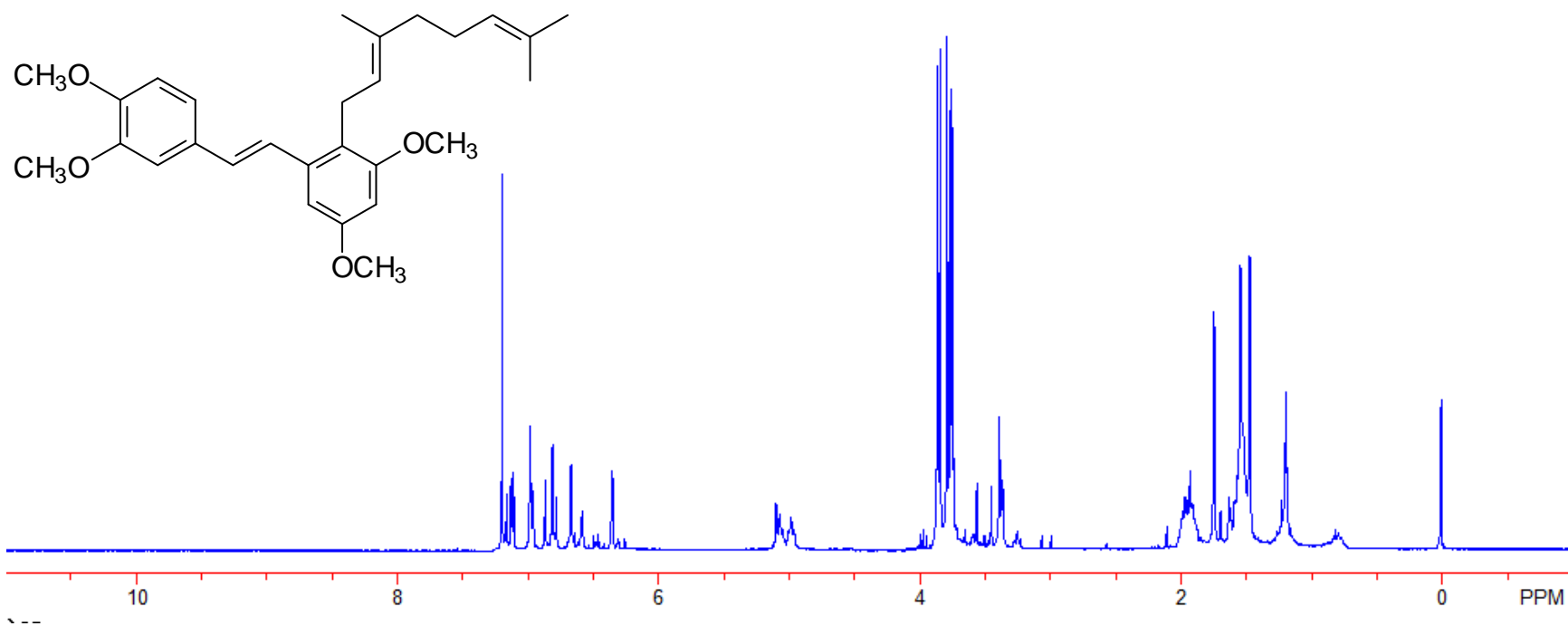


Figure A-67. ¹H NMR spectrum of compound **91**

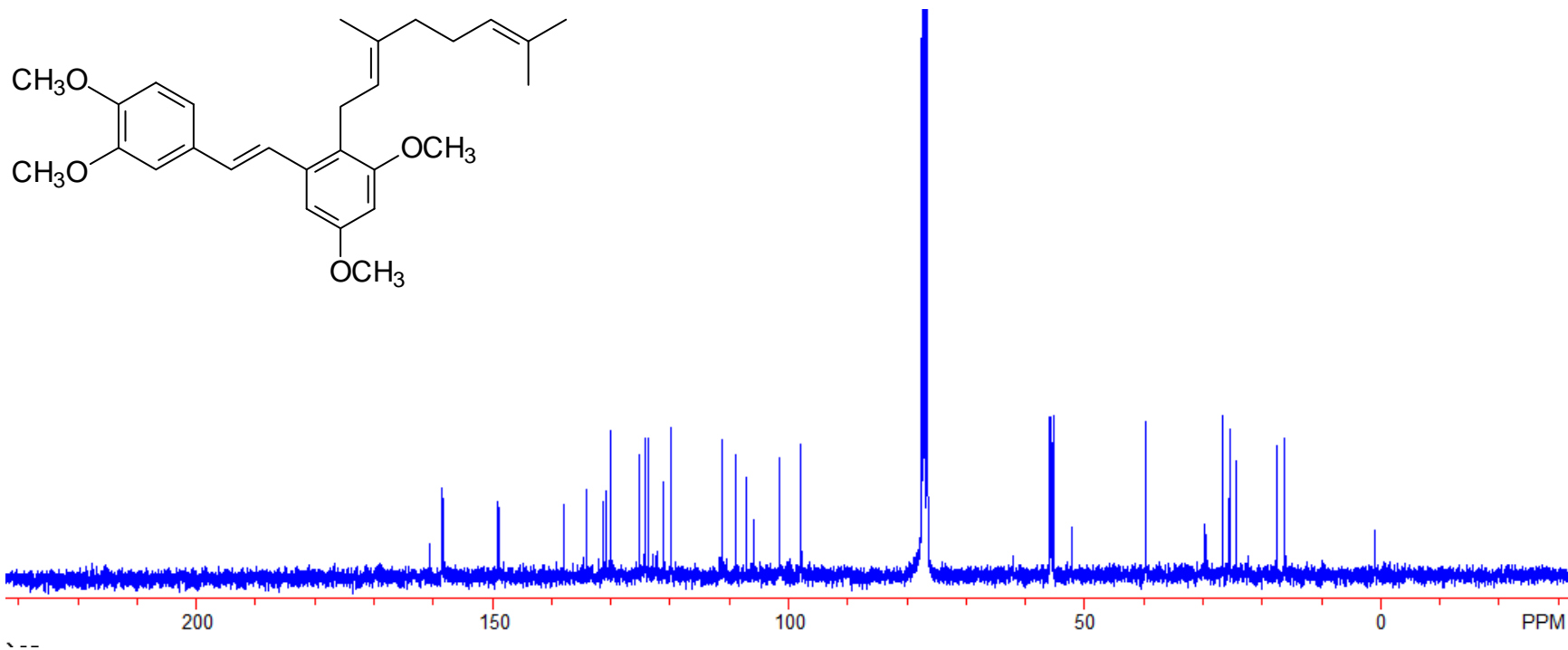


Figure A-68. ^{13}C NMR spectrum of compound **91**

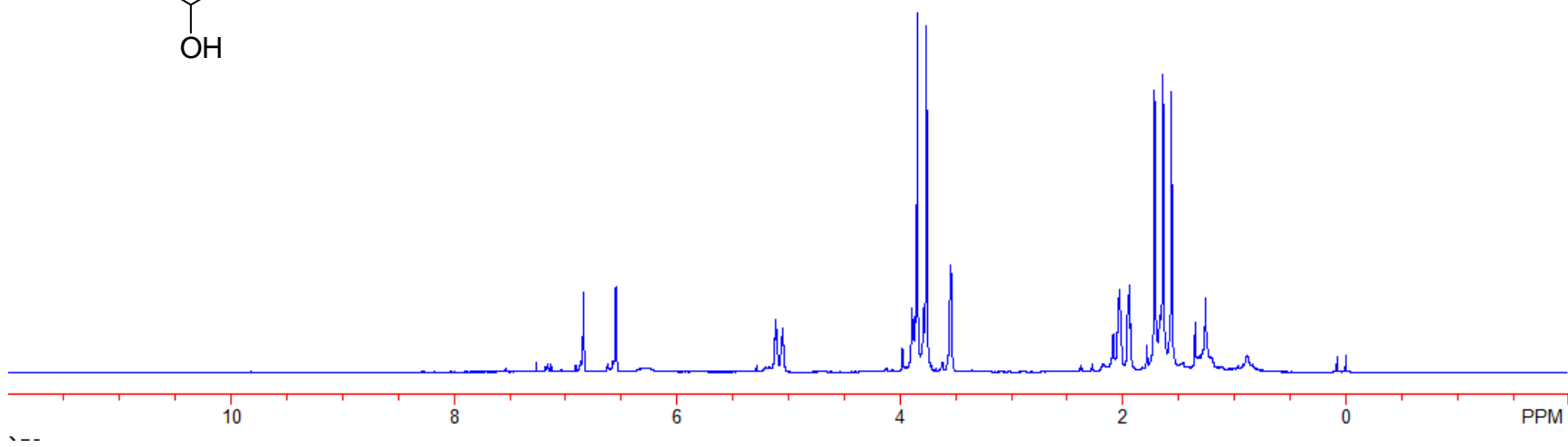
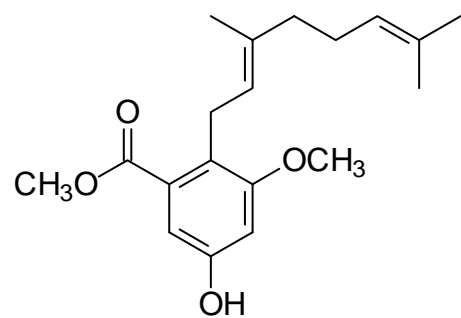


Figure A-69. ¹H NMR spectrum of compound **94**

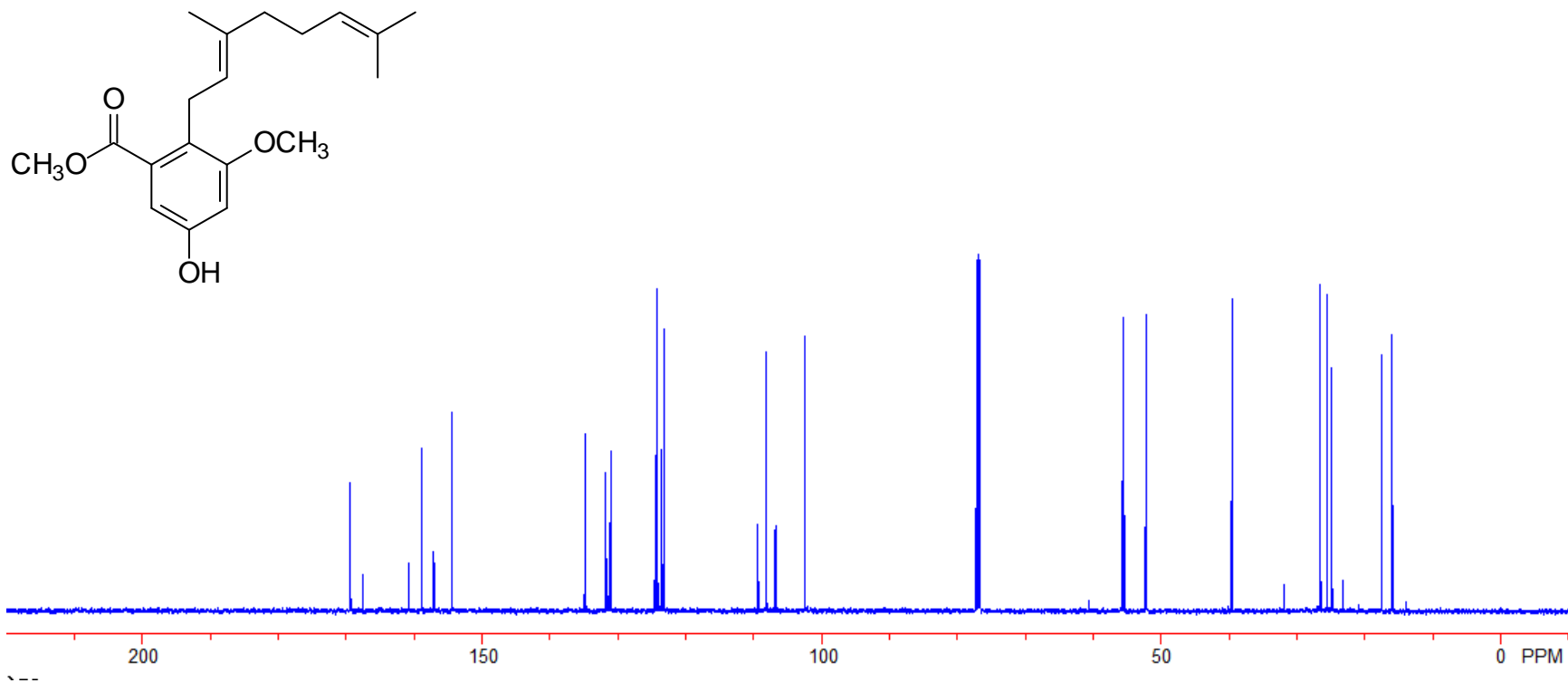


Figure A-70. ^{13}C NMR spectrum of compound **94**

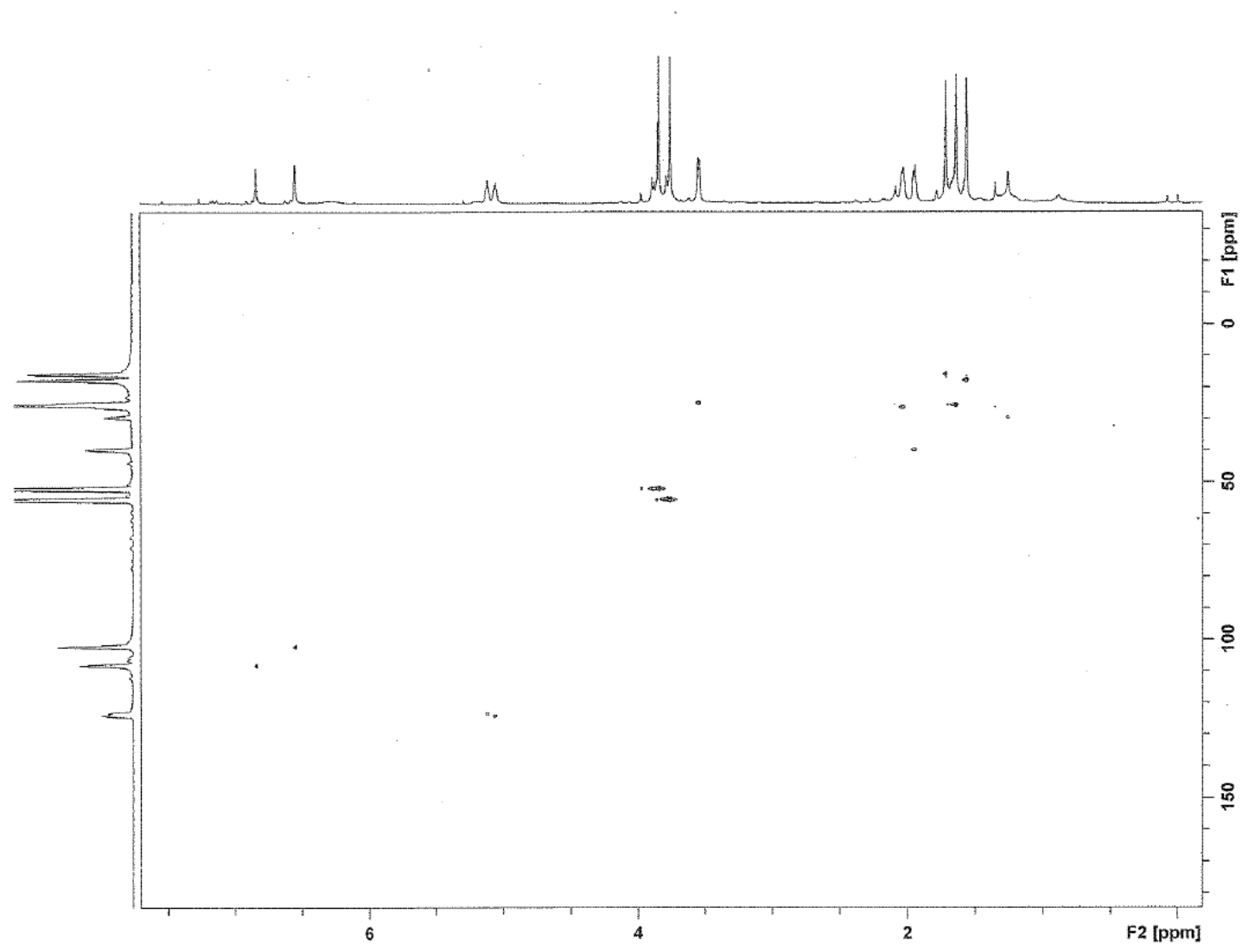


Figure A-71. HSQC spectrum of compound **94**

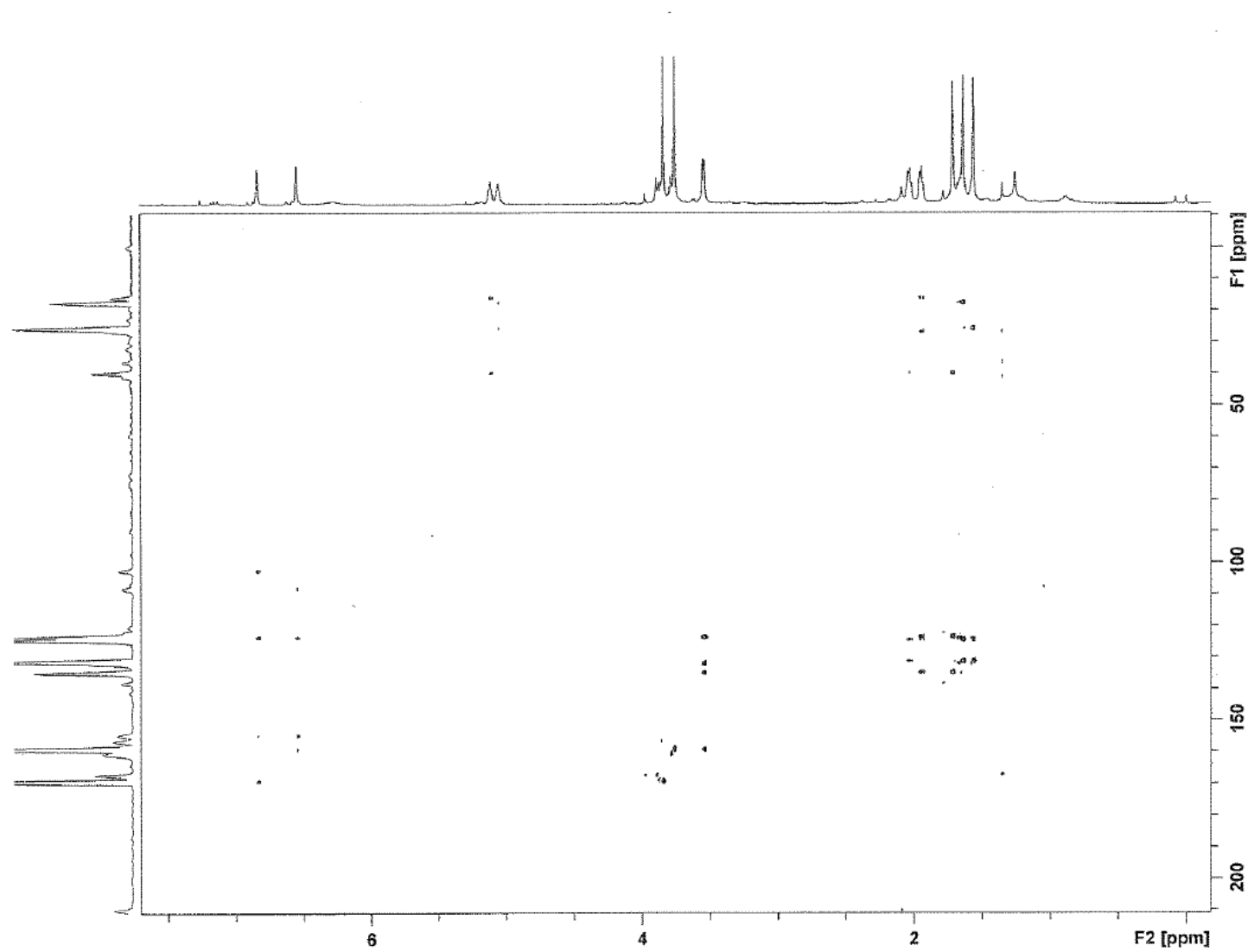


Figure A-72. HMBC spectrum of compound **94**

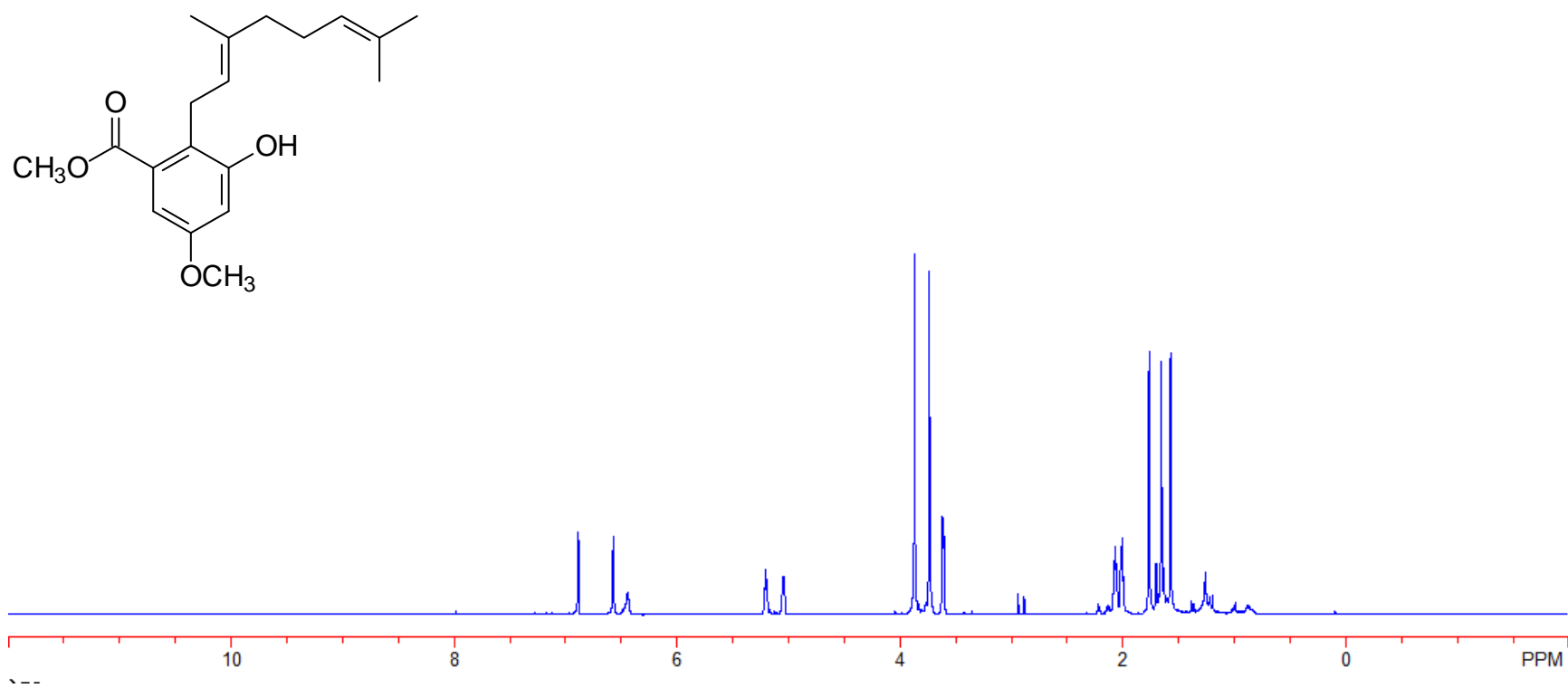


Figure A-73. ^1H NMR spectrum of compound **95**

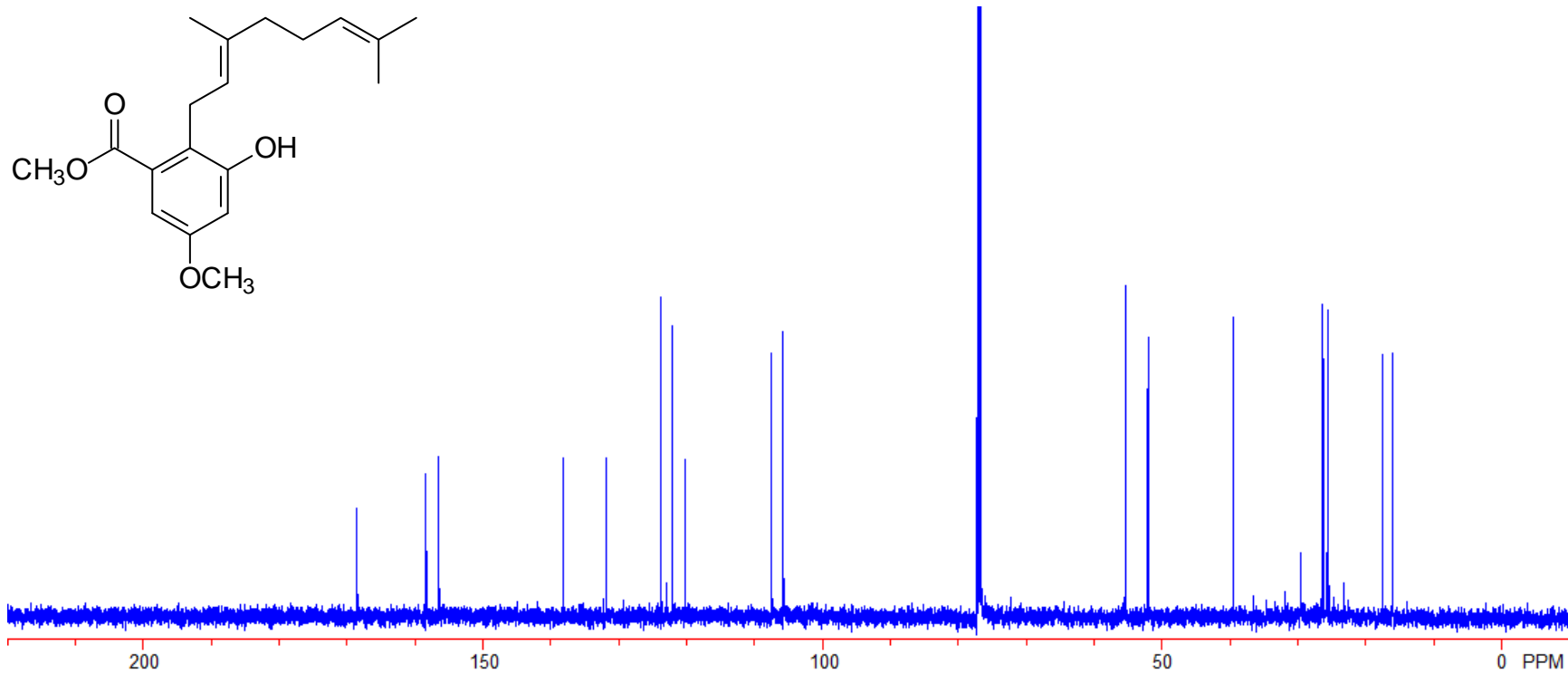


Figure A-74. ^{13}C NMR spectrum of compound **95**

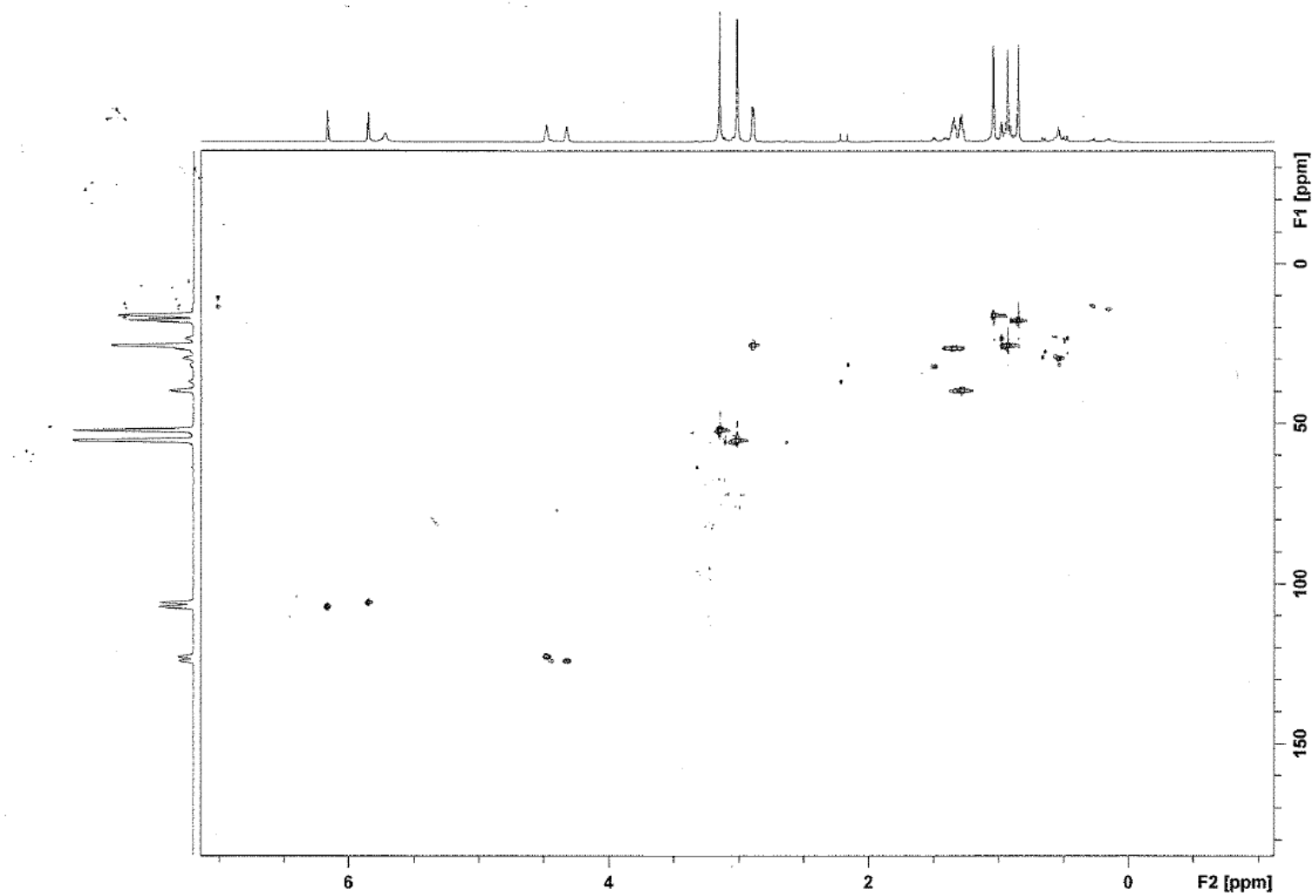


Figure A-75. HSQC spectrum of compound **95**

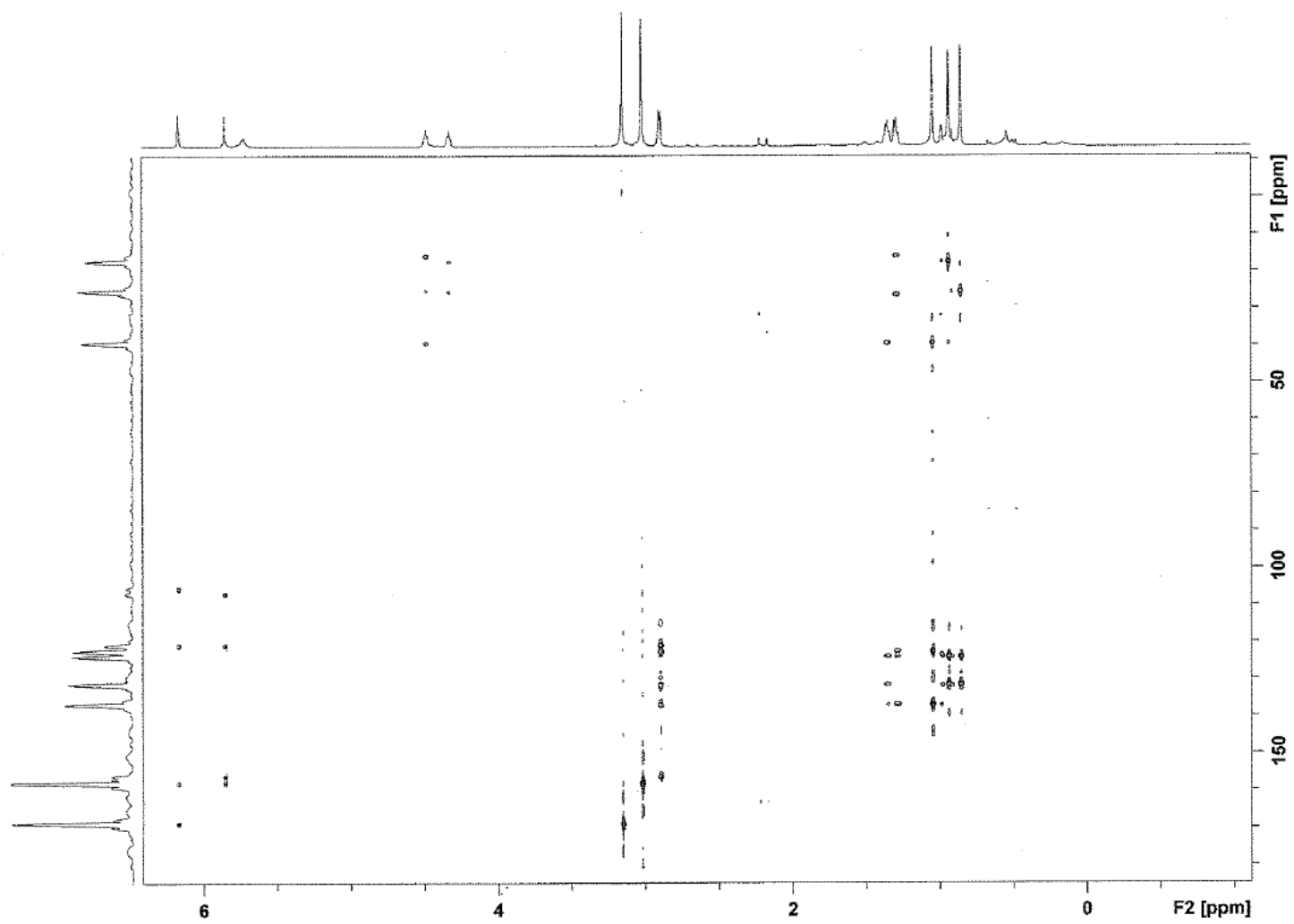


Figure A-76. HMBC spectrum of compound **95**

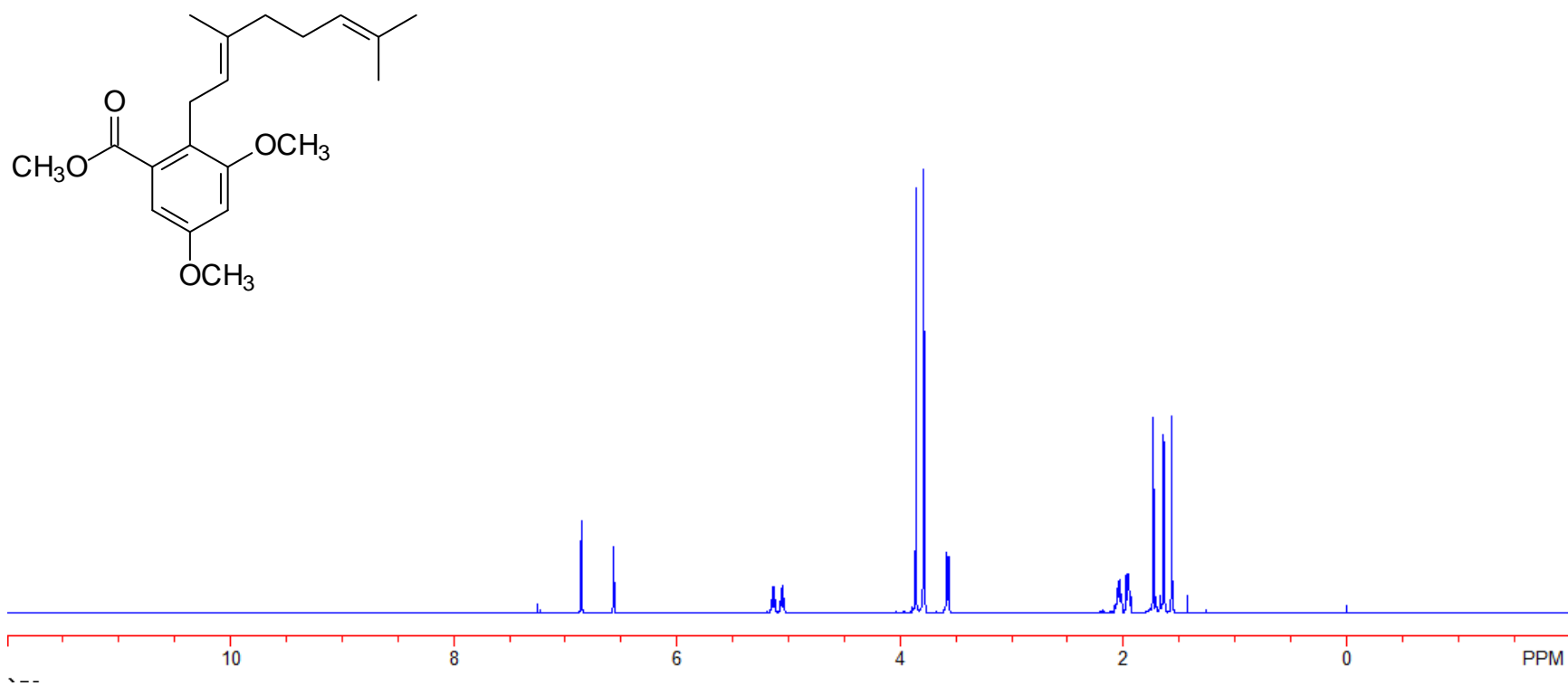


Figure A-77. ^1H NMR spectrum of compound **93**

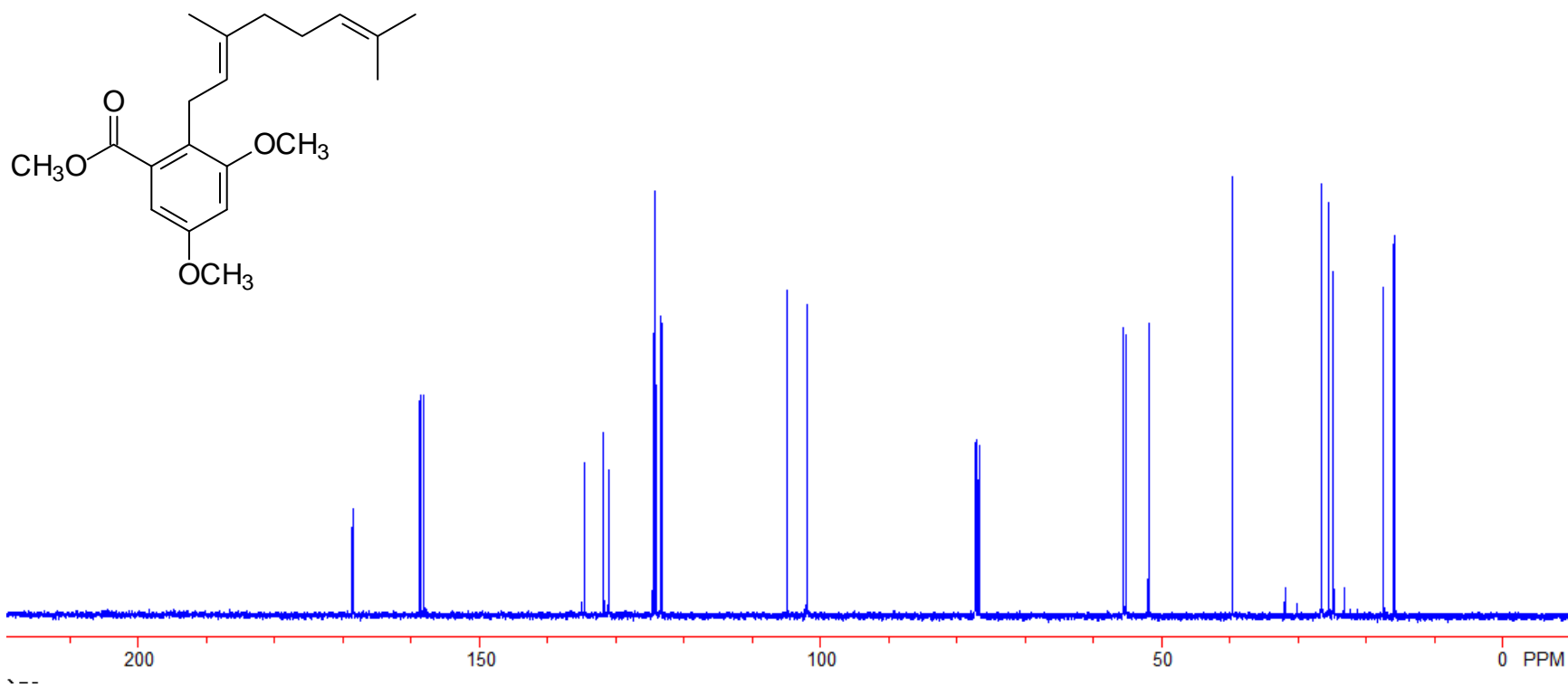


Figure A-78. ^{13}C NMR spectrum of compound **93**

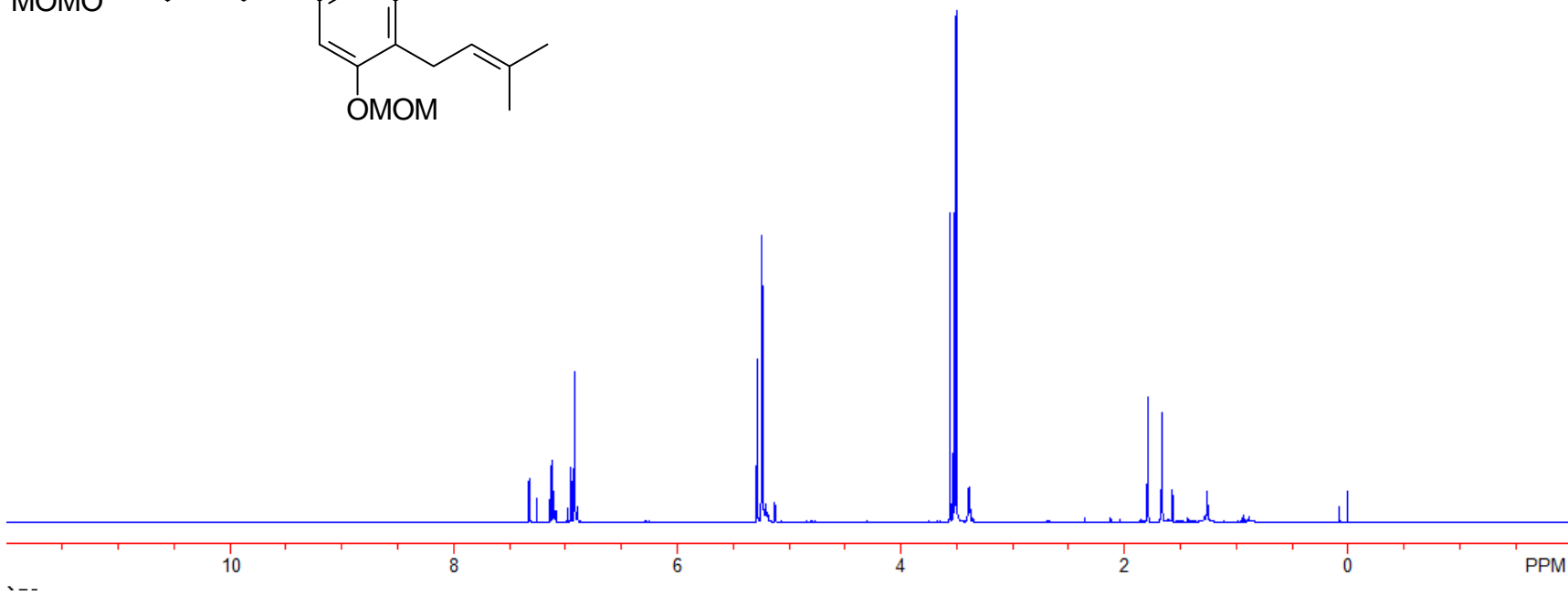
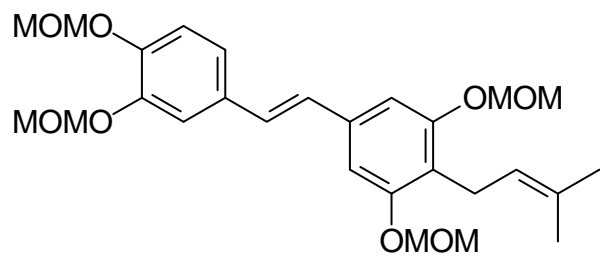


Figure A-79. ^1H NMR spectrum of compound **109**

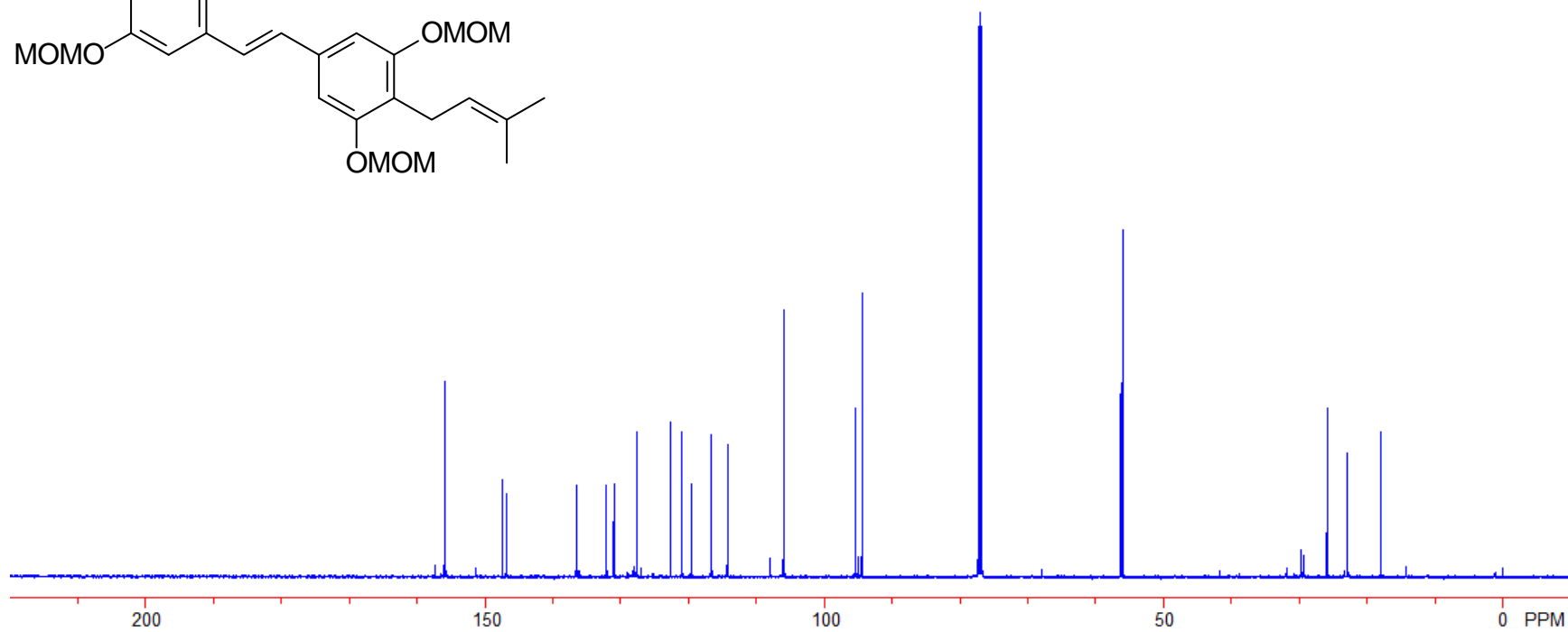
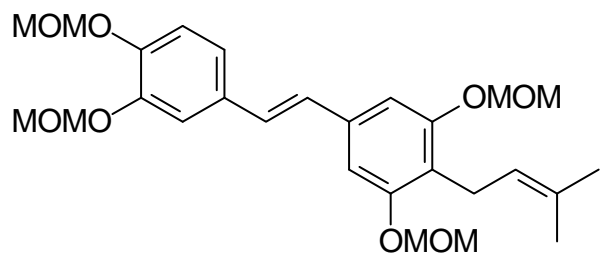


Figure A-80. ^{13}C NMR spectrum of compound **109**

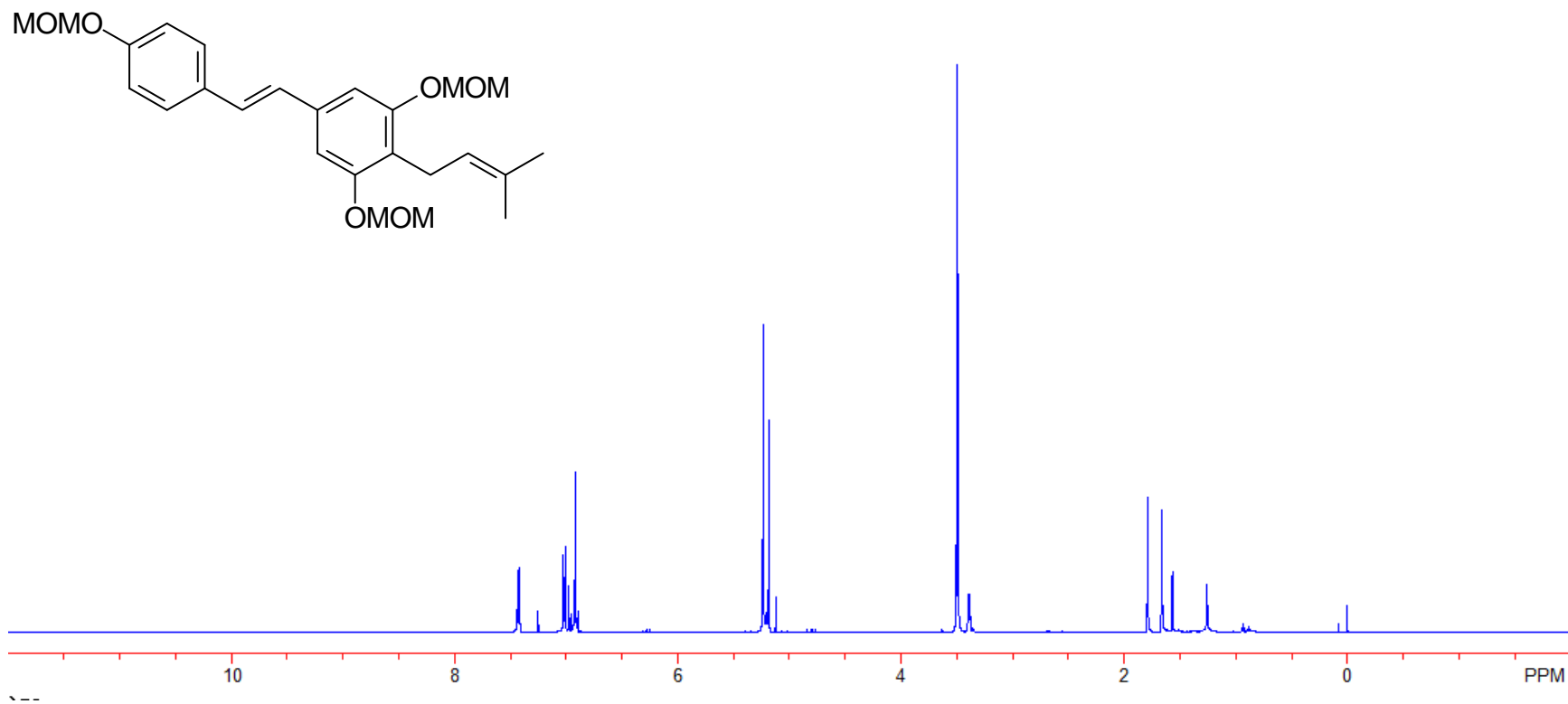


Figure A-81. ^1H NMR spectrum of compound **112**

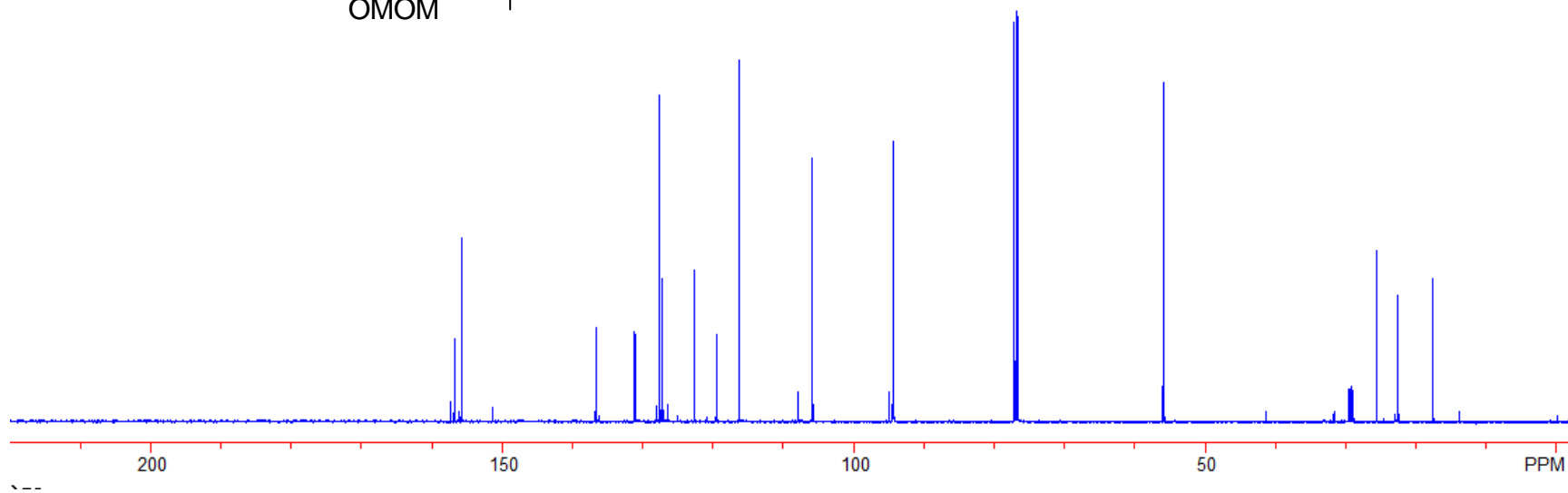
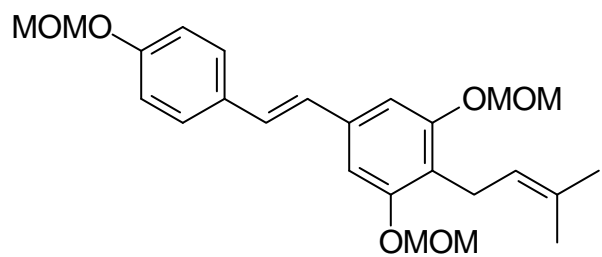


Figure A-82. ^{13}C NMR spectrum of compound **112**

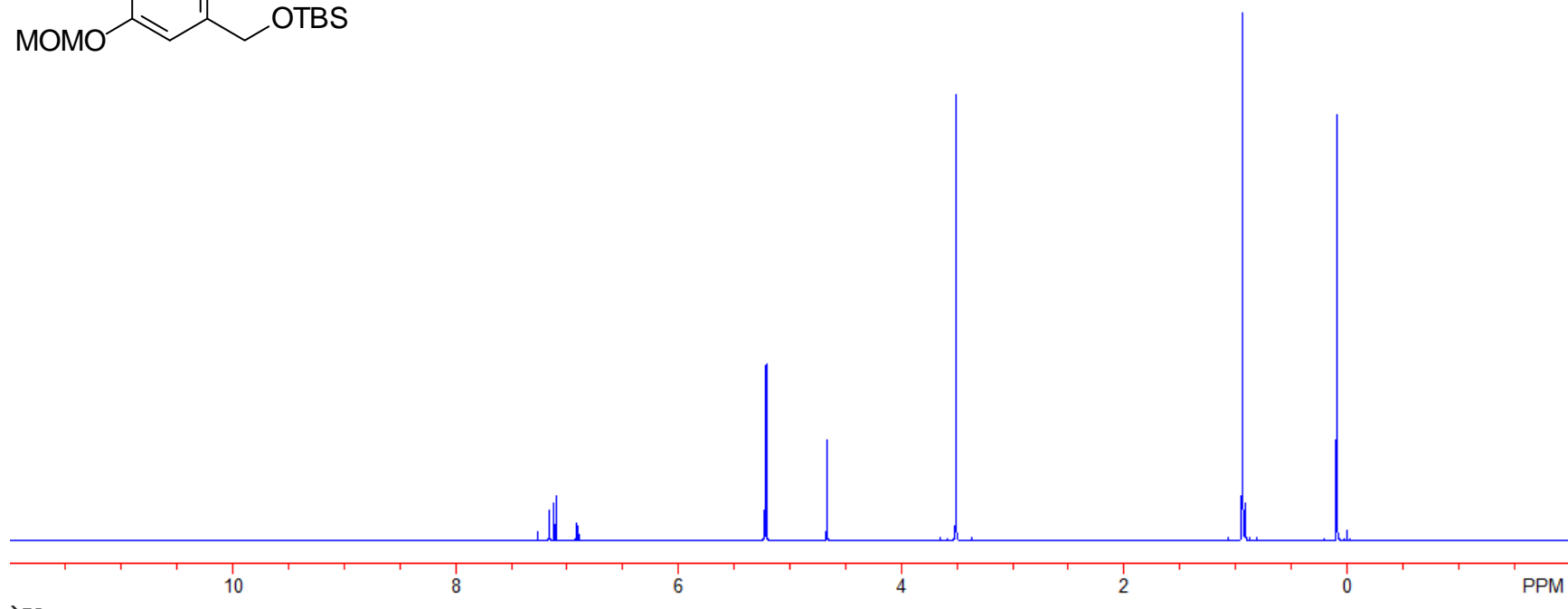
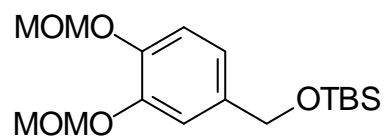


Figure A-83. ¹H NMR spectrum of compound **128**

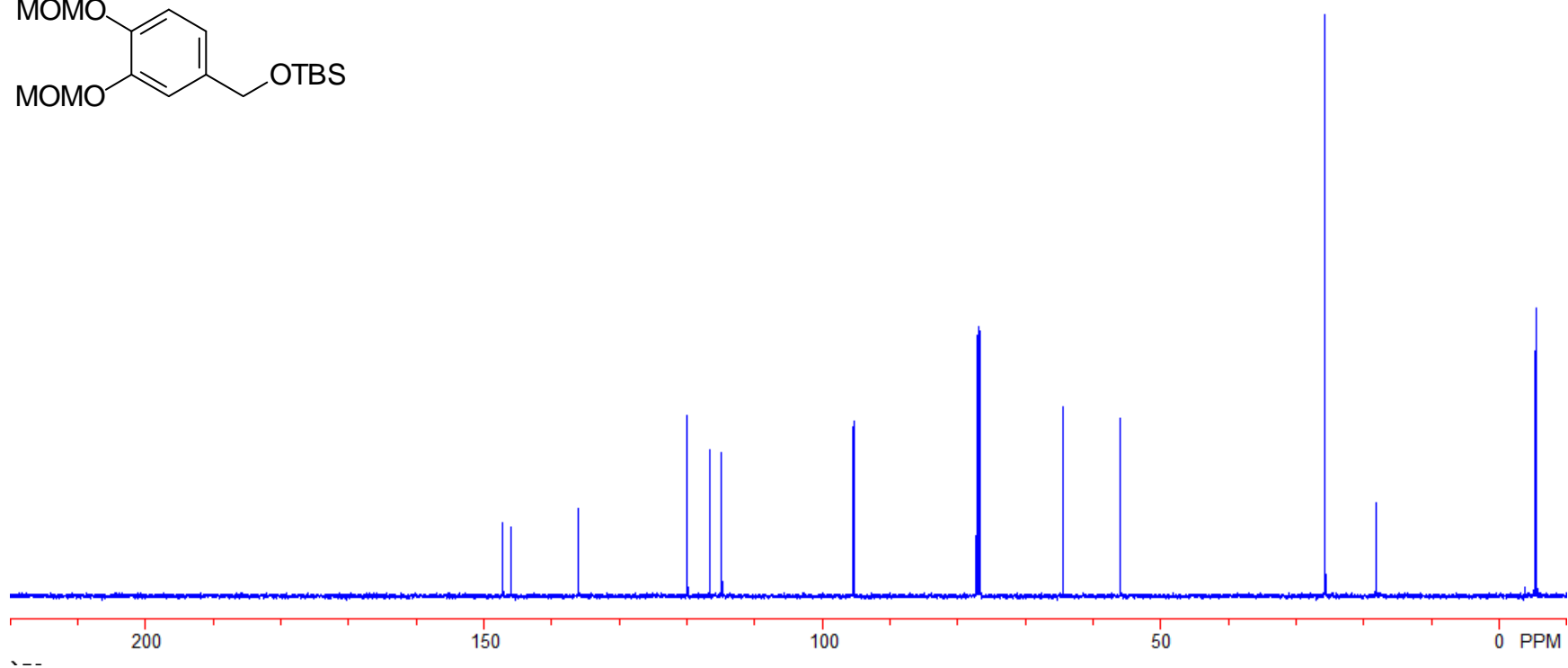
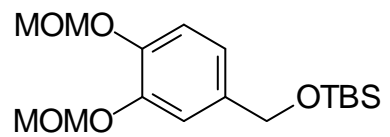


Figure A-84. ^{13}C NMR spectrum of compound **128**

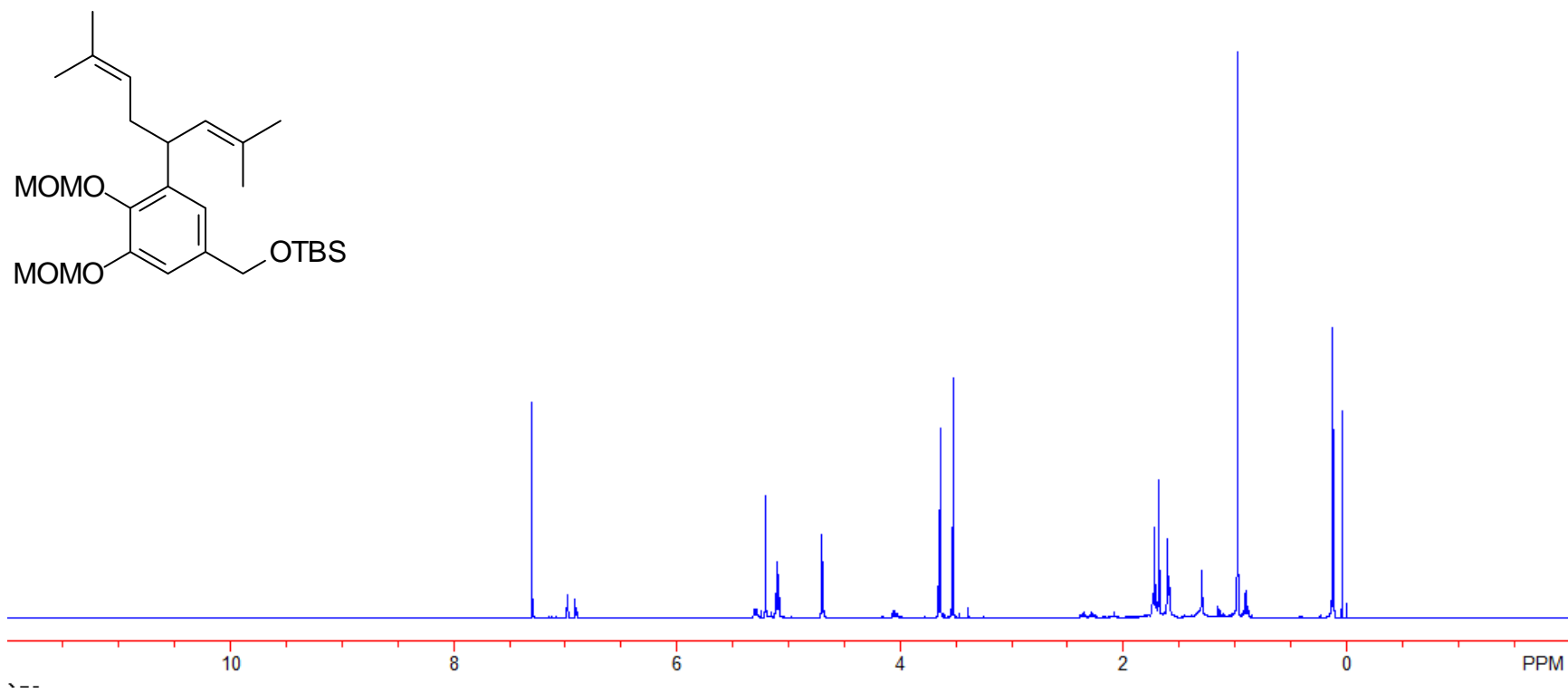


Figure A-85. ¹H NMR spectrum of compound **129**

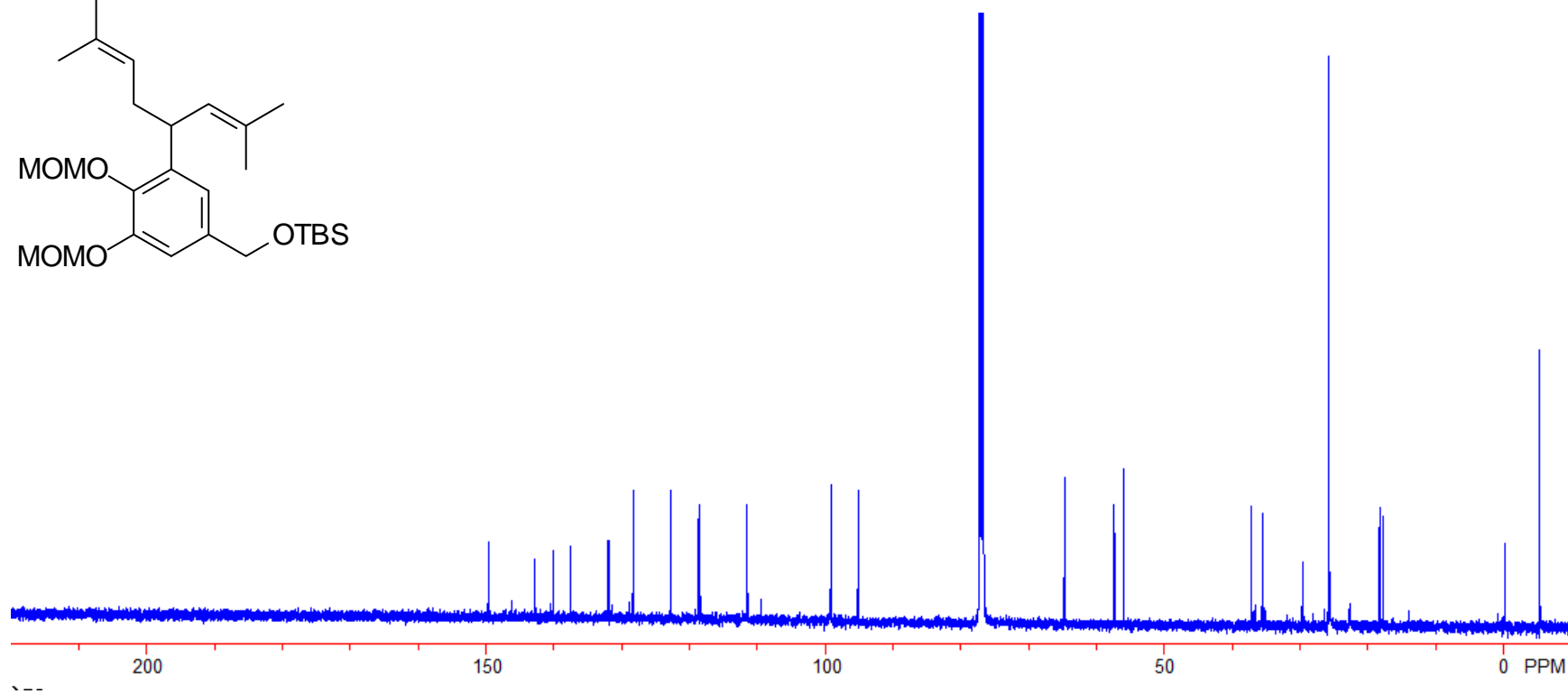
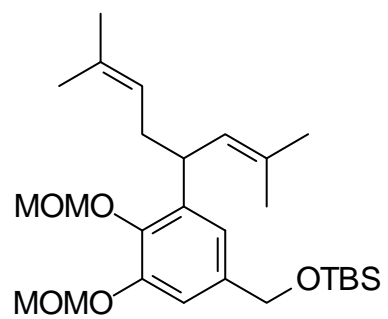


Figure A-86. ^{13}C NMR spectrum of compound 129

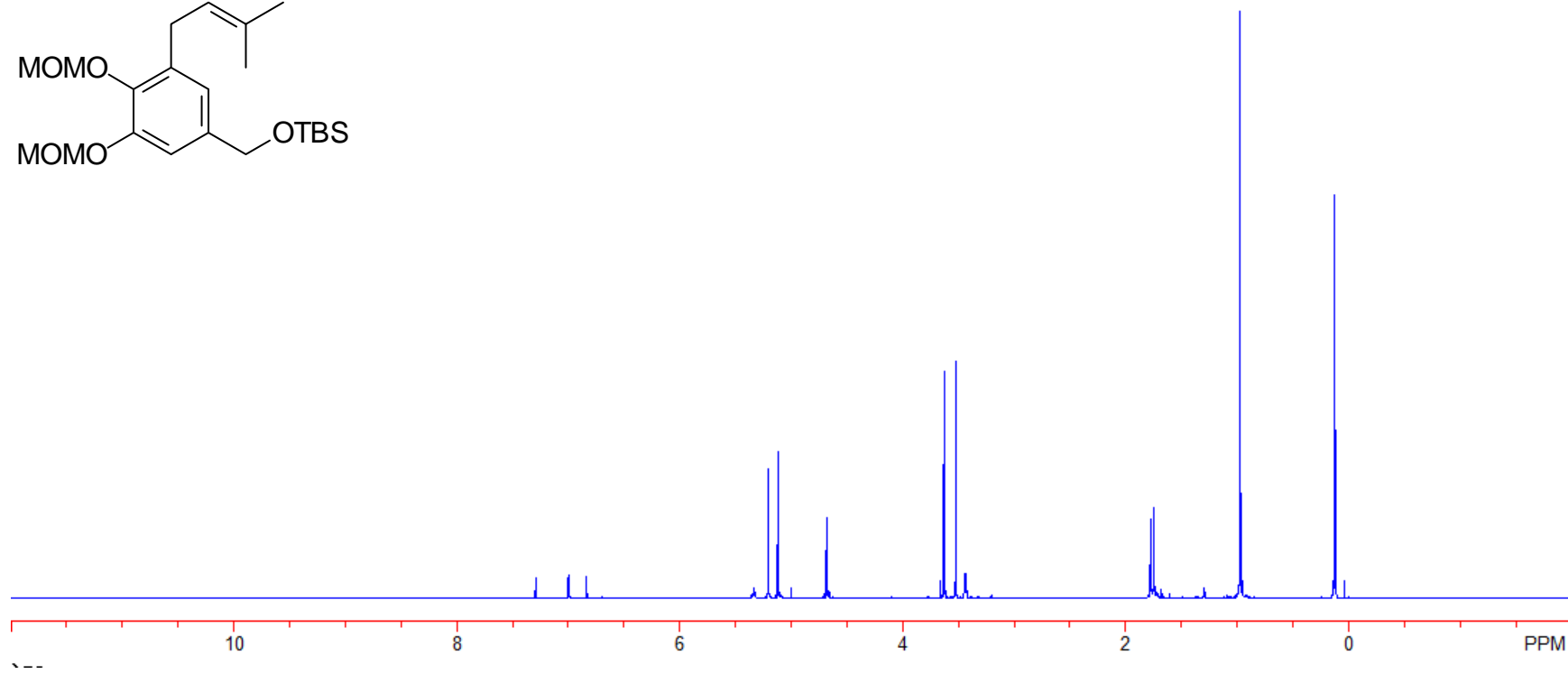
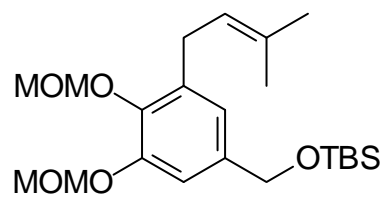


Figure A-87. ^1H NMR spectrum of compound **130**

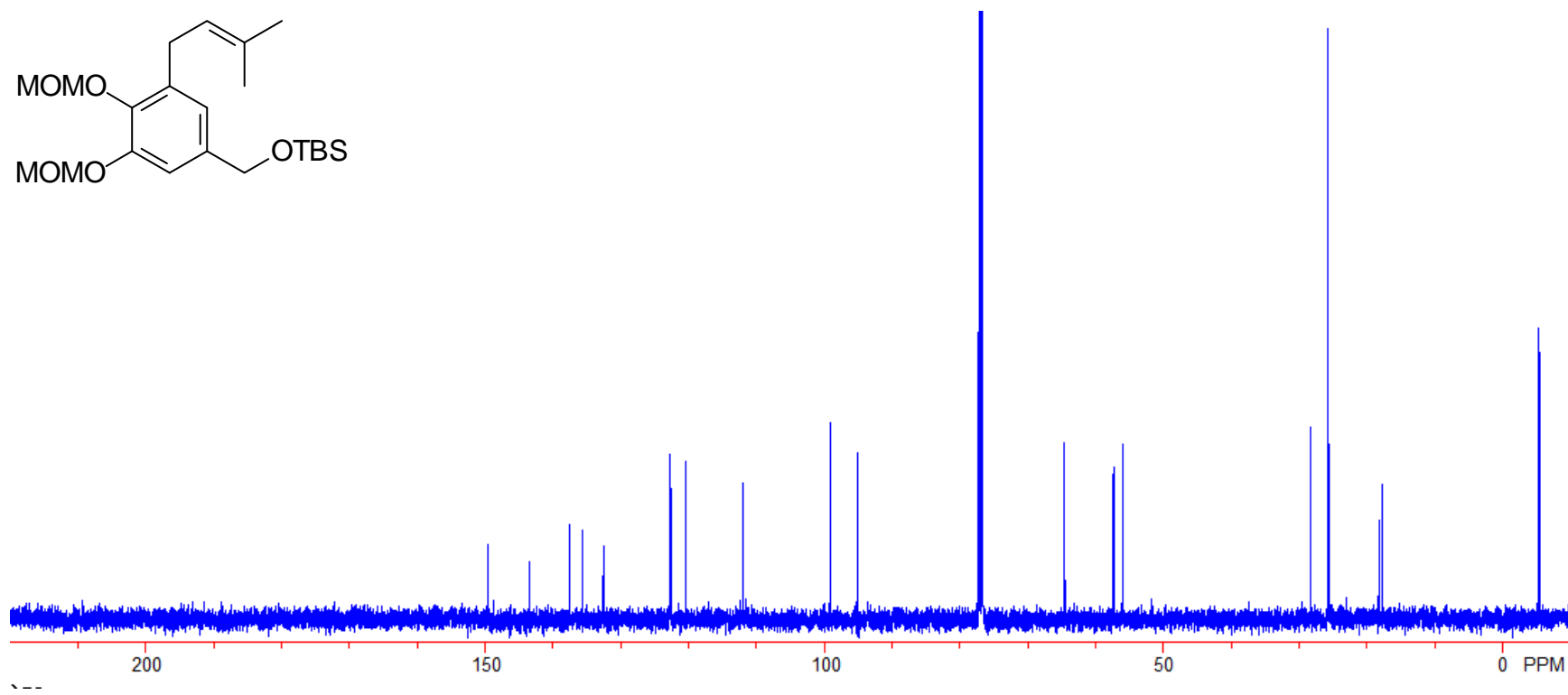
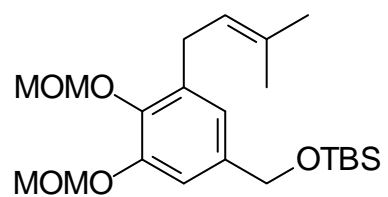


Figure A-88. ^{13}C NMR spectrum of compound **130**

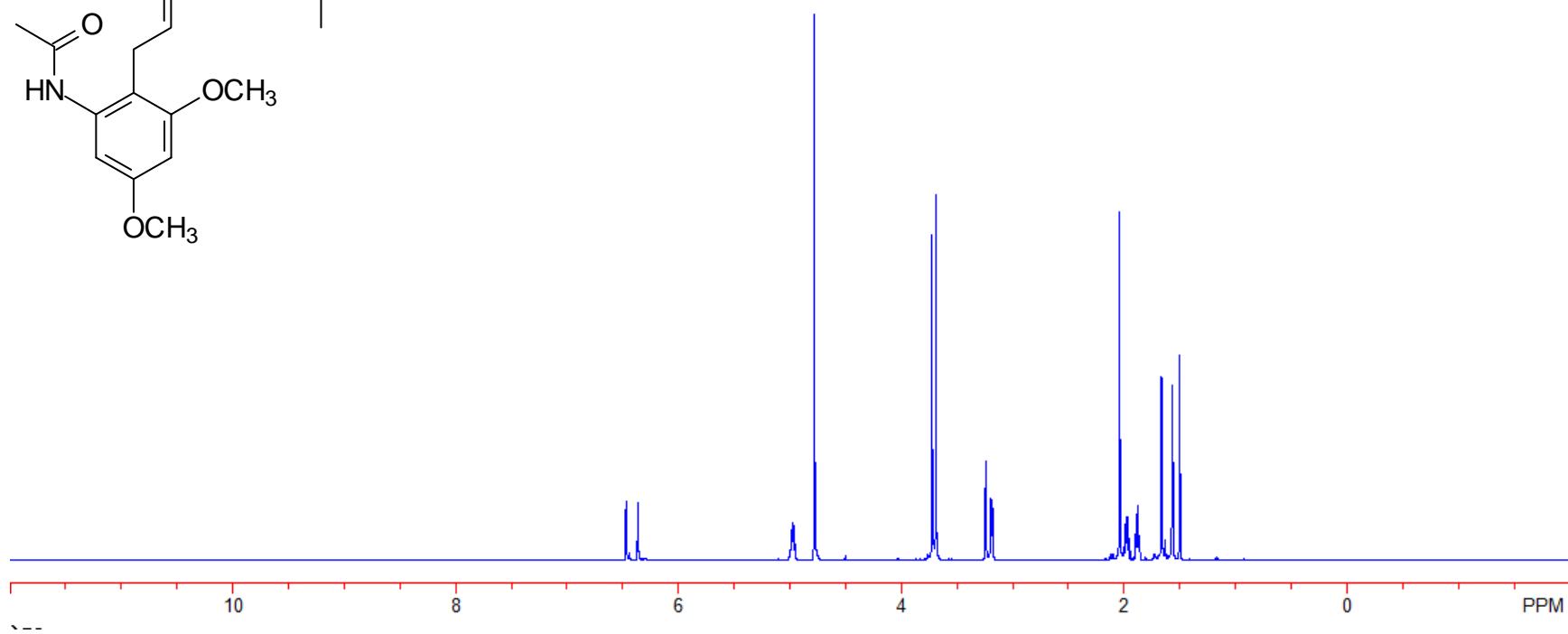
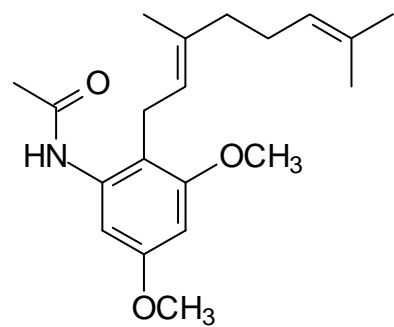


Figure A-89. ¹H NMR spectrum of compound **138**

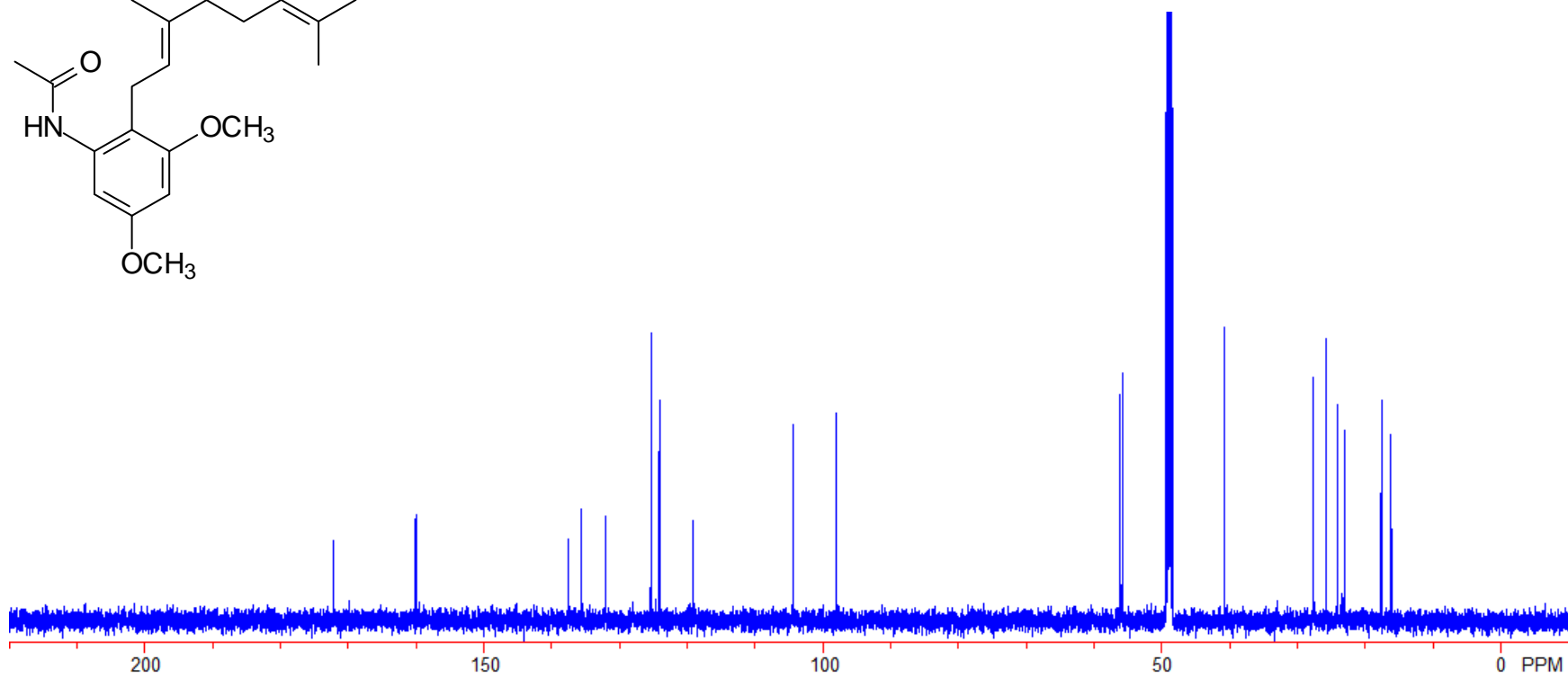
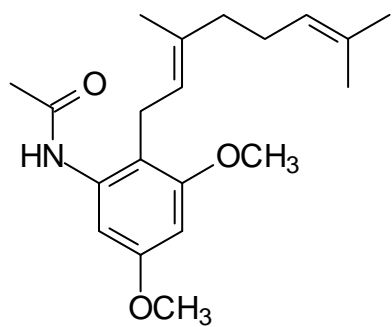


Figure A-90. ¹³C NMR spectrum of compound 138

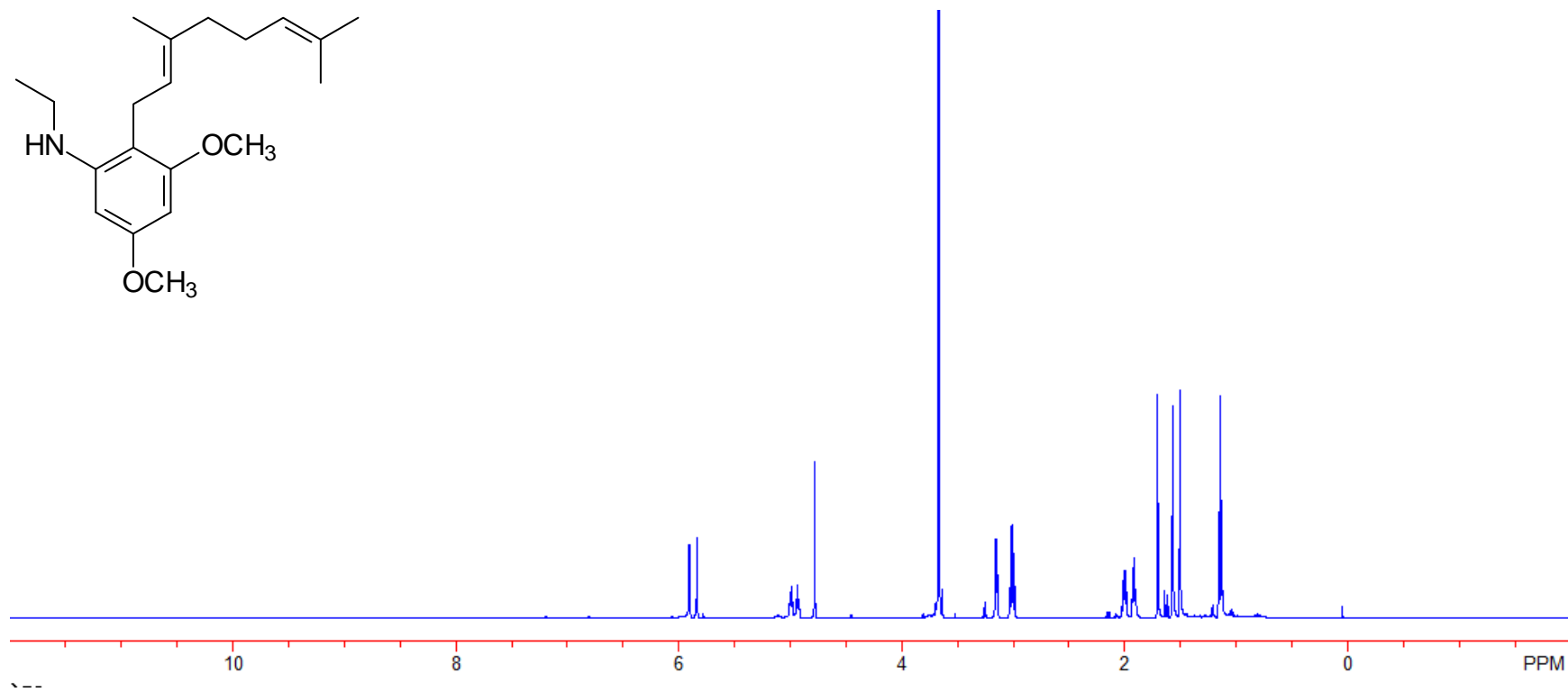
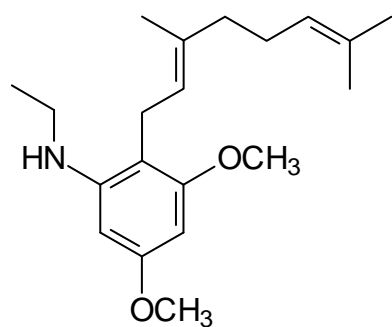


Figure A-91. ¹H NMR spectrum of compound 139

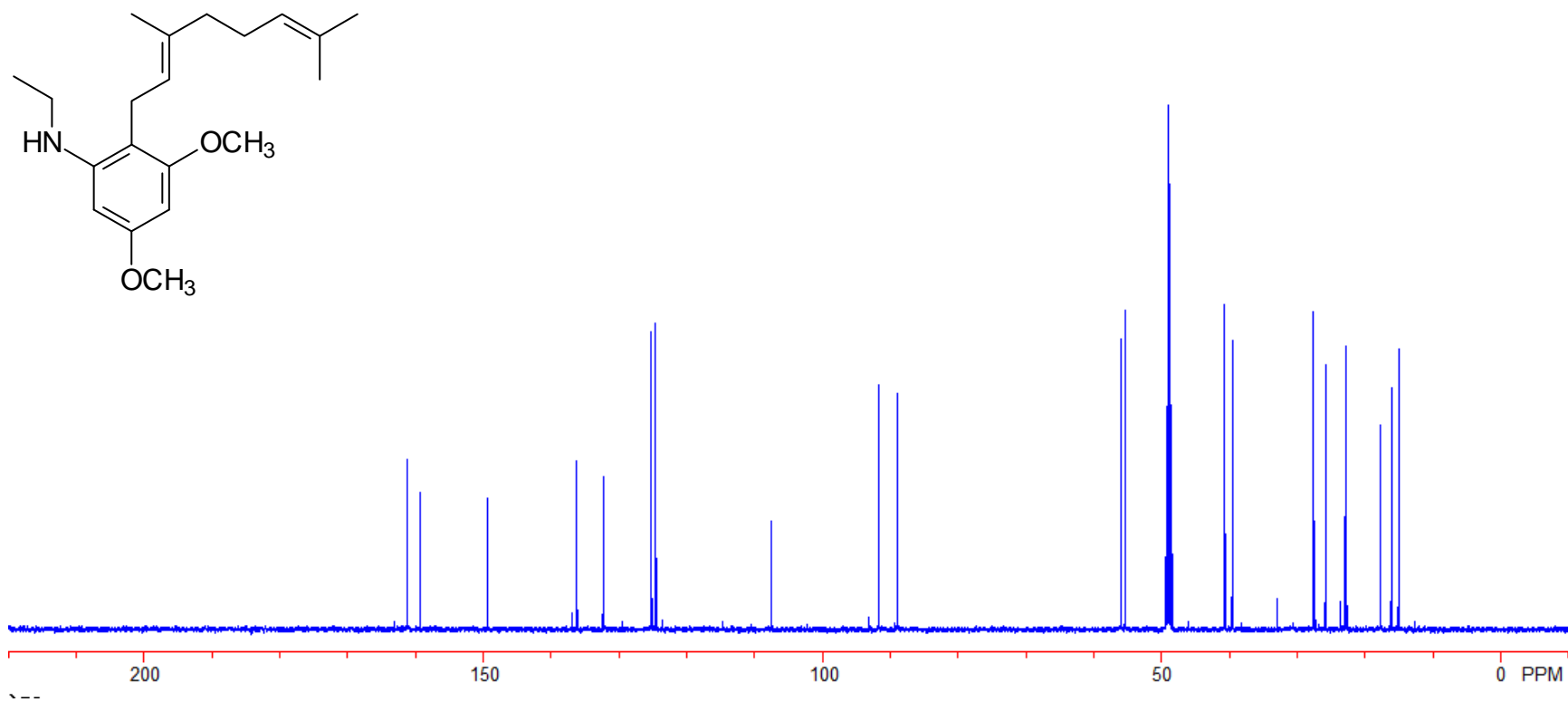


Figure A-92. ¹³C NMR spectrum of compound 139

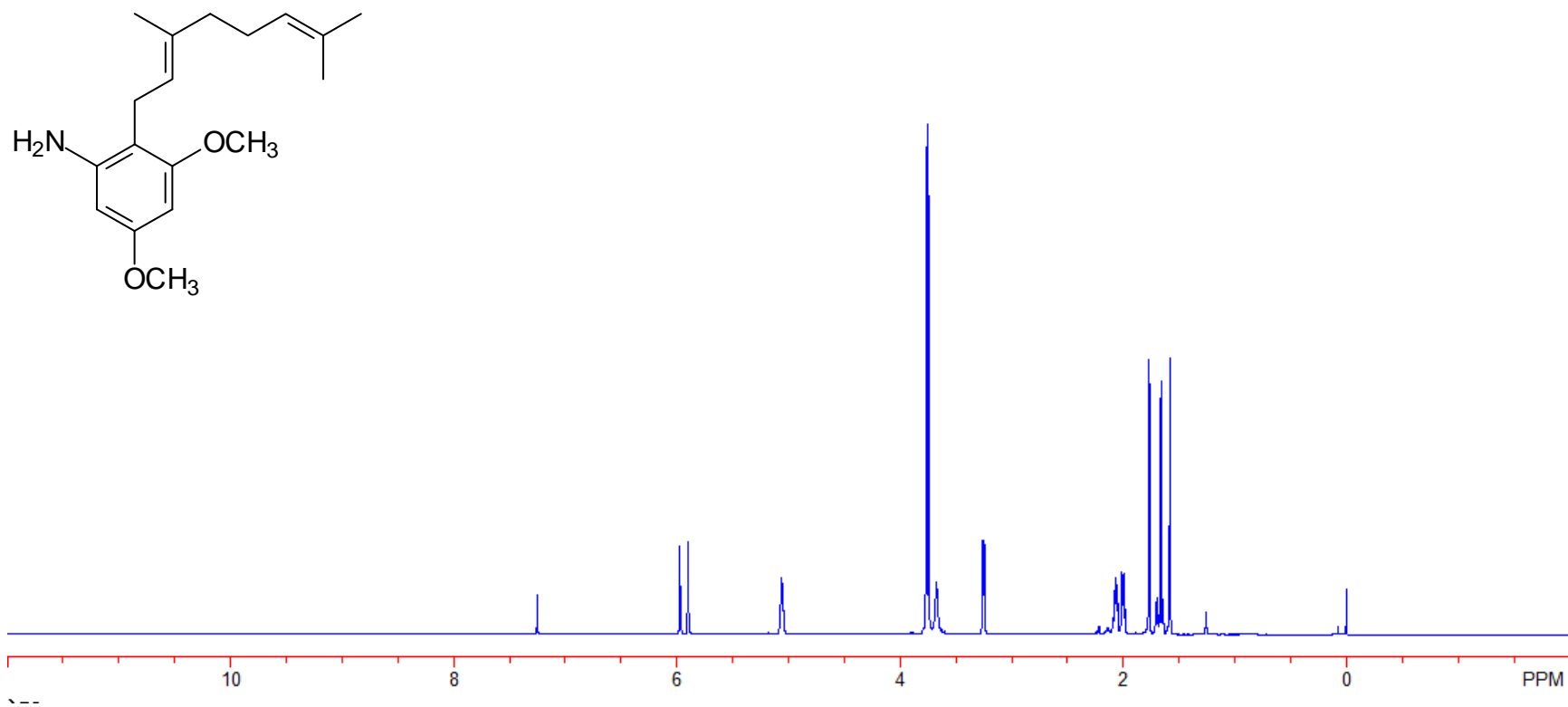


Figure A-93. ¹H NMR spectrum of compound **140**

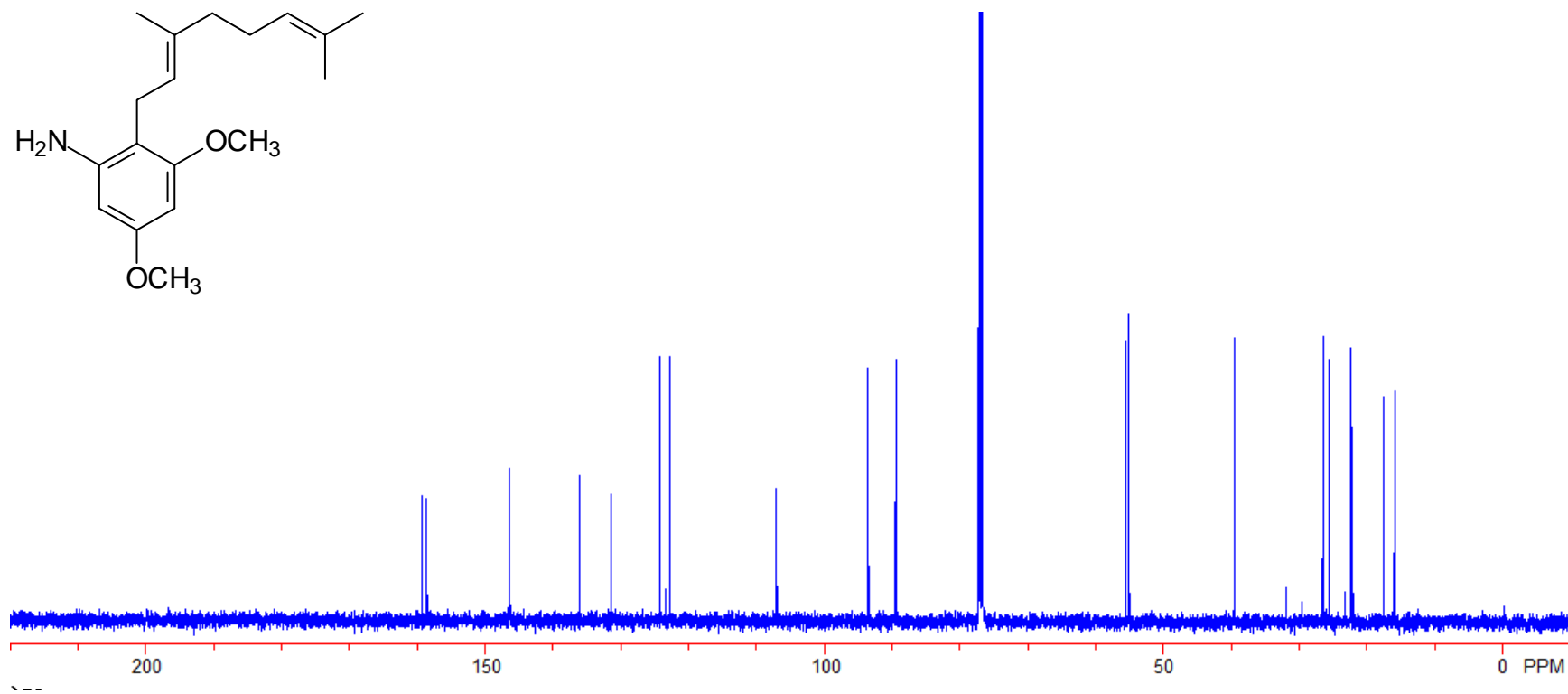
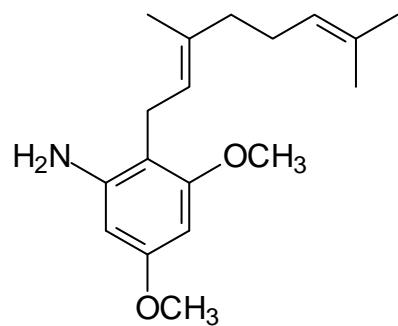


Figure A-94. ¹³C NMR spectrum of compound 140

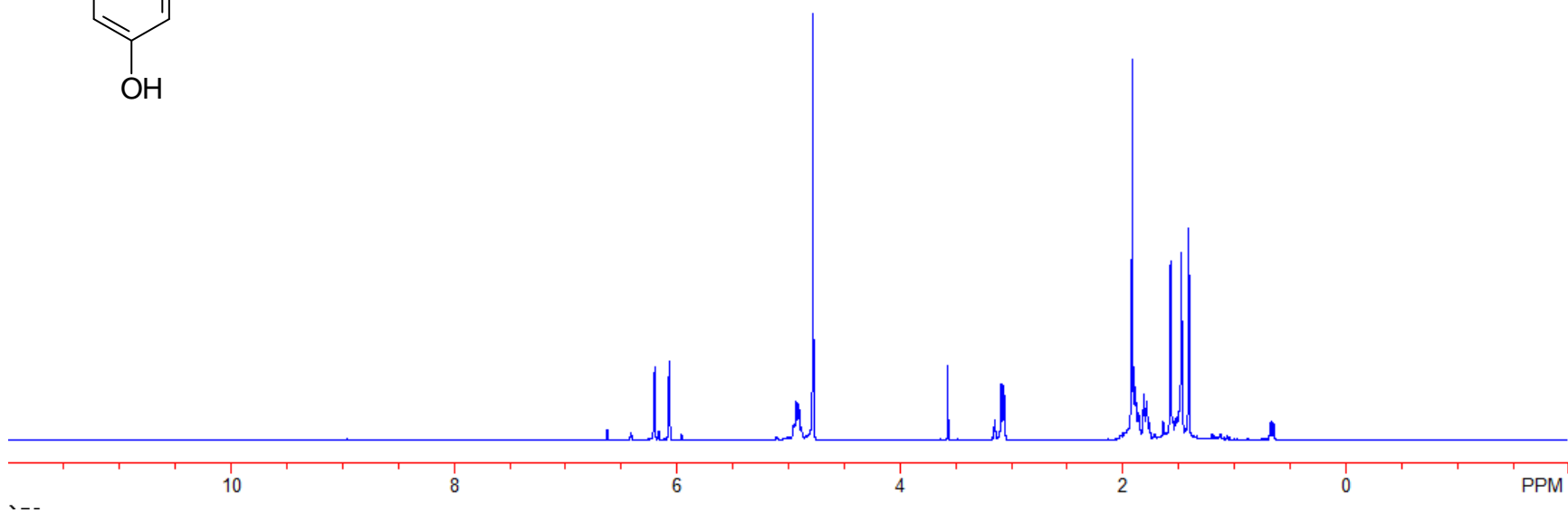
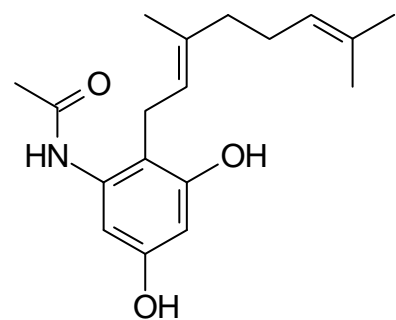


Figure A-95. ¹H NMR spectrum of compound **142**

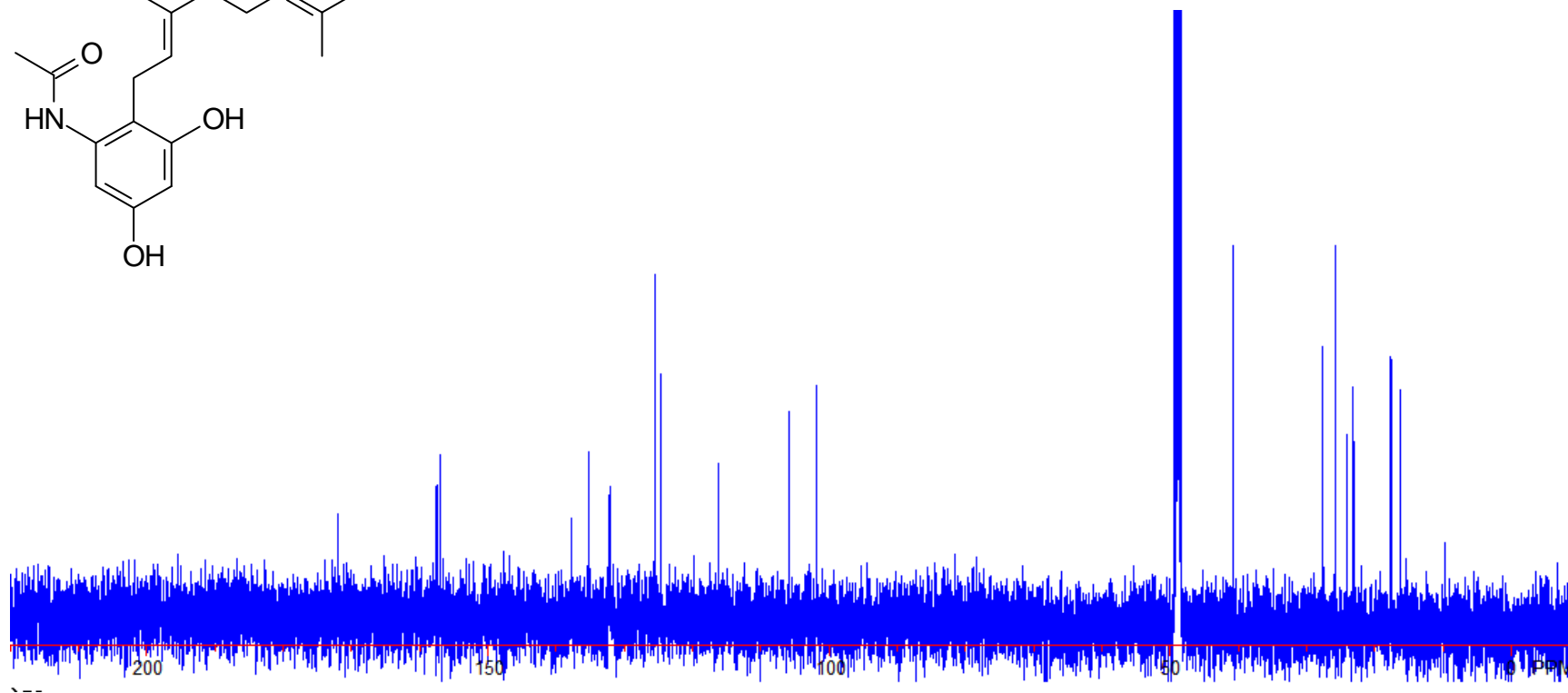
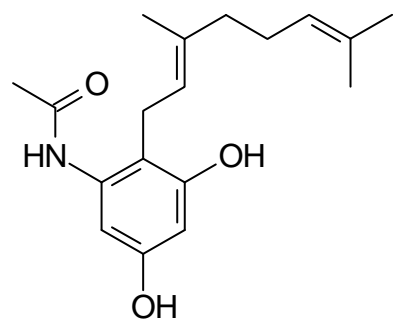


Figure A-96. ^{13}C NMR spectrum of compound **142**

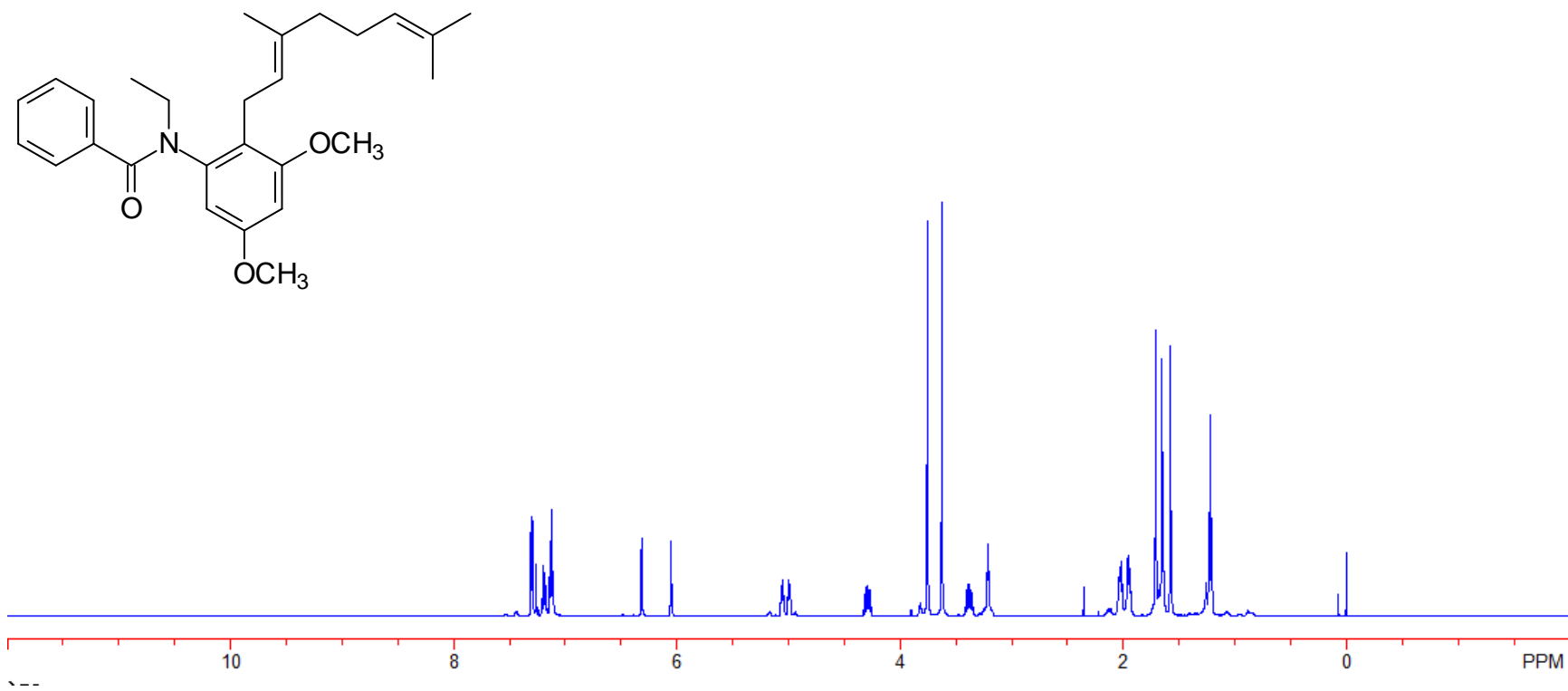


Figure A-97. ^1H NMR spectrum of compound **145**

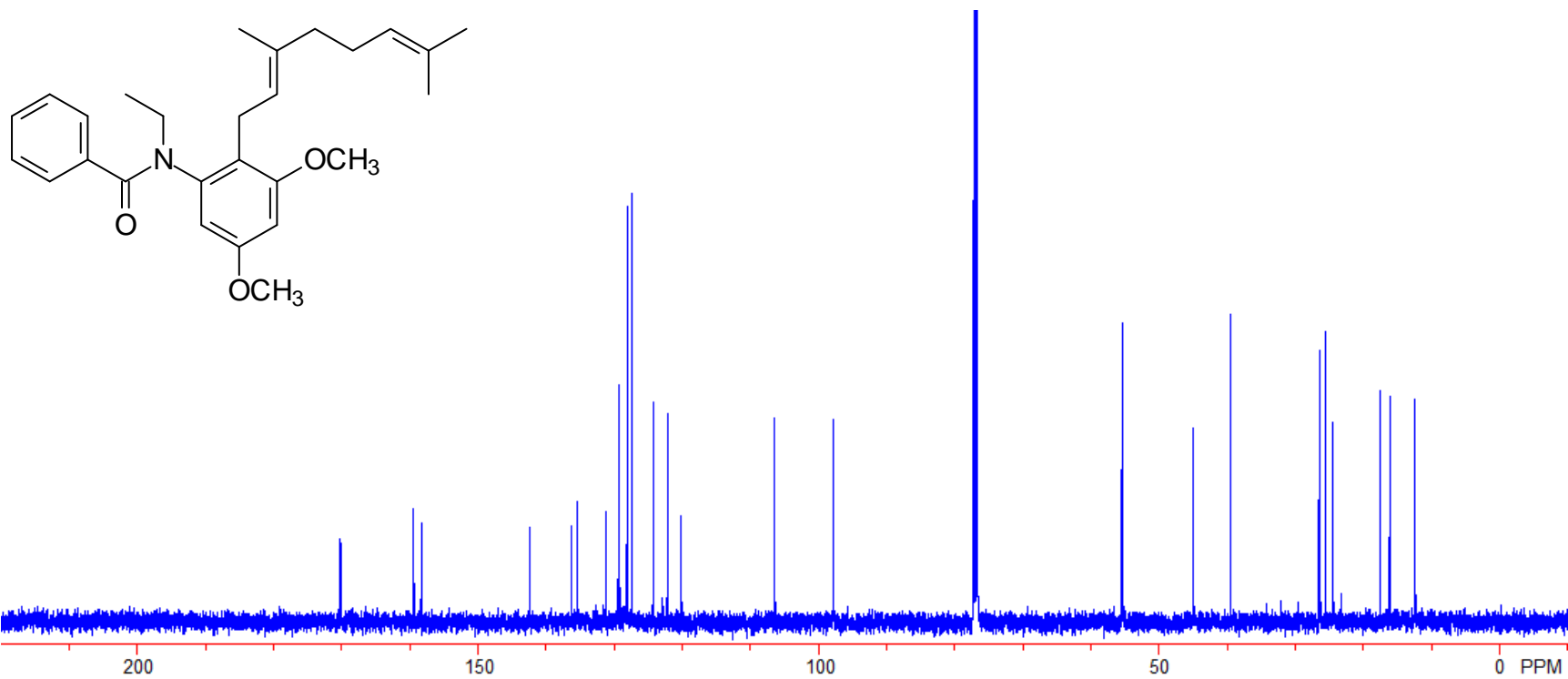


Figure A-98. ¹³C NMR spectrum of compound 145

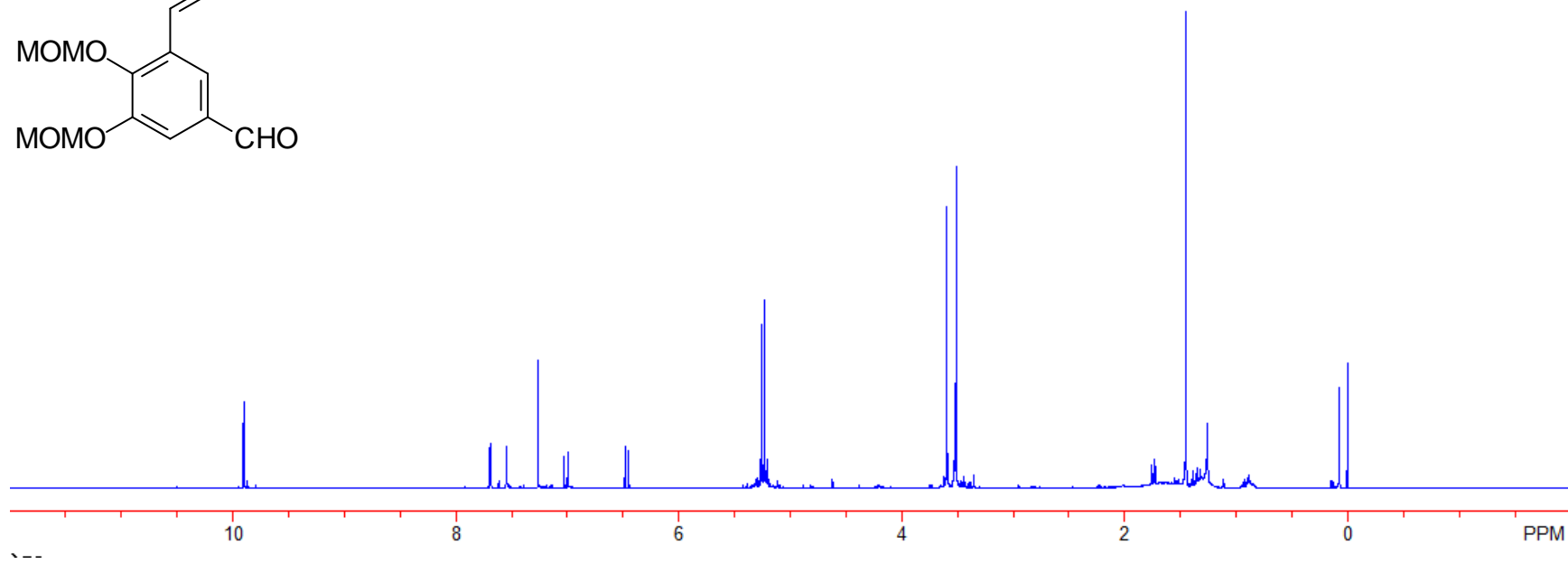
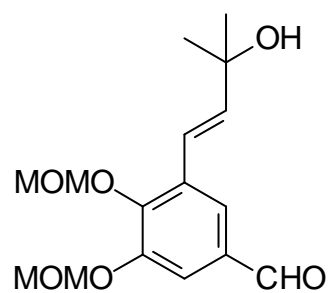


Figure A-99. ¹H NMR spectrum of compound **150**

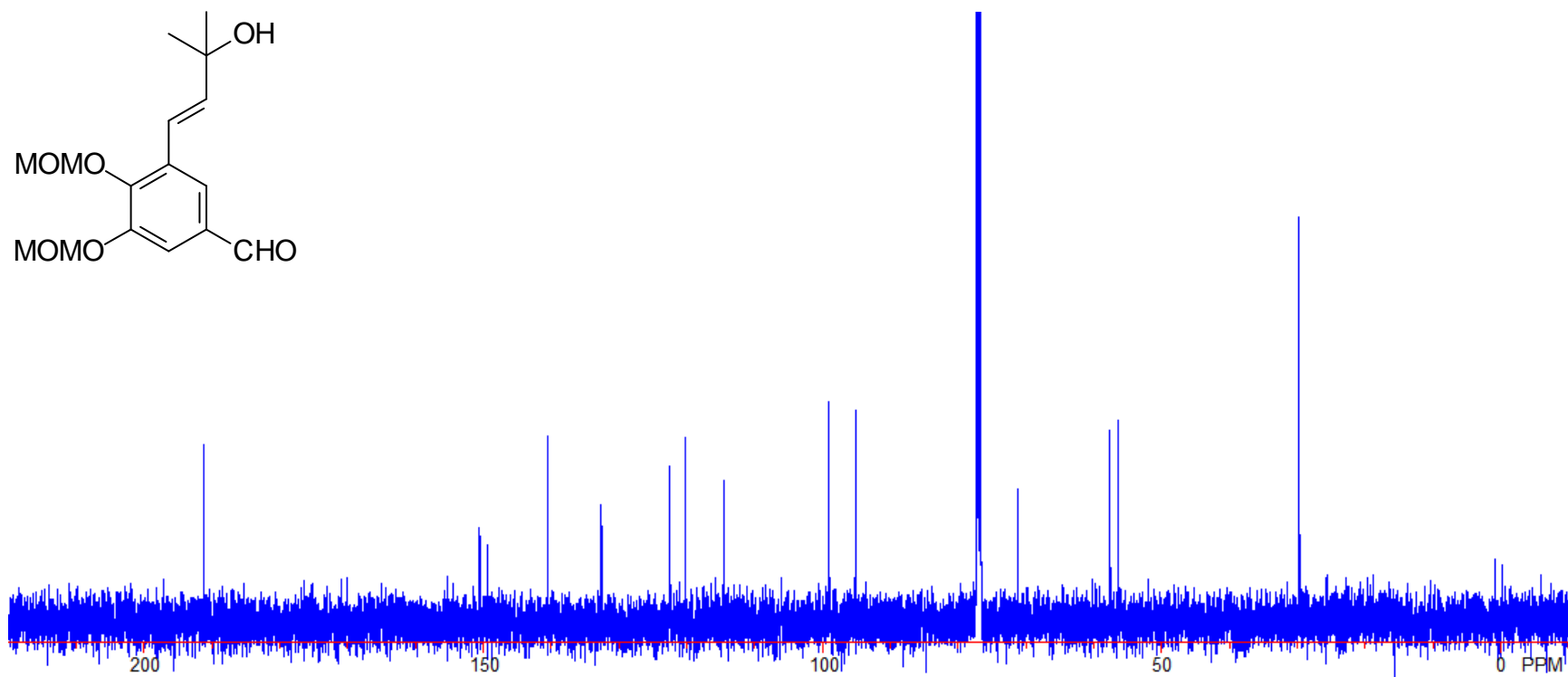
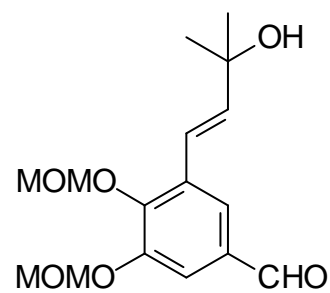


Figure A-100. ^{13}C NMR spectrum of compound **150**

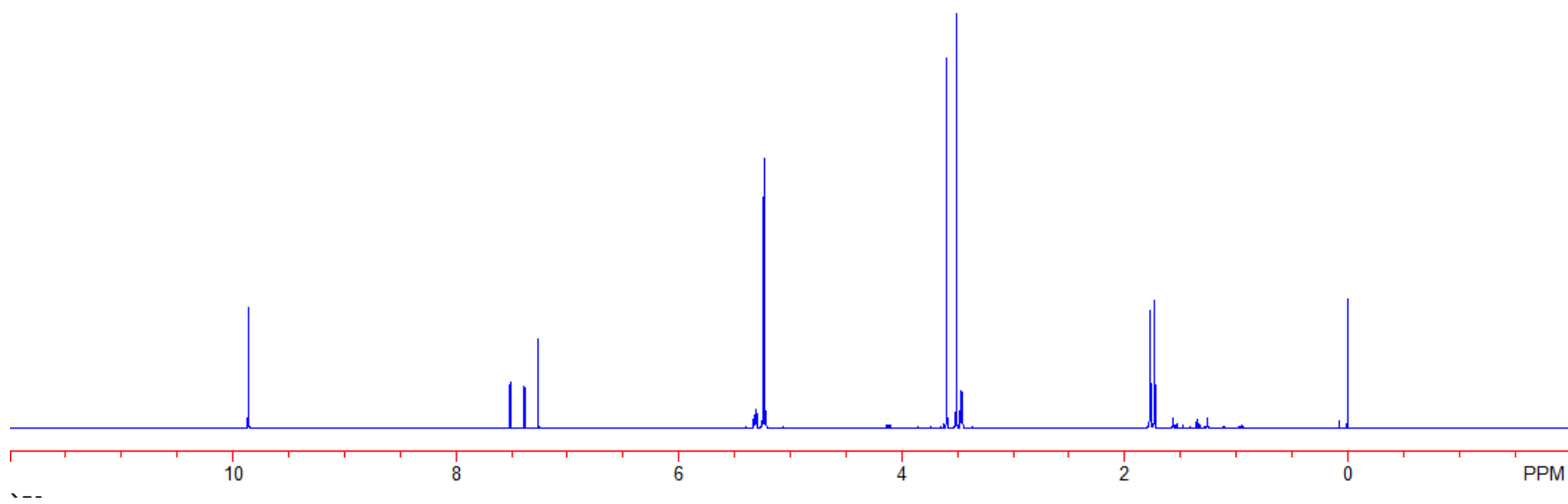
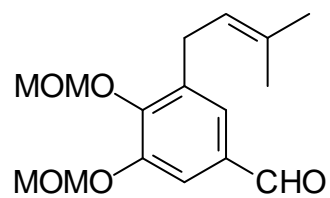


Figure A-101. ^1H NMR spectrum of compound **151**

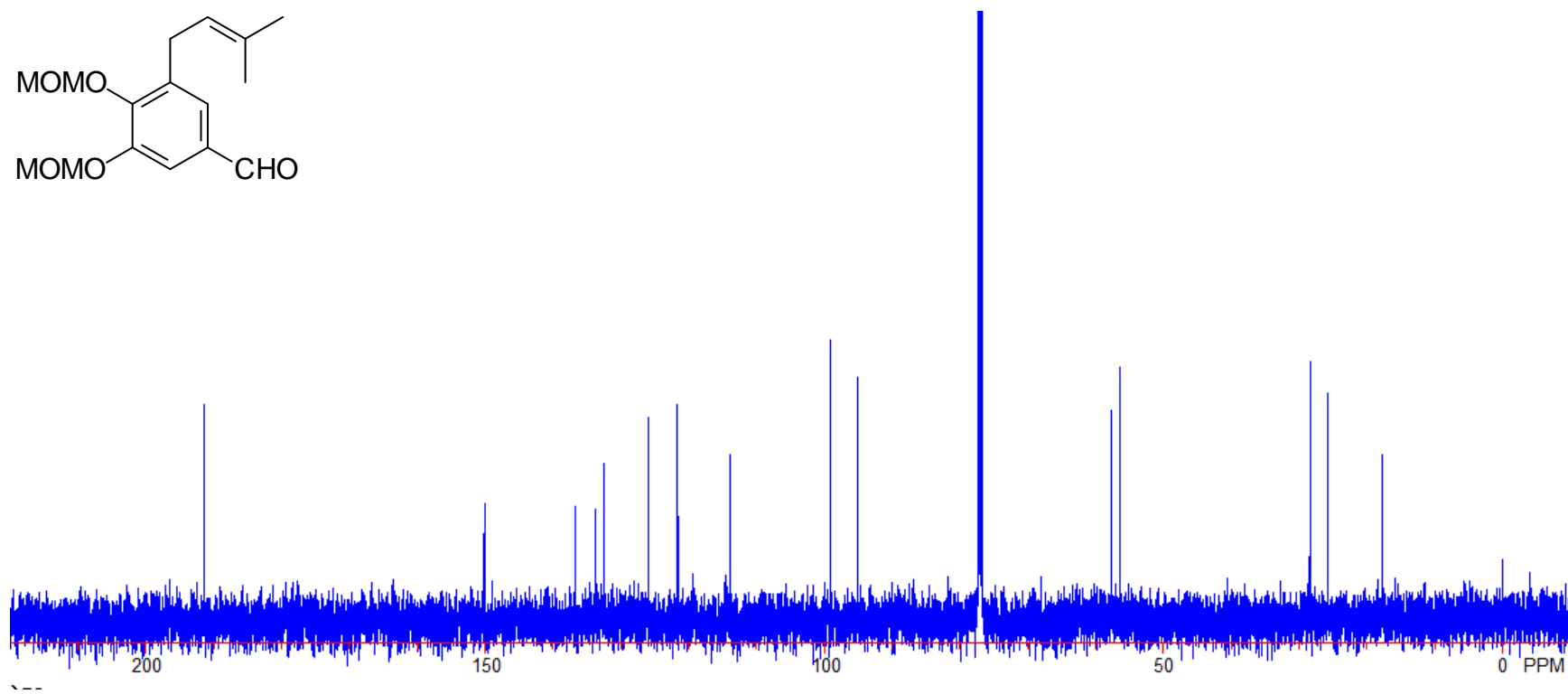
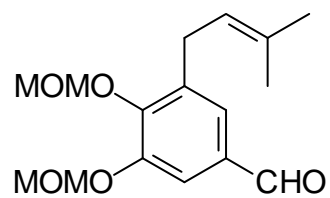


Figure A-102. ^{13}C NMR spectrum of compound **151**

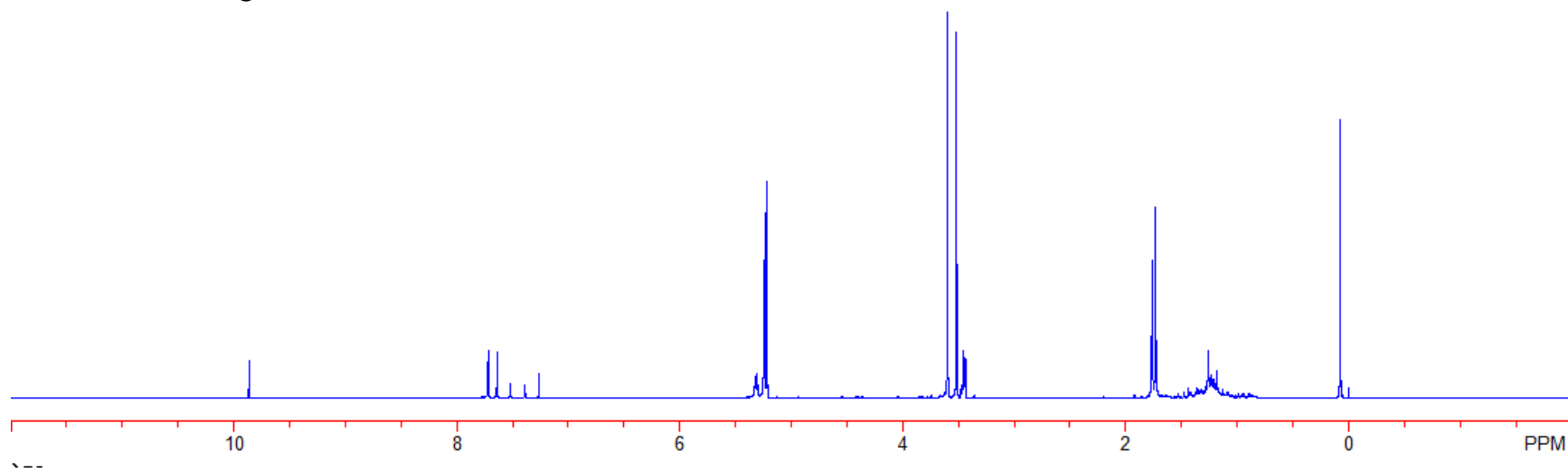
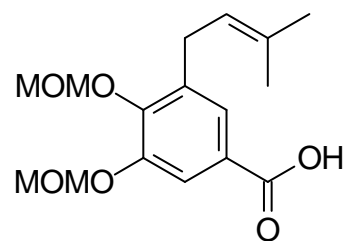


Figure A-103. ¹H NMR spectrum of compound **149**

Please note, it has been taken into account there is a 3.3:1 ratio of compound **149** to aldehyde **151**.

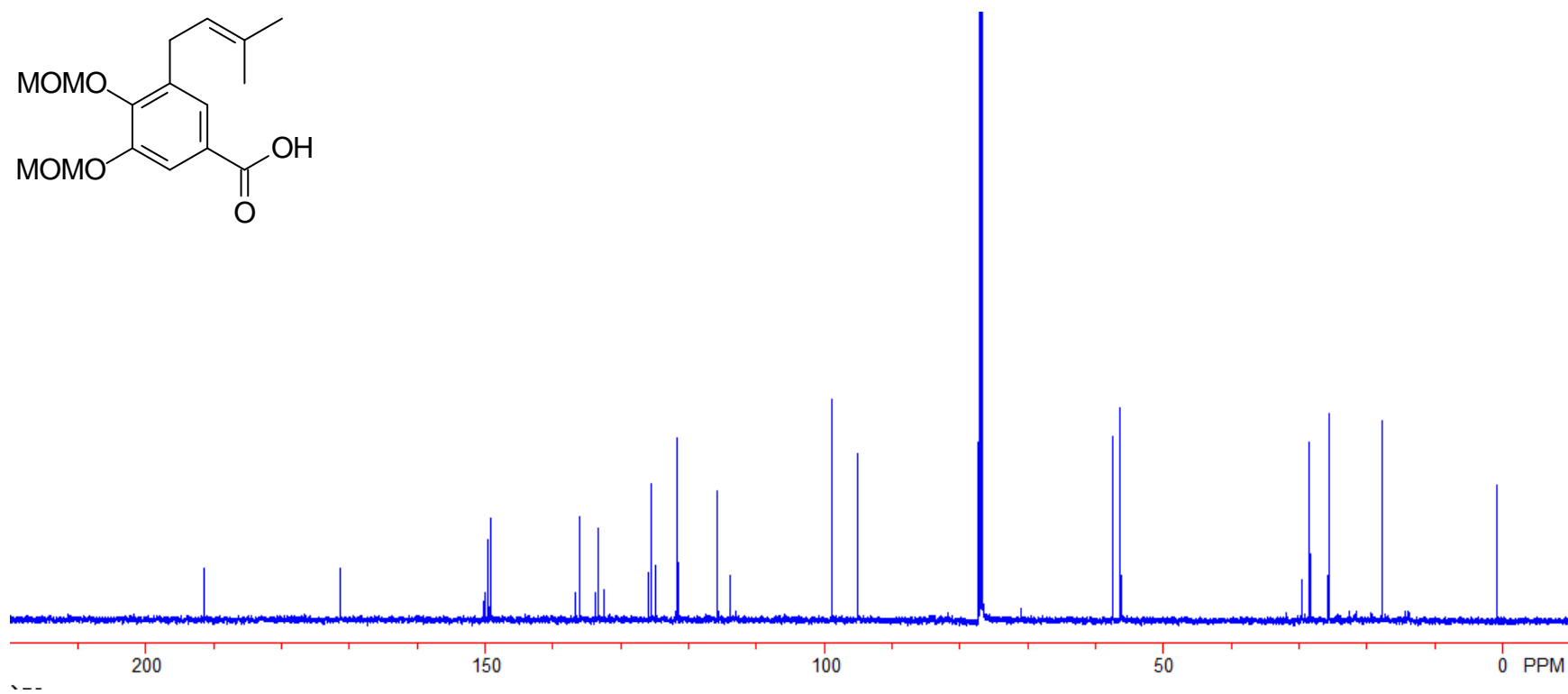
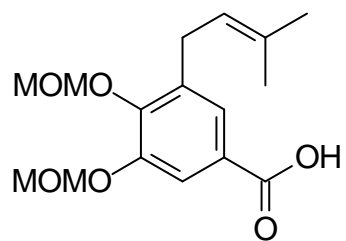


Figure A-104. ^{13}C NMR spectrum of compound **149**

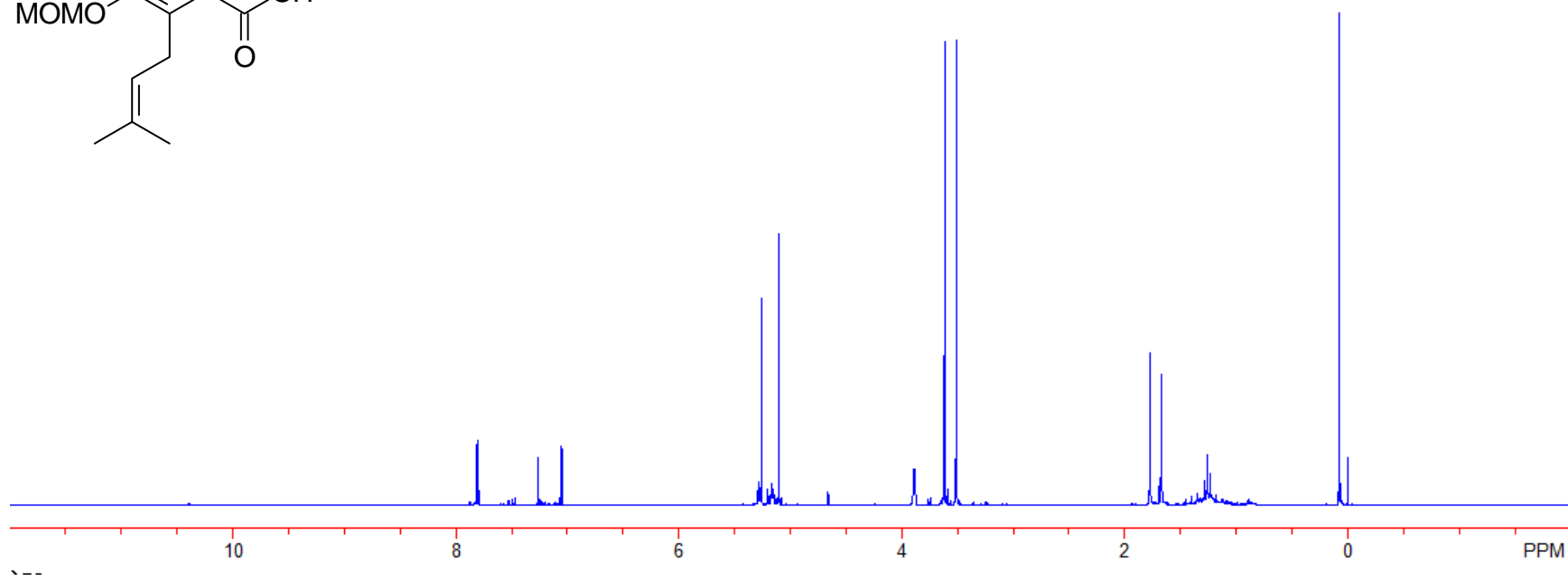
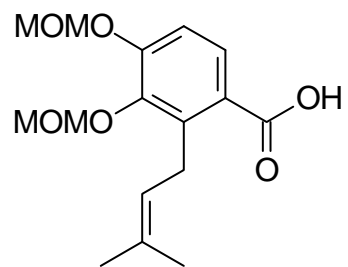


Figure A-105. ¹H NMR spectrum of compound **152**

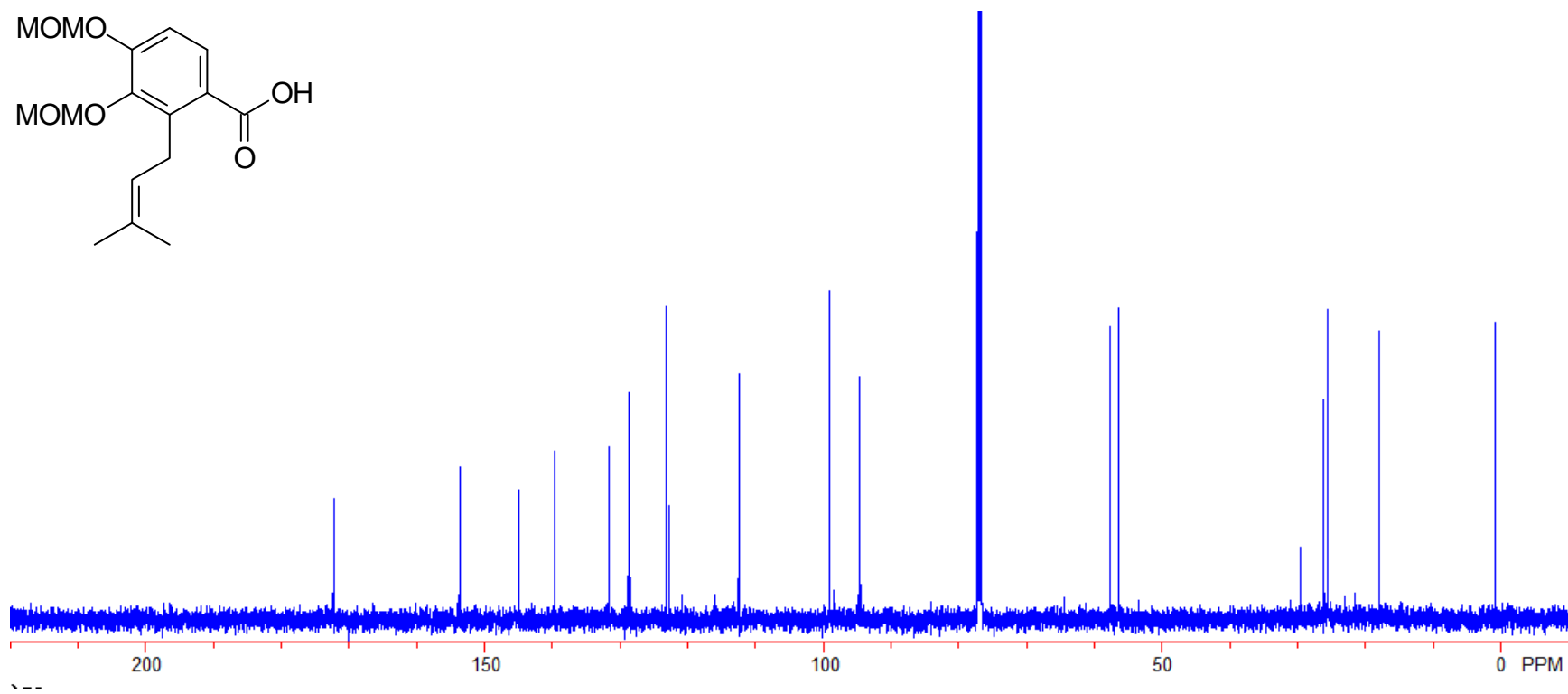
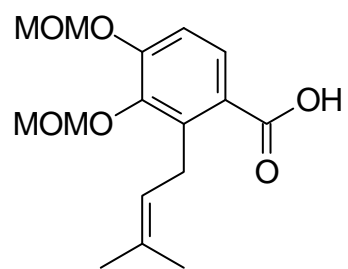


Figure A-106. ^{13}C NMR spectrum of compound **152**

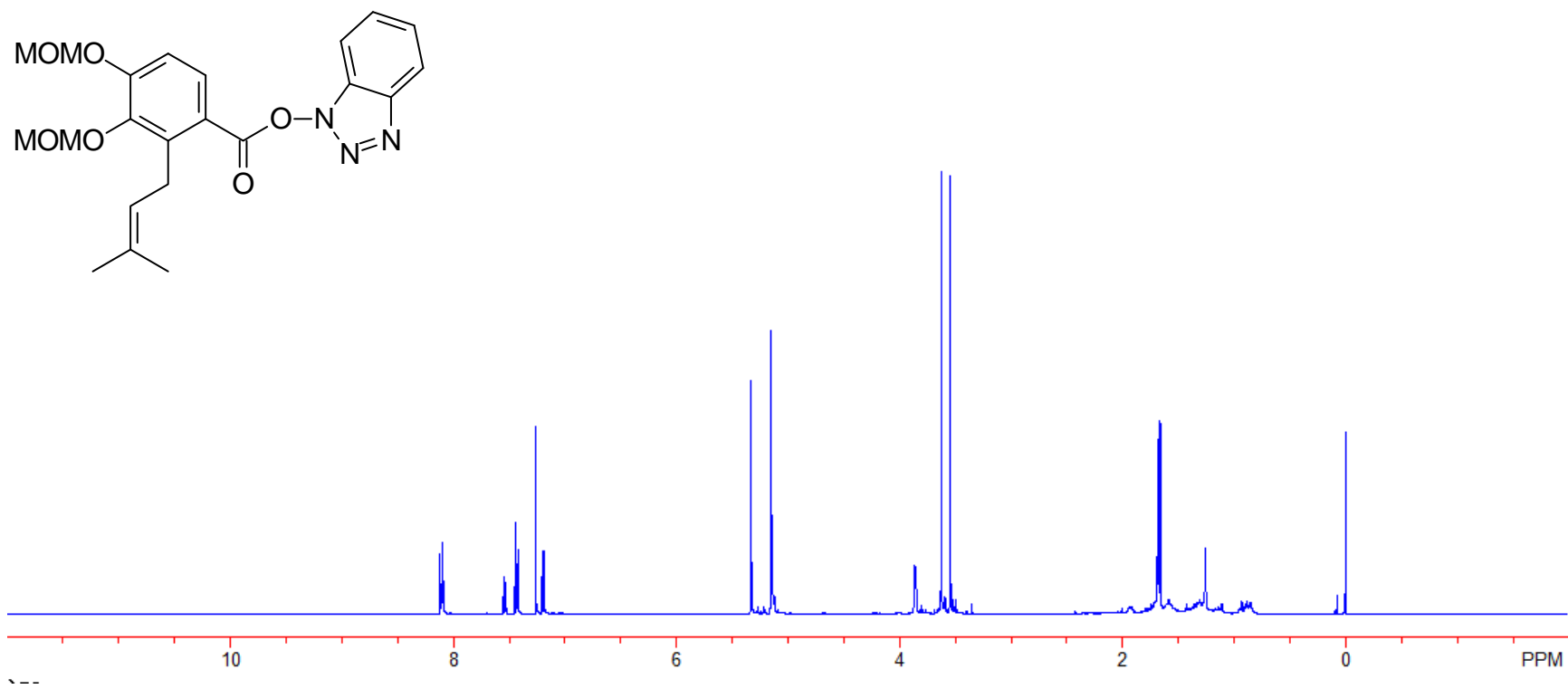


Figure A-107. ¹H NMR spectrum of compound **154**

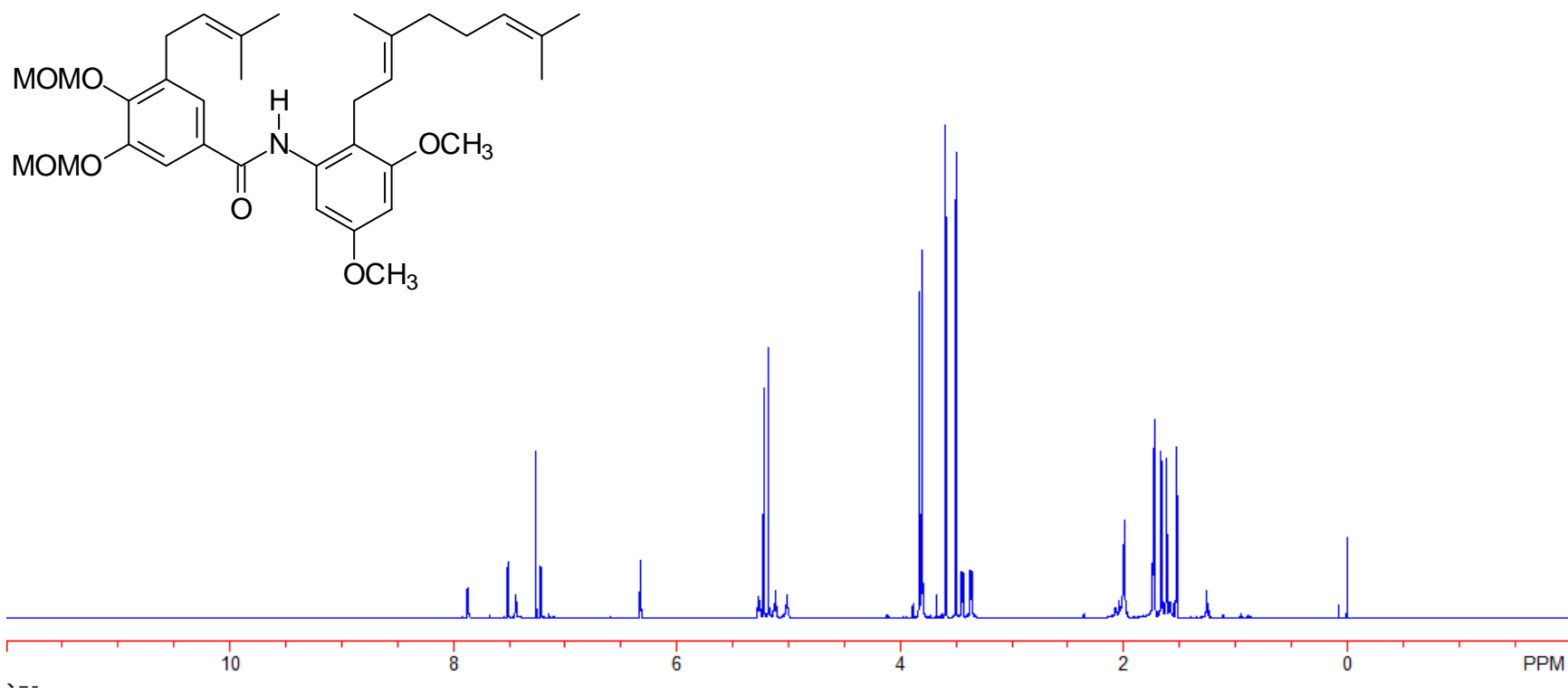


Figure A-108. ^1H NMR spectrum of compound **155**

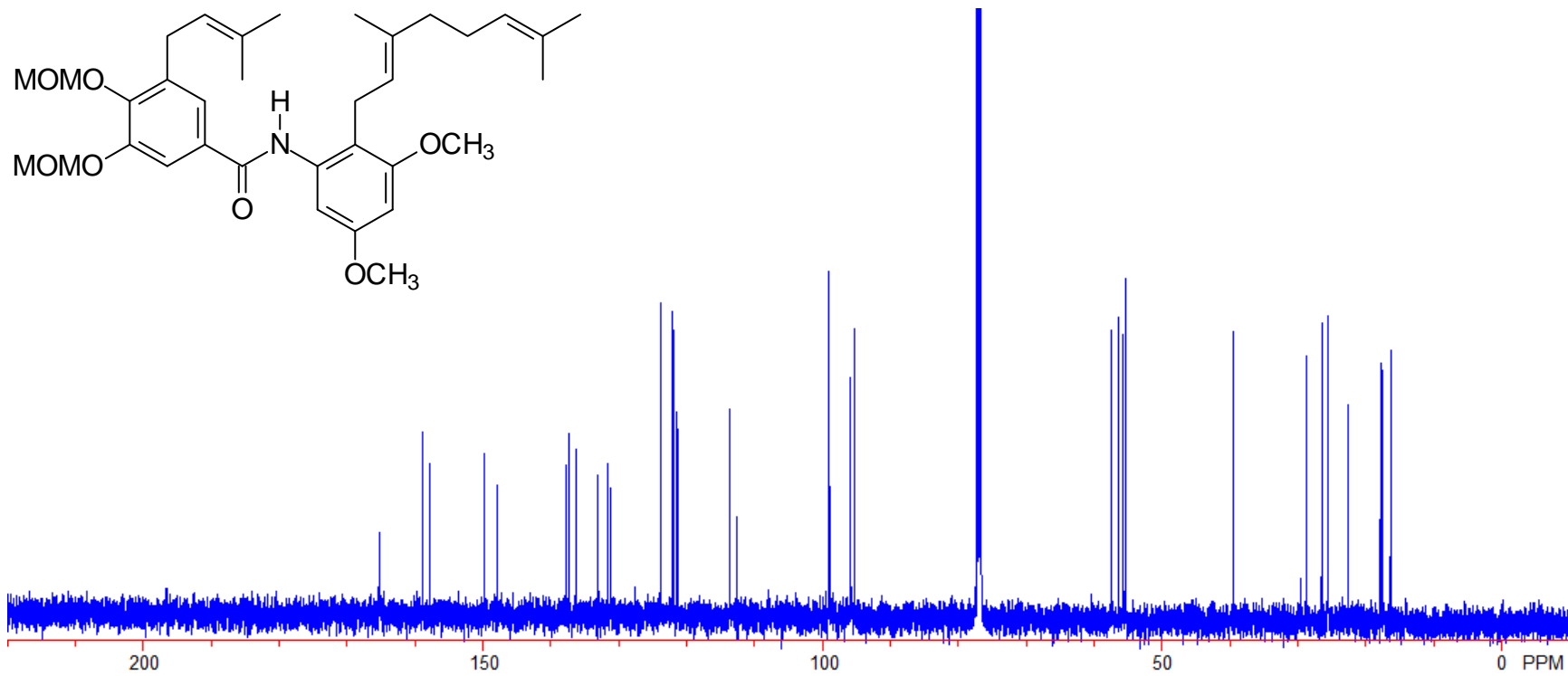


Figure A-109. ^{13}C NMR spectrum of compound **155**

References

1. Treadwell, E. M.; Cermak, S. C.; Wiemer, D. F. *J. Org. Chem.* **1999**, *64*, 8718-8723.
2. Topczewski, J. J.; Kodet, J. G.; Wiemer, D. F. *J. Org. Chem.* **2011**, *76*, 909-919.
3. Topczewski, J. J.; Kuder, C. H.; Neighbors, J. D.; Hohl, R. J.; Wiemer, D. F. *Bioorg. Med. Chem.* **2010**, *18*, 6734-6741.
4. Topczewski, J. J.; Neighbors, J. D.; Wiemer, D. F. *J. Org. Chem.* **2009**, *74*, 6965-6972.
5. Neighbors, J. D.; Salnikova, M. S.; Beutler, J. A.; Wiemer, D. F. *Bioorg. Med. Chem.* **2006**, *14*, 1771-1784.
6. Neighbors, J. D.; Beutler, J. A.; Wiemer, D. F. *J. Org. Chem.* **2005**, *70*, 925-931.
7. Treadwell, E. M.; Neighbors, J. D.; Wiemer, D. F. *Org. Lett.* **2002**, *4*, 3639-3642.
8. Mente, N. R.; Neighbors, J. D.; Wiemer, D. F. *J. Org. Chem.* **2008**, *73*, 7963-7970.
9. Mente, N. R.; Wiemer, A. J.; Neighbors, J. D.; Beutler, J. A.; Hohl, R. J.; Wiemer, D. F. *Bioorg. Med. Chem. Lett.* **2007**, *17*, 911-915.
10. Topczewski, J. J.; Wiemer, D. F. *Tetrahedron Lett.* **2011**, *52*, 1628-1630.
11. Mente, N. R. Ph.D. Thesis, University of Iowa, 2008.
12. Belofsky, G.; French, A. N.; Wallace, D. R.; Dodson, S. L. *J. Nat. Prod.* **2004**, *67*, 26-30.
13. Hufford, C. D.; Jia, Y.; Croom, E. M., Jr.; Muhammed, I.; Okunade, A. L.; Clark, A. M.; Rogers, R. D. *J. Nat. Prod.* **1993**, *56*, 1878-1889.
14. Huang, L.; Fullas, F.; McGivney, R. J.; Brown, D. M.; Wani, M. C.; Wall, M. E. *J. Nat. Prod.* **1996**, *59*, 290-292.
15. Gilmore, M. In *Uses of Plants by the Indians of the Missouri River Region*; University of Nebraska Press: Lincoln, NE, 1977; pp 41-62.
16. Hartung, A. M.; Beutler, J. A.; Navarro, H. A.; Wiemer, D. F.; Neighbors, J. D. *J. Nat. Prod.* **2014**, *77*, 311-319.
17. Prisinzano, T. E. *J. Med. Chem.* **2013**, *56*, 3435-3443.

18. Benyhe, S. *Life Sci.* **1994**, *55*, 969-979.
19. Gourlay, G. K. *Support. Care Cancer* **2005**, *13*, 153-159.
20. Verhoest, P. R.; Basak, A. S.; Parikh, V.; Hayward, M.; Kauffman, G. W.; Paradis, V.; McHardy, S. F.; McLean, S.; Grimwood, S.; Schmidt, A. W.; Vanase-Frawley, M.; Freeman, J.; Van Deusen, J.; Cox, L.; Wong, D.; Liras, S. *J. Med. Chem.* **2011**, *54*, 5868-5877.
21. Melief, E. J.; Miyatake, M.; Carroll, F. I.; Béguin, C.; Carlezon, W. A., Jr.; Cohen, B. M.; Grimwood, S.; Mitch, C. H.; Rorick-Kehn, L.; Chavkin, C. *Mol. Pharmacol.* **2011**, *80*, 920-929.
22. Siebert, D. J. *J. Ethnopharmacol.* **1994**, *43*, 53-56.
23. Lovell, K. M.; Vasiljevik, T.; Araya, J. J.; Lozama, A.; Prevatt-Smith, K. M.; Day, V. W.; Dersch, C. M.; Rothman, R. B.; Butelman, E. R.; Kreek, M. J.; Prisinzano, T. E. *Bioorg. Med. Chem.* **2012**, *20*, 3100-3110.
24. Scheerer, J. R.; Lawrence, J. F.; Wang, G. C.; Evans, D. A. *J. Am. Chem. Soc.* **2007**, *129*, 8968-8969.
25. Hagiwara, H.; Suka, Y.; Nojima, T.; Hoshi, T.; Suzuki, T. *Tetrahedron* **2009**, *65*, 4820-4825.
26. Harding, W. W.; Schmidt, M.; Tidgewell, K.; Kannan, P.; Holden, K. G.; Dersch, C. M.; Rothman, R. B.; Prisinzano, T. E. *Bioorg. Med. Chem. Lett.* **2006**, *16*, 3170-3174.
27. Harding, W. W.; Schmidt, M.; Tidgewell, K.; Kannan, P.; Holden, K. G.; Gilmour, B.; Navarro, H. A.; Rothman, R. B.; Prisinzano, T. E. *J. Nat. Prod.* **2006**, *69*, 107-112.
28. Simpson, D. S.; Katavic, P. L.; Lozama, A.; Harding, W. W.; Parrish, D.; Deschamps, J. R.; Dersch, C. M.; Partilla, J. S.; Rothman, R. B.; Navarro, H.; Prisinzano, T. E. *J. Med. Chem.* **2007**, *50*, 3596-3603.
29. Holden, K. G.; Tidgewell, K.; Marquam, A.; Rothman, R. B.; Navarro, H.; Prisinzano, T. E. *Bioorg. Med. Chem. Lett.* **2007**, *17*, 6111-6115.
30. Tidgewell, K.; Harding, W. W.; Lozama, A.; Cobb, H.; Shah, K.; Pavitra, K.; Dersch, C. M.; Parrish, D.; Deschamps, J. R.; Rothman, R. B.; Prisinzano, T. E. *J. Nat. Prod.* **2006**, *69*, 914-918.

31. Lozama, A.; Cunningham, C. W.; Caspers, M. J.; Douglas, J. T.; Dersch, C. M.; Rothman, R. B.; Prisinzano, T. E. *J. Nat. Prod.* **2011**, *74*, 718-726.
32. Polepally, P. R.; White, K.; Vardy, E.; Roth, B. L.; Ferreira, D.; Zjawiony, J. K. *Bioorg. Med. Chem. Lett.* **2013**, *23*, 2860-2862.
33. Almeida, E. R.; Almeida, R. N.; Navarro, D. S.; Bhattacharyya, J.; Silva, B. A.; Birnbaum, J. S. P. *J. Ethnopharmacol.* **2003**, *88*, 1-4.
34. Bhattacharyya, J.; Majetich, G.; Jenkins, T. M.; Almeida, R. N. *J. Nat. Prod.* **1998**, *61*, 413-414.
35. Batista, J. S.; Almeida, R. N.; Bhattacharyya, J. *J. Ethnopharmacol.* **1995**, *45*, 207-210.
36. Almeida, R. N.; Navarro, D. S.; Agra, M. F.; Almeida, E. R.; Majetich, G.; Bhattacharyya, J. *J. Pharm. Biol.* **2000**, *38*, 394-395.
37. Katavic, P. L.; Lamb, K.; Navarro, H.; Prisinzano, T. E. *J. Nat. Prod.* **2007**, *70*, 1278-1282.
38. Gao, J.; León, F.; Radwan, M. M.; Dale, O. R.; Husni, A. S.; Manly, S. P.; Lupien, S.; Wang, X.; Hill, R. A.; Dugan, F. M.; Cutler, H. G.; Cutler, S. J. *J. Nat. Prod.* **2011**, *74*, 1636-1639.
39. Gao, J.; Radwan, M. M.; León, F.; Dale, O. R.; Husni, A. S.; Wu, Y.; Lupien, S.; Wang, X.; Manly, S. P.; Hill, R. A.; Dugan, F. M.; Cutler, H. G.; Cutler, S. J. *J. Nat. Prod.* **2013**, *76*, 824-828.
40. Lovell, K. M.; Simpson, D. S.; Cunningham, C. W.; Prisinzano, T. E. *Future Med. Chem.* **2009**, *1*, 285-301.
41. Jang, M. S.; Cai, E. N.; Udeani, G. O.; Slowing, K. V.; Thomas, C. F.; Beecher, C. W. W.; Fong, H. H. S.; Farnsworth, N. R.; Kinghorn, A. D.; Mehta, R. G.; Moon, R. C.; Pezzuto, J. M. *Science* **1997**, *275*, 218-220.
42. Gupta, Y. K.; Sharma, M.; Briyal, S. *Methods Find. Exp. Clin. Pharmacol.* **2004**, *26*, 667-672.
43. Sobolev, V. S.; Khan, S. I.; Tabanca, N.; Wedge, D. E.; Manly, S. P.; Cutler, S. J.; Coy, M. R.; Becnel, J. J.; Neff, S. A.; Gloer, J. B. *J. Agric. Food Chem.* **2011**, *59*, 1673-1682.
44. Roth, B. L.; Baner, K.; Westkaemper, R.; Siebert, D.; Rice, K. C.; Steinberg, S.; Ernsberger, P.; Rothman, R. B. *Proc. Natl. Acad. Sci. USA* **2002**, *99*, 11934-11939.

45. Carroll, F. I.; Carlezon, W. A., Jr. *J. Med. Chem.* **2013**, *56*, 2178-2195.
46. Staples, M.; Acosta, S.; Tajiri, N.; Pabon, M.; Kaneko, Y.; Borlongan, C. V. *Int. J. Mol. Sci.* **2013**, *14*, 17410-17419.
47. Lamberts, J. T.; Traynor, J. R. *Curr. Pharm. Des.* **2013**, *19*, 7333-7347.
48. Shaqura, M. A.; Zöllner, C.; Mousa, S. A.; Stein, C.; Schäfer, M. *J. Pharmacol. Exp. Ther.* **2004**, *308*, 712-718.
49. Pfeiffer, A.; Brantle, V.; Herz, A.; Emerich, H. M. *Science* **1986**, *233*, 744-776.
50. Goodman, A. J.; Bourdonnec, B. L.; Dolle, R. E. *Chem. Med. Chem.* **2007**, *2*, 1552-1570.
51. Boyd, R. E.; Reitz, A. B.; (Janssen Pharmaceutica, N. V.). International Patent WO 2004035574 A2, 2004.
52. Newton, S. S.; Thome, J.; Wallace, T. L.; Shirayama, Y.; Schlesinger, L.; Sakai, N.; Chen, J.; Neve, R.; Nestler, E. J.; Duman, R. S. *J. Neurosci.* **2002**, *22*, 10883-10890.
53. Carlezon, W. A., Jr.; Béguin, C.; Knoll, A. T.; Cohen, B. M. *Pharmacol. Ther.* **2009**, *123*, 334-343.
54. Neighbors, J. D.; Salnikova, M. S.; Wiemer, D. F. *Tetrahedron Lett.* **2005**, *46*, 1321-1324.
55. Neighbors, J. D.; Beutler, J. A.; Wiemer, D. F. *J. Org. Chem.* **2005**, *70*, 925-931.
56. Neighbors, J. D.; Buller, M. J.; Boss, K. D.; Wiemer, D. F. *J. Nat. Prod.* **2008**, *71*, 1949-1952.
57. Kreek, M. J.; Koob, G. F. *Drug Alcohol Depend.* **1998**, *51*, 23-47.
58. Sinha, R.; Fuse, T.; Aubin, L. R.; O'Malley, S. S. *Psychopharmacology* **2000**, *152*, 140-148.
59. McMahon, R. C. *J. Subst. Abuse Treat.* **2001**, *21*, 77-87.
60. Thomas, J. B.; Atkinson, R. N.; Vinson, N. A.; Catanzaro, J. L.; Perretta, C. L.; Fix, S. E.; Mascarella, S. W.; Rothman, R. B.; Xu, H.; Dersch, C. M.; Cantrell, B. E.; Zimmerman, D. M.; Carroll, F. I. *J. Med. Chem.* **2003**, *46*, 3127-3137.
61. Beardsley, P. M.; Howard, J. L.; Shelton, K. L.; Carroll, F. I. *Psychopharmacology* **2005**, *183*, 118-126.

62. Carey, A. N.; Borozny, K.; Aldrich, J. V.; McLaughlin, J. P. *Eur. J. Pharmacol.* **2007**, *569*, 84-89.
63. Arunlakshana, O.; Schild, H. O. *Br. J. Pharm. Chemother.* **1959**, *14*, 48-58.
64. Kuder, C. H.; Neighbors, J. D.; Hohl, R. J.; Wiemer, D. F. *Bioorg. Med. Chem.* **2009**, *17*, 4718-4723.
65. Kodet, J. G. Ph.D. Thesis, University of Iowa, 2010.
66. Ulrich, N. C.; Kodet, J. G.; Mente, N. R.; Kuder, C. H.; Beutler, J. A.; Hohl, R. J.; Wiemer, D. F. *Bioorg. Med. Chem.* **2010**, *18*, 1676-1683.
67. Thomas, J. B.; Fix, S. E.; Rothman, R. B.; Mascarella, S. W.; Dersch, C. M.; Cantrell, B. E.; Zimmerman, D. M.; Carroll, F. I. *J. Med. Chem.* **2004**, *47*, 1070-1073.
68. Li, Y. L.; Zhao, Y. L. *Chin. Chem. Lett.* **1994**, *5*, 935-938.
69. Topczewski, J. J.; Callahan, M. P.; Kodet, J. G.; Inbarasu, J. D.; Mente, N. R.; Beutler, J. A.; Wiemer, D. F. *Bioorg. Med. Chem.* **2011**, *19*, 7570-7581.
70. Kaiser, F.; Schwink, L.; Velder, J.; Schmalz, H. G. *Tetrahedron* **2003**, *59*, 3201-3217.
71. Cushman, M.; Nagarathnam, D.; Gopal, D.; Chakraborti, A. K.; Lin, C. M.; Hamel, E. *J. Med. Chem.* **1991**, *34*, 2579-2588.
72. Merlic, C. A.; Aldrich, C. C.; Albaneze-Walker, J.; Saghatelian, A.; Mammen, J. J. *Org. Chem.* **2001**, *66*, 1297-1309.
73. Tan, Y. L.; White, A. J. P.; Widdowson, D. A.; Wilhelm, R.; Williams, D. J. *J. Chem. Soc., Perkin Trans. 1* **2001**, 3269-3280.
74. Wang, Y.; Mathis, C. A.; Huang, G.; Holt, D. P.; Debnath, M. L.; Klunk, W. E. *J. Labelled Compd. Radiopharmaceut.* **2002**, *45*, 647-664.
75. Neighbors, J. D.; Salnikova, M. S.; Beutler, J. A.; Wiemer, D. F. *Bioorg. Med. Chem.* **2006**, *14*, 1771-1784.
76. Klausmeyer, P.; Van, Q. N.; Jato, J.; McCloud, T. G.; Beutler, J. A. *J. Nat. Prod.* **2010**, *73*, 479-481.
77. Singh, M.; Argade, N. P. *Synthesis* **2012**, *44*, 2895-2902.
78. Huang, C. P.; Au, L. C.; Chiou, R. Y. Y.; Chung, P. C.; Chen, S. Y.; Tang, W. C.; Chang, C. L.; Fang, W. H.; Lin, S. B. *J. Agric. Food Chem.* **2010**, *58*, 12123-12129.

79. Chang, J. C.; Lai, Y. H.; Djoko, B.; Wu, P. L.; Liu, C. D.; Liu, Y. W.; Chiou, R. Y. *Y. J. Agric. Food Chem.* **2006**, *54*, 10281-10287.
80. Hu, K.; Yang, Z.; Pan, S. S.; Xu, H.; Ren, J. *Eur. J. Med. Chem.* **2010**, *45*, 3453-3458.
81. Park, B. H.; Lee, H. J.; Lee, Y. R. *J. Nat. Prod.* **2011**, *74*, 644-649.
82. Leeson, P. *Nature* **2012**, *481*, 455-456.
83. Gaslonde, T.; Covello, F.; Velazquez-Alonso, L.; Léonce, S.; Pierré, A.; Pfeiffer, B.; Michel, S.; Tillequin, F. *Eur. J. Med. Chem.* **2011**, *46*, 1861-1873.
84. González-Antuña, A.; Lavandera, I.; Rodríguez-González, P.; Rodríguez, J.; García Alonso, J. I.; Gotor, V. *Tetrahedron* **2011**, *67*, 5577-5581.
85. Wang, G. B.; Wang, L. F.; Li, C. Z.; Sun, J.; Zhou, G. M.; Yang, D. C. *Res. Chem. Intermed.* **2012**, *38*, 77-89.
86. Baggelaar, M. P.; Huang, Y.; Feringa, B. L.; Dekker, F. J.; Minnaard, A. J. *Bioorg. Med. Chem.* **2013**, *21*, 5271-5274.
87. Hassan, M. Z.; Khan, S. A.; Amir, M. *Eur. J. Med. Chem.* **2012**, *58*, 206-213.
88. Burlison, J. A.; Neckers, L.; Smith, A. B.; Maxwell, A.; Blagg, B. S. J. *J. Am. Chem. Soc.* **2006**, *128*, 15529-15536.
89. Ooi, H.; Ishibashi, N.; Iwabuchi, Y.; Ishihara, J.; Hatakeyama, S. *J. Org. Chem.* **2004**, *69*, 7765-7768.
90. Gowda, R. R.; Chakraborty, D. *Chin. J. Chem.* **2011**, *29*, 2379-2384.
91. Foot, J. S.; Kanno, H.; Giblin, G. M. P.; Taylor, R. J. K. *Synthesis* **2003**, *2003*, 1055-1064.
92. Arima, Y.; Kinoshita, M.; Akita, H. *Tetrahedron: Asymmetry* **2007**, *18*, 1701-1711.
93. Huczyński, A.; Janczak, J.; Stefańska, J.; Antoszczak, M.; Brzezinski, B. *Bioorg. Med. Chem. Lett.* **2012**, *22*, 4697-4702.
94. Mohamed, M. A.; Yamada, K.; Tomioka, K. *Tetrahedron Lett.* **2009**, *50*, 3436-3438.
95. Shvartsbart, A.; Smith, A. B. *J. Am. Chem. Soc.* **2014**, *136*, 870-873.

96. Pettit, G. R.; Singh, S. B.; Margaret, N.; Hamel, E.; Schmidt, J. M. *J. Nat. Prod.* **1987**, *50*, 119-131.
97. Wu, H.; Wacker, D.; Mileni, M.; Katritch, V.; Han, G. W.; Vardy, E.; Liu, W.; Thompson, A. A.; Huang, X. P.; Carroll, F. I.; Mascarella, S. W.; Westkaemper, R. B.; Mosier, P. D.; Roth, B. L.; Cherezov, V.; Stevens, R. C. *Nature* **2012**, *485*, 327-332.
98. Lu, J.; Ma, J.; Xie, X.; Chen, B.; She, X.; Pan, X. *Tetrahedron: Asymmetry* **2006**, *17*, 1066-1073.
99. Tae, E. L.; Lee, S. H.; Lee, J. K.; Yoo, S. S.; Kang, E. J.; Yoon, K. B. *J. Phys. Chem. B.* **2005**, *109*, 22513-22522.
100. Gester, S.; Pietzsch, J.; Wuest, F. R. *J. Labelled Compd. Radiopharmaceut.* **2007**, *50*, 105-113.
101. Kumano, T.; Tomita, T.; Nishiyama, M.; Kuzuyama, T. *J. Biol. Chem.* **2010**, *285*, 39663-39671.
102. Wright, G. E.; Tang Wei, T. Y. *Tetrahedron* **1973**, *29*, 3775-3779.
103. McNulty, J.; McLeod, D. *Tetrahedron Lett.* **2013**, *54*, 6303-6306.
104. Li, H.; Wang, Y.; Tang, L.; Wu, F.; Liu, X.; Guo, C.; Foxman, B. M.; Deng, L. *Angew. Chem. Int. Ed.* **2005**, *44*, 105-108.